

## Using Composites in Seismic Retrofit Applications

20 April 2005

Prepared by

V. M. KARBHARI  
Outside Consultant

### **DISTRIBUTION STATEMENT A**

Approved for Public Release  
Distribution Unlimited

Prepared for

STATE OF CALIFORNIA  
DEPARTMENT OF TRANSPORTATION  
Sacramento, CA 94273

Contract No. 59A088

Engineering and Technology Group

20050602 001




**THE AEROSPACE  
CORPORATION**

El Segundo, California

PUBLIC RELEASE IS AUTHORIZED

## USING COMPOSITES IN SEISMIC RETROFIT APPLICATIONS

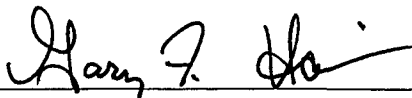
Prepared



---

V. M. KARBHARI  
Outside Consultant

Approved



---

G. F. HAWKINS, Principal Director  
Space Materials Laboratory  
Laboratory Operations

## **Abstract**

This report was prepared to provide a comprehensive review of the state-of-the-art for using composite materials for seismic retrofit applications. The emphasis is on seismic retrofit of reinforced concrete columns. The report is presented in eleven chapters. Chapters 1–3 provide a basic introduction to composite materials, including discussions on the types of matrix and reinforcement materials, processing methods, and basic mechanics. Polymer matrix composites with continuous carbon or glass fibers as reinforcement are emphasized since they are the most frequently used composite materials for seismic retrofit applications. Chapters 4–6 review methods for designing and applying composite jackets onto columns and performing structural tests on columns with composite jackets. Environmental durability test protocols and data for composite systems for seismic retrofit are reviewed in Chapters 7–10. Examples of commercially available composite retrofit systems are presented in Chapter 11.

## CHAPTER 1: INTRODUCTION

### 1.1 Materials Perspective

The development of materials is often considered to be the key to social and technological growth of *homo sapiens*. In archeological terms man has developed through the *stone* age (about 10,000 BC), the *copper* age (4000-3000 BC), the *bronze* age (2000-1000 BC), the *iron* age (1000 BC–1620 AD) and modern times are often denoted as the *plastic* or the *silicon* age. Irrespective of the focus from an archeological perspective it is clear that since the beginning of mankind the human race has attempted to create new materials with enhanced properties.

Structural materials are generically differentiated into the four basic classes of metals, ceramics, polymers and composites. Ashby [1] has schematically shown the relative development and importance of these classes in the context of a historical time line as shown in Figure 1.1.

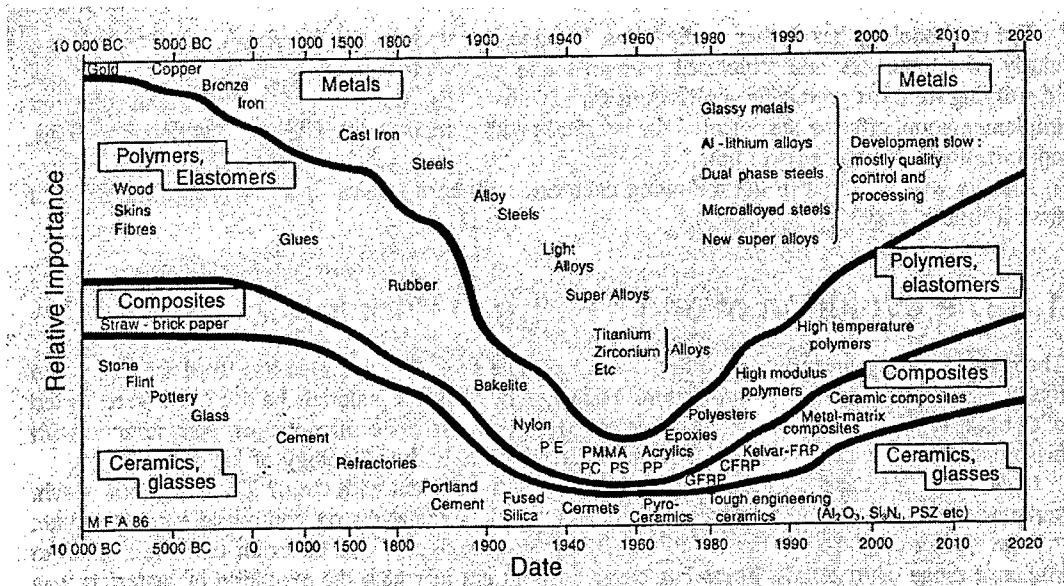


Figure 1.1: The Evolution of Engineering Materials With Time [1]



A reasonable argument could be made that composites, defined as a combination of two or more constituents in a macroscopic structural unit, were one of the first materials in nature. Wood consists of fibrous cellulose held together by lignin, whereas even bones are combinations of collagen in fibrular form surrounded by a proteinous calcium-phosphate binder [2]. The first reference to a man-made composite comes from the Bible referring to the ancient Israelites use of straw reinforcement, albeit to probably control shrinkage cracks, in mud bricks. The Egyptians in about 3500 BC also came up with the concept of *laminated composites* through the development of a rudimentary form of plywood. Several thin layers of wood were glued together to form a thick layer of useable material from a combination of good veneer (on the outside) and substandard veneer towards the center. By about 700 BC this concept was taken further towards orienting the grain in layers perpendicular to each other to provide a more uniform board. The concept of gluing thinner veneer cross-grain to thicker pieces of lumber, primarily for purposes of aesthetics was widely used in 18<sup>th</sup> century furniture. Modern plywood, called veneered wood at that time, draws from the patents of John Mayo (1865, 1868) and George Gardner (1872-1876), principally for use in chair seats [3,4]. Interestingly similar concepts of lamination were used in medieval armor and in laminated Japanese swords.

In more modern times, reinforced concrete is in fact a macroscopic composite consisting of steel rods as reinforcement in a particulate reinforced ceramic matrix. The difference between this form of composite and the *advanced* composite materials discussed in this book is that the fiber in the latter case has a diameter of a few microns rather than millimeters and greater, and that the fiber volume fraction for structural applications ranges between 35-65% rather than levels of less than 0.5-2% as used in conventional reinforced concrete.

## 1.2 Composite Materials

In the context of the present discussion, composite materials are defined as a macroscopic combination of two or more distinct materials having a finite interface between them. One of the constituents is the reinforcement, or reinforcing phase, while the other is the matrix phase. The major, or at least clearly apparent, difference between a material such as a plastic and a

composite is thus that the composite consists of both reinforcement (fibers for example) and a matrix (which could be the polymer used to form the plastic itself).

The ability to macroscopically combine the phases provides immense opportunities for the tailoring of materials. This in fact enables a true creation of “materials by design” since properties and performance can be designed through selection and proportion of constituent materials, orientation of the reinforcing phase and lay-up of different layers in a laminated structure. Thus, depending on the set of requirements it is possible to create a range of materials from those that are homogeneous and isotropic to those that are heterogenous and anisotropic, as well as all combinations in between. A composite, if conceptualized in correct fashion is a designers dream, whereas in the hands of a novice it could well become a nightmare.

### 1.3 Classification

Composite materials are generically classified at two different levels. The first, and more generic, is related to the matrix phase. It is noted that the matrix serves a number of functions besides being the binder to hold the reinforcing phase together. It provides environmental and damage protection to the reinforcing phase, toughness and multi-functional non-mechanical properties to the composite, and enables forming into shapes. Figure 1.2 depicts the 3 main classes of composites based on matrix type.

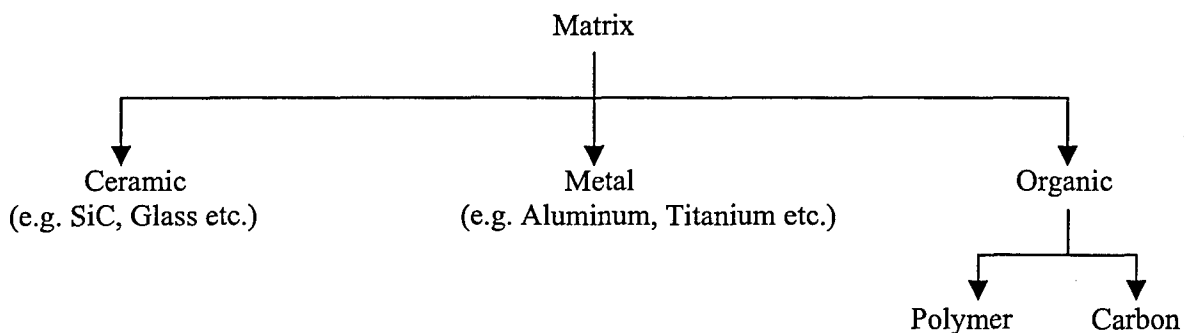


*Figure 1.2: Classification Based on Matrix Type*

Ceramic matrix composites (CMC) incorporate a ceramic as the matrix phase. Reinforcements such as silicon carbide and silicon nitride are combined using specialized processing methods with matrices such as alumina, mullite, silicon carbide and silicon nitride. The addition of reinforcement enhances the innate brittleness, i.e. low fracture toughness, of ceramics through toughening mechanisms while also increasing tensile, flexural and shear properties. CMC's can withstand high temperatures and are used in applications such as turbine engines, heat shields, rocket nozzles, and hypervelocity flight structures. Due to their inert nature they are also used in biomedical applications, and of late have even found application in high performance sporting goods such as skating blades and golf club heads.

Metal matrix composites (MMC) use metals and metallic alloys as the matrix phase. The reinforcements, in the form of fibers, whiskers or particulates enhance the strength and stiffness of the alloys while also enhancing performance attributes such as light weight, dimensional stability, and shear performance. The use of these materials is in its infancy but there is increased use in automotive engine and airframe components, trusses for structures in space and even in sporting goods.

The last class of composites is that of Organic matrix composites (OMC) and is further divided into the two classes of Polymer matrix composites (PMC) and Carbon matrix composites. Polymer matrix composites are the most widely used of all types of composites and have already found significant application in areas such as transportation, civil infrastructure and commercial/industrial applications. These generically involve the use of strong and stiff fibers encapsulated in a polymer resin. Our discussion in later chapters will focus on this class of composites. Carbon matrix composites are typically manufactured from specially developed polymer matrix composites through high temperature carbonization and densification. In these processes the fibers do not undergo changes but the polymer matrix is converted into carbon. A large percentage of these composites use carbon reinforcements and the material is then known as a Carbon carbon composite (CCC). These are invaluable in applications requiring high temperature capabilities and high thermal shock resistance. These materials are used in aircraft and high performance automobile brakes, ablative structures, rocket nozzles, spacecraft thermal protection systems and parts in missiles and satellites.

While the first method of classification is based on the type of matrix used, the second method of classification, shown schematically in Figure 1.3, is based on form of reinforcement used.

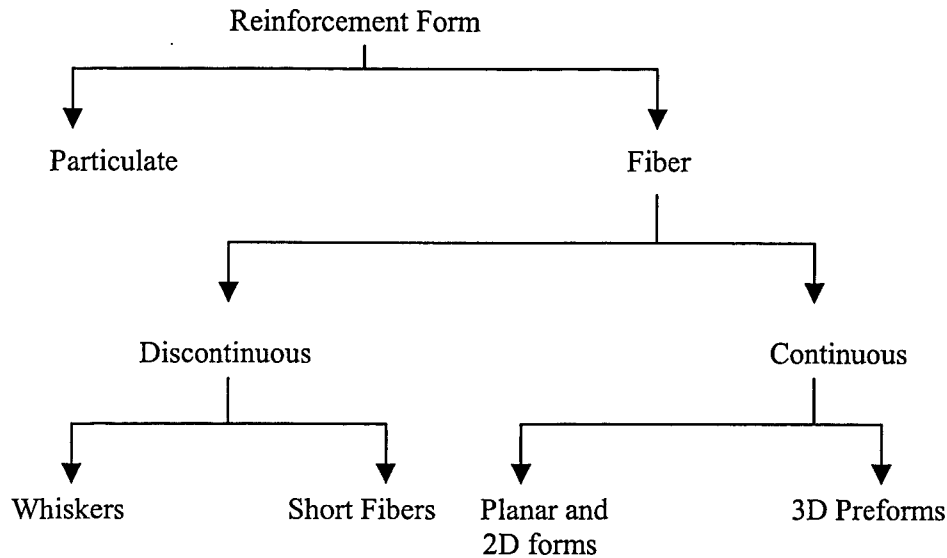
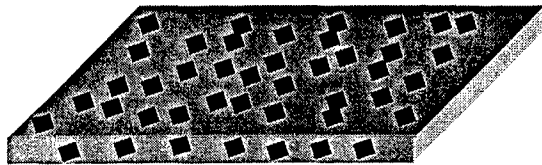


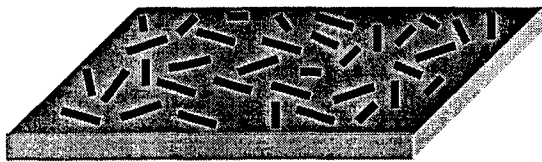
Figure 1.3: Classification Based on Form of Reinforcing Phase

For the reinforcing phase to provide a useful enhancement in the properties provided by the matrix phase alone a minimum fiber volume fraction, generally not lower than 10%, is required. This can, however, be in a variety of forms. Particulate reinforcements are those whose dimensions are all roughly equal. These are used for non-structural applications, and are often termed as fillers, such as for the enhancement of fire resistance, electro-magnetic shielding, thermal conductivity, fracture toughness etc. In contrast *fiber* reinforcement is a term used to denote a phase having one dimension substantially larger than the others. Discontinuous reinforcements have low aspect ratios (ratio of length to diameter). Whiskers are extremely short, generally in the form of single crystals with almost no crystalline defects. Their diameters usually fall in the range of 1-25  $\mu\text{m}$ , and have aspect ratios less than 100. Short fibers are fibers with aspect ratios between 100-250 and are of the same material as used in continuous reinforcement. Continuous fiber reinforced composites contain reinforcements having lengths much greater than their cross-sectional dimensions. Although the fiber length does not

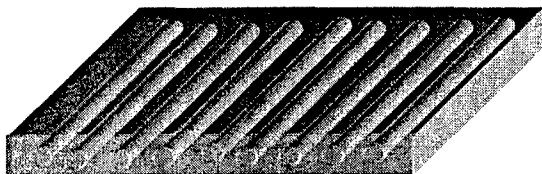
necessarily have to be comparable in dimension to the part being fabricated it is essential that the length be such that any further increase in length will not change properties such as modulus or strength. These reinforcements are usually used in the form of bundles called rovings and tows, and in the form of fabrics wherein a number of bundles are woven, knitted, or braided in specific patterns. In some cases the reinforcement is specially formed using textile processes into a 3-dimensional formwork. This allows the entire skeleton of reinforcement to be formed prior to the introduction of the resin and could be considered, albeit at a much smaller dimensional scale, as analogous to the steel reinforcement cages that are tied prior to pouring of concrete.



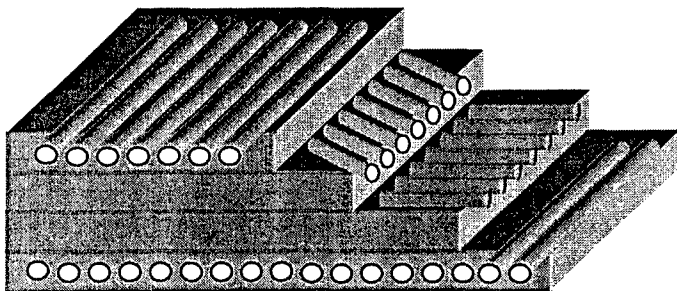
**Particulate Reinforced Composite**  
"Isotropic"



**Short Fiber Reinforced Composite**  
"Orthotropic", "Transversely"



**Continuous Fiber Reinforced Composite**



**Laminate**  
"Anisotropic"

*Figure 1.4: Types of Fiber Reinforced Composites*

A major advantage of fiber-reinforced composites is the ability to place, or orient, the reinforcement depending on the direction in which strength, or stiffness, is required. This enables the placement of reinforcement following specific load paths, or directions of optimized performance leading to tailored anisotropy. This, again, can be the basis for classification, as in Figure 1.4. Most particulate reinforced composites by their very nature are isotropic. Short, or discontinuous, reinforced composites in contrast are orthotropic or transversely isotropic in nature. A major building block of continuous reinforced composites is a lamina, which essentially is a single layer formed of reinforcement aligned parallel to each other. The stacking of these unidirectional laminae with the orientation of fibers differing from layer to layer results in a laminate.

As will be discussed later, laminae and laminated composites are the most common form of polymer matrix composites. However, it should be noted that since the reinforcement is all in the plane of the lamina these composites are weak in the through-thickness direction. Although laminae are well bonded, or consolidated to each other, the potential for separation of the laminae along the interface, or delamination, is a major concern since the interlaminar properties are matrix dominated.

#### **1.4 Matrix Materials for Polymer Matrix Composites**

Polymers are high molecular weight organic compounds whose structure can be represented by repeated units called monomers. These long chained materials are the most widely used matrices in composites. Although polymers can be classified in a number of ways we will only focus on the scheme based on mechanical response at elevated temperatures. Under this classification scheme polymers are either thermoplastic or thermosetting.

Thermoplastic polymers soften when heated, eventually liquefying, and harden on being cooled. This reversibility is because the change upon heating is more physical, through sliding and movement of adjacent chains, than chemical, and enables reshaping and reforming. However, irreversible degradation can result when the polymer is subject to temperatures at which

molecular motion is strong enough to break the primary covalent bonds. Examples of thermoplastics used in composites are polyether ether ketone (PEEK), polyphenylene sulfide (PPS), polyether sulfone (PES), polyether ketone (PEK) and polyether imide (PEI).

Thermosetting polymers, on the other hand, undergo cure in which polymer molecules are bound in a cross-linked three-dimensional network. Once cured the material is essentially infusible and insoluble without decomposition. On application of high temperature, after being formed, the material can show a softening stage but cannot be reformed or reshaped since it degrades rather than returning to the melt stage. Examples of thermosets used in composites are epoxies, polyesters, vinylesters, phenolics, polyimides, bismaleimides (BMI) and urethanes.

Although both thermosets and thermoplastics are used as matrices in polymer matrix composites there is significantly higher use of thermosets, to date, based on aspects related to cost, ease of processing and overall environmental durability. Nonetheless, thermoplastic resins provide a number of significant advantages as shown in the comparison in Table 1.1.

*Table 1.1: Trade-offs Between Thermoplastics and Thermosets*

Characteristic	Thermoplastic Polymers	Thermosetting Polymers
Formulation	Simple	Complex
Recyclability	Reformable on heating	Non-reformable. Can only be reused as regrind
Impact Resistance	Good, tough material	Low, Brittle material
Interlaminar Fracture Toughness	High	Low-Moderate
Strain Limits	Higher strain-to-failure	Low Ultimate strain
Melt Viscosity	High, can interfere in fabric impregnation	Low
Creep Resistance	Not as good, variable	Good
Shelf-Life	Virtually Unlimited	Limited
Resistance to Solvents	Variable, can be degraded by some solvents	Good
Need for refrigeration	Not needed for prepreg	Generally needed for prepreg
Crystallinity Issues	Affects solvent resistance Can cause premature ageing	Non-Crystalline
Cure Cycle	Simple	More complex with ramp and dwell time requirements

PEEK is a linear aromatic thermoplastic which is available in both semi-crystalline and amorphous forms. The introduction of fibers increases the degree of crystallinity, as fibers act as nucleation sites for crystal formation, also resulting in an increase in resin modulus and yield strength, but a decrease in ultimate strain. [5]. Because of its semi-crystalline nature it does not dissolve in common solvents and has good environmental durability. It also has a very low level of moisture absorption (less than 0.5% at 23°C compared to 3-5% for conventional aerospace grade resins).

PPS is a linear semi-crystalline polymer, which has the capability of behaving like a thermoset at elevated temperatures, in that it undergoes cross-linking by air induced oxidation. It has a high degree of solvent and fluid resistance in this state and has outstanding flame resistance and insulation characteristics. However, because of the cross-linking it is brittle and is extremely susceptible to environmental stress cracking.

PES is an amorphous thermoplastic with good temperature resistance but a relatively high level of water absorption. It has poor fatigue characteristics and is susceptible to environmental stress cracking. However, it is often used because of its exceptional thermal ageing characteristics and resistance to radiation.

PEK is a crystalline aromatic thermoplastic with very good mechanical property retention at high temperatures. Polyetherketone ketone (PEEK) exhibits excellent properties and has very good resistance to strong solvents such as methylene chloride.

PEI is an amorphous thermoplastic processible in the melt and is used extensively in aircraft galleys, stowage bins, wing fairings and floor panels. However, it has a much lower solvent resistance than PPS or PEEK and has been found to be extremely susceptible in some cases to hydraulic fluid.

An overall comparison of characteristic temperature levels for high performance thermoplastics used in aircraft grade composites is given in Table 1.2.



Table 1.2: Characteristic Temperature Levels of Thermoplastics [6]

Polymer	Acronym	Glass Transition Temperature (° C)	Melt Temperature (° C)	Continuous Operating Temperature (° C)	Processing Temperature (° C)
Polyether ether ketone	PEEK	143	343	250	360-400
Polyether ketone	PEK	165	365	-	400-450
Polyphenylene sulfide	PPS	138	288	240	340-370
Polyether sulfone	PES	260	-	-	400-450
Polyether imide	PEI	217a	-	-	350-400
		270b	380	-	380-420

a: Amorphous

b: Semicrystalline

Thermosetting resins are the most widely used class of polymers used in polymer matrix composites and in general have very good environmental and creep resistance due to their cross-linked morphology. Cross-linking occurs due to chemical reactions that are affected by thermal history during processing. Most of these materials can be processed, both under ambient conditions or at elevated temperatures, through selection of appropriate catalyst, initiator, and promotor stoichiometry. In general, the glass transition temperature is controlled by the temperature at which the material is processed and the level of exotherm attained. Since thermosets cannot be reheated and reformed, both the material and the resulting structure/geometrical configuration are achieved at the same time.

Polyesters are perhaps the most widely used of the thermoset systems, accounting for about 75% of total resin usage. They are macromolecules formed by the condensation polymerization of dibasic acids or anhydrides with dihydric alcohols (glycols). In addition, unsaturated polyester contain materials such as maleic anhydride, adipic acid (added to enhance flexibility and toughness), isophthalic acid (added to increase toughness, moisture-and-chemical-resistance) and fumaric acid in unsaturated form. The polymer is generally dissolved in a reactive monomer diluent, such as styrene, to give a viscosity in the range of 0.2-2 pa.s (200-2000 cps). There are four primary types of polyester resins. Orthopolyesters are blends of phthalic anhydride and maleic anhydride or fumaric acid and are cheap and easy to use. However, they have relatively poor thermal stability and chemical resistance. Isopolyesters are blends of isophthalic acid and

maleic anhydride or fumaric acid. These are commonly used in the fabrication of corrosion resistant equipment and have better thermal stability and resistance to moisture and solvents. Bisphenol A fumarates are blends of propoxylated or ethoxylated BPA with fumaric acid and have very good thermal stability and chemical resistance. Chlorendics are blends of chlorendic anhydride or chlorendic acid and maleic anhydride or fumaric acid. The addition of the chlorendic component provides enhanced fire retardancy. A comparison of typical mechanical characteristics is given in Table 1.3.

*Table 1.3: Typical Mechanical Properties of Clear Cast Resin*

<b>Material Type</b>	<b>Tensile Strength (MPa)</b>	<b>Tensile Modulus (GPa)</b>	<b>Ultimate Strain (%)</b>	<b>Flexural Strength (MPa)</b>	<b>Flexural Modulus (GPa)</b>	<b>Compressive Strength (MPa)</b>
Orthophthalic	40-55	3-3.5	1.5-2.1	70-85	3-3.5	80-90
Isophthalic	55-85	2.8-3.8	3.0-3.5	110-140	3-4.0	100-120
BPA fumarate	30-40	2.5-3.0	1.2-1.6	100-120	3-3.5	80-100
Chlorendic	15-20	3.0-3.5	1.0-1.5	110-130	3.5-4.0	80-100

An important aspect for use of these materials is the temperature at which they begin to lose their ability to carry load. A characteristic used to define this temperature is the heat distortion, or deflection, temperature (HDT). This temperature is a function of the degree of cure and of the conditions under which cure was achieved. Obviously, higher HDTs reflect higher potential operating temperatures. Table 1.4 provides a comparison of heat distortion temperatures and hardness.

*Table 1.4: Typical Values of Hardness and Heat Distortion Temperature*

<b>Material Type</b>	<b>Barcol Hardness</b>	<b>Heat Distortion Temperature (°C)</b>
Orthophthalic	38 – 42	65 – 85
Isophthalic	40 – 45	75 – 90
BPA fumarate	30 – 35	125 – 135
Chlorendic	35 - 42	140 - 150

Vinylesters represent a series of unsaturated resins prepared by the reaction of a monofunctional methacrylic or acrylic acid with an epoxy such as bisphenol diepoxide. They are superior in many cases to polyesters insofar as environmental durability is concerned since the unsaturated sites are only in the terminal positions of the chains. As with polyesters, styrene is added to vinylesters as a diluent in quantities between 20 and 60%. An increase in styrene content increases hydrophobicity and hence decreases moisture uptake. However, it also increases volumetric shrinkage and cure based microcracking potential. Further, since the cure of a vinylester essentially consists of 3 simultaneous reactions, homopolymerization of vinylester monomer, homopolymerization of styrene monomer, and copolymerization of vinylester with styrene – all of which have different rates, there is a high potential for incomplete polymerization, especially under ambient temperature conditions [7,8]. They are often considered to be as good or better than epoxies combining their excellent chemical resistance and tensile strength with low viscosity and potential for rapid cure. Volumetric shrinkage is however higher than that of comparable epoxies.

Epoxies are used extensively as matrices in structural composites and offer a broad range of physical attributes, mechanical properties and process windows. In general they give off very few (or none) byproducts during cure making them more environmentally friendly than polyesters and vinylesters. These resins constitute a very broad class of polymers in which cross-linking occurs primarily through the reaction of an epoxide group, although this may be replaced by an oxirane group or an ethoxylene group. They are available in a wide range of viscosities from low-viscosity liquids (albeit having viscosities higher than polyesters) to high-melting solids. Their processing characteristics and resulting performance depend on the selection of base resin, curatives, hardeners, and modifiers, and can vary significantly based on choice and stoichiometry. The three primary classes of hardeners are based on temperature of cure. Room temperature curing agents include aliphatic amines, polyamides and amidamines of which the aliphatic amines are the most commonly used. These can enable cure under adverse conditions and are often highly exothermic. With the exception of a few types (such as tertiary amines and cycloaliphatics) the glass transition temperature,  $T_g$ , is restricted by the cure temperature and even on elevated temperature cure or post-cure will remain at 10-20°C below the maximum processing temperature.  $BF_3$  (Lewis –Acid) complexes and imidazoles can be

used as both room and elevated temperature curing agents.  $T_g$ s of up to 200°C can be attained. Elevated cure additives include include some aromatic amines and anhydrides and generally provide superior  $T_g$ s and greater chemical resistance. Some of these, however, are susceptible to moisture degradation during cure and hence must be used under controlled conditions of humidity and temperature. It is emphasized that the intrinsic properties of epoxies are affected by both temperature of cure and schedule, and the actual curing agent used, changes in both of which can result in significant difference in properties as shown in Table 1.5. Epoxies in general have a higher degree of toughness than polyesters and significantly lower levels of shrinkage.

*Table 1.5: Effect of Curing Agent and Cure Schedule\**

Epoxy	Curing Agent	Cure Schedule	Flexural Strength (MPa)	Flexural Modulus (GPa)
DGEBA	TETA	7 days at 25°C	370	14
		2 hours at 110°C	490	21
DGEBA	BGE/TETA	7 days at 25°C	330	19
		2 hours at 110°C	530	20

\*With E-glass reinforcement at 67% weight fraction (normalized)

Phenolic resins are used in cases where superior fire resistance, high-temperature performance and resistance to hydrocarbon and chlorinated solvents is required. These are the product of the condensation reaction of phenol with an aldehyde (most commonly formaldehyde). The materials however are unstable when exposed to ultraviolet radiation and are in the main, brittle. Additives and fillers can, however, be added to improve toughness and to reduce shrinkage.

### 1.5 Fiber Reinforcement Systems

Fiber reinforcements are available in a variety of types typically classified as Natural fibers, synthetic organic fibers and synthetic inorganic fibers. Natural fibers, such as jute, flax, kenef and sisal, are extremely economical but do not have the strengths and stiffness required for most structural applications. They also absorb a large amount of water and can be difficult to process. Synthetic organic fibers have low densities and high strengths and consist of reinforcements such

as nylon, polyester, polypropylene, aramids and polyethylene. With the exception of the last two, however, they generally have low moduli. Glass, boron, carbon and silicon carbide belong to the class of synthetic inorganic fibers. These fibers have low densities, high strengths and high moduli. It is emphasized that all these, even individually, represent classes of fibers with a range of properties within each class and therefore it is as misleading to refer generically to a carbon fiber as it is to an aluminum without specifying grade. Typical properties of a number of fibers are given in Table 1.6 for purposes of comparison.

*Table 1.6: Overall Comparison of Fiber Properties*

Fiber Type	Density (g/cm <sup>3</sup> )	Tensile Modulus (GPa)	Tensile Strength (MPa)
Polyester	1.30	14	1100
E-Glass	2.54	76	3100
S-Glass	2.48	88	4400
Spectra 900	0.97	117	2590
Kevlar 149	1.47	26	3500
Standard Modulus Carbon	1.8	228	3800
Boron	2.57	400	3600
Silicon Carbide	2.55	220	3000
Grade 60 Steel	6.20	200	Yield: 415 Ultimate: 620

Glass fibers are perhaps the most common reinforcement type used in composites, accounting for, perhaps, about 90% of all fibers used. Glass is made by fusing silicates with potash, lime, or various metallic oxides. The manufacture of glass filaments, which are between typically 3-20µm in diameter, begins with the blending of silica and select minerals in a furnace where the melt is homogenized. Once refined, the melt is drawn into fibers by extrusion through platinum-rhodium bushings. The filaments are rapidly cooled to prevent crystallization. These filaments are highly abrasive and are susceptible to moisture-induced degradation hence treated with a sizing/binder soon after forming and prior to gathering into strands.

Glass fibers are differentiated based on chemical composition and have letter designations implying specific characteristics and uses [9]. A brief summary of some of the more common types is given in Table 1.7 and the chemical composition ranges for a subset are shown, purposes of identification, in Table 1.8.

*Table 1.7: Major Grades of Glass Fibers*

Type/Designation	Description
A Glass	Soda lime silicate glass. Used where strength, durability and electrical resistivity are not the main factors. Often used in filters and insulation.
AR Glass	Alkali resistant glass containing alkali zirconium silicates. Introduced for use as chopped reinforcement in concrete.
C Glass	Chemical glass composed of calcium borosilicates. Used in corrosive acid environments to provide greater chemical stability.
D Glass	Dielectric glass composed of borosilicates. Used in electrical and electronic applications where a low dielectric constant is required.
E Glass	Electrical grade glass composed of alumina-calcium borosilicates with a maximum alkali content of 2% by weight. Most commonly used grade in composites.
ECR Glass	Calcium aluminosilicate glasses with a maximum alkali content of 2% by weight. Combines strength and electrical resistivity of E-Glass with higher corrosion resistance of C Glass
R Glass	Calcium aluminosilicate glass with good strength and corrosion resistance
S/S2 Glass	Magnesium aluminosilicate glass with higher strength and modulus than E-Glass. Used in aerospace applications and in areas where higher stability in high temperature and corrosive environments is needed.
T-Glass	Thermal glass. Used for high temperature applications and has a 40% decrease in the coefficient of thermal expansion as compared to E-Glass.
Z-Glass	Zirconia glass. Similar to AR Glass

*Table 1.8: Composition Ranges (%) for Glass Fibers [10,11]*

Oxide	A-Glass	ECR-Glass	S-Glass	E-Glass	Boron Free E-Glass
SiO <sub>2</sub>	63-72	54-62	64-65	52-56	52-62
Al <sub>2</sub> O <sub>3</sub>	0-6	9-15	24-25	12-16	12-16
B <sub>2</sub> O <sub>3</sub>	0-6			0-10	0-10
CaO	6-10	17-25	0-0.1	16-25	16-25
MgO	0-4	0-4	9.5-10	0-5	0-5
ZnO		0-5			
BaO					
Li <sub>2</sub> O					
Na <sub>2</sub> O + K <sub>2</sub> O	14-16	0-1	0-0.3	0-2	0-2
TiO <sub>2</sub>	0-0.6	0-4		0-1.5	0-1.5
ZrO <sub>2</sub>					
Fe <sub>2</sub> O <sub>3</sub>	0-0.5	0-0.8	0-0.2	0-0.8	
F <sub>2</sub>	0-0.4			0-1	0-1

The Boron-free E-Glass listed in Table 1.8 is a modification of conventional E-glass that has been introduced to remove pollutants associated with boron. It should, however, be noted that

the overall concern is that related to condensation of boron, fluorine and alkali species as primary volatiles during the glass fiber forming process. Additional details regarding composition and forming processes are given in [9-14].

E- and S-Glass fibers are commonly used in structural applications. They have good strength and modulus and are easy to form. These materials are available in various forms ranging from yarn and rovings to uniaxial, multi-axial weaves and knits. These fibers are however susceptible to degradation in the presence of moisture and alkalis in the bare state (i.e. when not protected by the use of an appropriately selected resin matrix). Further they undergo creep and stress-rupture and therefore should not be used under high levels of sustained load. Typical properties for some glass fibers are given in Table 1.9.

*Table 1.9: Typical Properties of Glass Fibers [10,11,13]*

Property	A-Glass	ECR-Glass	S-Glass	E-Glass	Boron Free E-Glass
Density (g/cc)	2.44	2.66-2.68	2.46-2.49	2.52-2.56	2.62
Refractive Index	1.538	1.576	1.523-1.525	1.547-1.562	1.56-1.562
Softening Point (°C)	705	880	1056	830-860	916
Coefficient of Linear Expansion (x10-6/°C)	7-9	5.9	2.9	4.9-6	6
Dielectric Constant at 23°C & 1 Mhz			4.53-4.6	5.86-6.6	7
Tensile Strength at 23°C (MPa)	3310	3100-3800	4590-4830	3100-3800	3100-3800
Tensile Modulus at 23°C (GPa)	69	80-81	88-91	76-78	80-81
Elongation at Break (%)	4.8	4.5-4.9	5.4-5.8	4.5-4.9	4.6

The first use of carbon fibers is often ascribed to Thomas Alva Edison who carbonized cotton and bamboo for use as filaments in incandescent lamps [15]. However, practical forms for use in structural applications did not appear till the work of Bacon [16] and Bacon and Tang [17] based on the use of rayon and cellulose as precursors. The use of isotropic pitch as a precursor was initially pursued by Union Carbide [18]. Later Shindo in Japan [19] and Walt in the UK [20] both developed carbon fibers from polyacrylonitrile (PAN). Otani later developed high modulus

fibers from pitch [21,22]. Carbon fibers can be classified in three ways as depicted in Figure 1.5.

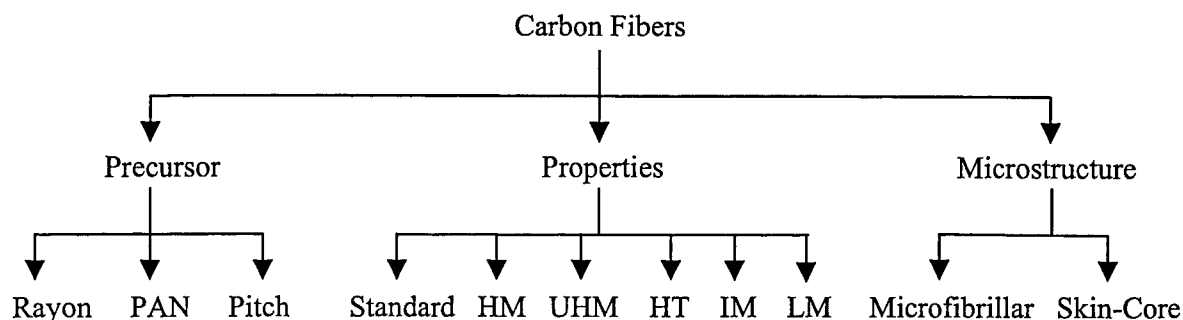


*Figure 1.5: Classification Schema for Carbon Fibers*

Precursors are materials from which carbon fibers are derived. The three general types used currently are rayon, polyacrylonitrile (PAN) and pitch. Properties of the resulting fiber, as well as the economics of the process, change based on choice of precursor. Rayon based precursors are derived from cellulose and have a low conversion efficiency. PAN precursors are the basis for a majority of commercially available carbon fibers and generally yield the highest tensile strengths. Although most fibers are circular in cross-section the use PAN as a precursor enables formation of rectangular, dog-boned and "x" type cross-sections, which can yield closer fiber packing. Pitch precursors are of low cost and are a complex mixture of aromatic hydrocarbons generally derived from petroleum, coal tar, or Polyvinylchloride. Mesophase pitch which has long highly oriented molecules yields very high modulus fibers. The use of pitch, depending on process, can yield either very low modulus or high modulus fibers and until recently had associated problems related to batch-to-batch variation.

Irrespective of precursor used the process for formation of the fibers is similar and is shown schematically in Figure 1.6. The PAN precursor is first spun into filament form and then stretched during heating at 200°C-300°C to cause orientation and cross-linking of molecules such that decomposition does not take place in subsequent steps. The stretching is essential for attainment of an oriented molecular structure for high strength and stiffness. In the case of the pitch precursor the fiber is spun and then stabilized in similar fashion. Once stabilization is



completed, carbonization at 1000°-1500°C causes precursor pyrolysis to about 95% carbon content. Restraint on shrinkage during this stage and graphitization (1500°-2800°C) results in higher orientation and attainment of high tensile modulus and enhanced tensile strength. It is essential at this stage to emphasize that although the terms carbon and graphite are often used interchangeably, there is a major point of distinction as related to chemical composition. Graphite fibers are subjected to a much higher degree of pyrolysis than carbon fibers resulting in carbon content being about 99% compared to a 95% content for conventional carbon fibers. Yield, defined as the weight of carbon fiber resulting per unit of precursor, is an important factor for economical production of carbon and examples of yield are given in Table 1.10. It is noted, however, that attainment of uniformity and standard modulus, rather than low modulus, results in a pitch yield similar to, or just slightly higher than PAN.

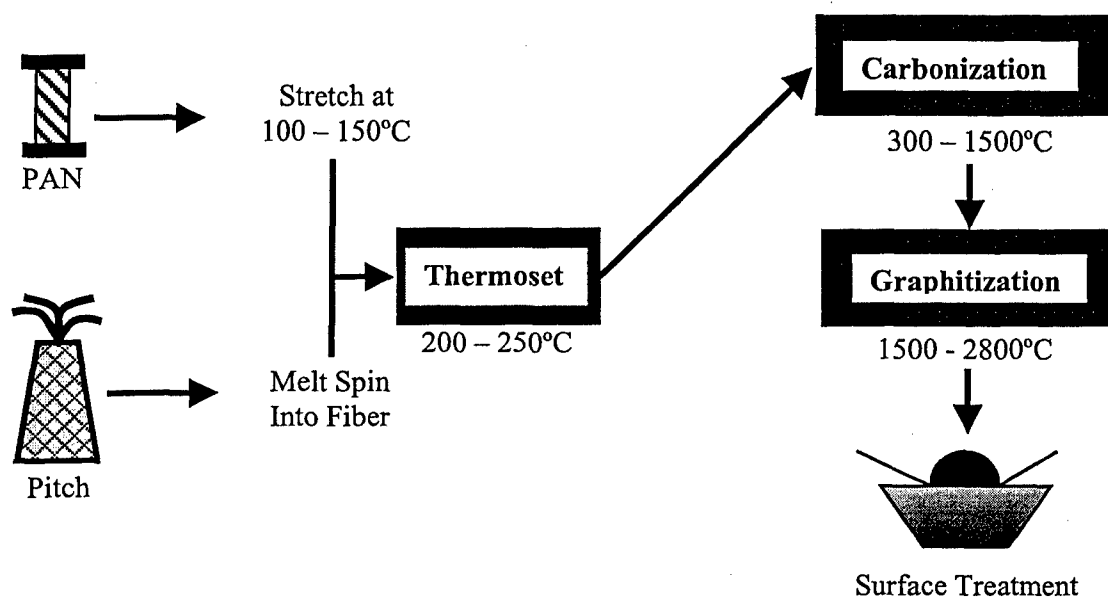


Figure 1.6: Process Flow for Carbon Fiber Production [after 23]

The PAN precursor is first spun into filament form and then stretched during heating at 200°C-300°C to cause orientation and cross-linking of molecules such that decomposition does not take place in subsequent steps. The stretching is essential for attainment of an oriented molecular structure for high strength and stiffness. In the case of the pitch precursor the fiber is spun and then stabilized in similar fashion. Once stabilization is completed, carbonization at 1000°-

1500°C causes precursor pyrolysis to about 95% carbon content. Restraint on shrinkage during this stage and graphitization (1500°-2800°C) results in higher orientation and attainment of high tensile modulus and enhanced tensile strength. It is essential at this stage to emphasize that although the terms carbon and graphite are often used interchangeably, there is a major point of distinction as related to chemical composition. Graphite fibers are subjected to a much higher degree of pyrolysis than carbon fibers resulting in carbon content being about 99% compared to a 95% content for conventional carbon fibers. Yield, defined as the weight of carbon fiber resulting per unit of precursor, is an important factor for economical production of carbon and examples of yield are given in Table 1.10. It is noted, however, that attainment of uniformity and standard modulus, rather than low modulus, results in a pitch yield similar to, or just slightly higher than PAN.

*Table 1.10: Carbon Yield From Various Precursors [24-27]*

Precursor	Carbon Fraction	Expected Yield
Rayon	0.44	0.1-0.3
Pitch	0.92-0.96	0.8-0.9
PAN	0.68	0.3-0.5
Lignin	0.68	0.45-0.55
PET	0.58	*
PE	0.85	0.09-0.4
PP	0.88	0.05-0.54

Carbon fibers are available with a large range of moduli and strength values as shown in Figure 1.7, and therefore need to be carefully specified and referred-to in order to avoid the use of erroneous data in design. Low modulus (LM) fibers are attained from pitch and generally have strengths between 350-1000 MPa and a modulus of less than 100 GPa. Intermediate modulus (IM) fibers have moduli up to 300 GPa and a strength to modulus ratio greater than 0.01. High modulus (HM) fibers have moduli higher than 300 GPa and a strength to modulus ratio of less than 0.01. Ultra-high modulus (UHM) fibers have moduli in excess of 500 GP and generally have strengths in the range of 1700-2600 MPa. These fibers can be both from pitch and PAN precursors, however, fibers at the higher range of modulus (>700 GPa) are formed exclusively from mesophase pitch. High tensile (HT) strength fibers have a strength higher than 3000 MPa and a strength to modulus ratio of between 0.015 and 0.02. Typical grades and properties of a

range of Carbon fibers are listed in Table 1.11 (with properties measured using the impregnated strand method).

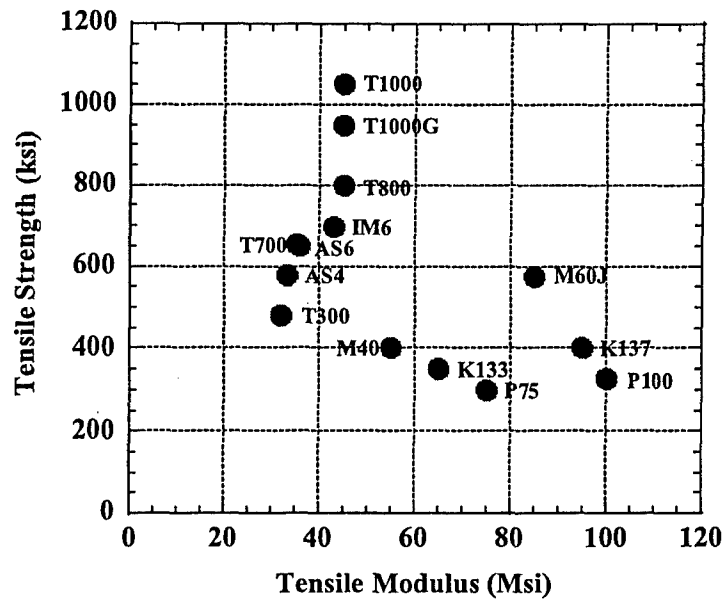


Figure 1.7: Range of Performance Levels for Carbon Fibers

Table 1.11: Typical Performance Ranges of Carbon Fibers (courtesy Toray)

Fiber Type	Density (g/cm <sup>3</sup> )	Tensile Strength <sup>1</sup> (MPa)	Tensile Modulus <sup>1</sup> (GPa)	Elongation <sup>1</sup> (%)
T300	1.76	3530	230	1.5
T300J	1.76	4210	230	1.8
T400H	1.80	4410	250	1.8
T600S	1.79	4140	230	1.8
T700S	1.80	4900	230	2.1
T700G	1.80	4900	240	2.0
T800H	1.81	5490	294	1.9
T1000G	1.80	6370	294	2.2
M35J	1.75	4700	343	1.4
M40J	1.77	4410	377	1.2
M46J	1.84	4210	436	1.0
M50J	1.88	4120	475	0.8
M55J	1.91	4020	540	0.8
M60J	1.93	3920	588	0.7
M30S	1.73	5490	294	1.9
M30G	1.73	5100	294	1.7
M40	1.81	2740	392	0.7

The properties of carbon fiber are derived from their structure, in both the axial and transverse directions. PAN based fibers generally have a micro-fibrillar structure consisting of tiny undulating ribbon like crystallites [28] which are intertwined and oriented more or less parallel to the fiber longitudinal axis (Figure 1.8). The higher the straightness of these fibrillates, the higher the properties of the fiber itself. It should, however, be noted that this results in an intrinsically anisotropic structure for the fiber with substantially different properties in the longitudinal and transverse directions (Table 1.12). Transverse textures (Figure 1.9) can range from an onion skin type microstructure, wherein the graphene planes towards the surface are aligned in layers with a randomly oriented core, to a more radial structure shown by pitch based fibers [29-31].

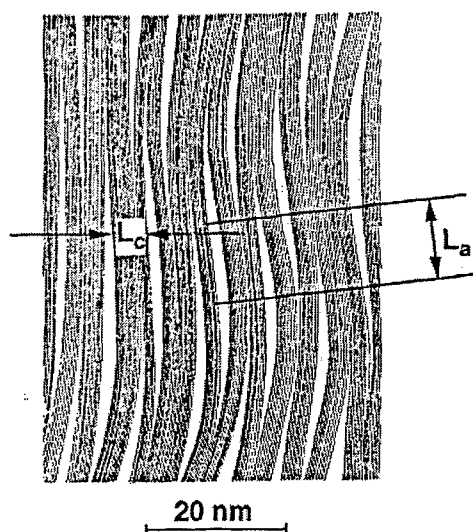


Figure 1.8: Microfibrillar Structure of Carbon  
(after 28)

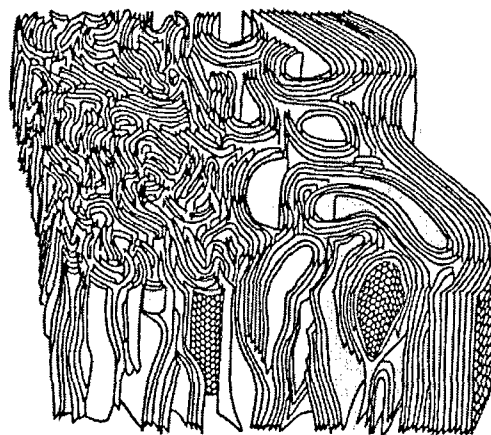


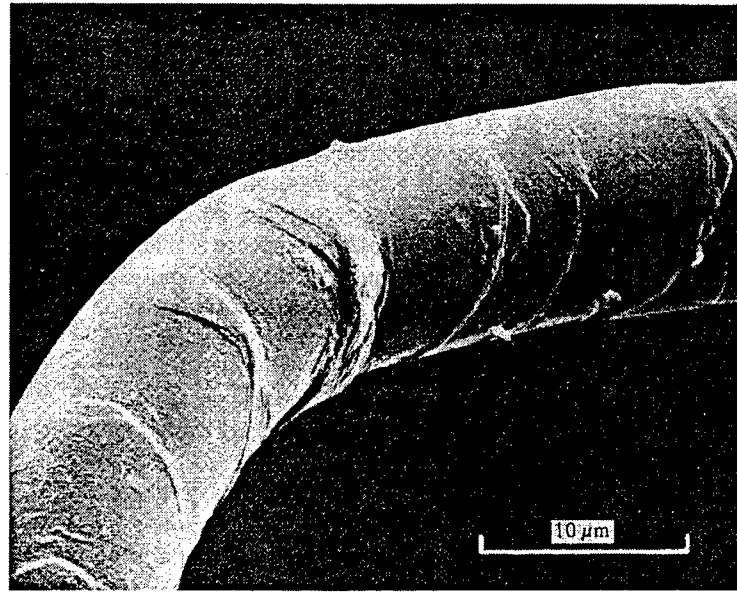
Figure 1.9: Transverse Textures in Carbon  
Fibers

Table 1.12: Comparison of Longitudinal and Transverse Properties of Carbon Fibers

Characteristics	Direction	Standard Modulus Fiber	High Modulus Fiber
Tensile Modulus	Axial Transverse	230 GPa 40 GPa	390 GPa 21 GPa
Coefficient of Thermal Expansion	Axial Transverse	$-0.7 \times 10^{-6}/^{\circ}\text{K}$ $10 \times 10^{-6}/^{\circ}\text{K}$	$-0.5 \times 10^{-6}/^{\circ}\text{K}$ $7 \times 10^{-6}/^{\circ}\text{K}$

As seen in Table 1.12 the transverse properties are substantially different than the longitudinal properties and adequate care must be taken in design because of this. For example, although carbon fibers have high strengths and moduli in the axial direction, properties transverse to this direction are extremely low and actions such as bending around sharp corners and impact will actually cause fiber rupture. Neglecting this aspect has often caused failure due to low impact resistance and brittleness, as well as lack of drapeability over sharp changes in configuration. It is also because of this that individual filaments rupture when tied in a knot or when placed across a sharp edge. Nonetheless, carbon fibers present many advantages for high performance applications. They are inert to most terrestrial environmental conditions, undergo almost imperceptible creep and stress-rupture and have very good fatigue properties. Due to their inertness, and the non-polar nature of their surfaces, carbon fibers have to be treated with active groups such as hydroxyls, carboxyls and carbonyls, through processes such as electrochemical oxidation and even etching to enable a good bond with polymer matrices. Oxidation of these fibers can be an issue at elevated temperatures, since impurities can catalyze oxidation at temperatures as low as 350°C for PAN based fibers and 450°C for pitch based fibers, when exposed for extended periods of time.

Aramid fibers are organic fibers consisting of aromatic polyamides generally manufactured by the extrusion of a polymer solution through a spinneret. These liquid crystalline polymers have an extended chain structure containing aromatic rings, which provide high levels of thermal stability, and amide (-NH-) and carbonyl (-CO-) bonds which are highly resistant to rotation and provide high strength and modulus. The microstructure of aramid fibers, due to the alignment of long, parallel polymer chains is fibrillar and gives an anisotropic nature with higher strength and modulus in the axial direction as compared to the radial (transverse) direction. Because of the fibrillar structure, the fibers are susceptible to the formation of kink-bands or microbuckling (Figure 1.10) in compression. Fiber response is linear in tension but plastic in compression with yield at levels of compressive strain as low as 0.3-0.5%.



*Figure 1.10: Kink-bank Formation in Aramid Fibers*

A number of varieties of aramid (Kevlar, Technora, Twaron) are available and although Kevlar is often mistakenly used as a generic name for aramids it must be noted that it refers specifically to a type of poly para-phenyleneterephthalimide (PPD-T) developed by the Du Pont Company [32,33]. Aramids have high tensile strength and stiffness (Table 1.13), very good impact and abrasion resistance and damage tolerance. However, they do swell in the presence of moisture with equilibrium moisture content at 60% RH being between 1.5-5% depending on fiber type with diameter increasing by 0.5% with a change in 1% moisture content [34]. The fiber is susceptible to creep but has a higher creep rupture threshold than E-glass, and shows degradation in the presence of sunlight due to ultraviolet radiation (Table 1.14)

*Table 1.13: Typical Properties of Representative Aramid Fibers*

Fiber Type	Density (g/cm <sup>3</sup> )	Tensile Modulus (GPa)	Tensile Strength (GPa)	Elongation (%)
Kevlar 29	1.44	83	3.6	4
Kevlar 49	1.44	131	3.6-4.1	2.8
Kevlar 119	1.45	99	3.3	2.5
Kevlar 129	1.47	186	3.4	2.0
Kevlar 149	1.39	77	3.1	4.0-4.2
Technora (HM-50)	1.44	55	4.4	3.0

*Table 1.14: Effect of UV Radiation on 0.5" diameter (3 strand) Kevlar Rope in the Florida Sun  
(from E.I. duPont brochures 1979, 1981)*

Time of Exposure	Breaking Load (kN)	Strength Reduction (%)
Unexposed	64.1	100
6 months	58.0	90
12 months	51.6	81
18 months	44.3	69
24 months	44.2	69

Kevlar, like carbon, is an anisotropic material and has a coefficient of thermal expansion of  $-1.1 \times 10^{-6}/^{\circ}\text{F}$  in the fiber direction and  $33 \times 10^{-6}/^{\circ}\text{F}$  in the transverse direction. This anisotropy also extends to the modulus and strength. However, due to the inherent toughness of the fiber it does not result in fracture of the filament, as with carbon, when subjected to local transverse pressure.

In addition to these fibers other fibers such as Boron, Silicon carbide, polyethylene and aluminum oxide are used for specific applications. Further details on these and other fibers can be in [6,35,36].

## 1.6 Fiber Assemblies and Fabrics

Although the basic reinforcing element of a composite is a fiber, it is almost never used in that form in the fabrication of a composite. Rather, a collection of filaments is used in a fibrous assembly or in fabric form as shown schematically in Figure 1.11. The primary 1-D structure in a fibrous assembly is a bundle of fibers described variously as rovings, tows, strand and yarns, each consisting of hundreds of filaments arranged together in a unit. It should be noted that bundle is a general term for a collection of essentially parallel filaments or fibers. Tows are untwisted bundles of continuous filaments, whereas strands are untwisted assemblies of filaments. Yarns are assemblages of twisted filaments forming a continuous length suitable for further use in textile processes such as weaving. Rovings are collections of yarns, strands or

tows in parallel with little to no twist. These units are used in a variety of textile processes such as weaving, knitting, stitching and braiding to create a variety of woven and non-woven fabric architectures (Figure 1.12) used as building blocks in the fabrication of composites [37-39].

Axis Dimension		0 NON - AXIAL	1 MONO - AXIAL	2 BIAXIAL	3 TRIAxIAL	4 ~ MULTI - AXIAL
1 D			ROVING - YARN			
2 D		CHOPPED STRAND MAT	PRE-IMPREG- NATION SHEET	PLANE WEAVE	TRIAxIAL WEAVE 1)-3)	MULTI-AXIAL WEAVE, KNIT
3 D	Linear Element		3-D BRAID	MULTI-PLY WEAVE	TRIAxIAL 3-D WEAVE	(MULTI-AXIAL 3-D WEAVE) 4)-n, 12)-14)
	Plane Element		LAMINATE TYPE	H or I BEAM	HONEY-COMB TYPE	

Figure 1.11: Classification of Reinforcing Structures

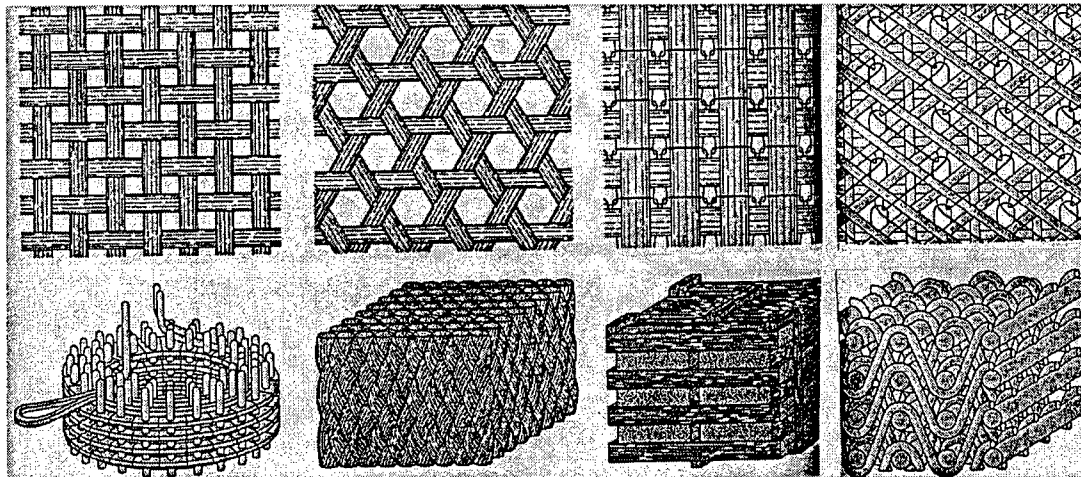
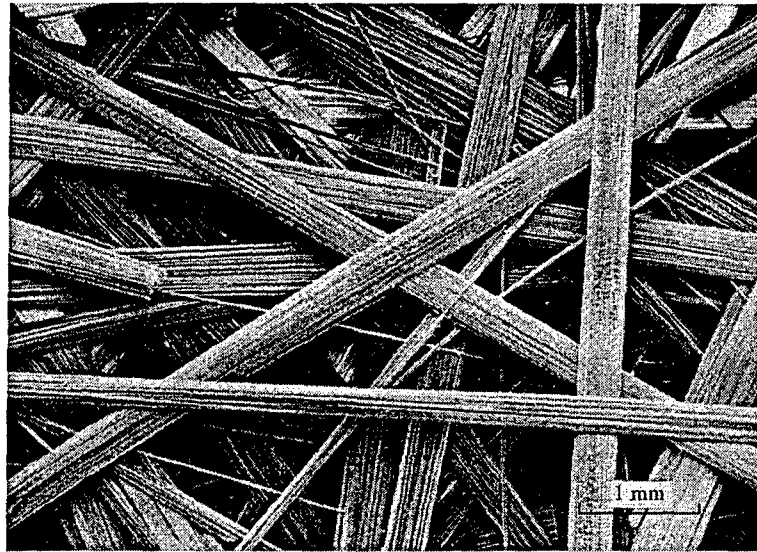


Figure 1.12: Examples of Reinforcement Architecture (after [37])

The simplest form of fibrous assembly in one consisting of a collection of chopped strands or swirled continuous strands placed in a random network and held together by a binder. The



chopped strand mat and continuous strand mat assemblies are used for secondary structural assemblies. The general structure of a chopped strand mat showing random agglomeration of bundles is shown in Figure 1.13.



*Figure 1.13: Typical Structure of Chopped Strand Mat*

The unidirectional architecture is the principal building block of a set of oriented, and non-woven fabrics. In this form roving, yarn or tow and oriented parallel to each other and held in place with the use of transversely oriented threads which either stitch the assembly together or are bonded to the assembly using a heating process. Although the “stitch-bonded” assemblies are easier to handle the points of bond serve as local points of weakness and crack initiation in the composite since in general good bond with the matrix is not achieved at these sites.

Woven fabrics are formed by interlocking two or more sets of bundles at prescribed oriented. Biaxial weaves (where the sets of bundles are perpendicular to each other as shown in Figure 1.14) and triaxial weaves (shown schematically in Figure 1.12) are the most common forms of this type. The fibrous assembly in the principal direction of the loom/weaving machine is known as the warp, whereas the one angled to the warp is known as the weft or fill. Although plain weaves, wherein bundles alternate in the weave pattern, are the most common form of assembly, other architectures of yarns perpendicular to each other, yet interwoven at specified intervals

(every 3rd, 4th or 5th bundle for example) are also used as needed for specific property ratios and for ease of conformance. These assemblies are often known as “satins.”

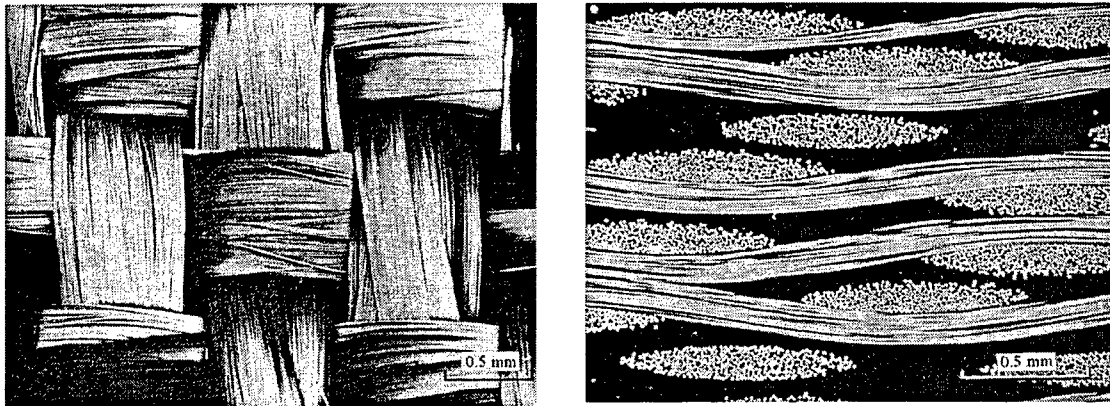


*Figure 1.14: Architecture and Microstructure of a Plane-Weave Fabric Assembly*

Although woven structures enable a high degree of conformance and are easy to handle the interwoven structure involves undulation of fibers, which results in a loss of effective modulus. An alternative to the use of this is the use of stitched, non-woven assemblies wherein layers of unidirectionals are placed at different orientations in a stack and then stitched together, as shown schematically in Figure 1.15. In a number of cases a backing of chopped strand mat is also added to increase resistance to fabric shear during handling.

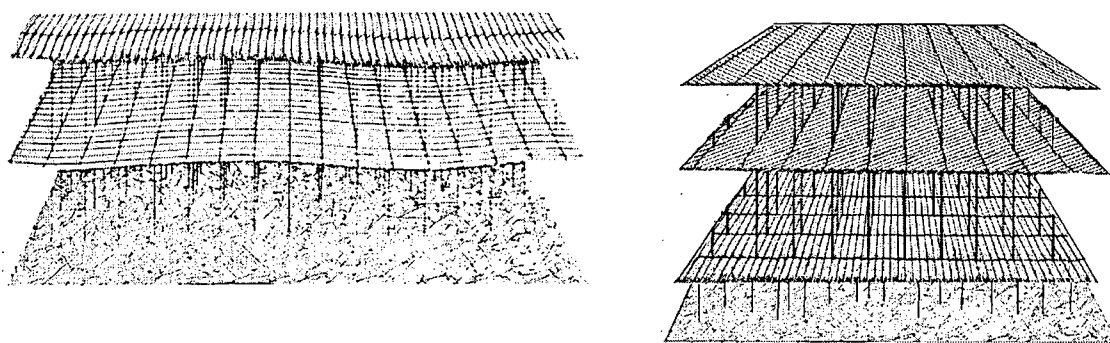


*Figure 1.15: Schematic of Non-woven Fabric Structures*

Knitted fabrics are a special form of non-woven assemblies made by mechanically interlocking yarns by the formation of loops for fibrous elements with hooked needles which draw the

element through previously formed ones as in Figure 1.16. The non-woven assemblies shown in Figure 1.15 can be also formed by knitting if the interlocking unit is a monofilament.

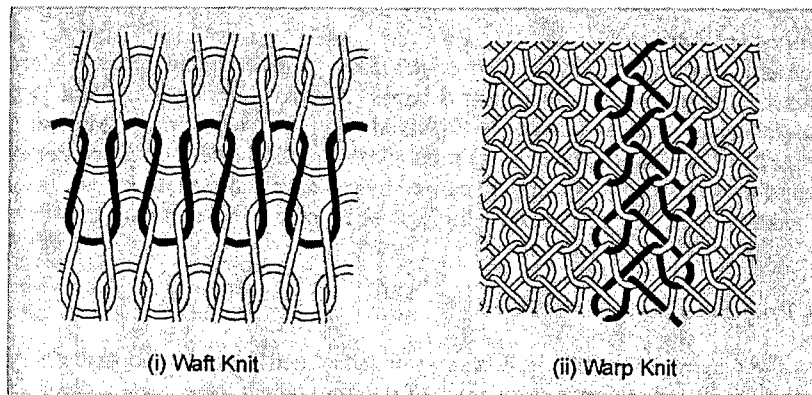


*Figure 1.16: Knitted Construction*

In most composite processes (see Chapter 2) the polymeric resin has to be introduced into the fibrous assembly as part of the manufacturing process. This necessitates that the resin be formulated and mixed in batches and can lead to substantial concerns related to uniformity of “wet-out” of the reinforcement and variation in properties due to changes in constituent volume content. In order to maintain a high level of uniformity in resin formulation, fiber wet-out, and volume content, fibrous assemblies (usually in the form of individual tows or unidirectional sheets) are preimpregnated with resin and partially cured (“B” staged) before delivery to the end-user. Layers of this *prepreg* can then be stacked to form the structure and cured under heat and pressure. Prepreg, which is available in the form of tow, tape or fabric is the basic building block for composite fabrication in the aerospace industry.

## REFERENCES

1. Ashby, M.F. (1999), **Materials Selection in Mechanical Design**, 2nd edition, Butterworth-Heinemann, Oxford.
2. Wainwright, S.A., Biggs, W.D., Currey, J.D. and Gosline, J.M. (1976), **Mechanical Design in Organisms**, Princeton University Press, Princeton, NJ.

3. Perry, T. (1942), **Modern Plywood**, Pitman Publishing Corporation, New York
4. Wood, A. ( 1963), **Plywoods of the World**, W. and A.K. Johnston, London.
5. Nguyen, H.X. and Ishida, H. (1987), "Poly (aryl-ether-ether-ketone) and its Advanced Composites; A Review" *Polymer Composites*, 8, pp. 57-.
6. Schwartz, M.M. (1997), **Composite Materials, Volume 1**, Prentice Hall, Inc. Upper Saddle River, NJ.
7. Ziaee, S. and Palmese, G.R. (1999), "Effects of Temperature on Cure Kinetics and Mechanical Properties of Vinyl-Ester Resins," *Journal of Polymer Science: B*, 37, pp. 725-744.
8. Karbhari, V.M. and Lee, R. (2002), "On the Effect of E-Glass Fiber on the Cure Behavior of Vinylester Composites," *Journal of Reinforced Plastics and Composites*, 21 [10], pp. 901-918.
9. Gupta, P.K. (1988), "Glass Fibers for Composite Materials," in *Fibre Reinforcements for Composite Materials*, Editor - A.R. Bunsell, Elsevier Publishers, pp.19-72.
10. Hartman, D.R. Greenwood, M.E. and Miller, D.M. (1994), "High Strength Glass Fiber," *Proceedings of the 39th International SAMPE Symposium and Exhibition*, pp. 521-533.
11. Wagner, T.L. (2001), "The New Wave of Boron-Free Glass Fibers," *Proceedings of Composites 2001*, 10 pp.
12. Lowenstein, K.L. (1993), **The Manufacturing Technology of Continuous Glass Fibers**, 3rd edition, Elsevier.
13. Wallenberger, F.T., Watson, J.C. and Li, H. (2001), "Glass Fibers," in *ASM Handbook*, Vol. 21: Composites, Chairs – D.B. Miracle and S.L. Donaldson, ASM International.
14. Starr, F.T. (1995), **Carbon and High Performance Fibers, Directory and Databook**, 6th edition, Chapman and Hall.
15. Edison, T.A. (1880), U.S. Patent 233, 898
16. Bacon, R. (1960), "Growth, Structure and Properties of Graphite Whiskers," *Journal of Applied Physics*, 31, pp. 283-290.
17. Bacon, R. and Tang, M.M. (1964), "Carbonization of Cellulose Fibers, I," *Carbon*, 2, pp. 211.
18. Bacon, R. and Smith W.H. (1965), *Proceedings of the 2nd Conference Ind. Carbon and Graphite*, Soc. Chem. Ind. Pp. 203.

19. Shindo, A. (1961), Report No. 317, Government Industrial Research Institute, Osaka.
20. Watt, W., Phillips, L.N. and Johnson, W. (1986), Engineer London, 221
21. Otani, S., Watanabe, S. Orion, H., Iikma, K. and Koitabashi, T. (1972), "High Modulus Carbon Fibers from Pitch Materials," *Bulletin of the Chemical Society of Japan*, Vol. 45, pp. 3710.
22. Otami, S. and Fukuoka, Y. (1969) U.S. Patent 3, 461, 082.
23. Diefendorf, R.J. (1987), "Carbon/Graphite Fibers," in Composites, Vol. 1, **Engineered Materials Handbook**, ASM International, Metals Park, Ohio.
24. Leitten, C.F., Griffith, W.L., Compere, A.L. and Shaffer, J.T. (2001), "High-Volume, Low-Cost Precursors for Carbon Fiber Production," *SAE Paper #02FCC-144*, 8pp.
25. Chemical Marketing Reporter (1996)
26. Watt, W. (1985), "Carbon fibers from Polyacrylonitrile," in Strong Fibers, Vol. 1 Handbook of Composites, Eds. – W.Watt and B.V. Perov, Elsevier Science Publishing Co., Inc., pp. 327-390.
27. Leon y Leon, C.A. (2001), "Polyethylene and Polypropylene as Low Cost Carbon Fiber (LCCF) Precursors," Proceedings of the 33rd SAMPE Technical Conference, pp. 1289-1296.
28. Perret, R. and Ruland, W. (1970), "The Microstructure of PAN-Based Carbon Fibers," *Journal of Applied Crystallography*, 3, pp. 525-
29. Le Maistre, C.W. and Diefendorf, R.J. (1973), "The Origin of Structure in Carbonized PAN Fibers," *SAMPE Quarterly*, 4, pp. 1-
30. Bennett, S.C. and Johnson, D.J. (1976), "Structural Characterization of a High Modulus Carbon Fibre by High-Resolution Electron Microscopy and Electron Diffraction," *Carbon*, 14, pp. 177
31. Diefendorf, R.J. and Tokarsky, E.W. (1971-1975), "The Relationships of Structure to Properties in Graphite Fibers, Parts I-IV," AFML TR-72-133, Air Force Materials Laboratory
32. Kwolek, S.L. Morgan, P.W., Schaefgen, J.R. and Gulrich, L.W. (1977), *Macromolecules*, 10, pp. 1390-
33. Blades, H. (1973), U.S. Patent 3, 767,756.

34. Chang, K.K. (2001), "Aramid Fibers," in ASM Handbook, Volume 21, Composites, Volume Chairs: D.B. Miracle and S.L. Donaldson, ASM International, pp. 41-45.
35. Katz, H.S. and Milesoski, J.V. (1978), **Handbook of Fillers and Reinforcements for Plastics**, Van Nostrand Reinhold Co., New York.
36. Chou, T.W. (2000), Volume Editor, **Fiber Reinforcements and General Theory of Composites**, Volume 1 of Comprehensive Composite Materials, Elsevier Science, Ltd., Oxford, UK.
37. Chou, T.W., McCullough, R.L. and Pipes, R.B. (1986), "Composites", *Scientific American*, 255 [4], pp. 192-203.
38. Chou, T.W. and Ko, F.K. (1989), eds, **Textile Structural Composites**, Elsevier Science Ltd., Oxford, UK.
39. Ko, F.K. (1994), "Three-Dimensional Fabrics for Composites," in Concise Encyclopedia of Composite Materials, Revised Edition, Editor: A. Kelly, Pergamon Press/Elsevier, pp. 297-305.

## CHAPTER 2: MANUFACTURING PROCESSES

### 2.1 Introduction

Manufacturing methods for composite structures need to be considered as important as aspects of materials design and development since the successful integration of fibrous reinforcement and matrix materials to create a composite is largely dependent on the choice of processing method used. This is especially true with thermoset resin based composites where the material is itself formed at the same time as the structure. The selection of a manufacturing process is, in general, much more critical for composites than for most conventional engineering materials. This is because each process is limited in the shapes and microstructures that can be created, as well as the material combinations that can be utilized. As with more traditional materials, manufacturing processes for composites consist of a series of steps or stages as shown in Figure 2.1. Within each step there are a number of choices, including in some cases the possibility of skipping a step. Obviously, process economics and reliability are tied to the number of steps needed within a process to move from the raw materials stage to the finished product.

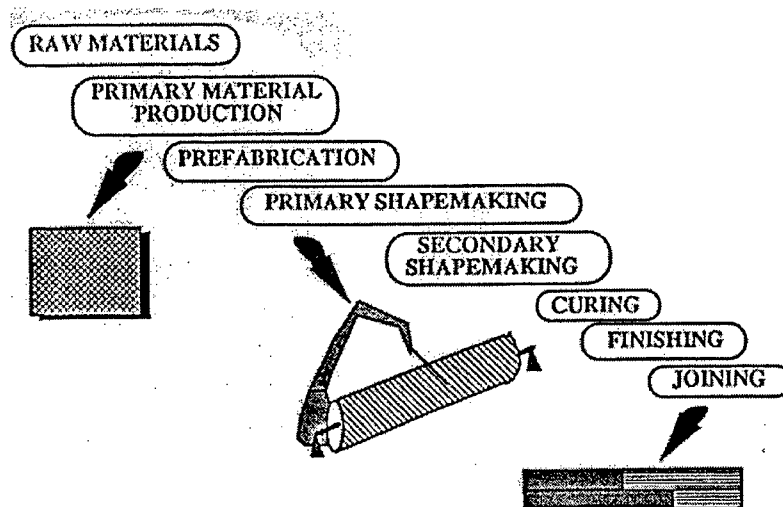


Figure 2.1: The Materials Transformation Process

The successful integration of fibrous reinforcement and matrix materials to create a composite is largely dependent on the choice of processing method used. There are a large number of processing methods available and each process has specific attributes. In general, the fabrication scheme for any composite structure can be outlined using eight generic steps:

1. Design – stress and geometric envelope
2. Materials selection
3. Arrangement (orientation and configuration) of the reinforcement
4. Assembly of the reinforcement and resin system
5. Application of heat and pressure as appropriate to cure the composite
6. Finishing processes
7. Assembly
8. Quality control and non-destructive inspection

In the ideal sense a process should be such that it has the following attributes:

1. High Productivity – i.e. short cycle times, low manpower requirements, low requirements for capital expenditures and minimum permanent use of space
2. Minimal Conversion Cost – minimum cost spent on processing stages used to combine the fiber and matrix in order to form the composite
3. Maximum Tailorability – maximum ability to tailor the performance of the composite through materials and configurational choices
4. Maximum geometrical flexibility – ability to mold parts of varying dimensions and shapes with the ability to include cores, inserts etc.
5. Minimal Finishing – near and net-shape processes are preferred since operations such as deflashing, trimming, etc. are reduced
6. Quality Control – each step in the process should be capable of being controlled on-line, without causing significant changes to the process

The tailorability of composites for specific applications is one of the biggest advantages of the material, and simultaneously one of its most perplexing challenges. The wide choice of materials combinations, processing methods and shapes possible, present bewildering problems of selection. In the isotropic world of traditional materials it was



possible to use tables, charts, and simple formulae to check the validity of a concept, thereby relegating the need for specialists to the final stage before prototyping. This is not possible in composites, where every decision made during the product development process is intricately linked to the three interacting decision areas of materials, configuration and process plan (Figure 2.2), with a decision to select one automatically resulting in a narrowing of choices for the other two [1].

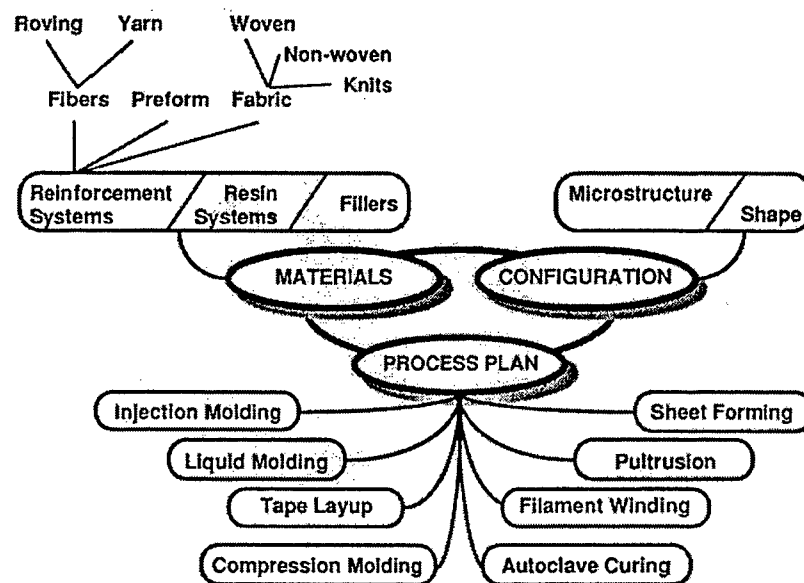


Figure 2.2: Interacting Decision Areas

Each of the elements in Figure 2.2 presents a spectrum of choices. The configuration of a composite is unique in that it includes both shape and microstructure, any one of both of which could be varied to attain a specific attribute. Unlike manufacturing methods for metals the processes related to the fabrication of composites have limitations based on shape, microstructure, and materials. Theoretically, any combination of the three aspects should be possible. Yet, the development is a complex process and requires the simultaneous consideration of parameters such as component geometry, production volume, reinforcement and matrix types and relative volumes, tooling requirements, and process and market economics.

In this chapter we briefly review aspects related to processes pertinent to fabrication of components or systems related to civil infrastructure. Thus not all methods are covered, neither is this a comprehensive review of composite processing techniques. Although only a few of these techniques are currently used for the fabrication of composite shells/wraps/jackets for the seismic retrofit of concrete columns, a number of these could potentially be used, and these are briefly discussed.

## 2.2 Classification of Methods

In general, processes can be divided into direct (i.e. those that utilize the reinforcement and resin directly without any preprocessing changes) and those that are indirect (i.e. those requiring that the reinforcing and matrix phases are first preprocessed into a form suitable for processing). The preparation of prepreg, injection molding pellets, and sheet molding compound are examples of preprocessed material forms used in indirect methods. Table 2.1 provides a list of processes belonging to each group.

*Table 2.1 Classification of Processes*

Direct Methods	Indirect Methods
Wet Layup	Compression Molding
Spray Up	Pultrusion
Pultrusion	Autoclave Molding of Prepreg
Filament Winding	Filament Winding
Liquid Molding	Injection Molding

Processes such as filament winding and pultrusion appear in both categories since they can be used with reinforcement both in the form of dry roving, tape or fabric (direct) or as prepreg (indirect). Although quality assurance is generally higher through the use of an indirect method the costs can be substantially higher with the resulting control on dimensions or other aspects sometimes being at a much higher level than routinely required in infrastructure rehabilitation.

### 2.3 Wet Layup

Wet layup is probably the oldest and most commonly used composite process. Fabric is cut to the appropriate size and is placed on a mold layer by layer, onto each of which resin is applied by pouring, brushing/rolling, or spraying. Entrapped air is removed from the fibrous assembly and resin impregnation of the reinforcement is achieved through the manual application of pressure using rollers/squeegees. The process is extremely flexible and can be used over a wide range of sizes and shapes. Since tooling is generally simple and low-cost and there is no need for specialized equipment capital costs are low. Foam cores, inserts and attachments can easily be built into the part. Often a vacuum bag is used to apply further pressure on the impregnated assembly leading to a higher level of fabric compaction with lower void content. A wide range of thermosets can be used in this process both under ambient and heated conditions with impregnation being more uniform and easier when the resin viscosity is low. Volume fractions achievable are based on the level of compaction achieved with levels just reaching 35% without the use of a vacuum bag and up to 55 % with a vacuum bag under specific conditions. Although the manual nature of the process lends it flexibility and to an extent lower cost it also results in greater variability from part to part and even within the same part.

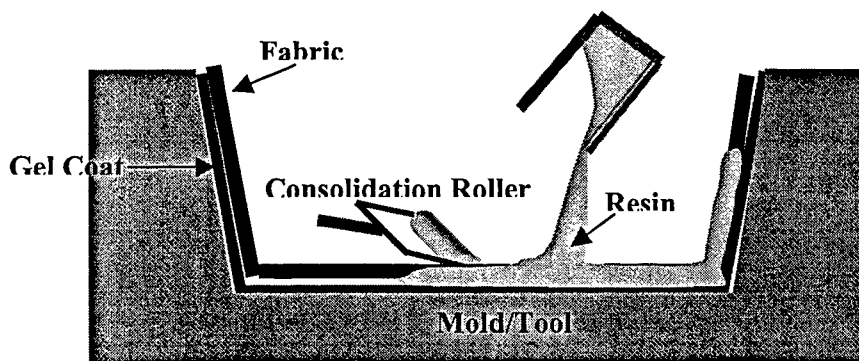


*Figure 2.3 Schematic of the Wet Layup Process*

The process is widely used to fabricate jackets/wraps directly onto the column (as is described in more detail in Chapter 4). However, the process could also be used within a factory to prefabricate jackets, which could then be adhesively bonded in the field.

## 2.4 Spray Up

The spray up process is one in which resin and chopped fibers are applied simultaneously onto the mold surface. A specially designed spray head impels catalyzed resin in a spray into which chopped fibers are introduced (Figure 2.4) in lengths of 25-75 mm. The fibers are carried by the force of the spray onto the mandred surface onto which pressure is applied through rollers, and sometimes even a vacuum bag. The process enables greater flexibility of shape than wet layup and has a very high rate of production (up to 2000 lbs. of material per hour) but limits reinforcement to random architectures only. As with the wet layup process ambient conditions are normally used although elevated temperatures can be used for cure and post-cure. In some cases, spray up is combined with the wet layup process to enable the use of fabric architectures as needed in conjunction with the lower cost and higher bulk of the random sprayed architecture. Fiber volume fractions are necessarily lower than those achieved by wet layup and there can be significant variation in content and even uniformity within the same part. Because the reinforcement is sprayed in the chopped form it is often difficult to maintain smooth and uniform surfaces and even appropriate levels of dimensional tolerance.

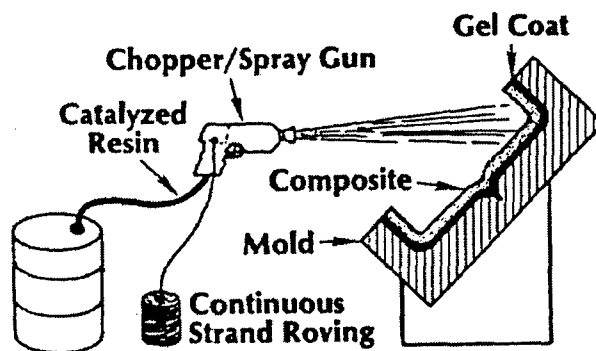


Figure 2.4: Schematic of the Spray Up Process

Due to the random nature of the reinforcement the process does not provide reinforcement in an optimal orientation (hoop). However, the process is relatively cheap, easy to use, and is analogous to shotcreting. It could hence, potentially, be used for

retrofit of columns where the demand is very small and use of other methods was not felt to be needed.

## 2.5 Injection Molding

Injection molding is an automated process with very high versatility for production of large runs of relatively complex shapes with a high degree of dimensional accuracy. Although the process is commonly used with thermoplastic resins it can also be used with thermosets. Essentially, injection molding is a high pressure process in which precompounded molding pellets, consisting of short fibers and encapsulating resin, are fed through a hopper to a screw or ram device (Figure 2.5). This mechanism conveys the charge through the barrel while subjecting it to strong shearing action that results in a viscous homogeneous mix. The mix is then injected into the mold where it is allowed to cure. Since the mold is closed complex shaped parts can be fabricated very rapidly as long as flow of the filled resin can be achieved through the mold. Due to surface effects, fibers next to the mold surface have a preferential alignment parallel to the surface, whereas the orientation away from the surface is random, giving rise to a skin-core morphology. Fiber loadings are generally fairly low and parts are usually for non-structural or secondary structural applications.

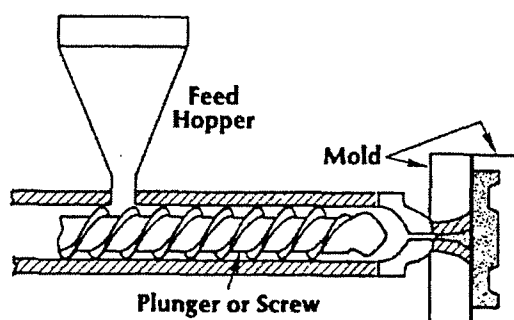
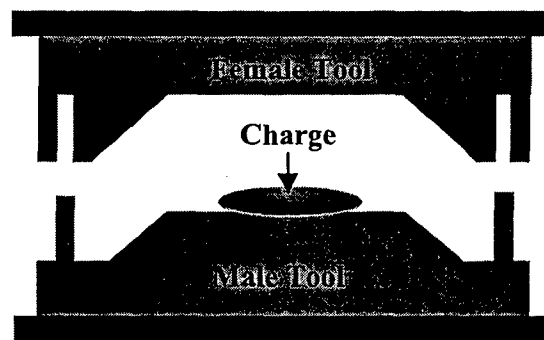


Figure 2.5: Schematic of the Injection Molding Process

Although prefabricated jackets could be made using this technique for adhesive or fusion bonding in the field the lack of reinforcement orientation and the existence of short fiber lengths makes this process generically of lower potential for seismic retrofit.

## 2.6 Compression Molding

This is a widely used process in the industrial and automotive sectors. Essentially the process consists of the application of pressure to a specially prepared “charge” (which is a preblended mixture of reinforcement, resin and filler) between two tool surfaces causing squeeze and shear-flow of the material to fill the mold cavity, which is then cured at elevated temperature within the tool. As shown in Figure 2.6 the process takes places between a pair of heated matched metal dies, mimicking steel stamping.



*Figure 2.6: Schematic of the Compression Molding Process*

The most common “blank” is the sheet-molding compound (SMC), which has polyester as the most prevalent resin. SMC is made in rolls, which are then stored in a freezer to retard the progression of cure. Figure 2.7 depicts a SMC machine showing how fiber is sandwiched between layers of a paste consisting of resin and filler. Although most compression molded parts use a random arrangement of fibers (which is an optimal form for squeeze-flow from a “charge”) SMC is also available in unidirectional, biaxial ( $\pm 45^\circ$ ), directional-discontinuous, and combined forms enabling a wide range of potential architectures. Since it is a closed mold process parts can be fairly complex with a very

high degree of dimensional tolerance. Fiber volume fraction is generally not very high and most parts are for secondary structural applications.

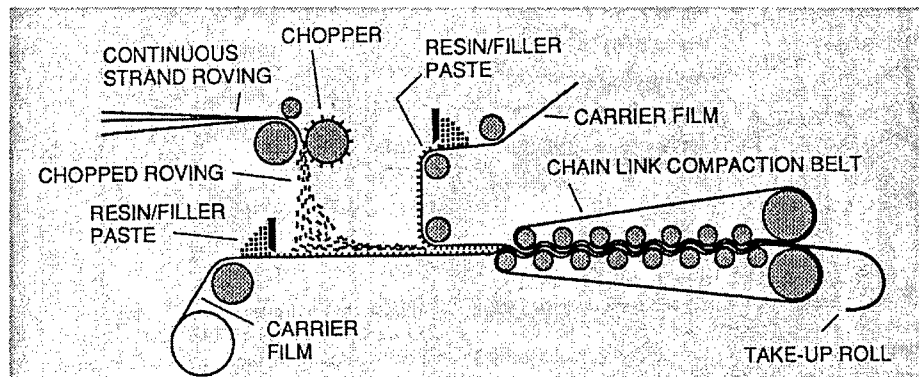


*Figure 2.7: Details for Processing of SMC*

Since SMS can be fabricated with long fibers, potentially jacket segments could be made for adhesive bonding in the field. However, due to the use of a press the shell would be made in segments requiring setup of a number of segments to completely cover the column surface once resulting in a significant shear lag effect.

## **2.7 Autoclave Molding**

This process is widely used in the aerospace industry for the production of high quality prepreg based parts. The prepregged laminae are laid onto the tool surface, on top of which a peel ply, bleeder ply and vacuum bag are placed. The entire assembly, once sealed, is placed in an autoclave (combination of an oven and pressure chamber) for cure (Figure 2.8). The use of the autoclave enables excellent control on pressure and temperature with appropriate ramps and dwells. The vacuum serves to assist in ply consolidation while continuously removing volatiles that may form during the molding operation to reduce the incidence of porosity. The combination of the vacuum and the pressure acting on the assembly serve to apply uniform pressure over the part surface resulting in a very high quality laminate with fiber volume fractions at 60-70% and a very high level of dimensional control. The process results in perhaps the highest quality

laminates with lowest void content but requires substantial capital investment in the autoclave itself.

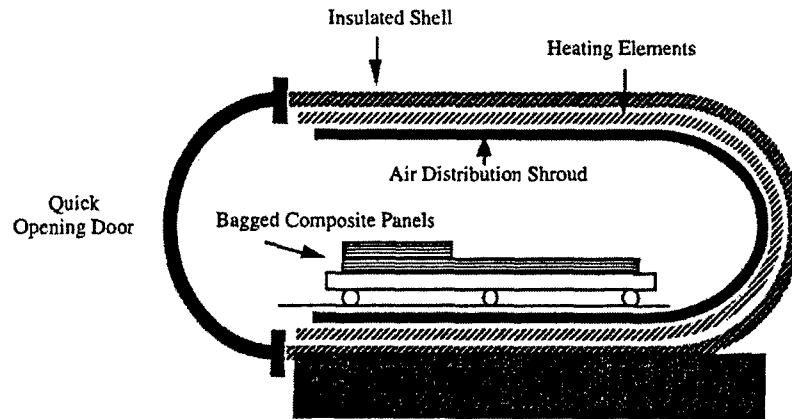


*Figure 2.8: Schematic of an Autoclave*

The process provides very high levels of uniformity, dimensional tolerance, and quality and hence could easily be used for the manufacture of prefabricated jackets to be adhesively bonded in the field. However, costs due to the need for an autoclave and for prepreg are likely to make this prohibitively expensive unless there is a requirement for the level of quality control and dimensional tolerance needed. It should be noted that the incoming materials level control afforded by prepreg can also be attained with the use of prepreg tow as elucidated in the next section and in Chapter 4.

## **2.8 Filament Winding**

The process is used for the fabrication of parts that are generally axisymmetric in nature, or which entail the placement of reinforcement around a mandrel that is rotated. In the simplest form of the process, reinforcement in tow or bundle form is fed through a wet bath wherein they are impregnated with resin and are then wound onto a rotating mandrel (Figure 2.9). Once the desired architecture and lay up thickness are achieved the part is bagged and then cured. In variations of the process, preimpregnated tow or tape is wound onto the mandrel, and the part is then cured. The process can be used with both



thermosetting and thermoplastic resins and provides excellent dimensional control and repeatability. In principle labor content is fairly low and there is a high efficiency in the materials transformation process. Fiber architecture can be changed, within limits, from one layer to the next, and even within the same layer with orientations as low as  $\pm 2^\circ$  and as high as  $\pm 88^\circ$  being possible. Although the process is best suited to axisymmetric parts, complicated contours such as those on aircraft inlet ducts can be achieved through the use of special heads and the use of multiple tows as in the use of fiber placement machines.

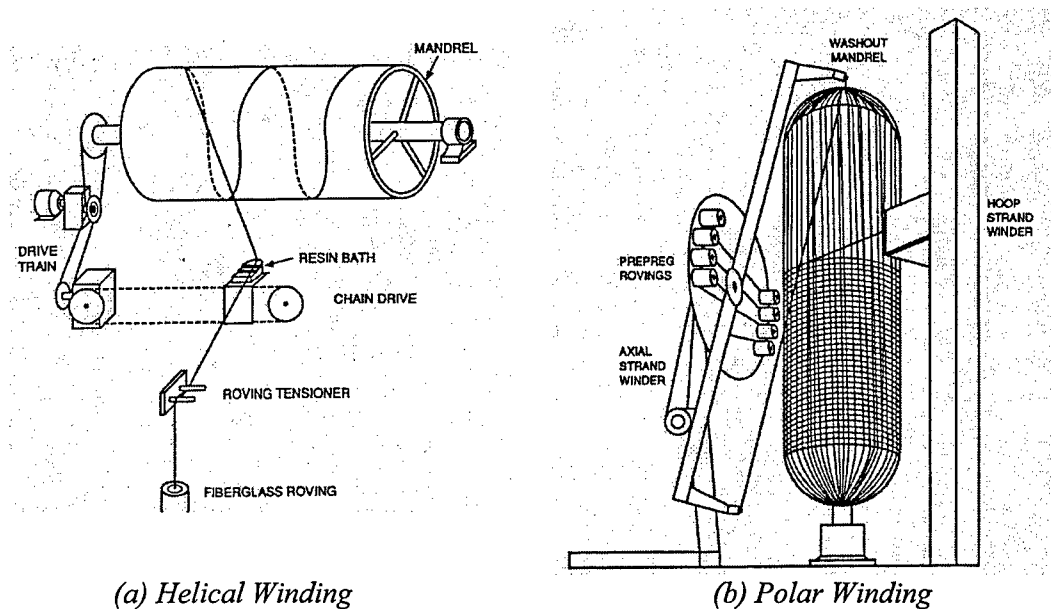


Figure 2.9: Schematic of the Filament Winding Process

This process is ideal for accurate and uniform placement of tow (either through a wet bath or in prepreg form) around a column and has already been adapted in two forms – wet winding of tow and prepreg winding, both using carbon fibers, wherein the winder itself rotates around the column on a ring like stage.

## 2.9 Pultrusion

The pultrusion process is similar to extrusion in that continuous lengths of constant cross-section can be formed although the reinforcement and resin is pulled through a die rather

than being pushed through it as in extrusion of plastics. In the generic form of the process impregnated fabric is shaped and pulled through a heated die which not only provides final shape, but also causes the composite to reach an adequate level of cure. The process is amenable to the use of dry roving and fabric which are impregnated in wet baths prior to being shaped (Figure 2.10) as well as prepreg. Final compaction is conducted within the die which also controls dimensional tolerance. Because the reinforcement has to be pulled through the die a high percentage of it has to be in the axial direction. Since the process is highly automated it provides a very high level of uniformity and can lead to the highest level of materials efficiency. The only drawback to the process is the constraint for constant cross-sections although innovative die designs have been demonstrated to allow changes, albeit at a very slow rate of pulling making the process analogous to sequential stamping. As in the case of compression molding the process uses a fairly high filler content both to reduce material cost and more importantly to control shrinkage and to reduce frictional resistance in the die.

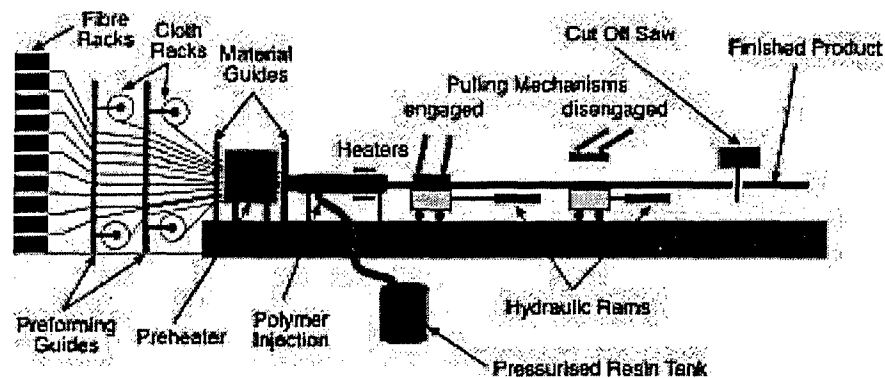


*Figure 2.10: Schematic of the Pultrusion Process*

Although the pultrusion process would appear to be ideal for the controlled prefabrication of circular cross-section shells the challenge lies in the fact that the fiber orientation required (hoop) is not in the pull direction. The perform could be fabricated using a braider and then used as a sock or wound just before entering the die. This, however, leads to a lower efficiency of material transformation since additional steps are required.

## 2.10 Liquid Molding

Liquid Molding refers to the family of processes in which a skeleton of dry reinforcement, the preform, is first placed in a tool, which is closed prior to injection of resin into the tool under pressure, after which the composite is cured under ambient or elevated temperature conditions (Figure 2.11). Resin Transfer Molding (RTM), Structural Reaction Injection Molding (SRIM) and Resin Infusion are the most commonly used subsets of this process. In resin transfer molding a two-sided tool is used resulting in fairly complex net-shape or near-net-shape parts with high fiber volume fractions and a high level of dimensional tolerance.

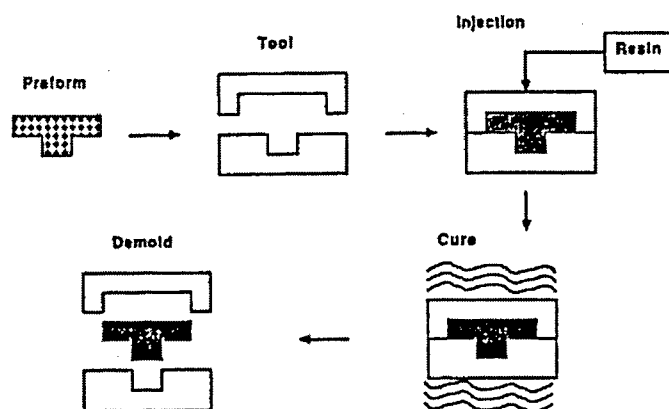


*Figure 2.11: Schematic of the Resin Transfer Molding Process*

The resin infusion version generally uses a one sided tool with a specially designed silicone or other bag on the other surface with resin being pulled into the preform by the application of vacuum (Figure 2.12). This enables fabrication of larger parts without the need for large presses for the movement of two-sided tooling. Overall since the processes separate the stages of reinforcement placement, and infusion, extreme level of architectural tailoring can be achieved at lower cost without excessive expenditure on equipment. Successful molding is highly dependent on flow necessitating a good understanding of preform permeability and flow phenomena especially under non-isothermal conditions. Void content and wet-out are highly dependent on flow. The

coupling of preform fabrication from both structural and an infusion perspectives brings with it challenges related to concurrent design for load and processing. Due to requirements of low viscosity to enable good infusion of resin into the preform the processes are almost completely restricted to thermosetting polymer systems although some recent work has shown the feasibility of using cyclic oligomers.

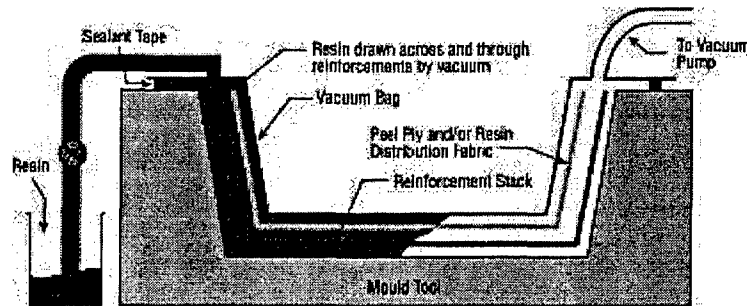


*Figure 2.13: Schematic of the Resin Infusion Process*

This set of processes can be used very efficiently for the fabrication of shells that can be adhesively bonded in the field. The use of resin infusion also provides a method by which the jacket can be directly infused onto the column. Both these versions have been used in the field and are further described in Chapter 4.

## **2.11 Process Selection**

It is emphasized that whereas it may be possible to fabricate a component using a variety of processes, the choice of the optimum process will depend on aspects such as size, shape complexity, type and level of reinforcement loading, speed required and number of parts to be fabricated, level of dimensional tolerance and part-to-part uniformity required. A variety of process discriminators are discussed in [2-4]. The reader is, however, cautioned that selection is not generic and depends largely on the specifics of the application and the capabilities of the fabricator in question. Thus, although wet layup is generally considered to be capable of far lower product quality than prepreg based

autoclave cure, the process when used by an expert crew can result in very high quality comparable parts without the capital expenditure of an autoclave.

#### REFERENCES

1. Wilkins, D.J and Karbhari, V.M. (1991), "Concurrent Engineering for Composites," International Journal of Materials and Product Technology, 6 (3), pp. 257-268.
2. Karbhari, V.M and Wilkikns, D.J. (1992), "The Use of Decision Support Systems for the Efficient Selection and Design of Composites and Their Products," International Journal of Materials and Product Technology, 7 [2], pp. 125-149.
3. Krolewski, S.M. (1989), Study of the Application of Automation to Composites Manufacture, US Army Materials Technology Laboratory, Watertown, MA, MTL-TR-89-47.
4. Gutowski, T., Henderson, R. and Shipp, C. (1991), "Manufacturing Costs for Advanced Composites Aerospace Parts," SAMPE Journal, 27 [3], pp. 37-43.

## CHAPTER 3: BASIC MECHANICS OF COMPOSITES

### 3.1 Introduction

In order to design an efficient structure, an engineer/designer must have a good understanding of the loads being applied to the structure and the materials used in the structure. The response of these materials to the loads characterize the details of the design used. With composite materials, the response can be characterized at three levels, (i) the constituent level, consisting of the fibers and the matrix, (ii) the lamina level, which consists of a single layer of unidirectional fibers, and (iii) the laminate level which characterizes response at the level of a composite plate (Figure 3.1).

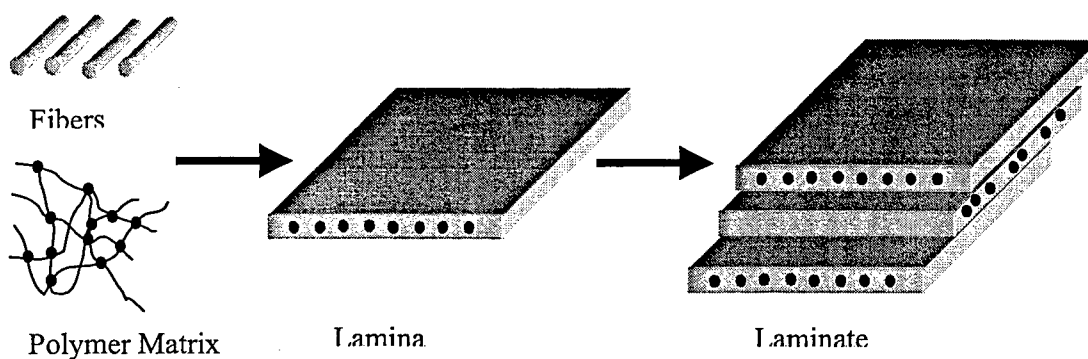


*Figure 3.1: Schematic of Levels Within a Laminated Composite*

Although this taxonomy is based on the assumed use of unidirectional prepreg, it is generally applicable, at least conceptually, to all forms of composites consisting of continuous aligned (or ordered) reinforcement. Under such a scheme it would be possible to determine the response of a composite laminate to external loadings using knowledge of constituent properties. The topic of mechanics of composites is a complex one and cannot be treated in a few pages. This chapter, therefore, presents some basic concepts that enable preliminary analysis and design. The reader is referred to [1-4] for a more in depth treatment necessary to develop an understanding of the subject.

### 3.2 Micromechanics

Although the term "Micromechanics" generally implies the study of mechanical behavior at the level of the molecular or crystal structure it also refers to the mechanics of composites at the constituent level. The study of structure-property relations is important at this level since the performance of the composite is intrinsically tied to fiber-matrix level interactions. Since fibers are used to provide reinforcement to the composite, one of the critical elements in designing/analyzing a composite is the characterization of the relative proportions of the fiber and matrix. We assume that the total volume of a composite can be expressed as the sum of the volume of the fibers,  $V_f$ , the volume of the matrix,  $V_m$ , and the volume of voids,  $V_v$ , within a composite. Generally these are expressed as volume fractions such that

$$V_f + V_m + V_v = 1 \quad \text{.....(3.1)}$$

Since it is easier to characterize components on the basis of weight rather than volume, the relative quantities of fiber and resin are often expressed in terms of weight fractions as

$$W_f + W_m = 1 \quad \text{.....(3.2)}$$

where  $W_f$  and  $W_m$  are the fiber and resin weight fractions respectively. Knowing the density of the fiber,  $\rho_f$ , and that of the matrix,  $\rho_m$ , a relationship can be determined between volume and weight fractions as

$$W_f = \frac{\frac{\rho_f}{\rho_m} V_f}{\frac{\rho_f}{\rho_m} V_f + V_m} \quad \text{.....(3.3)}$$

and,

$$W_m = \frac{1}{\frac{\rho_f}{\rho_m} (1 - V_m) + V_m} V_m \quad \text{.....(3.4)}$$

The void fraction,  $V_v$ , can be determined knowing constituent densities and mass of the fiber,  $M_f$ , and mass of the composite,  $M_c$ , in a given volume of composite  $V_{\text{comp}}$ , as

$$V_v = 1 - \frac{1}{V_{\text{comp}}} \left[ \frac{M_f}{\rho_f} + \frac{M_c - M_f}{\rho_m} \right] \quad \text{.....(3.5)}$$

It should be noted that volume fractions are conventionally used in the aerospace sector whereas weight fractions are more often used as descriptors of relative loading of fiber and matrix in the marine sector.

Since composite material are by their very nature anisotropic, we need to differentiate between properties and response attributes in the three principal directions. Conventionally the "1" direction is taken to represent the direction along the longitudinal axis of the fiber, while the "2" and "3" axes are normal to this axis (Figure 3.2).

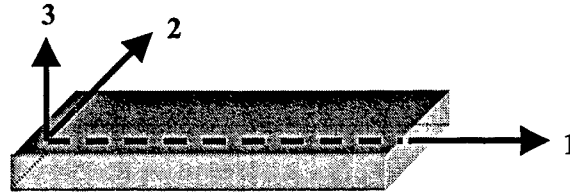


*Figure 3.2: Local Axes in a Unidirectional Lamina*

Using a strength of materials approach with assumptions of perfect bonding between fiber and matrix, deterministic and uniform properties of the constituents, regular spacing between continuous, parallel fibers and Hooke's law being followed, the longitudinal modulus of a unidirectional lamina can be determined as

$$E_1 = E_f V_f + E_m V_m \quad \text{.....(3.6)}$$

The transverse modulus can similarly be determined from

$$\frac{1}{E_2} = \frac{V_f}{E_f} + \frac{V_m}{E_m} \quad \text{.....(3.7)}$$

Keeping in mind that fibers such as carbon are anisotropic and have very different moduli in the direction of the fiber and transverse to it (for a standard modulus carbon fiber for example  $E_{f1} = 230$  GPa, whereas  $E_{f2} = 40$  GPa) the transverse modulus should actually be defined in terms of the transverse modulus of the fiber as

$$\frac{1}{E_2} = \frac{V_f}{E_{f2}} + \frac{V_m}{E_m} \quad \text{.....(3.8)}$$



Using the mechanics of materials approach the major Poissons' ratio,  $\nu_{12}$ , and the inplane Shear modulus,  $G_{12}$ , can be determined as

$$\nu_{12} = \nu_f V_f + \nu_m V_m \quad \text{.....(3.9)}$$

and,

$$\frac{1}{G_{12}} = \frac{V_f}{G_f} + \frac{V_m}{G_m} \quad \text{.....(3.10)}$$

where  $\nu_f$  and  $\nu_m$  are the Poissons ratios for the fiber and matrix, respectively, and  $G_f$  and  $G_m$  are the shear moduli for the fiber and matrix, respectively.

It should be noted that the values determined for the transverse modulus,  $E_2$ , and the in-plane shear modulus,  $G_{12}$ , using equations (3.7) or (3.8), and (3.10), respectively do not agree well with experimental results. Further, equations (3.7) and (3.8) provide incorrect answers when void fraction is considered in that both  $E_2$  and  $G_{12}$  increase with an increase in void fraction!

Semi-empirical models such as the Halpsin-Tsai [5] model have been developed to treat these inconsistencies. However, these are specific to a limited set of materials-process combinations. A modification is also presented by Hahn [6] to account for these effects and in this scheme the elastic property  $P$  is determined from

$$P = \frac{P_f + V_f + \eta P_m V_m}{V_f + \eta V_m} \quad \text{.....(3.11)}$$

where  $P_f$  and  $P_m$  are the properties at the fiber and matrix level, respectively, and  $\eta$  is a correction factor, with each being described as in Table 3.1

*Table 3.1: Constants and Factors*

Elastic Constant	$P$	$P_f$	$P_m$	$\eta$
$E_{11}$	$E_{11}$	$E_{11f}$	$E_m$	1
$\nu_{12}$	$\nu_{12}$	$\nu_{12f}$	$\nu_m$	L
$G_{12}$	$1/G_{12}$	$1/G_{12f}$	$1/G_m$	$\eta_6$
$G_{23}$	$1/G_{23}$	$1/G_{23f}$	$1/G_m$	$\eta_4$
$K_T$	$1/K_T$	$1/K_f$	$1/K_m$	$\eta_k$

wherein  $K_T$  is the plain strain bulk modulus and

$$K_f = \frac{E_f}{2(1-\nu_f)} \quad ; \quad K_m = \frac{E_m}{2(1-\nu_m)} \quad \dots\dots(3.12)$$

$$\eta_6 = \frac{1 + \frac{G_m}{G_{12f}}}{2} \quad \dots\dots(3.13)$$

$$\eta_4 = \frac{3 - 4\nu_m + \frac{G_m}{G_{23f}}}{4(1-\nu_m)} \quad \dots\dots(3.14)$$

$$\eta_K = \frac{1 + \frac{G_m}{K_f}}{2(1-\nu_m)} \quad \dots\dots(3.15)$$

$$\nu_{23} = \nu_{12f} \nu_f + \nu_m (1 - \nu_f) \left[ \frac{1 + \nu_m - \nu_{12} \left( \frac{E_m}{E_1} \right)}{1 - \nu_m^2 + \nu_m \nu_{12} \frac{E_m}{E_1}} \right] \quad \dots\dots(3.16)$$

$$E_{22} = E_{33} = \frac{4K_T G_{23}}{K_T + mG_{23}} \quad \dots\dots(3.17)$$

where

$$m = 1 + \frac{4K_T \nu_{12}^2}{E_1} \quad \dots\dots(3.18)$$

### 3.3 Lamina Level Mechanics

With reference to Figure 3.1 the basic building block for a laminated composite is assumed to be a lamina. Since laminae are stacked one on top of another to form a laminate it is necessary that coordinate systems of reference are clearly defined. Conventionally the local frame of reference is defined by a set of orthogonal axes with the "1" axis in the direction of the longitudinal fiber axis and the "2" axis transverse to it. The "global", or elemental geometric axes are denoted by x and y as in Figure 3.3.

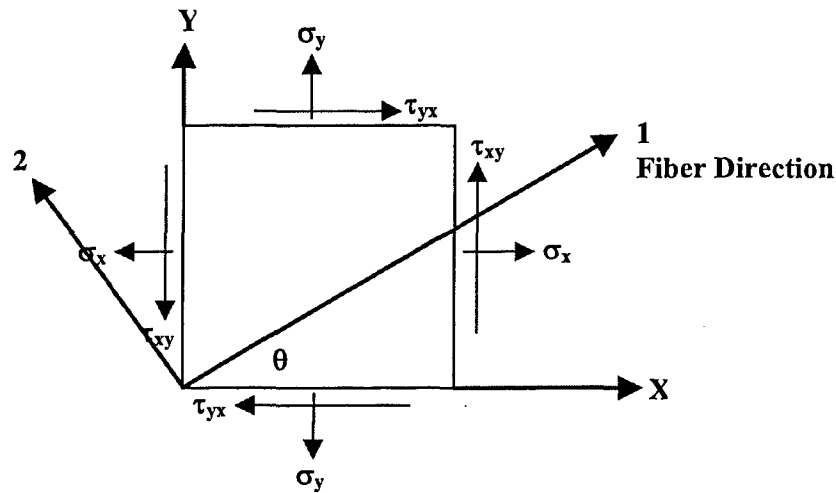


Figure 3.3: Material and Reference Coordinate Systems

Considering that a lamina is representative of a thin plate, and assuming that there are no out-of-plane loads the plate can be considered to be under a state of plane stress. Under these conditions  $\sigma_3 = \tau_{31} = \tau_{23} = 0$ , and the unidirectional lamina is considered to be an orthotropic material such that

$$\begin{Bmatrix} \sigma_1 \\ \sigma_2 \\ \tau_{12} \end{Bmatrix} = \begin{bmatrix} Q_{11} & Q_{12} & 0 \\ Q_{12} & Q_{22} & 0 \\ 0 & 0 & Q_{66} \end{bmatrix} \begin{Bmatrix} \epsilon_1 \\ \epsilon_2 \\ \gamma_{12} \end{Bmatrix} \quad \text{.....(3.19)}$$

where the  $Q_{ij}$  are the reduced stiffness coefficients and can be determined from the lamina elastic constants as

$$Q_{11} = \frac{E_1}{1 - \nu_{12} \nu_{21}} \quad \text{.....(3.20a)}$$

$$Q_{12} = \frac{\nu_{12} E_2}{1 - \nu_{12} \nu_{21}} \quad \text{.....(3.20b)}$$

$$Q_{22} = \frac{E_2}{1 - \nu_{12} \nu_{21}} \quad \text{.....(3.20c)}$$

$$Q_{66} = G_{12} \quad \text{.....(3.20d)}$$

Considering force equilibrium to relate stresses in one coordinate system to those in the other, we can write

$$\begin{Bmatrix} \sigma_1 \\ \sigma_2 \\ \tau_{12} \end{Bmatrix} = \begin{bmatrix} \cos^2 \theta & \sin^2 \theta & 2\cos\theta \sin\theta \\ \sin^2 \theta & \cos^2 \theta & -2\cos\theta \sin\theta \\ -\cos\theta \sin\theta & \cos\theta \sin\theta & \cos^2 \theta - \sin^2 \theta \end{bmatrix} \begin{Bmatrix} \sigma_x \\ \sigma_y \\ \tau_{xy} \end{Bmatrix} \quad \text{.....(3.21)}$$

or simply

$$\{\sigma_1\} = [T] \{\sigma_x\} \quad \text{.....(3.22)}$$

where [T] is the transformation matrix.

Stresses in the global axes can then be related to strains in the same axes through the transformed reduced stiffness matrix  $[\bar{Q}]$  wherein

$$\begin{Bmatrix} \sigma_x \\ \sigma_y \\ \tau_{xy} \end{Bmatrix} = [T]^{-1} [Q] [R] [T] [R]^{-1} \begin{Bmatrix} \epsilon_x \\ \epsilon_y \\ \gamma_{xy} \end{Bmatrix} \quad \text{.....(3.23)}$$

where R is the Reuter Matrix defined as

$$R = \begin{bmatrix} 1 & 0 & 0 \\ 0 & 1 & 0 \\ 0 & 0 & 2 \end{bmatrix} \quad \text{.....(3.24)}$$

so that

$$\begin{Bmatrix} \sigma_x \\ \sigma_y \\ \tau_{xy} \end{Bmatrix} = \begin{bmatrix} \bar{Q}_{11} & \bar{Q}_{12} & \bar{Q}_{16} \\ \bar{Q}_{12} & \bar{Q}_{22} & \bar{Q}_{26} \\ \bar{Q}_{16} & \bar{Q}_{26} & \bar{Q}_{66} \end{bmatrix} \begin{Bmatrix} \epsilon_x \\ \epsilon_y \\ \gamma_{xy} \end{Bmatrix} \quad \text{.....(3.25)}$$

where

$$\bar{Q}_{11} = Q_{11} c^4 + Q_{22} s^4 + 2 (Q_{12} + 2Q_{66}) s^2 c^2 \quad \text{...(3.26a)}$$

$$\bar{Q}_{12} = (Q_{11} + Q_{22} - 4Q_{66}) s^2 c^2 + Q_{12} (c^4 + s^4) \quad \text{.....(3.26b)}$$

$$\bar{Q}_{22} = Q_{11} s^4 + Q_{22} c^4 + 2 (Q_{12} + 2Q_{66}) s^2 c^2 \quad \text{.....(3.26c)}$$

$$\bar{Q}_{16} = (Q_{11} - Q_{12} - 2Q_{66}) c^3 s - (Q_{22} - Q_{12} - 2Q_{66}) s^3 c \quad \text{..... (3.26d)}$$

$$\bar{Q}_{26} = (Q_{11} - Q_{12} - 2Q_{66}) c s^3 - (Q_{22} - Q_{12} - 2Q_{66}) c^3 s \quad \text{..... (3.26e)}$$

$$\bar{Q}_{66} = (Q_{11} + Q_{22} - 2Q_{12} - 2Q_{66}) s^2 c^2 + Q_{66} (s^4 + c^4) \quad \text{.....(3.26f)}$$

where  $c = \cos \theta$  and  $s = \sin \theta$ .

Using the transformations to relate strains to stresses using the inverse relationship of (3.25) the engineering constants of a lamina can be defined as

$$\frac{1}{E_x} = \frac{c^4}{E_1} + \left( \frac{1}{G_{12}} - \frac{2\nu_{12}}{E_1} \right) s^2 c^2 + \frac{s^4}{E_2} \quad \text{.....(3.27)}$$

$$\frac{1}{E_y} = \frac{s^4}{E_1} + \left( \frac{1}{G_{12}} - \frac{2\nu_{12}}{E_1} \right) s^2 c^2 + \frac{c^4}{E_2} \quad \text{.....(3.28)}$$

$$\frac{1}{G_{xy}} = 2 \left( \frac{2}{E_1} + \frac{2}{E_2} + \frac{4\nu_{12}}{E_1} - \frac{1}{G_{12}} \right) s^2 c^2 + \frac{1}{G_{12}} (s^4 + c^4) \quad \text{.....(3.29)}$$

$$\nu_{xy} = E_x \left[ \frac{\nu_{12}}{E_1} (s^4 + c^4) - \left( \frac{1}{E_1} + \frac{1}{E_2} - \frac{1}{G_{12}} \right) s^2 c^2 \right] \quad \text{.....(3.30)}$$

These equations clearly show that the effective properties change with orientation and examples of this variation for an E-glass/epoxy laminate ( $E_f = 10.5$  msi,  $E_m = 0.4$  msi,  $\nu_f$

$= 0.2$  and  $\nu_m = 0.3$ , which at  $V_f = 0.35$ , representative of a glass/epoxy wet layup results in  $E_1 = 3.935$  msi,  $E_2 = 0.603$  msi,  $G_{12} = 0.2323$  msi, and  $\nu_{12} = 0.265$ ) is shown in Figure 3.4. As can be seen a minor change in orientation of a  $0^\circ$  lamina results in a dramatic drop in effective longitudinal modulus. It should be noted that this misorientation can result from misalignment of the fabric during placement, or even errors in cutting samples.

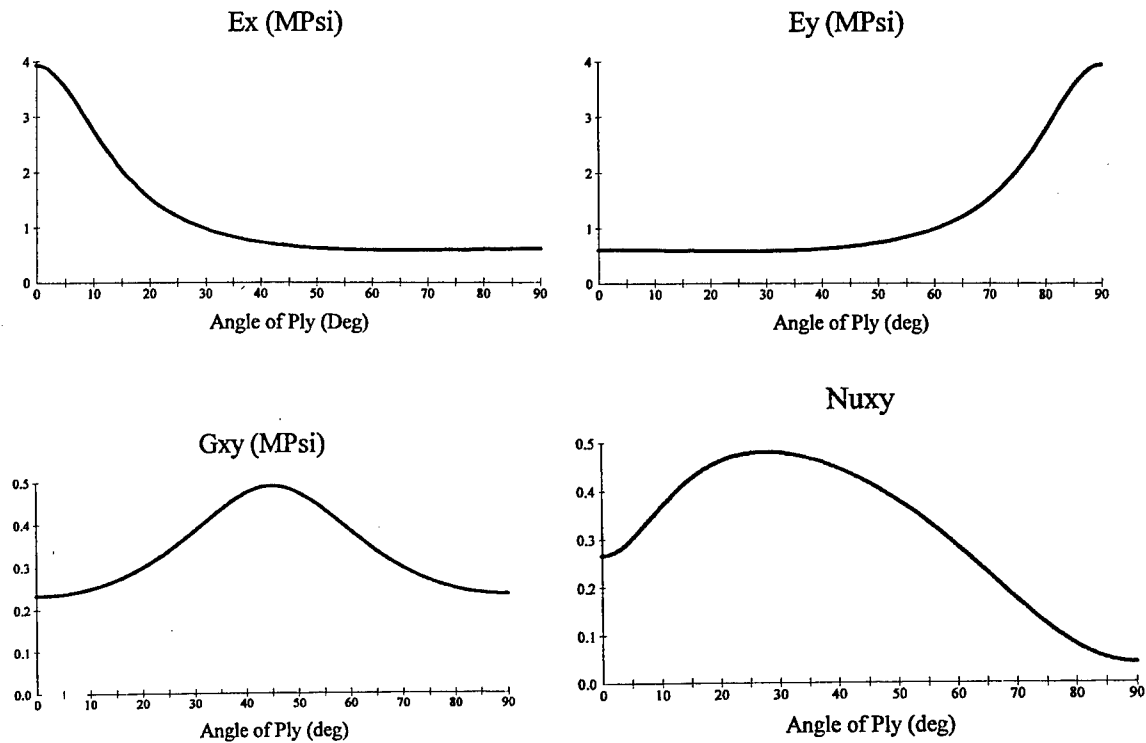


Figure 3.4: Effect of Orientation on Global Properties

For successful design of a composite system a designer needs to address both material coefficients. ( $E, \nu, G$ ) and strength. For a laminate strength is related to each individual lamina and for the use of failure theories in composites 5 different parameters need to be known, i.e.

$(\sigma^T)_{ult}$ : Ultimate longitudinal tensile strength

$(\sigma^c_1)_{ult}$ : Ultimate longitudinal compressive strength

$(\sigma_2^T)_{ult}$ : Ultimate transverse tensile strength

$(\sigma_2^c)_{ult}$ : Ultimate transverse compressive strength

$(\tau_{12})_{ult}$ : Ultimate in-plane shear strength

With these parameters failure can be assessed using a number of theories of which the most commonly used are the maximum stress failure theory, the maximum strain failure theory, the Tsai-Hill failure theory and the Tsai-Wu failure theory.

The maximum stress failure theory is similar to the one used for isotropic materials in that stresses are resolved into normal and shear stresses and failure is predicted if any of the stresses are equal to or exceed the corresponding ultimate strengths. Thus the lamina is considered to have failed if stress states violate any of the following three criteria

$$-(\sigma_1^c)_{ult} < \sigma_1 < (\sigma_1^T)_{ult} \quad \dots\dots(3.31a)$$

$$-(\sigma_2^c)_{ult} < \sigma_2 < (\sigma_2^T)_{ult} \quad \dots\dots(3.31b)$$

$$-(\tau_{12})_{ult} < \tau_{12} < (\tau_{12})_{ult} \quad \dots\dots(3.31c)$$

The maximum strain failure theory is based on St. Venants maximum normal strain theory in which strains applied to a lamina are resolved to strains in the local axes. Failure is then predicted if any of the strains are equal to or exceed the corresponding ultimate strains. This theory does consider Poisson's ratio effects and is thus considered to have more applicability than the maximum stress failure theory. As with the maximum stress failure theory, in the maximum strain failure theory, a lamina is considered to have failed if the state of loading results in a violation of any of three criteria

$$-(\epsilon_1^c)_{ult} < \epsilon_1 < (\epsilon_1^T)_{ult} \quad \dots\dots(3.32a)$$

$$-(\epsilon_2^c)_{ult} < \epsilon_2 < (\epsilon_2^T)_{ult} \quad \dots\dots(3.32b)$$

$$-(\gamma_{12})_{ult} < \gamma_{12} < (\gamma_{12})_{ult} \quad \dots\dots(3.32c)$$

Both the maximum stress failure theory and the maximum strain failure theory neglect coupling between the five possible failure modes. The Tsai-Hill theory [7] which is based on the concept of distortion energy postulates that failure occurs when the following inequality is violated

$$\left[ \frac{\sigma_1}{(\sigma_1^T)_{ult}} \right]^2 - \left[ \frac{\sigma_1 \sigma_2}{(\sigma_1^T)_{ult}^2} \right] + \left[ \frac{\sigma_2}{(\sigma_2^T)_{ult}} \right]^2 + \left[ \frac{\tau_{12}}{(\tau_{12})_{ult}} \right]^2 < 1 \quad \text{.....(3.33)}$$

Although the Tsai-Hill theory is more general it does not differentiate between the tensile and the compressive strengths of a lamina. The Tsai-Wu theory [8] addresses this but requires significantly more data as well as an experiment (or appropriate assumption) for an interaction term. In this theory a lamina is considered to have failed if there is a violation of the following inequality

$$H_1 \sigma_1 + H_2 \sigma_2 + H_6 \tau_{12} + H_{11} \sigma_1^2 + H_{22} \sigma_2^2 + H_{66} \tau_{12}^2 + 2H_{12} \sigma_1 \sigma_2 < 1 \quad \text{.....(3.34)}$$

where  $H_1 = \frac{1}{(\sigma_1^T)_{ult}} - \frac{1}{(\sigma_1^c)_{ult}}$

$$H_2 = \frac{1}{(\sigma_2^T)_{ult}} - \frac{1}{(\sigma_{21}^c)_{ult}}$$

$$H_6 = 0$$

$$H_{11} = \frac{1}{(\sigma_1^T)_{ult} (\sigma_1^c)_{ult}}$$

$$H_{22} = \frac{1}{(\sigma_2^T)_{ult} (\sigma_2^c)_{ult}}$$

$$H_{66} = \frac{1}{(\tau_{12})_{ult}^2}$$

and  $H_{12}$  is determined by experiment or through empirical values.

### 3.4 Macromechanical Analysis of a Laminate

Composites are formed by the stacking of laminae with adjacent laminae being bonded to each other through the thickness. Each layer in a laminate can be identified by its location in the laminate (with the first ply being the top), constituent materials, and its orientation with reference to an axis. The laminate stacking sequence thus provides details about layup of a laminate and some examples are given in Figure 3.5.



+45	15	45
-45	15	30
-45	30	45
+45	60	30
	30	30
	15	45
	15	30
		45

$[45/-45/-45/45]$   
 $[45/-45]_s$   
 $[\pm 45]_s$

$[15_2/30/60/30/15_2]$   
 $[15_2/30/\overline{60}]_s$

$[(45/30)_2]_s$

Figure 3.5: Examples of Laminate Stacking Sequences

Using strain-displacement relations for a plate under in-plane loads laminate strains can be determined as the combination of midplane strains and curvatures through

$$\begin{Bmatrix} \epsilon_x \\ \epsilon_y \\ \gamma_{xy} \end{Bmatrix} = \begin{Bmatrix} \epsilon_x^o \\ \epsilon_y^o \\ \gamma_{xy}^o \end{Bmatrix} + z \begin{Bmatrix} \kappa_x \\ \kappa_y \\ \kappa_{xy} \end{Bmatrix} \quad \text{.....(3.35)}$$

where  $E_x^o, E_y^o$  and  $\gamma_{xy}^o$  are the normal and shear strains, respectively, determined at the laminate midplane,  $z$  is the distance of a lamina from the midplane and  $\kappa$ 's are curvatures. Using the earlier developed reduced transformed stiffness matrix to relate global stresses to strains as

$$\begin{Bmatrix} \sigma_x \\ \sigma_y \\ \tau_{xy} \end{Bmatrix} = \begin{bmatrix} \overline{Q}_{11} & \overline{Q}_{12} & \overline{Q}_{16} \\ \overline{Q}_{12} & \overline{Q}_{22} & \overline{Q}_{26} \\ \overline{Q}_{16} & \overline{Q}_{26} & \overline{Q}_{66} \end{bmatrix} \begin{Bmatrix} \epsilon_x \\ \epsilon_y \\ \gamma_{xy} \end{Bmatrix} \quad \text{.....(3.36)}$$

in conjunction with equation (3.35) we get

$$\begin{Bmatrix} \sigma_x \\ \sigma_y \\ \tau_{xy} \end{Bmatrix} = \begin{bmatrix} \overline{Q}_{11} & \overline{Q}_{12} & \overline{Q}_{16} \\ \overline{Q}_{12} & \overline{Q}_{22} & \overline{Q}_{26} \\ \overline{Q}_{16} & \overline{Q}_{26} & \overline{Q}_{66} \end{bmatrix} \begin{Bmatrix} \epsilon_x^o \\ \epsilon_y^o \\ \gamma_{xy}^o \end{Bmatrix} + z \begin{bmatrix} \overline{Q}_{11} & \overline{Q}_{12} & \overline{Q}_{16} \\ \overline{Q}_{12} & \overline{Q}_{22} & \overline{Q}_{26} \\ \overline{Q}_{16} & \overline{Q}_{26} & \overline{Q}_{66} \end{bmatrix} \begin{Bmatrix} \kappa_x \\ \kappa_y \\ \kappa_{xy} \end{Bmatrix} \quad \text{.....(3.37)}$$

Consideration of equation (3.37) shows that although strains vary linearly through the laminate thickness stresses vary linearly only through the thickness of each lamina with changes at interfaces, since the transformed reduced stiffness matrix  $[\bar{Q}]$  changes from ply to ply based on material and orientation. Summing the effects of forces and moments over a laminates thickness a relationship can be derived between resultant forces and moments, and the corresponding strains and curvatures as

$$\begin{Bmatrix} N_x \\ N_y \\ N_{xy} \\ M_x \\ M_y \\ M_{xy} \end{Bmatrix} = \begin{bmatrix} A_{11} & A_{12} & A_{16} & B_{11} & B_{12} & B_{16} \\ A_{12} & A_{22} & A_{26} & B_{12} & B_{22} & B_{26} \\ A_{16} & A_{26} & A_{66} & B_{16} & B_{26} & B_{66} \\ B_{11} & B_{12} & B_{16} & D_{11} & D_{12} & D_{16} \\ B_{12} & B_{22} & B_{26} & D_{12} & D_{22} & D_{26} \\ B_{16} & B_{26} & B_{66} & D_{16} & D_{26} & D_{66} \end{bmatrix} \begin{Bmatrix} \epsilon_x^0 \\ \epsilon_y^0 \\ \gamma_{xy}^0 \\ \kappa_x \\ \kappa_y \\ \kappa_{xy} \end{Bmatrix} \quad \text{.....(3.38)}$$

where  $N_x$  and  $N_y$  are normal forces per unit length,  $N_{xy}$  is the shear force per unit length,  $M_x$  and  $M_y$  are bending moments per unit length,  $M_{xy}$  is the twisting moment per unit length and the  $A_{ij}$ ,  $B_{ij}$ , and  $D_{ij}$  are the extensional, coupling, and bending stiffness matrices, respectively.

Using the equations developed a laminate can be analyzed when subjected to applied forces and moments, or conversely the forces and moments corresponding to allowable strains and curvatures can be determined.

It should be noted that in general laminates can be subjected to a combination of mechanical, thermal, and moisture related loads which can be combined through use of appropriate superposition of effects. In the case of seismic retrofit of columns the thermal stresses can be due to cool down from process related exotherms and elevated cure temperatures.

## REFERENCES

- [1] Vinson, J.R. and Sierakowski, R.L. (1986), The Behavior of Structures Composed of Composite Materials, Martinus Nijhoff, Dordrecht.
- [2] Vinson, J.R. and Chou, T. (1975), Composite Materials and Their Use in Structures, John Wiley & Sons, New York.
- [3] Kaw, A.K. (1997), Mechanics of Composite Materials, CRC Press, New York.
- [4] Gibson, R.F. (1994), Principles of Composite Material Mechanics, McGraw Hill, Inc., New York.
- [5] Halpin, J.C. and Tsai, S.W. (1969), Effect of Environment Factors on Composite Materials, AFML-TR-67-423, June 1969.
- [6] Tsai, S.W. and Hahn, H.T. (1980), Introduction to Composite Materials, Technomic Publishing, Lancaster, PA.
- [7] Tsai, S.W. (1968), Strength Theories of Filamentary Structures in Fundamental Aspects of Fiber Reinforced Plastic Composites, Eds. R.T. Schwartz and H.S. Schwartz, Wiley Interscience, New York, 3
- [8] Tsai, S.W. and Wu, E.M. (1971), A General Theory of Strength for Anisotropic Materials, Journal of Composite Materials, Vol. 5, 58.

## CHAPTER 4: METHODS OF SEISMIC RETROFIT USING FIBER REINFORCED POLYMER COMPOSITE MATERIALS

### 4.1 Introduction

Recent earthquakes in urban areas such as Loma Prieta '89, Northridge '94, and Kobe '95, have repeatedly demonstrated the vulnerabilities of older reinforced concrete columns to seismic deformation demands [1-3]. Particularly vulnerable are reinforced concrete bridge piers that were designed prior to the lessons learned from the 1971 San Fernando earthquake, which showed the inadequacy of the then typically used nominal transverse reinforcement consisting of 13 mm (#4) ties or hoops spaced at 305 mm (12 in.) [4]. This reinforcement layout was utilized independent of column size, longitudinal reinforcement, or seismic demands. Furthermore, inadequate seismic detailing in the form of short laps of the column hoop reinforcement in the cover concrete and 90° L-shaped corner hooks for rectangular column ties, contribute to premature column failures as soon as cover concrete spalling occurs during the seismic event.

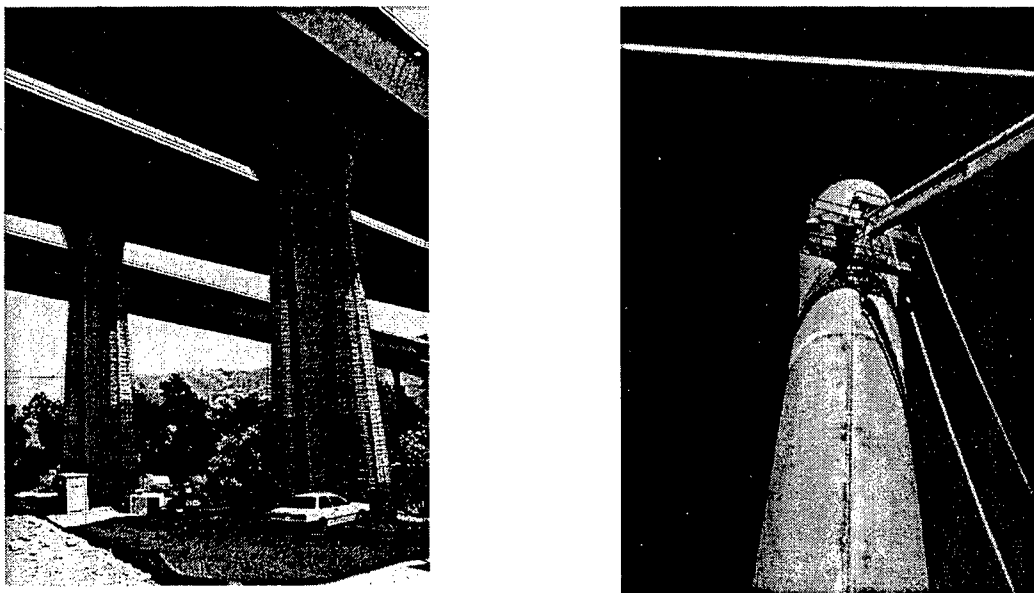


*Figure 4.1: Use of Concrete and Steel Jackets for Seismic Retrofit*

For reinforced concrete columns with these substandard reinforcement details, retrofit systems consisting of concrete or steel jackets (Figure 4.1) have been developed and experimentally validated, and thousands of steel jacket installations based on this technology have been deployed in California alone. Their structural effectiveness has also been demonstrated by observed excellent performance of steel jacketed bridge columns during the 1994 Northridge earthquake.

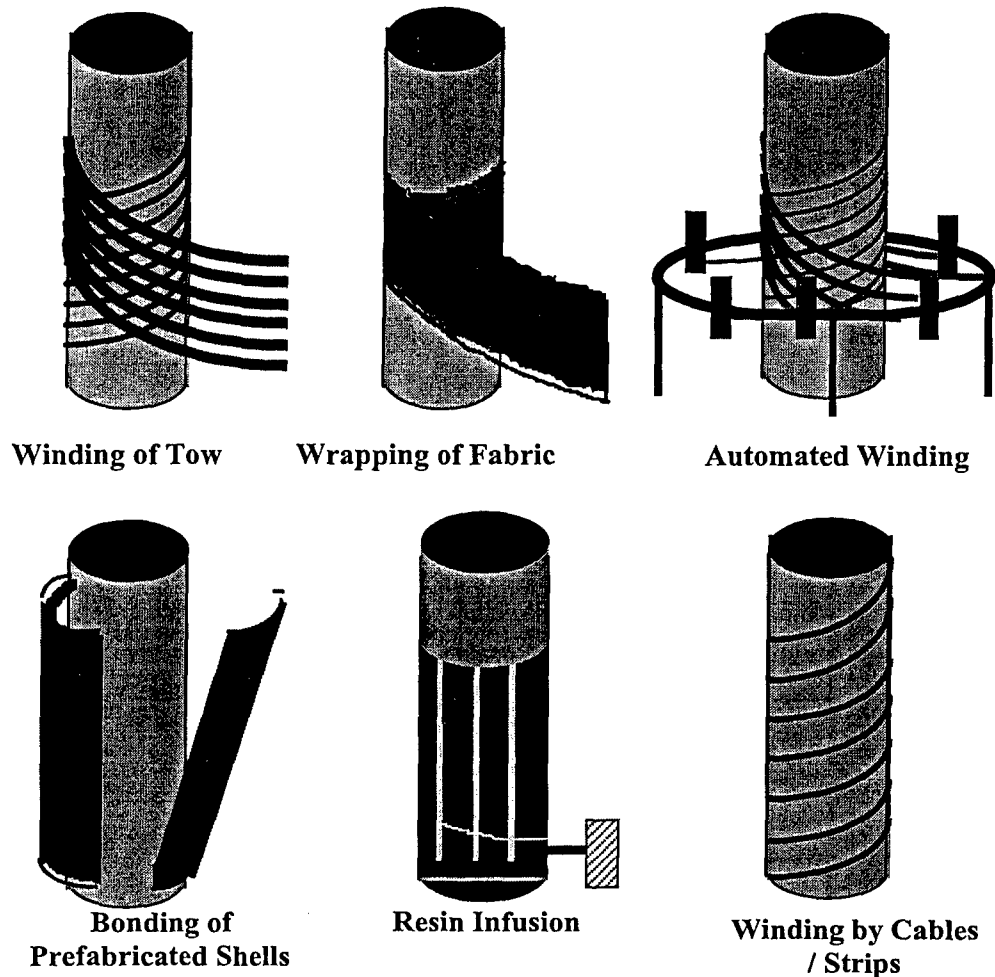


*Figure 4.2: Schematic of Methods of Application of Composite Jackets*

In order to increase speed of installation of column jackets, to reduce maintenance, and to improve durability, different types of advanced composite column jacketing systems have been investigated and developed, ranging from hand lay-up of glass or carbon fabrics to winding of tow and adhesive bonding of premanufactured layered glass or carbon shell systems. These

methods can generically be differentiated into six basic types (illustrated schematically in Figure 4.2) based on the method of processing/installation, including:

- (a) the use of the wet lay-up process using fiber tow
- (b) the use of wet lay-up processes using fabric or tape,
- (c) the use of prepreg in the form of tow, tape or fabric,
- (d) the use of prefabricated shells,
- (e) the use of resin infusion processes, and
- (f) the use of external composite cables or prefabricated strips.

These methods are briefly discussed in this chapter to provide the reader with an overview of the variations possible for the application of FRP composite jackets for purposes of seismic retrofit of columns. Wherever possible cautions, as appropriate, as related to the methods are also discussed. It should, however be noted that as with all composites the final performance of the system depends intrinsically on the choice of constituents and the details of the processing steps used. Fabrication in uncertain environments and on substrates such as concrete has its own difficulties, which need to be considered [5].

#### **4.2 Wet Layup Processes Using Fiber Tow**

In this set of processes fiber in tow form is taken through a resin bath to enable fiber wetout with resin and is then wound around the column. This method was initially developed in Japan during the 80's for the retrofit of chimneys and smoke stacks (Figure 4.3). The winding is done through mechanical means and can result in fairly uniform jackets as long as the tension and lay down rates are controlled. This was the first method attempted for the retrofit of columns using carbon tows and has been used successfully in Japan [6-8]. In variations of the method a layer of unidirectional fabric is first placed on the concrete substrate with fibers in the axial direction, prior to winding of carbon tow in the hoop direction.

Since impregnation is through a wet bath there are likely to be concerns related to uniformity of wet out and as related to resin distribution, dripping and spray (depending on speed of winding). Cure is generally conducted under ambient conditions and hence can be affected by local

environmental conditions. The use of this method generically requires the use of a winder that moves circumferentially around the column while also traversing upwards. This requires specialized, albeit not very complicated or expensive, equipment that also needs space for setup and operation and hence may not be efficient in applications where space is restricted.

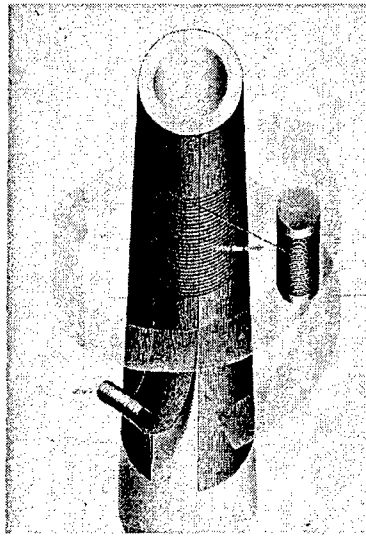


*Figure 4.3: Wet winding of Tow for the Retrofit of a Smoke Stack*

#### **4.3 Wet Layup Processes Using Fabric**

The process essentially is a modification of the previously described process with the replacement of the individual tow by fabric. The fabric is impregnated with resin and is applied to the requisite thickness onto the column itself. Although fabric wet-out can be either done manually through the use of rollers and squeegees or through the use of an impregnator, the actual application process is manual with the use of ambient cure. Although it is possible to heat the system after application to achieve higher cure temperatures and hence higher  $T_g$  (glass transition temperature) this is rarely done in the field. Four general subclasses can be identified within this general process type:

(a) *Wet Layup through manual impregnation away from the column*

In this process the fabric is first impregnated using manual means and is then carried (either folded or in a roll) to the actual column and then applied to the concrete substrate, duly prepared with primer. Additional resin is applied as needed to the fabric to ensure wet-out and adequacy of the resin, with application being through a roller, bush or squeegee.

(b) *Wet Layup through mechanical impregnation away from the column*

In this process the fabric is impregnated through use of a mechanical impregnator (Figure 4.4a), carried (either folded or in a roll) to the actual column and then applied to the concrete substrate, duly prepared with primer (Figure 4.4b). Additional resin is applied as needed to the fabric to ensure wet-out and adequacy of the resin, with application being through a roller, bush or squeegee. A putty or paste is generally applied to fill gaps between lifts of fabric in the joint area (Figure 4.4c) and the entire assembly, once completed is coated with a protective surface (Figure 4.4d). Since initial impregnation is through the use of an impregnator considerably greater wet-out and uniformity can be assumed, as well as a higher level of resulting material quality.



*Figure 4.4(a): Use of Impregnator*



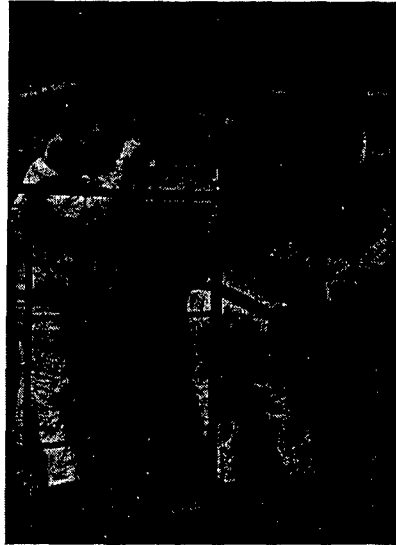


*Figure 4.4(b): Application of Fabric to Column*



*Figure 4.4(c): Application of Putty Between Lifts*

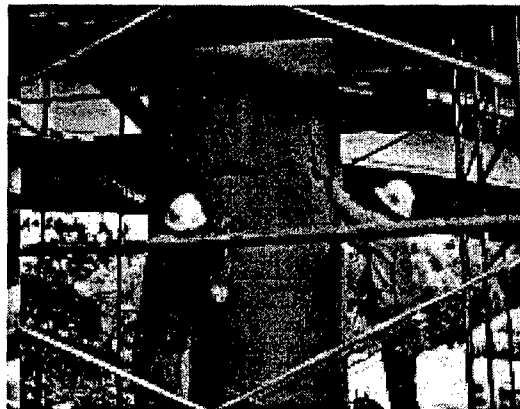


*Figure 4.4(d): Coating of Retrofitted Column*

(c) *Wet Layup through manual means on the concrete substrate itself*

In this process the fabric, usually with paper backing is applied onto the concrete substrate on which resin has already been applied. The fabric/paper system is then pressured against the surface to enable resin to move into the tows and cause the fabric to "stick" to the surface (Figure 4.5). After removal of the paper backing additional resin is applied to the tow through roller application and then the next layer of material is applied and the process repeated. Since the actual impregnation is conducted on the column there is less potential for contamination and shearing of the fabric itself. However the process is generically slower.

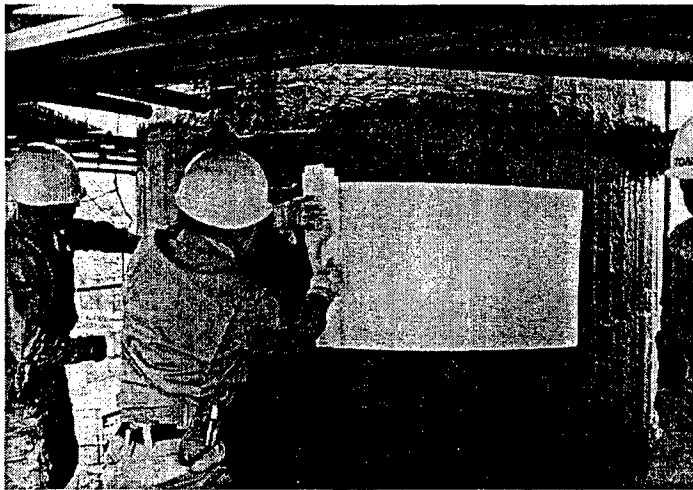


*Figure 4.5: Application of Paper Backed Fibrous System to Resin Rich Surface*

(d) *Wet Layup through use of higher viscosity paste*

In this process the resin system, generically an epoxy, is formulated to have a paste like consistency. Rather than achieving wet out through impregnation, the fabric is pushed into the paste. This results in a rapid and easy method of placement but essentially results in only coating the tow surface rather than actually effecting a uniform wet out of individual fibers. The system can be loosely considered to have partially dry fabric enclosed between layers of paste. It should be noted that the lack of wet out results in a lowering of effective properties especially as related to stress transfer and load sharing, shear, and even damage tolerance.

The wet layup process affords considerable flexibility of use especially in restricted spaces, but there are concerns related to the quality control of the resin mix, attainment of good wet-out of

fibers with uniform resin impregnation without entrapment of excessive voids, good compaction of fibers without excessive wrinkling of the predominantly hoop directed fibers, control of cure kinetics and achievement of full cure, and aspects related to environmental durability during and after cure. It does, however, represent the highest level of flexibility of installation in the field and has been used widely with good overall results [9-11]. A variety of fabric widths have been used ranging from large widths such as depicted in Figure 4.4(b) to strips [12,13] with the choice based on availability, specifications of the project, and considerations of ease of placement on the configuration of the column.

In some cases attempts have been made to pre-stress the glass fibers in order to increase the effectiveness of confinement [14] at an earlier stage of response through placement of a rubber bladders between the column and the jacket during its fabrication. After placement of the jacket the bladders are pressurized to about 100 psi with a grout slurry to activate earlier confinement. Although this is structurally viable as a means of enhancing effectiveness it can result in potential stress-rupture of the fibers resulting in premature failure [15]. This technique is hence to be discouraged.

#### **4.4 Use of Prepreg**

The use of prepreg material generically uses an elevated cure, with the winding process for tow (Figure 4.6a) and tape being automated, and the fabric process being manual in terms of lay-down. Both these variants use an elevated cure and hence concerns related to  $T_g$  and durability are assuaged, to an extent, as long as appropriate fabrication techniques are followed and anhydride-based systems are not used (due to the moisture sensitivity of these systems during cure) [16]. The use of a prepreg based system potentially provides a higher level of quality control over the incoming material, albeit at added cost, but also necessitates the adherence to a good cure schedule without which all advantages gained through material form are likely to be lost. Elevated temperature can be attained through the use of heat blankets or reflective heating applied within a clam shell placed around the column (Figure 4.6b). This method has been extensively characterized through laboratory testing [17].

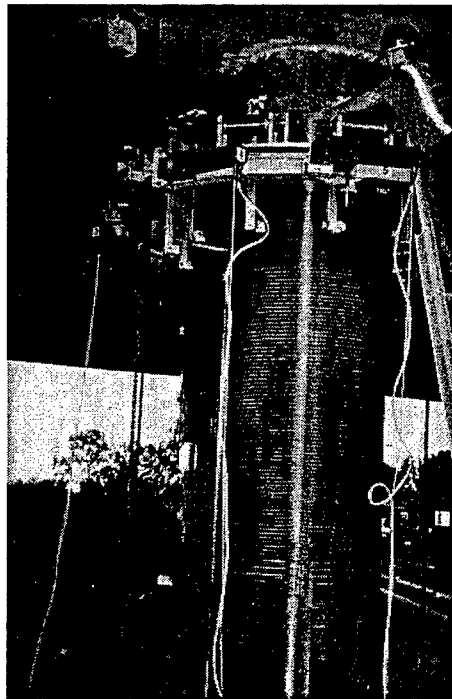


*Figure 4.6(a): Automated Winding of Prepreg Tow*

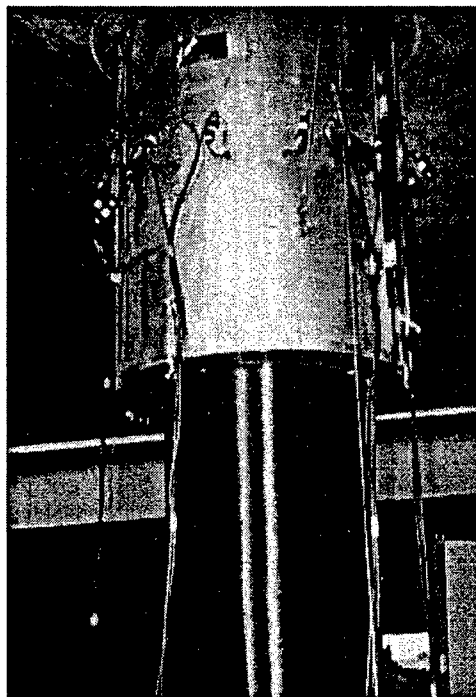


*Figure 4.6(b): Application of Heat Through a Shell to Cure The Prepreg Tow Based Jacket*

The necessity of curing under elevated temperatures (usually in the range of 175-300°F) can cause problems if the substrate concrete is very moist resulting in water vapor driven blistering in the curing composite jacket.

In the case of prepreg fabric, the concrete substrate is first coated with an appropriate elevated temperature cure resin and the prepreg is then applied onto the resin which holds it in place. Plates for application of heat and pressure are then clamped on to allow cure at elevated temperature. Although the method guarantees quality control of incoming material including strict requirements of resin content the method of heat application onto concrete which essentially is a heat sink can cause problems associated with blistering, and nonuniform cure through the thickness, including effects of overheating.

#### **4.5 Use of Prefabricated Shells**

In the case of prefabricated shells, the sections are fabricated in a factory and are adhesively bonded in the field so as to form the jacket. This method is thus somewhat analogous to the fabrication of steel shells which are field welded and thus provides a level of familiarity to some engineers. Further the use of prefabricated components ensures that the material can be processed under controlled conditions and to high standards of quality under controlled conditions.

The fabrication of the shells can be done using either two sections or a single section, which is stretched apart, so as to encapsulate the column. In both cases multiple layers are used to attain the requisite thickness with joints being staggered in order to reduce the effect of non-continuity. Figure 4.7 shows the installation scheme associated with the use of shells fabricated to the full size of the column and installed by spreading each shell apart at the single slit. It is noted that in this method sections are placed in horizontal alignment with gaps between vertical lifts. These gaps are filled with putty or with the excess adhesive that is squeezed out from between layers during compaction.

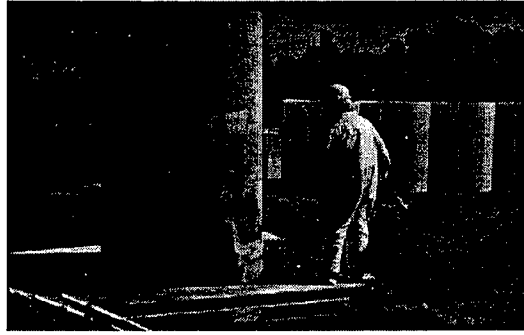


*Figure 4.7(a): Application of Adhesive to Column*

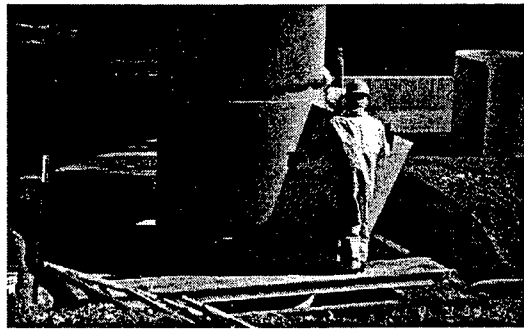


*Figure 4.7(b): Placement of Shell Around Column*

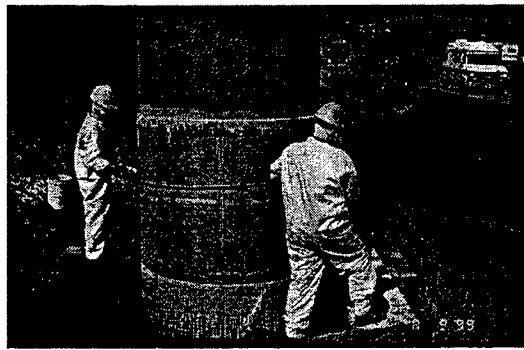


*Figure 4.7(c): Placement of Straps Over Assembly*

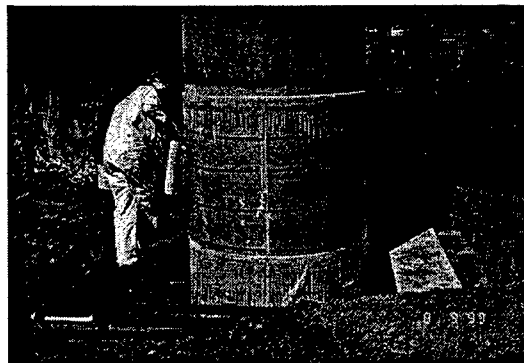


*Figure 4.7 (d): Overwrap by Plastic Sheeting*

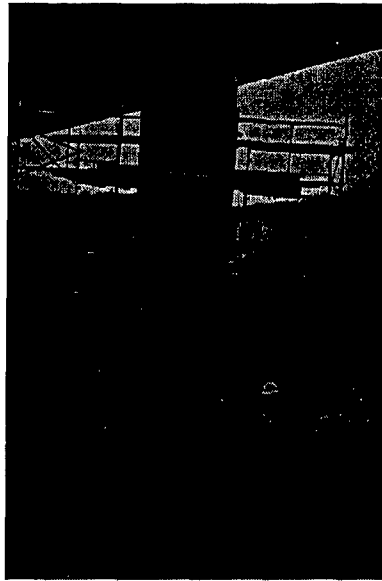


*Figure 4.7(e): Completed Column With Lifts of Individual Shell Segments*

A variation of this process entails the use of sections that are slightly less than half the circumference. Hence each layer has two joint regions (or regions of non-continuity). This affords certain flexibility in fitting the prefabricated sections onto columns having a certain level of irregularity and provides ease of fabrication. The process of application, with this one change is exactly the same as before. It should, however, be noted that the shear lag concern is greater in this case. An example of retrofit using this scheme and showing different layers is given in Figure 4.8, which also shows a sectional view showing alternate layers of prefabricated composite and adhesive.



*Figure 4.8: Retrofit Using the Segmental Adhesive Jacket Process*

This set of processes affords a high level of materials quality control due to controlled factory-based fabrication of the shells. However, the efficiency and durability of the system rests on the ability of the adhesive to transfer load, and hence is dependent on the integrity of the bond which is constructed in the field and on the durability of the adhesive in a harsh and widely varying environment which could include excessive moisture (or immersion in water, in the case of a flood plain) and large temperature gradients. Typically the adhesives used to date in such applications are cured under ambient conditions and are either polyurethanes or epoxies. It should be noted that polyurethanes generically contain moisture sensitive components and may undergo reversion in the presence of heat and/or moisture. Although they have good properties at low temperatures they typically show significant reductions in shear performance at elevated temperatures. Epoxies in comparison have a higher range and show less creep and shrinkage, although they have a lower overall peel strength. Unfortunately, to date, very little attention has been paid to the temperature and moisture related deleterious effects on bond performance. The structural performance of such jacketed systems is seen to be good [18, 19]

#### **4.6 Fabrication of a Jacket Using Resin Infusion**

In the case of resin infusion, the dry fabric is applied manually and resin is then infused using vacuum with cure being under ambient conditions. This method allows for placement over irregular geometries without having recourse to significant patching. Further, cracks in the substrate can also be filled through the infusion resin itself since the entire assembly is under vacuum pressure. Although attractive, there are concerns related to holding vacuum, nonuniform wet-out and/or compaction, and even the excessive drainage of resin into the column itself through large cracks.



#### **4.7 Retrofit Through External Composite Cables Or Prefabricated Strips**

The last method, involving the use of cables or prefabricated strips, has not been investigated to a large extent as yet. In this method confinement is achieved through additional external placement of reinforcement over the height of the column in the form of composite cables or prefabricated strips. The former case mimics the conventional use of steel cables for external helical confinement. The primary concern here is of integrity of the end anchorages and the cost of the composite system, which in general is multiple times that of a steel cable used in the same manner. In the latter case, prefabricated strips of unidirectional material and bonded into grooves cut into the surface of the column in helical fashion. This allows for the retrofit to be flush with the original surface but necessitates both careful cutting of grooves into the concrete (generally to a depth of 2-3 mm) and requires a reliable method of anchorage at the ends, without which the prefabricated element is likely to unravel.

#### **4.8 Summary**

Irrespective of the method used, it is important to note that aspects related to material forms (tow, dry fabric, impregnated fabric, etc.), processing (lay-up, cure, etc.), and location of fabrication (field versus prefabricated) will have an effect on the final performance and longevity of the material system in use. Further it is important to keep in mind that the effective properties of the jacketing system depend not just on the amount of material used but rather on the degree of confinement attained and the overall level of durability that can be potentially assured through the selection of materials-process combinations. Thus whereas the prefabricated jackets definitely provide a very high degree of materials assurance as related to the shells themselves the use of adhesive and the associated shear-lag phenomenon decreases its overall efficiency. Similarly while the use of continuous prepreg tow wound around the column in automated fashion provides the most efficient use of material the aspects related to specialized equipment and cure schedule could result in the process being very expensive.

## References

1. Yashinsky, M. (1998), The Loma Prieta, California, Earthquake of October 17, 1989 – Highway Systems, US Geological Survey Professional Paper 1552-B, US Govt Printing Office, Washington
2. Priestly, M. J. N., Seible, F. and Uang, C.M. (1994), "The Northridge Earthquake of January 17, 1994: Damage Analysis of Selected Freeway Bridges," Department of Applied Mechanics and Engineering Sciences, University of California, San Diego, Report No. SSRP-94/06.
3. Seible, F., Priestley, M.J.N. and MacRae, G. (1995), "The Kobe Earthquake of January 17, 1995," Department of Applied Mechanics and Engineering Sciences, University of California, San Diego, Report No. SSRP 95-03.
4. Priestley, M.J.N., Seible, F. and Calvi, G.M. (1996), **Seismic Design and Retrofit of Bridges**, John Wiley & Sons, Inc., New York.
5. V.M. Karbhari, "Issues in Joining of Composites to Concrete - Rehabilitation and Retrofit," invited lecture, Proceedings of Composites '96, Manufacturing and Tooling Conference, Anaheim, CA, January 22-24, 1996, pp. 345-363. (invited paper)
6. Katsumata, H. and Kobatake, Y. (1997) "Retrofit of Existing Reinforced Concrete Columns Using Carbon Fibers," Proceedings of the 3rd International Symposium on Non-Metallic (FRP) Reinforcement for Concrete Structures, Vol 1., pp. 555-562.
7. Katsumata, H., Kobatake, Y. and Takeda, T. (1988), "A Study on Strengthening With Carbon Fiber for Earthquake-Resistant Capacity of Existing Reinforced Concrete Columns," Proceedings of the 9th World Conference on Earthquake Engineering, pp. 517-522.
8. Masajiro, K., Urugami, H., Uemura, M. and Hoshijima, T., (1994), "Rehabilitation and Strengthening of Concrete Structures With Carbon Fiber," Proceedings of the 10th US-Japan Bridge Engineering Workshop, 16 pp.
9. Ono, K., Matsumura, M., Sakanishi, S. and Miyata, K.(1988), "Strength Improvement of RC Bridge Piers by Carbon Fiber Sheet," Proceedings of the 3rd International Symposium on Non-Metallic (FRP) Reinforcement for Concrete Structures, Vol 1., pp. 563-570.
10. Isley, F.P. (1993), Fabric Reinforced Concrete Columns, US Patent No. 5218810.

11. Priestley, M.J.N., Seible, F. and Fyfe, E. (1992), "Column Seismic Retrofit using Fibreglass/Epoxy Jackets," Proceedings of ACMBS-1, pp. 287-297.
12. Seible, F. and Karbhari, V.M. (1996), "Advanced Composites for Civil Engineering Applications in the United States," Proceedings of the 1st International Conference on Composites in Infrastructure, pp. 21-37.
13. Kishi, N., Sato, M., Mikami, H. and Matsuoka, K. (1988), "Failure Behavior of RC Pier Models Strengthened With Winding Aramid Tapes Due to Lateral Impact Loads," Proceedings of the 3rd International Symposium on Non-Metallic (FRP) Reinforcement for Concrete Structures, Vol 1., pp. 257-264.
14. Priestley, M.J.N., Seible, F. and Fyfe, E. (1993), "Column Retrofit Using Prestressed Fiberglass/Epoxy Jackets," Proceedings of the '93 FIP Symposium, pp. 147-160.
15. Hawkins, G.F., Patel, N.R., Steckel, G.L. and Sultan, M. (1996), "Failure Analysis of Highway Bridge Column Composite Overwraps," Proceedings of the 1st International Conference on Composites in Infrastructure, pp. 1126-1140.
16. Karbhari, V.M. and Seible, F. (1997), "Durability and Systems Level Design Guidelines for the Use of Fiber Reinforced Composite Reinforcement in Civil Infrastructure," Proceedings of the 1st International Conference on Composites in Infrastructure, pp. 191-198.
17. Seible, F., Priestley, M.J.N., Hegemier, G. and Innamorato, D. (1997), "Seismic Retrofit of RC Columns With Continuous Carbon Fiber Jackets," *ASCE Journal of Composites for Construction*, Vol. 1[2], pp. 52-62.
18. Xiao, Y. and Ma, R. (1997), "Seismic Retrofit of RC Circular Columns Using Prefabricated Composite Jacketing," *ASCE Journal of Structural Engineering*, Vol. 123[10], pp. 1357-1364.
19. Xiao, Y., Wu, H. and Martin, G.R. (1999), "Prefabricated Composite Jacketing of Circular Columns for Enhanced Shear Resistance," *ASCE Journal of Structural Engineering*, Vol. 125[3], pp. 255-264.

## CHAPTER 5: DESIGN METHODS AND EXAMPLES\*

### 5.1 Introduction

In existing reinforced concrete columns where insufficient transverse reinforcement and/or seismic detailing is provided, three different types of failure modes can be observed under seismic excitation (Figure 5.1).

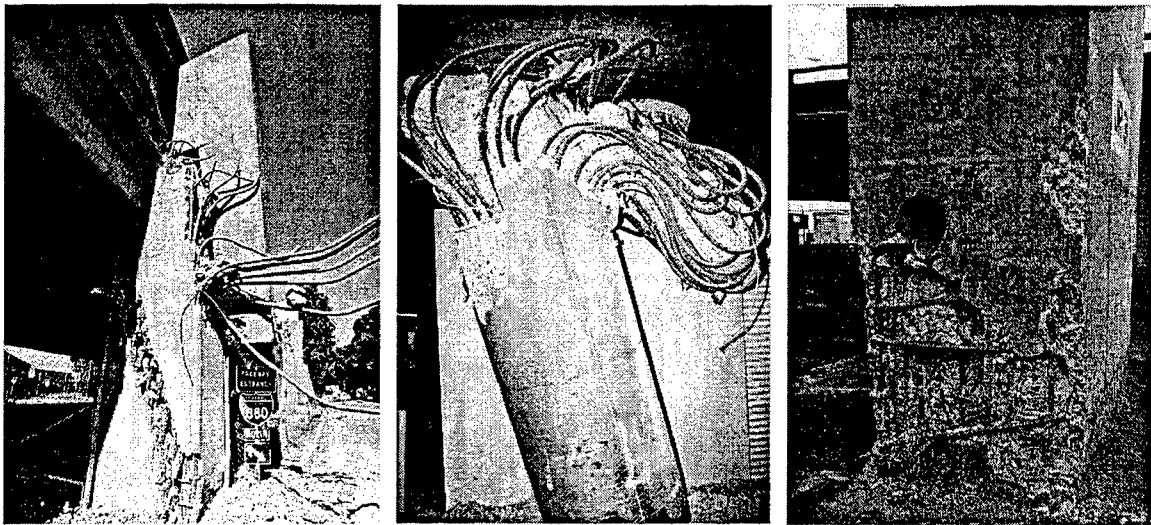


*Figure 5.1: Typical Column Failures from the 1989 Loma Prieta Earthquake (From Left to Right – Shear, Hinge, and Lap Splice Failure)*

The first and most critical failure mode is that of column shear failure where inclined cracking, cover concrete spalling, and rupture or opening of the transverse reinforcement can lead to brittle or explosive column failures. The failure sequence consists of 5 steps, namely:

- (1) the development of inclined cracks once the tensile strength of the concrete is exceeded,
- (2) the opening of inclined or diagonal cracks in the column and onset of cover concrete spalling,
- (3) rupture or opening of the transverse or horizontal reinforcement,
- (4) buckling of the longitudinal column reinforcement, and

---

\* Adapted in part from a paper presented by F. Seible and V.M. Karbhari at the National Seminar on Advanced

(5) disintegration of the column concrete core.

While new column designs feature engineered and better detailed transverse or shear reinforcement, the shear strength of existing substandard columns can be enhanced by providing external shear reinforcement or strength to the column through the application of composites with fibers oriented predominantly in the hoop direction. The shear capacity of columns needs to be checked, both in the column end regions or potential plastic hinge regions where the concrete shear capacity can degrade with increasing ductility demands, and in the column center portion between flexural plastic and/or existing built-in column hinges.

The second column failure mode consists of the potential confinement failure of the flexural plastic hinge region, where subsequent to flexural cracking, cover concrete crushing and spalling, buckling of the longitudinal reinforcement or compression failure of the core concrete initiate plastic hinge deterioration. Plastic hinge failures typically occur with some displacement ductility and are limited to shorter regions in the column. Thus, these failures are less destructive and, because of their large inelastic flexural deformations, are more desirable than the brittle column shear failures of the entire column as described above. This desired ductile flexural plastic hinging at the column ends can be achieved through added confinement in the form of increased hoop or transverse reinforcement in new construction, and through the use of external jacketing in existing columns. The objective of confinement is to simultaneously prevent cover concrete spalling, provide lateral support of the longitudinal reinforcement, and enhance concrete strength and deformation capacity.

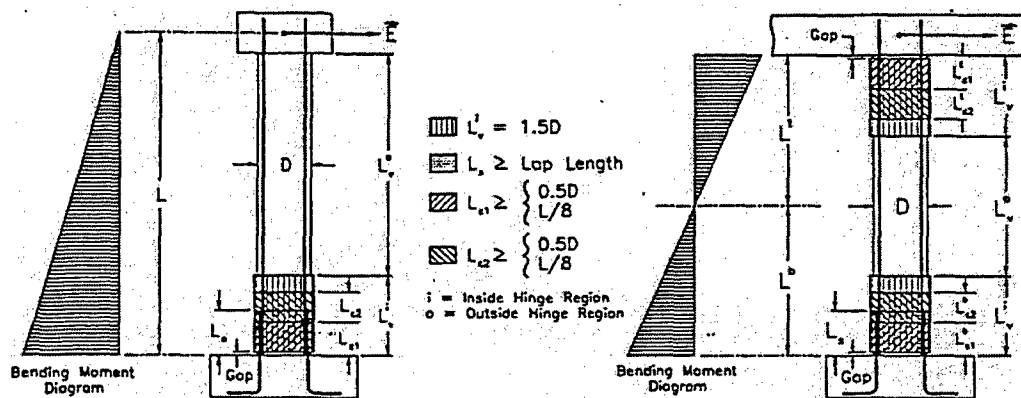
All these characteristics apply along the entire column perimeter and thus uniform confinement provided by circular hoops or circular external jackets would be the most beneficial. In rectangular columns either a circular or oval jacket can provide confinement along the entire column perimeter while rectangular jackets effectively only provide inward corner forces and significant jacket thickness needs to be provided between corners to restrain lateral dilation and column bar buckling. However, large scale tests have shown that appropriately designed

rectangular jackets can provide sufficient confinement and bar buckling restraint to achieve high flexural displacement ductility levels within specific geometric dimensions and aspect ratios [1].

Finally, some existing bridge columns feature lap splices in the column reinforcement, which for ease of construction are located at the lower column end to form the connection between the footing and the column. Starter bars for the column reinforcement are placed during the footing construction and lapped with the longitudinal column reinforcement in this region of maximum column moment demand, i.e. the potential plastic hinge region. While the confinement concepts discussed above for plastic hinge regions also apply to lap-spliced column ends, the flexural strength of the column can only be developed and maintained when debonding of the reinforcement lap splice is prevented. Lap splice debonding occurs once vertical cracks develop in the cover concrete and debonding progresses with increased dilation and cover concrete spalling. The associated flexural capacity degradation can occur rapidly at low flexural ductilities in cases where short lap splices are present and little confinement is provided, but can also occur more gradual with increased lap length and confinement. Confinement can again be provided by external jacketing, where jackets with convex curvature are again more advantageous to provide continuous lateral clamping pressures to the column bar lap splices along the entire column perimeter.

None of the above failure modes and associated column retrofits can be viewed separately since only retrofitting for one deficiency can shift the seismic problem to another location and failure mode, without necessarily improving the overall deformation capacity. For example, a shear critical column strengthened over the column center region with composite wraps is expected to develop flexural plastic hinges at the column ends which in turn need to be designed and retrofitted for the achievement of desired confinement levels. Furthermore, lap splice regions need to be checked not only for the required clamping force to develop the capacity of the longitudinal column reinforcement, but also for confinement and ductility of the flexural plastic hinge.

Based on the failure mechanisms discussed above different column regions which require different jacket designs can be identified, as shown in Figure 5.2.



(a) Single Bending

(b) Double Bending

Figure 5.2: Composite Jacket Regions for Bridge Column Retrofit

In this figure,  $L_s$  = lap splice length,  $L_{c1}$  = primary confinement region for plastic hinge,  $L_{c2}$  = secondary confinement region adjacent to plastic hinge, and  $L_v$  = shear strengthening region with  $L_v^i$  = shear retrofit inside the plastic hinge zone and  $L_v^o$  = shear retrofit outside the plastic hinge zone. The secondary confinement region is necessary to prevent flexural plastic hinging above the primary plastic hinge zone when confinement allows for significant overstrength development in the primary plastic hinge. Plastic hinge confinement lengths  $L_{c1}$  and  $L_{c2}$  are linked intrinsically to the column geometry based on the expected plastic hinge length both in terms of column depth or diameter in the loading direction, and to the shear span or distance from the column hinge to the point of contraflexure. The lap splice length  $L_s$  is directly defined by the lap length of the starter and column bars and the shear length  $L_v$  is taken as the remaining region between the previously defined end zones. In order to avoid direct contact between thick column end jackets and the adjacent bridge footing or cap-beam, a gap is designed to allow plastic hinge rotation without added strength or stiffness from longitudinal jacket action. For thin jackets wound directly onto the original column geometry this gap can be very small, i.e. less than 25 mm (1 in.), whereas in cases where concrete bolsters are added to convert column cross-sections to circular or oval shapes, gaps of 50 mm (2 in.) or more may be required to prevent contact between the retrofit and the adjacent bent portions. Since the principal deficiency in existing pre-1971 bridge columns is in the amount and detailing of the transverse reinforcement, composite jackets addresses this deficiency by applying primarily horizontal or

90° fibers to the column axis, to provide the required transverse confinement, clamping and buckling restraint.

## 5.2 Composite Aspects

As described in Chapter 4 a number of processes exist for the fabrication of composite wraps/jackets for the seismic retrofit of composites. As noted previously the primary requirement in such an application is for provision of additional hoop/transverse reinforcement. In addition, ideally this should be achieved without increasing axial stiffness of the column and thereby ensuring that the retrofit procedure itself does not also cause further attraction of load to the retrofitted element. Because of the inherent anisotropy possible with the use of composites through selection of fiber orientations and layup, both these goals can be efficiently attained through use of an architecture that is primarily in the hoop/transverse direction resulting in a predominantly uniaxial layup.

The key mechanical properties of a FRP composite jacket system, used to provide confinement, clamping and buckling restraints, are the elastic jacket modulus  $E_j$  in the hoop direction, the ultimate unidirectional tensile strength  $f_{ju}$ , and the ultimate unidirectional tension failure strain  $\epsilon_{ju}$ .

As a first approximation, assuming no voids, and all fibers in the hoop direction, the elastic jacket modulus in the hoop direction can be determined as

$$E_j = E_f V_f + E_m V_m$$

where  $E_f$  and  $E_m$  are the fiber and matrix moduli, respectively, and  $V_f$  and  $V_m$  are the corresponding fiber and matrix volume fractions. Since the composites require fiber dominated response for efficient confinement, the composite can be safely assumed to have a fiber volume fraction sufficient that failure occurs in a unidirectional lamina under uniaxial load through fiber rupture resulting in the determination of ultimate unidirectional tensile strength  $f_{ju}$ , through

$$(\sigma_1^T)_{ult} = (\sigma_f)_{ult} V_f + (\epsilon_f)_{ult} E_m (1 - V_f)$$



Since essentially linear elastic mechanical characteristics can be assumed for the composite fiber wrap, detailed knowledge of two of the three characteristic properties are sufficient for the jacket design. Appropriate reduction factors to the mechanical characteristics need to be defined for durability, non-uniformity in lay-up due to process variations, non-continuous fibers or jacket joints in the hoop direction, and for systems where ambient curing rather than elevated temperature cure is used. Examples of these are provided in [2].

### 5.3 Design Methodology

In the current section, general design guidelines to determine the composite jacket thickness for the different column regions in Figure 5.2 are discussed based on the previously described column failure modes. Detailed derivations of the presented design equations used can be found in [3,4]. It should, however, be noted that the approach presented herein is one of a number of approaches for the design of jackets from composite materials for the seismic retrofit of columns. The interested reader is referred to [5-8] for other approaches.

**a) Shear:** The column shear failure mode is primarily a strength and dilation problem. Shear strength can be added to concrete columns by hoop or horizontal reinforcement in the form of hoop oriented composite fibers. The opening of inclined cracks, and with it the loss of aggregate interlock in these cracks, which is one of the key shear force transfer mechanisms, can be controlled by limiting the column dilation in the loading direction to experimentally determined dilation strains of  $\epsilon_d < 0.004$  or 0.4% [1]. The jacket thickness for shear retrofit can be determined based on equation (5.1) for circular and rectangular columns as

$$\begin{aligned} \text{circular } t_j &= \frac{\frac{V_o}{\phi_v} - (V_c + V_s + V_p)}{\frac{\pi}{2} \times 0.004 E_j \cdot D} \\ \text{rectangular } t_j &= \frac{\frac{V_o}{\phi_v} - (V_c + V_s + V_p)}{2 \times 0.004 E_j \cdot D} \end{aligned} \quad (5.1)$$

where,  $V_o$  is the column shear demand based on full flexural overstrength in the potential plastic hinges,  $\phi_v$  a shear capacity reduction factor (typically taken as 0.85),  $V_c$ ,  $V_s$  and  $V_p$  the three shear capacity contributions from the concrete, horizontal steel reinforcement and axial load based on the three component shear model [9] with reductions for the concrete component  $V_c$  in the flexural plastic hinge region based on the ductility demand, and  $E_j$  and  $D$  the composite jacket modulus and the column dimension in the loading direction, respectively.

From Figure 5.3 it is obvious that the high strengths in the composite materials can typically not be utilized due to the limitation on the dilation strains to ensure aggregate interlock.

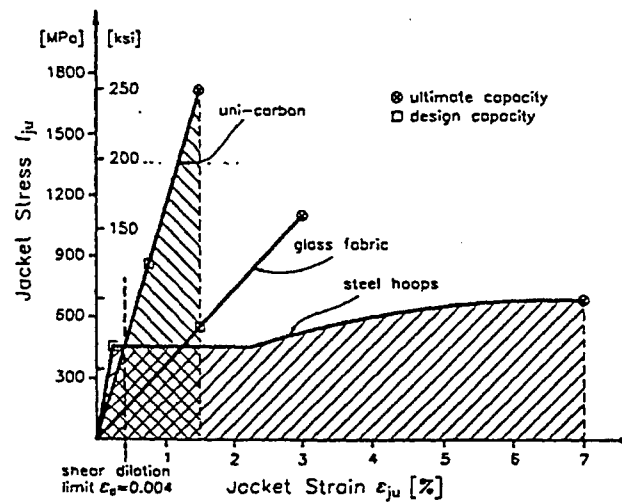


Figure 5.3: Typical Mechanical Characteristics of Column Jackets in the Hoop Direction

Thus, the proportional relationship for composite jacket thickness for shear retrofit can be expressed as

$$t_j^v \sim \frac{1}{E_j D} \times C_v \quad (5.2)$$

where  $C_v$  denotes the remaining general coefficient derived from Equation (5.1). Equation (5.2) shows that for most composite jacket retrofits the jacket thickness is inversely proportional to the jacket modulus and the column dimension in the loading direction.

***b) Flexural Hinge Confinement:*** Inelastic deformation capacity of flexural plastic hinge regions can be increased by confinement of the column concrete with hoop reinforcement from a advanced composite jacket system. For circular columns the required jacket thickness can be expressed as

$$t_j = 0.09 \frac{D(\varepsilon_{cu} - 0.004) f'_{cc}}{\phi_f \cdot f_{ju} \cdot \varepsilon_{ju}} \quad (5.3)$$

where  $f'_{cc}$  is the confined concrete compression strength which depends on the effective lateral confining stress and the nominal concrete strength and can be conservatively taken as  $1.5 f'_c$  for most retrofit designs,  $f_{ju}$  and  $\varepsilon_{ju}$  are the strength and deformation capacity of the composite jacket in the hoop direction,  $\phi_f$  is a flexural capacity reduction factor (typically taken as 0.9),  $\varepsilon_{cu}$  is the ultimate concrete strain which depends on the level of confinement provided by the composite jacket and can be determined as

$$\varepsilon_{cu} = 0.004 + \frac{2.8 \rho_j f_{ju} \varepsilon_{ju}}{f'_{cc}} \quad (5.4)$$

with  $\rho_j$  representing the volumetric jacket reinforcement ratio. In turn,  $\varepsilon_{cu}$  can be obtained from

$$\varepsilon_{cu} = \Phi_u \cdot c_u \quad (5.5)$$

based on the ultimate section curvature  $\Phi_u$  and the corresponding neutral axis depth  $c_u$  which both can be determined from a sectional moment-curvature analysis and directly related to a structural member ductility factor

$$\mu_\Delta = 1 + 3 \left( \frac{\Phi_u}{\Phi_y} - 1 \right) \frac{L_p}{L} \left( 1 - 0.5 \frac{L_p}{L} \right) \quad (5.6)$$

and a semi-empirical plastic hinge length assumption of

$$L_p = 0.08L + 0.022 f_{sy} \cdot d_b \quad (5.7)$$

where  $L$  represents the shear span to the plastic hinge,  $\Phi_y$  is the section yield curvature, and  $f_{sy}$  and  $d_b$  are the yield strength and bar diameter of the main column reinforcement.

Expressing the flexural jacket thickness for hinge confinement in proportional terms similar to the shear described in Equation (2) the required jacket thickness

$$t_j^c \sim \frac{D}{f_{ju} \varepsilon_{ju}} \times C_c \quad (5.8)$$

is proportional to the column dimension  $D$  in the loading direction and inversely proportional to the product of ultimate jacket stress and strain in the hoop direction.

To ensure that column bar buckling in the plastic hinge region does not control the flexural failure mode, additional checks on the transverse reinforcement ratio  $\rho_j$  need to be performed particularly for slender columns where  $M/(V \cdot D) > 4$  (with  $M$  and  $V$  the maximum column moment and shear). The expression for the required jacket thickness

$$t_j^b \sim \frac{D}{E_j} \times C_b \quad (5.9)$$

indicates that the required composite jacket thickness is inversely proportional to the jacket modulus  $E_j$  in the hoop direction and directly proportional to the column diameter.

The confinement effects provided by circular jackets originate directly from the radial pressure forces generated by the jacket curvature and the tensile hoop strains in the jacket generated by the dilation of the plastic hinge. For rectangular columns an oval jacket should be provided by means of added precast concrete segments, or other rigid filler material, with changing radii of curvature in the different loading directions. An equivalent circular column diameter  $D_e$  can be derived from the average of the oval jacket principal radii of curvature, and the jacket thickness calculations can follow those outlined for circular columns using the equivalent column diameter  $D_e$ .

In cases where the column side aspect ratio of depth/width  $\leq 1.5$  and for columns with side dimensions of depth/width = 0.75/0.5 m (30 in./20 in.), rectangular composite jackets with twice the theoretical thickness derived for an equivalent circular column of diameter  $D_e$  have been found to perform well up to the design target ductility levels. Thus, while rectangular column jackets are based on this empirical design assumption of doubling the equivalent circular column jacket thickness are feasible, extrapolations beyond the tested aspect ratios and column side dimensions need to be supported by additional tests or analyses.

**c) Lap Splice Clamping:** Lap splice clamping requires sufficient lateral pressure  $f_t$  onto the splice region to prevent the concrete prisms, which adhere to the starter bars and the column

reinforcement to slip relative to each other. Experimental test results show that onset of lap splice debonding or relative slippage starts when measured hoop or dilation strain levels are between 1,000 to 2,000  $\mu\epsilon$  as indicated by a loss in lateral load carrying capacity of the test columns. Limiting dilation strain levels to 1,000  $\mu\epsilon$ , the composite jacket thickness to ensure lap splice clamping can be derived as

$$t_j = 500 \frac{D(f_t - f_h)}{E_j} \quad (5.10)$$

where  $f_h$  represents the horizontal stress level provided by the existing hoop reinforcement in a circular column at a strain of 0.1% and  $f_t$  the lateral clamping pressure over the lap splice  $L_s$  can be determined as

$$f_t = \frac{A_s \cdot f_{sy}}{\left[ \frac{p}{2n} + 2(d_b + cc) \right] L_s} \quad (5.11)$$

where  $p$  is the perimeter line in the column cross-section along the lap spliced bar locations,  $n$  is the number of spliced bars along  $p$ ,  $A_s$  is the area of one main column reinforcing bar, and  $cc$  the concrete cover to the main column reinforcement with diameter  $d_b$ .

Expressing the splice clamping problem again in terms of a proportionality relationship in the form of

$$t_j^s \sim \frac{D}{E_j} \times C_s \quad (5.12)$$

indicates that the required composite jacket thickness is inversely proportional to the jacket modulus  $E_j$  in the hoop direction and directly proportional to the column diameter. For rectangular columns with lap splices, the curvature from circular or oval jackets is required to provide the necessary lateral clamping pressure and an equivalent circular column diameter  $D_e$  as outlined for the plastic hinge confinement can be used to determine jacket thicknesses. Table 5.1 gives relative jacket thicknesses for three hypothetical composite jacket systems for the four column failure modes given by equations (5.2), (5.8), (5.9) and (5.12). All values of thickness are normalized by the required thicknesses for system A.

*Table 5.1: Comparison of Hypothetical Jacket Thicknesses*

System	Mechanical Characteristics	Normalized Jacket Thickness			
		Shear Strength	Plastic Hinge Confinement	Bar Buckling Restraint	Lap Splice Clamping
System A	$E_j = 124 \text{ GPa}$ $f_{ju} = 1,380 \text{ MPa}$ $\epsilon_{ju} = 1\%$	1	1	1	1
System B	$E_j = 76 \text{ GPa}$ $f_{ju} = 1,380 \text{ MPa}$ $\epsilon_{ju} = 1.5\%$	1.6	0.7	1.6	1.6
System C	$E_j = 21 \text{ GPa}$ $f_{ju} = 655 \text{ MPa}$ $\epsilon_{ju} = 2.5\%$	6.0	0.9	6.0	6.0

1 MPa = 0.145 ksi, 1 GPa = 145 ksi

System A is representative of a towpreg based graphite/epoxy composite similar to that used in automated towpreg winding of jackets, system B is representative of a Kevlar/epoxy composite, and system C is representative of an E-glass/Vinylester composite similar to that used in prefabricated adhesively bonded shells. All values in Table 5.1 are normalized to the thickness values derived for System A which represents the unidirectional prepreg carbon tow winding system with an epoxy matrix used in the following experimental validation tests. Table 5.1 shows that jacket thicknesses for shear, bar buckling restraint and lap splice clamping are driven by the modulus of the jacket in the hoop direction which favors higher modulus materials, whereas the flexural plastic hinge confinement can also efficiently be achieved with a lower modulus and higher strain capacity material.

#### 5.4 Design Examples

This section provides design examples based on the above elucidated equations. For purposes of similarity all examples use a prespecified system with properties as listed in Table 5.2.

*Table 5.2: Summary of Design Example Column Specifications and Details*

	Specification	Design Examples 1 and 2		Design Example 3	Design Example 4
Column Section Properties	Column Height, H	2.438 m		3.658 m	3.658 m
	Shear Span, L	1.219 m		3.658 m	3.658 m
	Column Depth, D	0.610 m		0.730 m	0.610 m
	Column Width, B	0.406 m		0.489 m	--
	Concrete Cover, cc	19 mm		19 mm	19 mm
	Concrete Strength, $f'_c$	34.45 MPa		34.45 MPa	34.45 MPa
Longitudinal Reinforcement (Grade 40)	Bar Diameter, $d_b$	19 mm (#6 bars)= (22 tot.)		25 mm (#8 bars) and 22 mm (#7 bars) = (14 and 28 tot.)	19 mm (#6 bars) = (26 tot.)
	Bar Area, $A_s$	284 mm <sup>2</sup>		510 mm <sup>2</sup>	284 mm <sup>2</sup>
	Yield Strength, $f_{sy}$	303.16 MPa		303.16 MPa	303.16 MPa
Transverse Reinforcement (Grade 40)	Bar Diameter, $d_h$	6 mm (#2 bars)		6 mm (#2 bars)	6 mm (#2 bars)
	Bar Area, $A_h$	32 mm <sup>2</sup>		32 mm <sup>2</sup>	32 mm <sup>2</sup>
	Spacing, s	127 mm		127 mm	127 mm
Column Section Properties	Axial Load, P	507 kN		1780 kN	1780 kN
	Moment Capacity, $M_{yi}$	619 kN·m		2165 kN·m	815 kN·m
	Yield Curvature, $\Phi_y$	0.005472 1/m		0.004685 1/m	0.006339 1/m
	Neutral Axis Depth, $c_u$	116 mm		208 mm	211 mm
Jacket Material Properties	Jacket Modulus, $E_j$	#1	#2	124 GPa	124 GPa
		124 GPa	21 GPa		
		1.3 GPa	0.655 GPa		
Jacket Material Properties	Ultimate Strength, $f_{ju}$	1.3 GPa	0.655 GPa	1.3 GPa	1.3 GPa
	Ultimate Strain, $\epsilon_{ju}$	1.0%	2.5%	1.0%	1.0%

1 mm = 0.0394 in., 1 kN = 0.225 kips, 1 kN·m = 8.850 kip·in, 1 MPa = 0.145 ksi

However the same procedure, with appropriate modifications to the composite properties specified, can be used for other systems. Wherever possible results are compared to results from laboratory tests. In general, for laboratory tests, performance acceptance on 40% scale model bridge columns was defined as

- (1) meeting or exceeding retrofit performance of comparable steel jacket retrofits,
- (2) achieving a displacement ductility of at least  $\mu_\Delta = 8$ , or
- (3) more than doubling the displacement capacity achieved in comparison "As-built" and unretrofitted test specimens.

Test specimen geometry, reinforcement detailing, column section properties, and jacket material properties are summarized in Table 5.2.

#### 5.4.1 Design Example 1: Shear Retrofit of Rectangular Column in Double Bending Using Carbon/Epoxy Prepreg Tow

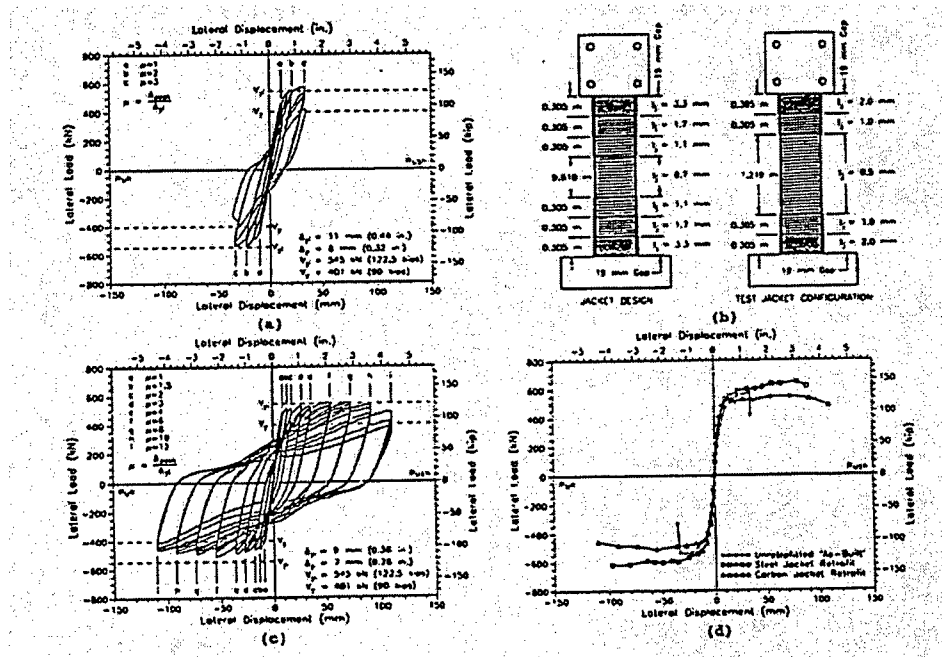


Figure 5.4: Shear Retrofit of Rectangular Column in Double Bending; (a) "As-Built" Load-Displacement Response; (b) Summary of Jacket Layouts; (c) Carbon Jacket Retrofitted Load-Displacement Response; and (d) Comparison of Load-Displacement Envelopes.

The objective of the design is to provide a jacket to convert the brittle shear failure (see Fig. 5.4(a)) to a ductile flexural failure with a target member displacement ductility of  $\mu_\Delta \geq 8$ .

#### Shear Strength Requirements:

Maximum expected plastic shear demand including overstrength  $V_o$  can be computed as

$$V_o = 1.5 V_{yi} = 1.5 \times \frac{M_{yi}}{L} = 1.5 \times \frac{618.8}{1.219} = 761.4 \text{ kN (171.1 kips)}.$$

Contributions from the shear mechanisms associated with the concrete ( $V_c^i$  and  $V_c^o$ ), the transverse reinforcement ( $V_s$ ), and the axial load ( $V_p$ ) were  $V_c^i = 48.8$  kN (11.0 kips) in the plastic hinge region, outside the plastic hinge region  $V_c^o = 209.7$  kN (65.3 kips),  $V_s = 88.3$  kN



(19.8 kips), and  $V_p = 102.7$  kN (23.1 kips), respectively. Using a shear capacity reduction factor of  $\phi_v = 0.85$ , the required jacket thickness inside the plastic hinge region ( $t_v^i$ ) and outside the plastic hinge region ( $t_v^o$ ) can be determined using Equation (1) as

$$t_v^i = \frac{\frac{V_o}{\phi_v} - (V_c^i + V_s + V_p)}{2 \times 0.004 E_j D} = \frac{\frac{761.4}{0.85} - (48.8 + 88.3 + 102.7)}{2 \times 0.004 (124,020 \times 610)} \times 10^3$$

$$= 1.1 \text{ mm (0.043 in.)}$$

$$t_v^o = \frac{\frac{V_o}{\phi_v} - (V_c^o + V_s + V_p)}{2 \times 0.004 E_j D} = \frac{\frac{761.4}{0.85} - (290.7 + 88.3 + 102.7)}{2 \times 0.004 (124,020 \times 610)} \times 10^3$$

$$= 0.7 \text{ mm (0.027 in.)}$$

#### Flexural Plastic Hinge Confinement Requirements:

The requirements for confinement of the plastic hinge region were achieved by using a rectangular jacket with twice the jacket thickness required for an equivalent circular jacket with an effective diameter  $D_e$  of 766 mm (30.2 in.). The expected plastic hinge length  $L_p$  can be determined by Equation (7) as

$$L_p = 0.08 L + 0.022 f_{sy} d_b = 0.08 \times 1219 + 0.022 \times 303.16 \times 19 = 224 \text{ mm (8.8 in.)}$$

To develop the full column capacity at a displacement ductility of  $\mu_\Delta = 8$ , the required curvature ductility  $\mu_\phi$  based on Equation (6) is

$$\mu_\phi = 1 + \frac{8 - 1}{3(224/1219) (1 - 0.5(224/1219))} = 15$$

resulting in a required ultimate concrete strain (using Equation (5)) of

$$\epsilon_{cu} = \Phi_u c_u = \mu_\phi \Phi_y c_u = 15 \times 0.005472 \times 0.116 = 0.0095.$$

The jacket thickness required to provide this ultimate concrete strain determined by Equation (3) equals

$$t_{c1} = 0.09 \frac{D_e (\epsilon_{cu} - 0.004)}{\phi_f f_{ju} e_{ju}} f'_{cc} \cdot 2 = 0.09 \frac{766(0.0095 - 0.004) \times 1.5 \times 34.45}{0.9 \times 1309 \times 0.01} \cdot 2$$

$$t_{c1} = 3.3\text{mm} (0.130\text{in.})$$

$$t_{c2} = t_{c1}/2 = 3.3/2 = 1.7\text{mm} (0.065\text{in.})$$

where  $t_{c1}$  and  $t_{c2}$  are the jacket thicknesses in the primary and secondary confinement regions, respectively. Since  $L/D = 2.0$  is less than 4, the anti-bar buckling criteria need not be checked.

Summary of Jacket Thickness Specifications:

$$L_v^i = 1.5D = 915\text{mm} (36\text{in.}) \rightarrow t_v^i = 1.1\text{mm} (0.043\text{in.})$$

$$L_v^o = L - 2 \cdot L_v^i = 610\text{mm} (24\text{in.}) \rightarrow t_v^o = 0.7\text{mm} (0.027\text{in.})$$

$$L_{c1}^t = L_{c1}^b = 0.5D = 305\text{mm} (12\text{in.}) \rightarrow t_{c1} = 3.3\text{mm} (0.130\text{in.})$$

$$L_{c2}^t = L_{c2}^b = 0.5D = 305\text{mm} (12\text{in.}) \rightarrow t_{c2} = t_{c1}/2 = 1.7\text{mm} (0.065\text{in.})$$

These required design jacket thicknesses are illustrated in Figure 5.4(b) together with the jacket configuration used in the actual laboratory tests. The differences in the jacket thickness and lay up regions arise from the fact that the test jacket configurations were designed in accordance with measured material properties which were modified and refined subsequent to the completion of the experimental validation tests. As shown in Figure 5.4(c), the carbon jacket significantly increased the ductility capacity of the “As-Built” column and allowed the column to reach and/or exceed the ideal or theoretical load capacity (except in the pull loading direction) while maintaining a constant load level without any significant cyclic capacity degradation. A direct comparison of the envelopes of the load-displacement peaks for the “As-Built” column, the steel jacket retrofitted column, and the carbon fiber retrofitted column is provided in Figure 5.4(d). From this figure, it can be seen that the increase in strength of the steel jacket retrofit is higher than that of the carbon fiber retrofit due to the isotropic characteristics of the steel jacket as compared to the tailored directionality of the fiber reinforcement. In general, both the steel

jacket and carbon fiber wrap system displayed very similar structural performance characteristics.

#### ***5.4.2 Design Example 2: Shear Retrofit of Rectangular Column in Double Bending with E-Glass/Vinylester Composite***

The objective of the retrofit is to provide an E-glass/Vinylester jacket to convert the brittle shear failure to a ductile flexural failure with a target member displacement ductility of  $\mu_{\Delta} \geq 8$ .

##### ***Shear Strength Requirements:***

Since the column section properties and reinforcement are the same as those used in Example 1, contributions from the shear mechanisms associated with the concrete ( $V_c^i$  and  $V_c^o$ ), the transverse reinforcement ( $V_s$ ), and the axial load ( $V_p$ ) will remain the same. Using a shear capacity reduction factor of  $\phi_v = 0.85$ , the required jacket thickness inside the plastic hinge region ( $t_v^i$ ) and outside the plastic hinge region ( $t_v^o$ ) can be determined using Equation (1) in similar fashion as in Example 1, but using the appropriate value of  $E_j$  to get

$$\begin{aligned} t_v^i &= 6.5 \text{ mm (0.256 in.)} \\ t_v^o &= 4.1 \text{ mm (0.161 in.)} \end{aligned}$$

##### ***Flexural Plastic Hinge Confinement Requirements:***

Using the formulation in Example 1, the expected plastic hinge length,  $L_p$ , curvature ductility,  $\mu_{\phi}$ , and the required ultimate compression strain in the concrete are 224 mm, 15 and 0.0095 respectively. The jacket thickness required to provide this ultimate concrete strain determined by Equation (3) equals

$$\begin{aligned} t_{c1} &= 0.09 \frac{D_t (\varepsilon_{cu} - 0.004) f'_{cc}}{\phi_f f_{ju} e_{ju}} \cdot 2 \\ &= 0.09 \frac{766 (0.0095 - 0.004) \times 1.5 \times 34.45}{0.9 \times 655 \times 0.025} \cdot 2 \\ t_{c1} &= 2.7 \text{ mm (0.106 in.)} \\ t_{c2} &= t_{c1} / 2 = \frac{2.7}{2} = 1.35 \text{ mm (0.053 in.)} \end{aligned}$$

where  $t_{c1}$  and  $t_{c2}$  are the jacket thicknesses in the primary and secondary confinement regions, respectively. Since  $L/D = 2.0$  is less than 4, the anti-bar buckling criteria need not be checked.

### Summary of Jacket Thickness Requirements:

$$L_v^i = 1.5D = 915\text{mm (36in.)} \rightarrow t_v^i = 6.5\text{mm (0.256in.)}$$

$$L_v^o = L - 2 \cdot L_v^i = 610\text{mm (24in.)} \rightarrow t_v^o = 4.1\text{mm (0.161in.)}$$

$$L_{cl}^t = L_{cl}^b = 0.5D = 305\text{mm (12in.)} \rightarrow t_{cl} = 2.7\text{mm (0.106in.)}$$

$$L_{c2}^t = L_{c2}^b = 0.5D = 305\text{mm (12in.)} \rightarrow t_{c2} = t_{cl}/2 = 1.35\text{mm (0.053in.)}$$

### **5.4.3 Design Example 3: Flexural Retrofit of a 5.0% Reinforced Rectangular Cantilever Column with Carbon/Epoxy Prepreg Tow**

The objective of the retrofit is to provide carbon jacket confinement to the plastic hinge region and retrofit the column to achieve at least twice the displacement ductility level of  $\mu_\Delta = 3$  observed in the "As-Built" test (see Figure 5.5(a)) namely  $\mu_\Delta \geq 6$ .

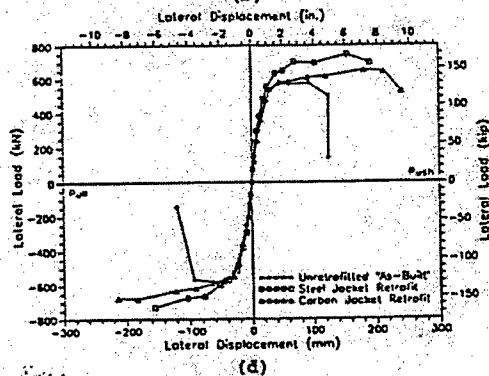
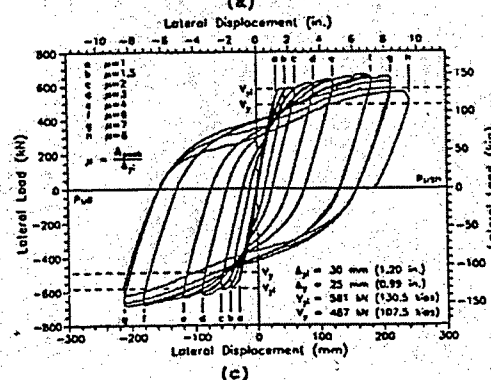
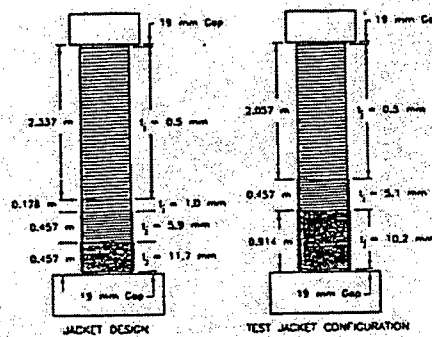
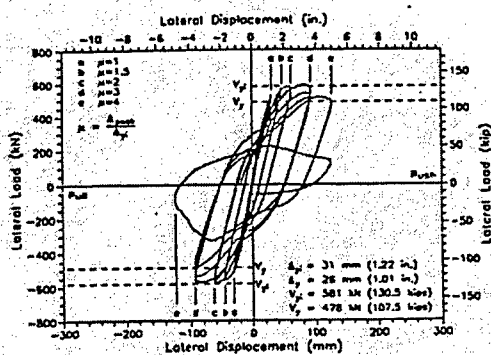


*Figure 5.5: Flexural Retrofit of a 5.0% Reinforced Rectangular Cantilever Column; (a) "As-Built" Load-Displacement Response; (b) Summary of Jacket Layouts; (c) Carbon Jacket Retrofitted Load-Displacement Response; and (d) Comparison of Load-Displacement Envelopes.*

Shear Strength Requirements:

Maximum expected plastic shear demand including overstrength  $V_o$  is

$$V_o = 1.5V_{yi} = 1.5 \times \frac{M_{yi}}{L} = 1.5 \times \frac{2164.5}{3.658} = 887.6 \text{ kN (199.5 kips)}.$$

Contributions from the shear mechanisms associated with the concrete ( $V_c^i$  and  $V_c^o$ ), the transverse reinforcement ( $V_s$ ), and the axial load ( $V_p$ ) were  $V_c^i = 70.4 \text{ kN (15.8 kips)}$  in the plastic hinge region, outside the plastic hinge region  $V_c^o = 419.0 \text{ kN (94.2 kips)}$ ,  $V_s = 106.6 \text{ kN (24.0 kips)}$ , and  $V_p = 127.0 \text{ kN (28.5 kips)}$ .

Using a shear capacity reduction factor of  $\phi_v = 0.85$ , the required jacket thickness inside the plastic hinge region ( $t_v^i$ ) and outside the plastic hinge region ( $t_v^o$ ) can be determined using Equation (1) as

$$t_v^i = \frac{\frac{V_o}{\phi_v} - (V_c^i + V_s + V_p)}{2 \times 0.004 E_j D} = \frac{\frac{887.6}{0.85} - (70.4 + 106.6 + 127.0)}{2 \times 0.004 (124,020 \times 730)} \times 10^3$$

$$= 1.0 \text{ mm (0.039 in.)}$$

$$t_v^o = \frac{\frac{V_o}{\phi_v} - (V_c^o + V_s + V_p)}{2 \times 0.004 E_j D} = \frac{\frac{887.6}{0.85} - (419.0 + 106.6 + 127.0)}{2 \times 0.004 (124,020 \times 730)} \times 10^3$$

$$= 0.5 \text{ mm (0.020 in.)}$$

#### Flexural Plastic Hinge Confinement Requirements:

The confinement of the plastic hinge region was designed using a rectangular jacket with twice the jacket thickness required for an equivalent circular jacket with an effective diameter  $D_e$  of 918 mm (36.1 in.). The expected plastic hinge length  $L_p$  can be determined from Equation (7) as

$$L_p = 0.08 L + 0.022 f_{sy} d_b = 0.08 \times 3658 + 0.022 \times 303.16 \times 25 = 462 \text{ mm (18.2 in.)}$$

To develop the full column capacity at a displacement ductility of  $\mu_\Delta \geq 6$  say  $\mu_\Delta = 8$ , the required curvature ductility  $\mu_\phi$  based on Equation (6) equals

$$\mu_\phi = 1 + \frac{8-1}{3(462/3658)(1-0.5(462/3658))} = 20.7$$

resulting in a required ultimate concrete strain (Equation (5)) of

$$\epsilon_{cu} = \Phi_u c_u = \mu_\phi \Phi_y c_u = 20.7 \times 0.004685 \times 0.208 = 0.0202.$$

The jacket thickness required to provide this ultimate concrete strain determined by Equation (3) equals

$$t_{c1} = 0.09 \frac{D_e (e_{cu} - 0.004) f'_{cc} \cdot 2}{\phi_f \cdot f_{ju} \cdot e_{ju}} = 0.09 \frac{915(0.0202 - 0.004) \times 1.5 \times 34.45}{0.9 \times 1309 \times 0.01} \cdot 2$$

$$t_{c1} = 11.7 \text{ mm (0.461 in.)}$$

$$t_{c2} = t_{c1} / 2 = 11.7 / 2 = 5.9 \text{ mm (0.232 in.)}$$

where  $t_{c1}$  and  $t_{c2}$  are the jacket thicknesses in the primary and secondary confinement regions, respectively.

#### Summary of Jacket Thickness Requirements:

$$L_v^i = 1.5D = 1095 \text{ mm (43.1 in.)} \rightarrow t_v^i = 1.0 \text{ mm (0.039 in.)}$$

$$L_v^o = L - 2 \cdot L_v^i = 2563 \text{ mm (100.9 in.)} \rightarrow t_v^o = 0.5 \text{ mm (0.020 in.)}$$

$$L_{c1} = 0.125L_e = 457 \text{ mm (18 in.)} \rightarrow t_{c1} = 11.7 \text{ mm (0.461 in.)}$$

$$L_{c2} = 0.125L_e = 457 \text{ mm (18 in.)} \rightarrow t_{c2} = t_{c1} / 2 = 5.9 \text{ mm (0.232 in.)}$$

These required design jacket thicknesses are illustrated in Figure 5.5(b) together with the jacket configuration used for the laboratory test specimen. The differences in the jacket thickness and lay-up regions arises again from the fact that the test jacket configurations were designed in accordance with earlier design criteria which were modified and refined subsequent to the completion of the experimental validation tests. As shown in Figure 5.5(c), the carbon jacket significantly increased the ductility capacity of the "As-Built" column and allowed the column to reach and/or exceed the ideal or theoretical load capacity while maintaining a constant load level without any significant cyclic capacity degradation. A direct comparison of the envelopes of the load-displacement peaks for the "As-Built" column, the steel jacket retrofitted column, and the carbon fiber retrofitted column is provided in Figure 5.5(d). From this figure, it can be seen that the increase in strength of the steel jacket retrofit again is higher than that of the carbon fiber retrofit. In general, both the steel jacket and carbon fiber wrap system displayed very similar structural performance characteristics.

#### ***5.4.4 Design Example 4: Lap Splice Clamping Retrofit of Circular Flexural Cantilever Column with Carbon/Epoxy Prepreg Tow***

The retrofit objective is to provide a carbon jacket over the column reinforcement lap splice region to develop the full column capacity to a displacement ductility level of  $\mu_{\Delta} = 8$ .

##### ***Shear Strength Requirements:***

Maximum expected plastic shear demand including overstrength  $V_o$  equals

$$V_o = 1.5V_{yi} = 1.5 \times \frac{M_{yi}}{(L)} = 1.5 \times \frac{815.2}{(3.658)} = 334.3 \text{ kN (75.1 kips)}.$$

Contributions from the shear mechanisms associated with the concrete ( $V_c^i$  and  $V_c^o$ ), the transverse reinforcement ( $V_s$ ), and the axial load ( $V_p$ ) were  $V_c^i = 57.6 \text{ kN (12.9 kips)}$  in the plastic hinge region, outside the plastic hinge region  $V_c^o = 343.1 \text{ kN (77.1 kips)}$ ,  $V_s = 69.4 \text{ kN (15.6 kips)}$ , and  $V_p = 97.1 \text{ kN (21.8 kips)}$ , respectively.

Using a shear capacity reduction factor of  $\phi_v = 0.85$ , the required jacket thickness inside the plastic hinge region ( $t_v^i$ ) and outside the plastic hinge region ( $t_v^o$ ) can be determined using Equation (1) as

$$t_v^i = \frac{\frac{V_o}{\phi_v} - (V_c^i + V_s + V_p)}{\frac{\pi}{2} \times 0.004 E_j D} = \frac{\frac{334.3}{0.85} - (57.6 + 69.4 + 97.1)}{\frac{\pi}{2} \times 0.004 (124,020 \times 610)} \times 10^3$$

$$t_v^i = 0.4 \text{ mm (0.016 in.)}$$

Outside the plastic hinge region, the nominal shear capacity  $V_n^o = V_c^o + V_s + V_p$  is greater than the factored ideal shear capacity  $V_o/\phi_v$ ; therefore, no shear retrofit is required in this column region.

#### Flexural Plastic Hinge Confinement Requirements:

The expected plastic hinge length  $L_p$  can be determined by Equation (7) as

$$L_p = 0.08 L + 0.022 f_{sy} d_b = 0.08 \times 3658 + 0.022 \times 303.16 \times 19 = 419 \text{ mm (16.5 in.)}$$

To develop the full column capacity at a displacement ductility of  $\mu_\Delta = 8$ , the required curvature ductility  $\mu_\phi$  based on Equation (6) equals

$$\mu_\phi = 1 + \frac{8-1}{3(419/3658)(1-0.5(419/3658))} = 22.6$$

resulting in a required ultimate concrete strain (Equation (5)) of

$$\epsilon_{cu} = \Phi_u c_u = \mu_\phi \Phi_y c_u = 22.6 \times 0.006339 \times 0.211 = 0.0302.$$

The jacket thickness required to provide this ultimate concrete strain determined by Equation (3) equals

$$t_{c1} = 0.09 \frac{D_c (\epsilon_{cu} - 0.004) f'_{cc}}{\phi_f \cdot f_{ju} \cdot e_{ju}} \cdot 2 = 0.09 \frac{610 (0.0302 - 0.004) \times 1.5 \times 34.45}{0.9 \times 1309 \times 0.01} \cdot 2$$

$$t_{c1} = 6.3 \text{ mm (0.248 in.)}$$

$$t_{c2} = t_{c1}/2 = 6.3/2 = 3.2 \text{ mm (0.124 in.)}$$



where  $t_{c1}$  and  $t_{c2}$  are the jacket thicknesses in the primary and secondary confinement regions, respectively. Since  $L/D = 6.0 > 4$ , again the anti-bar buckling criteria needs to be checked but does not control the jacket thickness in this case.

Lap Splice Clamping Requirements:

The available lateral clamping pressure provided by the hoop reinforcement  $f_h$  equals 0.165 MPa (0.024 ksi). The required clamping pressure to prevent lap splice debonding can be found from Equation (11) as

$$f_t = \frac{A_s f_{sy}}{\left[ \frac{p}{2n} + 2(d_b + cc) \right] L_s} = \frac{284 \times 303.16}{\left[ \frac{533\pi}{2 \times 26} + 2(19 + 19) \right] 381} = 2.088 \text{ MPa (0.303 ksi)}$$

The carbon jacket thickness can now be determined from Equation (10) as

$$t_s = 500 \frac{D(f_t - f_h)}{E_j} = 500 \frac{610(2.088 - 0.165)}{124,020} = 4.7 \text{ mm (0.185 in.)}$$

Summary of Jacket Thickness Specifications:

$$L_v^i = 1.5D = 915 \text{ mm (36 in.)} \rightarrow t_v^i = 0.4 \text{ mm (0.016 in.)}$$

$$L_{c1} = 0.125L_e = 457 \text{ mm (18 in.)} \rightarrow t_{c1} = 6.3 \text{ mm (0.248 in.)}$$

$$L_{c2} = 0.125L_e = 457 \text{ mm (18 in.)} \rightarrow t_{c2} = t_{c1}/2 = 3.2 \text{ in. (0.124 in.)}$$

$$L_s = 381 \text{ mm (15 in.)} \rightarrow t_s = 4.7 \text{ mm (0.185 in.)}$$

These required design jacket thicknesses are illustrated in Figure 5.6(a) together with the actual jacket configuration used on the laboratory test specimens. Again, differences in the jacket thicknesses arise from the fact that the test jacket configurations were designed in accordance with earlier design criteria which were modified and refined subsequent to the completion of the experimental validation tests. The lateral load-displacement history for the Carbon Jacket Test #1 is shown in Figure 5.6(b) indicating debonding of the lap splice after a displacement ductility level of  $\mu_\Delta = 5$  by a reduction in lateral load capacity. It is of interest to note that post-test measurements on the primary confinement jacket thickness  $t_{c1}$  of the first carbon test column

revealed that the actual jacket thickness was 20% less than the required design thickness, which does not meet the design requirements for lap splice clamping. A second test was performed where the column had a slightly higher jacket thickness than that required for confinement of the same region, see Figure 5.6(c). From Figures 5.6(b) and 5.6(c), it can be seen that during the Carbon Jacket Test #1 lap splice debonding occurred at a displacement ductility  $\mu_{\Delta} \geq 5$  occurred whereas Carbon Jacket Test #2 achieved displacement ductilities of  $\mu_{\Delta} = 8$  and more prior to starter bar rupture. A direct comparison of the envelopes of the load-displacement peaks for the "As-Built" column, the steel jacket retrofitted column, and the carbon fiber retrofitted columns is provided in Figure 5.6(d).

This is a good indication that the thickness of lap splice clamping Test #1 was not quite sufficient to prevent lap splice debonding and measured jacket strains also showed strain levels above  $2000 \mu\epsilon$  in the jacket hoop direction which is consistent with other observed slip dilation strain levels. On the other hand, in lap splice clamping Test #2 the jacket was thick enough to prevent lap splice debonding, forcing low cycle fatigue rupture in the starter bars.

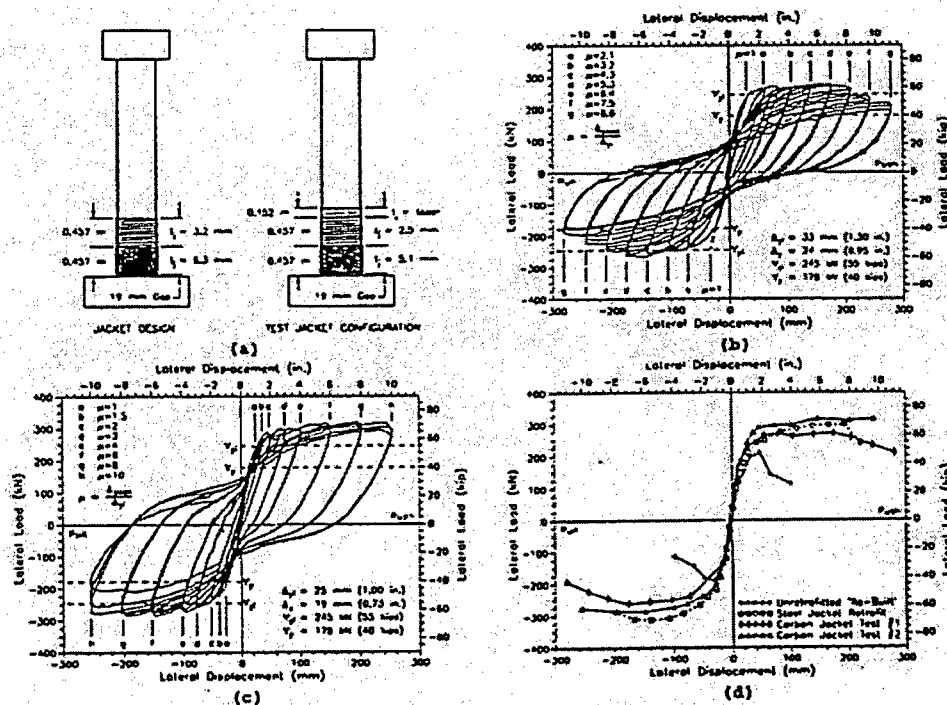


*Figure 5.6: Lap Splice Clamping Retrofit of Circular Flexural Cantilever Column; (a) Summary of Jacket Layouts; (b) Carbon Jacket Retrofitted Load-Displacement Response #1; (c) Carbon Jacket Retrofitted Load-Displacement Response #2; and (d) Comparison of Load-Displacement Envelopes*

## 5.5 Design Details

Notwithstanding the methodology provided by the design equations for the determination of jacket thickness, care must still be taken to provide appropriate design details. A few of these aspects are listed in this section

- (1) Unlike reinforcing steel, some fibers, such as carbon fibers, are anisotropic, having different properties in the longitudinal (i.e. along the length of the fiber) and transverse directions. For example, although the tensile modulus for T300 carbon fibers in the longitudinal direction is 230 GPa, in the transverse direction it is only about 40 GPa, a fact that must be considered when designing with fibers or fabrics that have to conform to tight radii and corners. Placement and tensioning around sharp corners can result in fiber fracture and hence at a minimum all corners should be rounded to a radius of 25 mm.
- (2) A related concern exists in large aspect ratio rectangular columns, wherein significant challenges exist in achievement of proper levels of confinement. Composite sheets can be easily applied to large aspect ratio columns or pier walls. However, due to the long length between the corners, the composite does not in actuality confine the internal concrete structure if just applied to the surface. In fact, if used in this manner, reinforcing fibers are often loose and unable to provide confinement. In order to achieve confinement, the composite wrap needs to be constrained on both sides along the length through the use of dowels or bolts that anchor the composite in the column core, thereby creating shorter distances of confinement. This is actually similar to the technique used in conventional reinforced concrete construction wherein the transverse reinforcement on the two side faces is tied together through the use of J-hooks. In the absence of the dowels/bolts/ties the jacket is not anchored and does not actually confine the material appropriately between the two shorter ends. The number of dowels or bolts needed to

prevent the opening of cracks in the concrete due to extreme dilation of the jacket can be established based on ACI 318 shear friction models, providing a minimum of shear friction capacity over the potential crack area.

- (3) In spandrel columns the column is often built on top of a stub, which is integral with the arch and with a construction joint between the stub and the column. This construction joint provides ductility to the assembly. In retrofitting such structures it is essential that the jacket be connected to the arch itself through the use of bolts/anchors to provide a link directly to the steel in the arch while ensuring that the construction joint is not covered by vertical or angled fibers, thereby providing fixity of the jacket where needed while still allowing the inherent mechanism of ductility to exist. Covering up the joint and leaving the jacket unanchored to the arch (even if adhesively bonded) will cause failure through a mechanism of the column sliding downwards along the arch with rigidity along the construction joint between the stub and column. Details of this can be found in [10].

## References

- [1] Priestley, M.J.N., Seible, F., and Calvi, M., (1996), **Seismic Design and Retrofit of Bridges**, John Wiley & Sons, Inc.
- [2] Karbhari, V.M. (2000), "Determination of Materials Design Values for the Use of Fibre-Reinforced Polymer Composites in Civil Infrastructure," *Proceedings of the Institution of Mechanical Engineers, Materials and Design*, Vol 214, Part L, 2000, pp. 163-171.
- [3] Seible, F., Priestley, M.J.N., and Innamorato, D., (1995). "Earthquake Retrofit of Bridge Columns with Continuous Fiber Jackets," Volume II, Design Guidelines, Advanced Composites Technology Transfer Consortium, Report No. ACTT-95/08, University of California, San Diego.
- [4] Seible, F., Hegemier, G.A., Priestley, M.J.N. and Innamorato, D. (1997), "Seismic Retrofit of RC Columns with Continuous Carbon Fiber Jackets," *ASCE Journal of Composites for Construction*, Vol. 1, pp. 52-62.
- [5] Mutsuyoshi, H., Ishibashi, T., Okano, M. and Katsuki, F. (1999), "New Design Method for Seismic Retrofit of Bridge Columns With Continuous Fiber Sheets – Performance Based

- Design," in **Fiber Reinforced Polymer for Reinforced Concrete Structures**, ACI SP-188, Eds. C.W. Dolan, S.H. Rizkalla and A. Nanni, pp. 229-240.
- [6] Monti, G., Nistico, N. and Santini, S. (in press), "Design of FRP Jackets for Upgrade of Circular Bridge Piers," *ASCE Journal of Composites in Construction*.
  - [7] Japan Concrete Institute (1998), Technical Report of Continuous Fiber Reinforced Concrete.
  - [8] Li, Y-F. and Sung, Y-Y (2001), "A Study on the Shear-Failure Circular Section Bridge Column Retrofitted by Using CFRP Jacketing," *Proceedings of FRP Composites in Civil Engineering, CICE I*, pp. 825-832.
  - [9] Priestley, M.J.N., Seible, F., and Chai, Y.H., (1992). "Design Guidelines for Assessment Retrofit and Repair of Bridges for Seismic Performance," Structural Systems Research Project, Report No. SSRP-92/01, University of California, San Diego.
  - [10] Seible, F., Innamarato, D., Baumgartner, J., Karbhari, V. and Sheng, L.H. (1999), "Seismic Retrofit of Flexural Bridge Spandrel Columns Using Fiber Reinforced Polymer Composite Jackets," in **Fiber Reinforced Polymer for Reinforced Concrete Structures**, ACI SP-188, Eds. C.W. Dolan, S.H. Rizkalla and A. Nanni, pp. 919-931.

## **CHAPTER 6: STRUCTURAL TEST PROTOCOLS AND ASSESSMENT**

### **6.1 Introduction**

Although the potential of composite retrofit schemes can be approximately evaluated through analytical computation of effectiveness through the use of pertinent models, it must be noted that models, to date, do not capture the complete mechanisms of response. Further, because the actual performance of composite jackets depends intrinsically on the details of fabrication it is essential that the performance of composite retrofit schemes be evaluated through actual structural tests. There are a large number of test protocols developed by individual manufacturers of composite jackets, materials suppliers, and even academic laboratories, varying in the approach of specimen scale, method of load introduction, number of cycles required per ductility level, amount of dead load etc. Because of these variations and the lack of a comprehensive and widely accepted baseline for testing there is a level of difficulty in comparing results.

In order to fill this set of lacunae, two major organizations have presented criteria for the conduct and evaluation of structural tests. The International Conference of Building Officials (ICBO) Evaluation Service has developed a set of criteria presented in AC125 [1] which relate to the seismic retrofit of columns in buildings as related to buildings, whereas under contract to the Federal Highway Administration, the Civil Engineering Research Foundation (CERF) under the aegis of the Highway Innovative Technology Evaluation Center (HITEC) developed through the use of a consensus panel (consisting of representatives of State Departments of Transportation, and leading academics) a test protocol and method of evaluation of structural performance [2] for bridge columns. Since the latter was developed in conjunction with the states representing AASHTO it is often considered to be the definitive testing and assessment methodology for bridge columns. A brief synopsis of both sets of criteria as well as a summary of tests conducted following the general principles of the HITEC criteria are presented in this chapter.

### **6.2 Acceptance Criteria Pursuant To AC125**

The ICBO criteria serve as guidelines on implementing performance features based on Section 104.2.8 of the Uniform Building Code, Section 104.11 of the International Building Code and Section R104.11 of the International Residential Code. Although AC215 addresses the strengthening of concrete and masonry using composite systems, only aspects related to seismic retrofit are discussed in this section. It is noted that AC125 does not as such provide criteria for assessment of performance, rather it provides a framework on the basis of which a jacketing system could be designed following general design rules presented in the document, and then tested with results to be assessed by a competent authority for applicability to the project under consideration.

Both flexural and shear tests are required for qualification with the requirements being that the column specimens be configured to induce flexural limit states in cantilever or double fixity modes for flexural strengthening, and shear limit states in double fixity for shear strengthening. Although no specific details for the specimen are given the procedure requires that "extremes of dimensional, reinforcing, and strength parameters" be considered. Lateral loads are required to be applied following the procedure depicted in Figure 6.1.

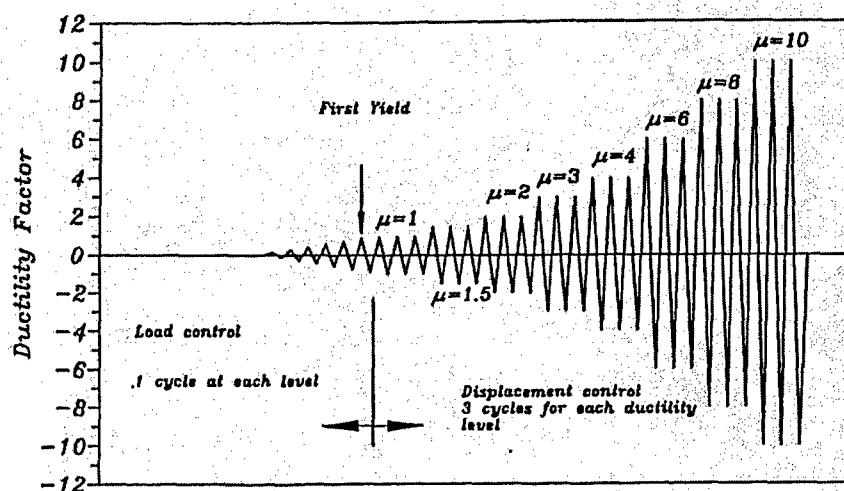


Figure 6.1: Test Sequence of Imposed Displacement [1]

The procedure restricts enhancement of flexural ductility through the application of composite material to circular columns, and rectangular columns where the aspect ratio does not exceed 1.5.

### **6.3 Test Requirements and Criteria for Structural Evaluation Pursuant to HITEC Criteria**

In contrast to AC125 [1] the HITEC protocol [2] defines both details of test methodology and criteria for the assessment of results. It thus provides a comprehensive set of guidelines for assessment of individual systems as well as the comparison of competing systems on the basis of a documented set of performance targets.

The protocol specifies that the evaluation of structural efficiency of the different systems needs to be conducted on the basis of large-scale laboratory tests. At a minimum, systems should be assessed on the basis of performance for three critical failure modes – shear failure, flexural hinge failure, and lap splice failure to show that the systems can successfully provide shear capacity enhancement, lap splice clamping, plastic hinge confinement and column bar buckling restraint, respectively. In order to ensure that tests conducted on different systems are not only structurally appropriate, but also comparable between systems, the protocol specifies ranges for critical test parameters. Since in reinforced concrete, damage and failure mechanisms are directly dependent on reinforcement detailing and on concrete properties (particularly those properties related to aggregate size), a minimum level of 1/3 scale specimens is required to provide meaningful data with column diameters being between 1 and 6 feet. Shear spans for flexure are required to exceed 4 feet, whereas those for shear are to be less than 3 feet. In case of non-circular columns, the side aspect ratio is not to exceed 2:1, considering that additional mechanisms such as dowels are necessary to ensure confinement over longer lengths. Reinforcement ratio in the concrete columns is restricted to values between 1 and 3% with lap splice lengths of 20-40  $d_b$  ( $d_b$  = bar diameter). The axial load ratio is



specified as between 10 and 30% of the product of gross concrete area and nominal concrete strength.

Acknowledging the difference in response between circular and rectangular columns a test matrix that differentiates between them is required and is given in Table 6.1. It is noted that a similar set of tests is required for each non-conventional, or special, geometry, outside the configurations listed.

*Table 6.1: Test Matrix Showing Modes*

<b>Column Geometry</b>	<b>Shear</b>	<b>Flexure (Continuous)</b>	<b>Flexure (Lap Splice)</b>
Circular	1	1	1
Square/Rectangular	1	1	1

Representative column geometries and reinforcement details for the six cases listed in Table 6.1 are shown schematically in Figures 6.2 - 6.7.

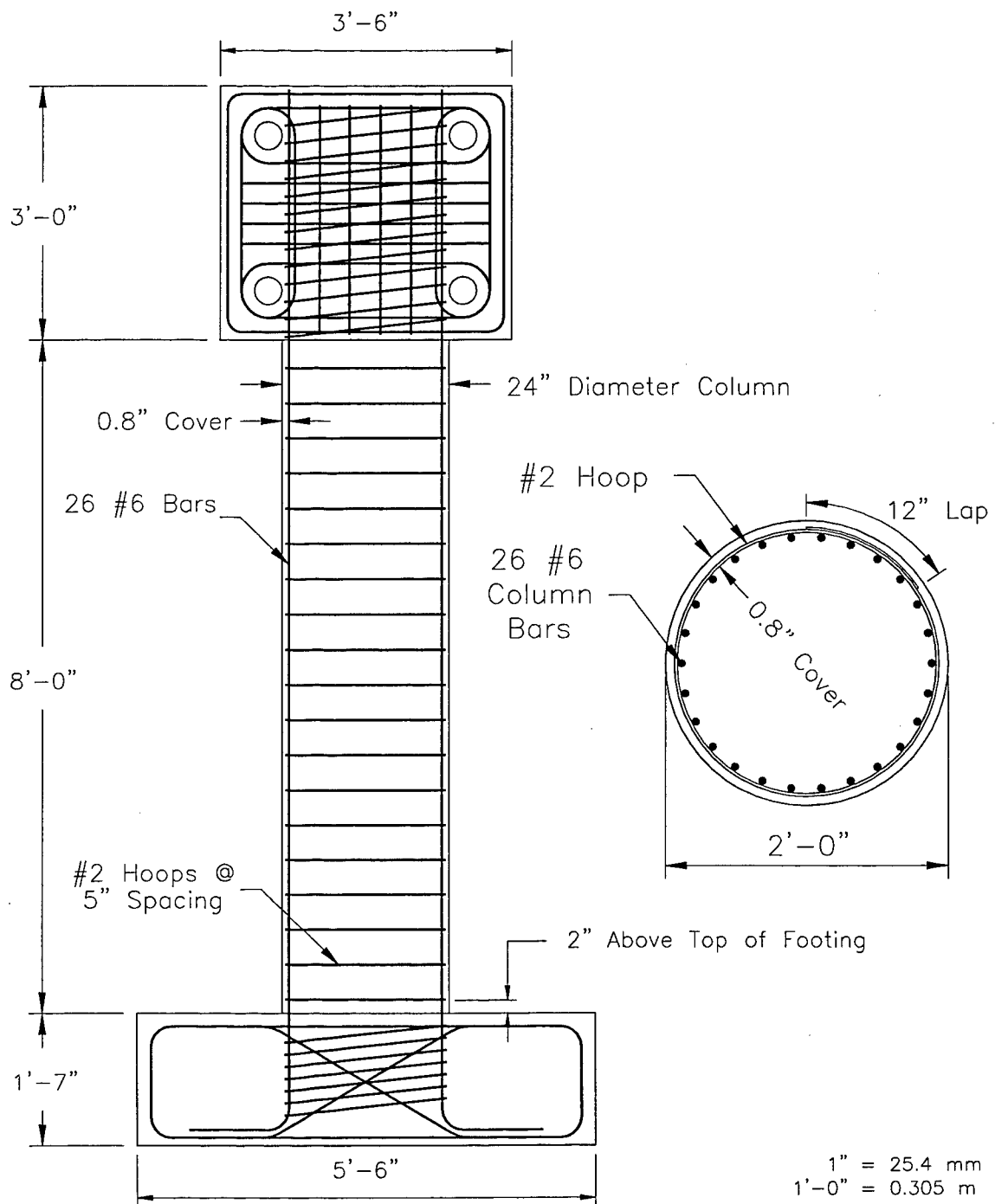
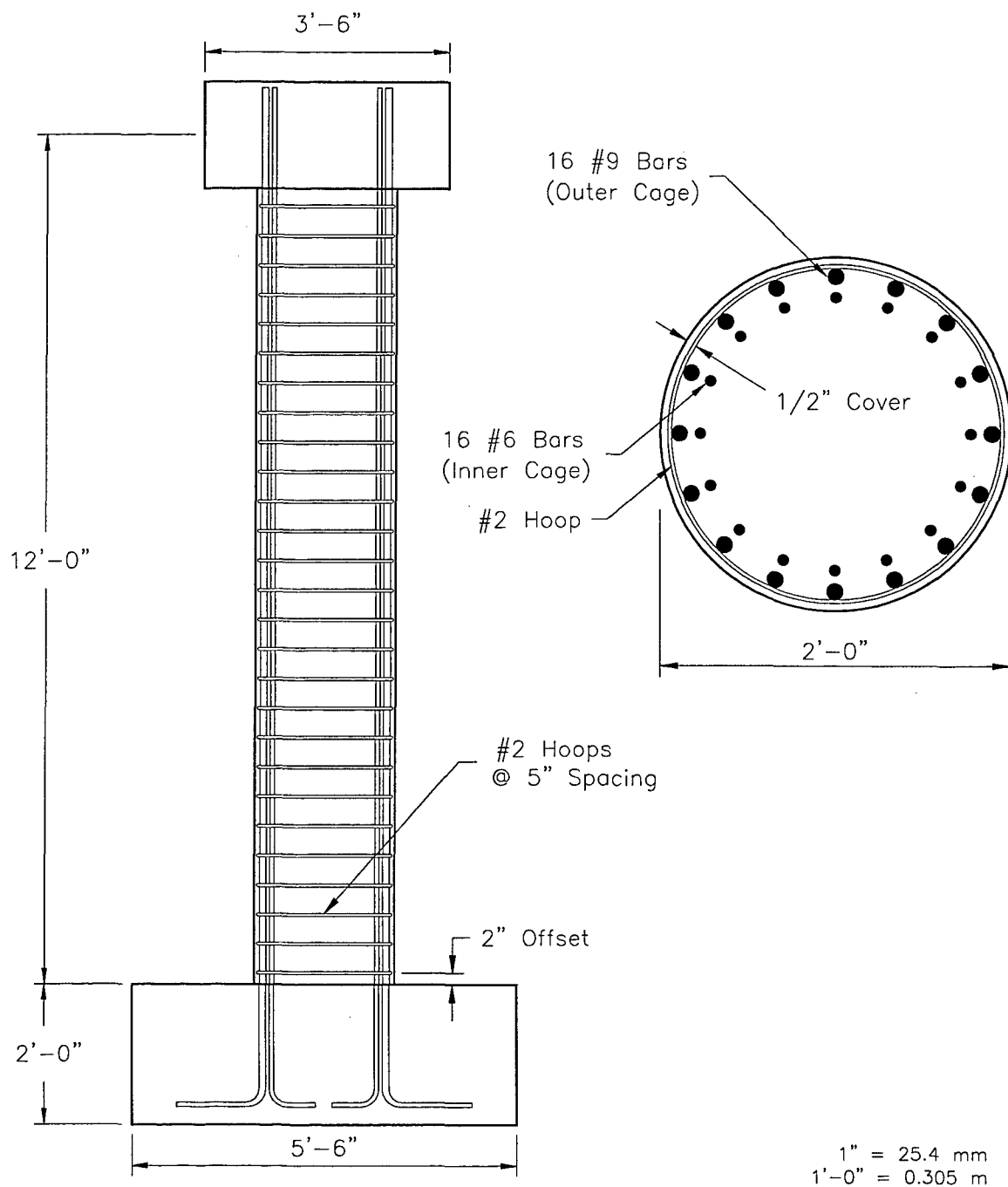
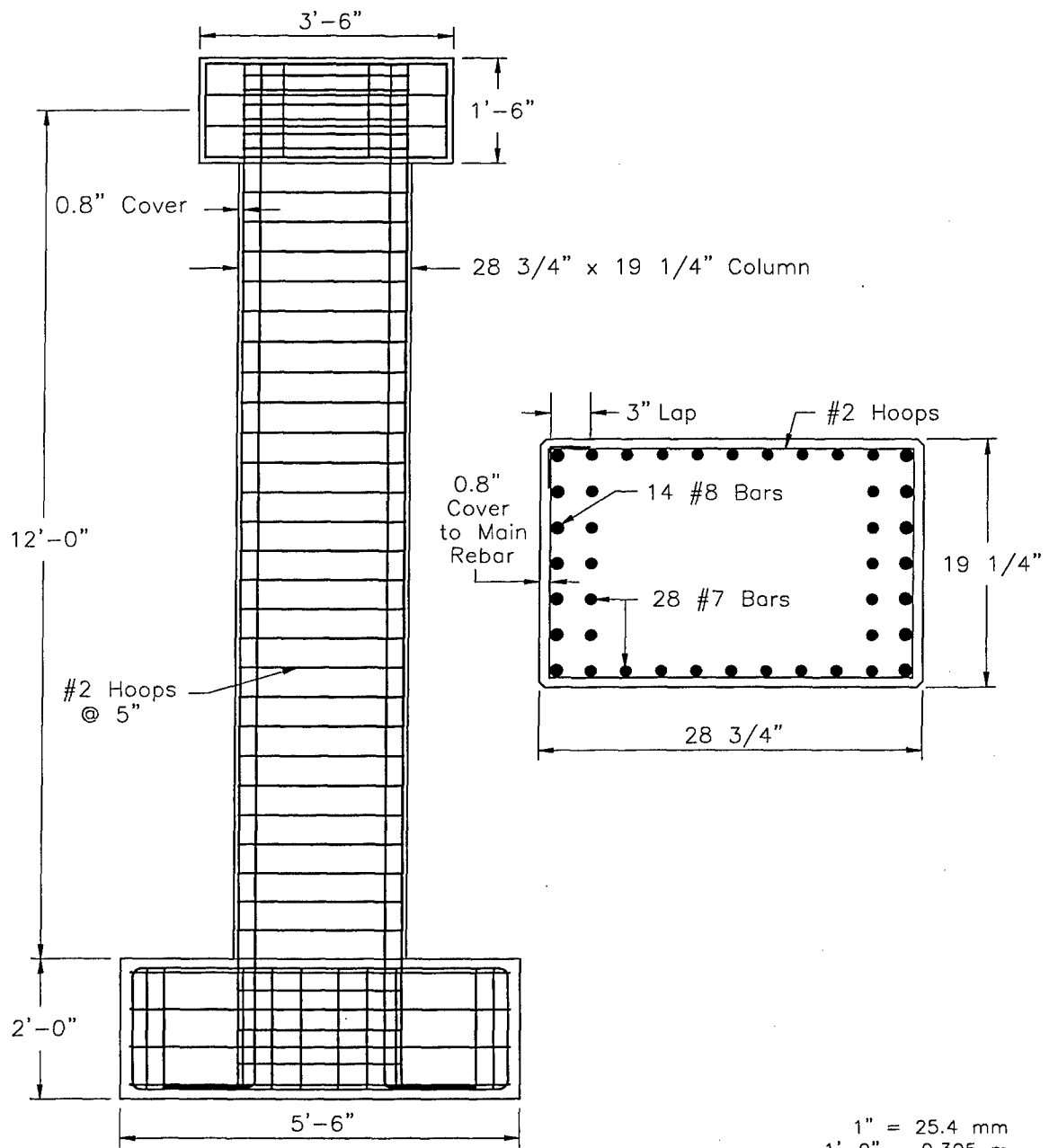


Figure 6.2: Representative Circular Shear Column Geometry and Reinforcement Details





*Figure 6.4: Representative Circular Flexure (Continuous) Column Geometry and Reinforcement Details*



*Figure 6.5: Representative Rectangular Flexure (Continuous) Column Geometry and Reinforcement Details*

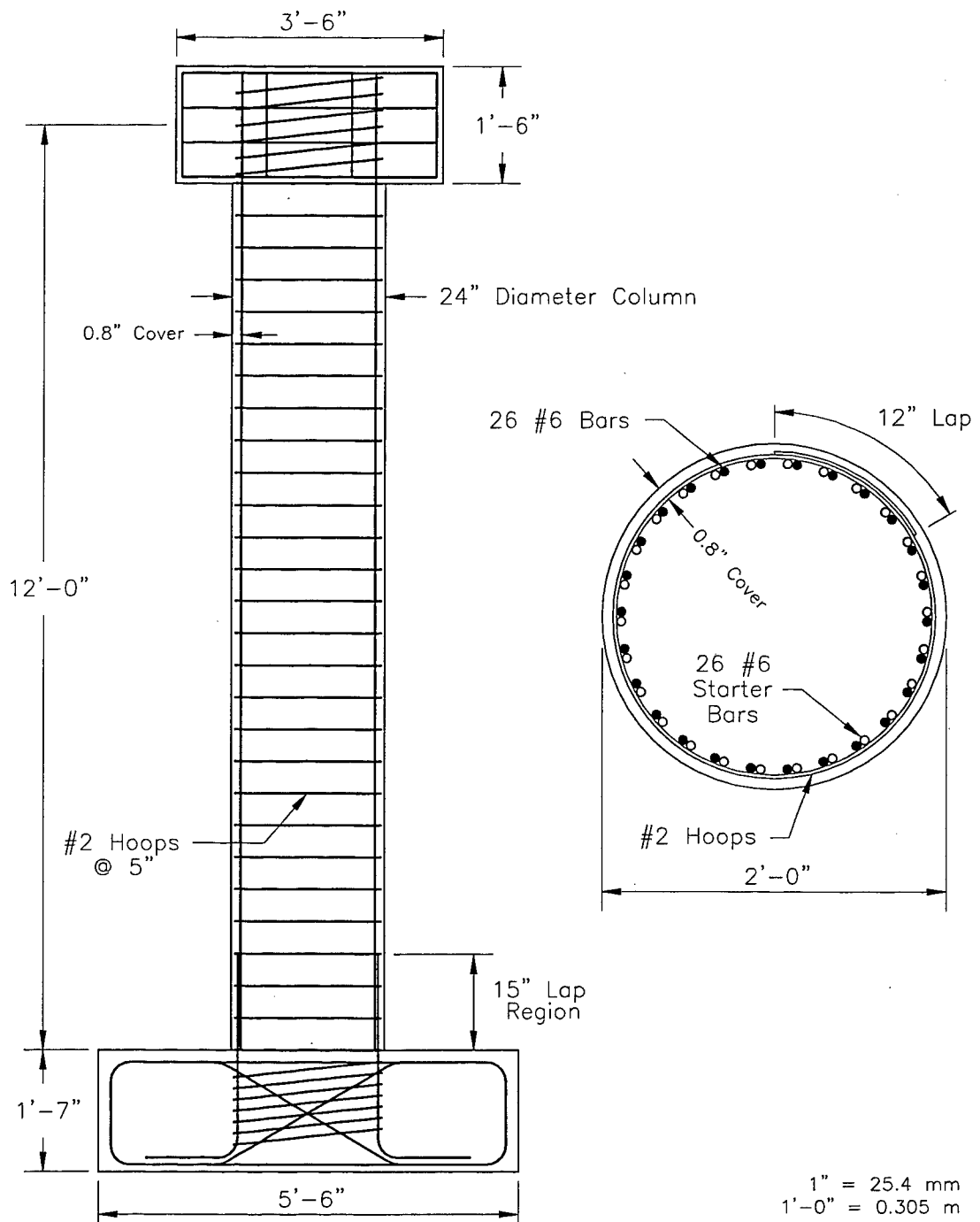


*Figure 6.6: Representative Circular Flexure (Lap Splice) Column Geometry and Reinforcement Details*

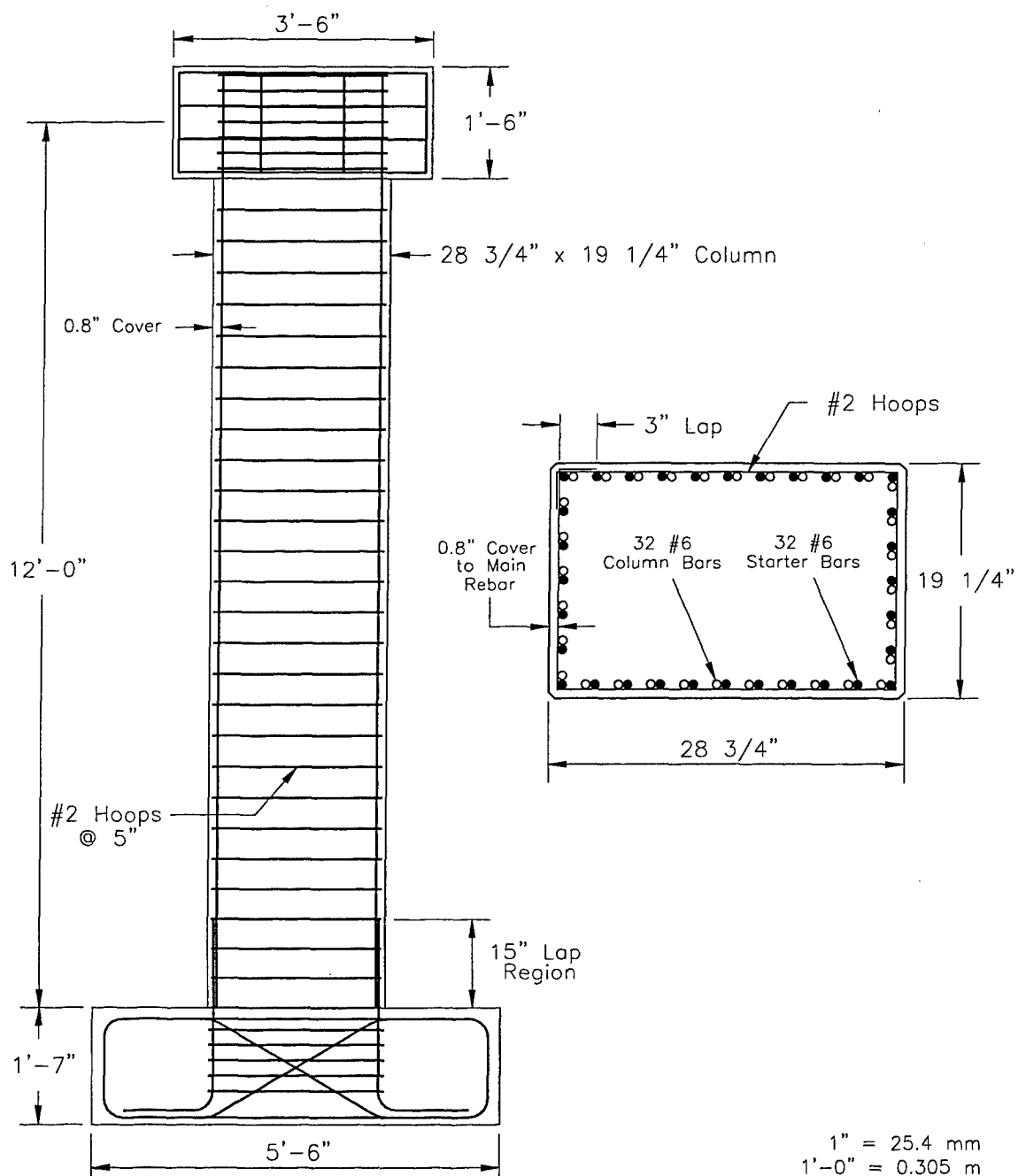


*Figure 6.7: Representative Rectangular Flexure (Lap Splice) Column Geometry and Reinforcement Details*

Schematics of typical test setups for shear and flexure are given, for purposes of reference, in Figures 6.8 and 6.9, respectively.

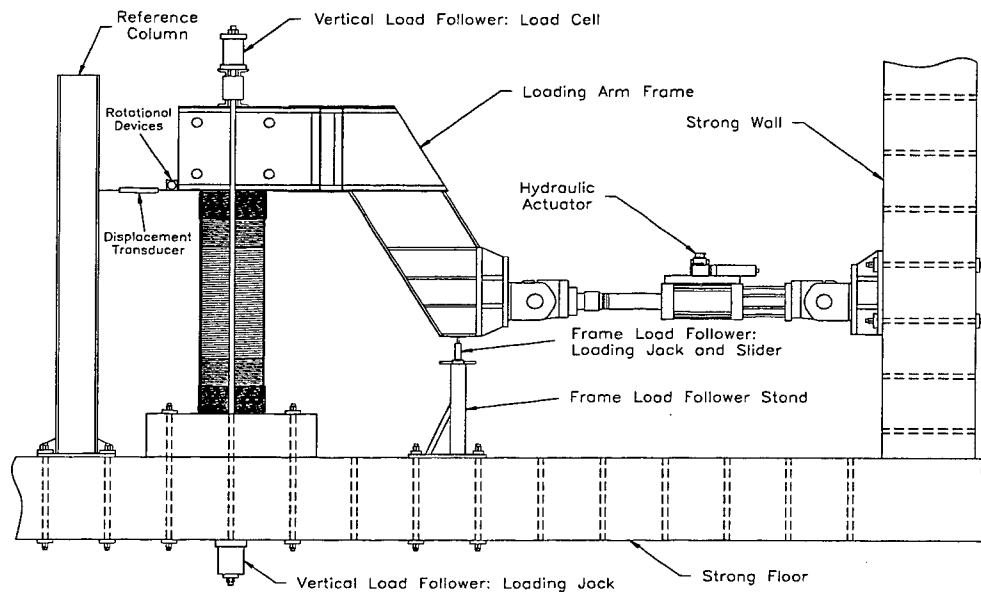


*Figure 6.8: Typical Test Setup for Shear Column*

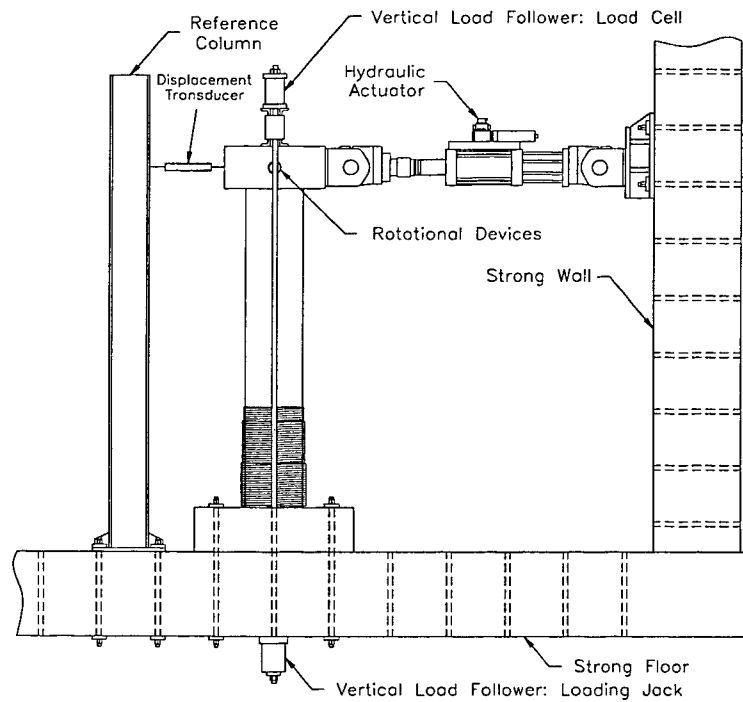


*Figure 6.9: Typical Test Setup for Flexure Column*



Since test results and failure modes are influenced significantly by the test sequence and procedure, it is important that test procedures are clearly defined, understood and followed. The performance of all retrofitted reinforced concrete columns is expected to be ductile through the formation of controlled inelastic rotations in predefined plastic hinges, the most important performance measure of which is ductility, which is defined in Figure 6.10.

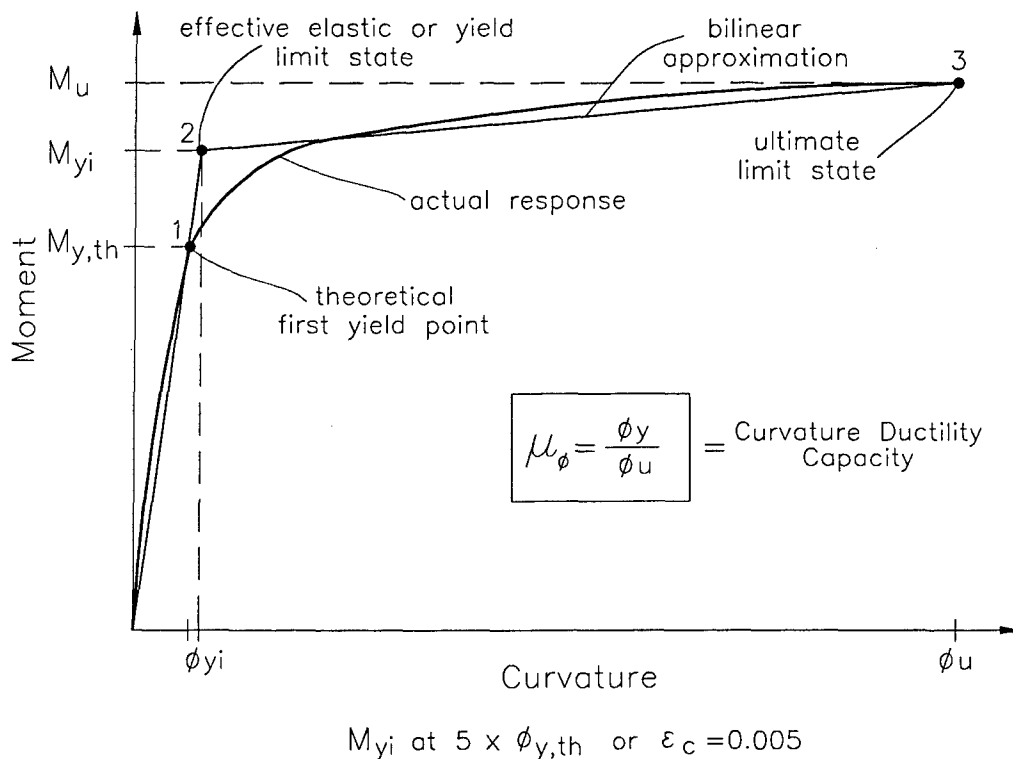


Figure 6.10: Definition of Ductility

The ultimate limit state, represented by point "3" in Figure 6.10, is assumed to be attained when the column capacity drops below 80% of the defined effective yield capacity. The effective elastic limit or yield limit state, represented by point "2" in Figure 6.10 is defined as the capacity at a given concrete strain and effective stiffness obtained at the first theoretical yield of the reinforcement. In a test, the first theoretical reinforcement yield can be calculated from sectional moment-curvature analysis and the required lateral load,  $f_{y,th}$ , to cause theoretical yield can be determined. The experimentally measured

displacement at first theoretical yield is then linearly extrapolated to the effective yield capacity obtained, again, from a moment curvature analysis at a concrete strain of 0.5%. Testing is required to subsequently proceed in displacement control following a loading history as outlined in Figure 6.11.

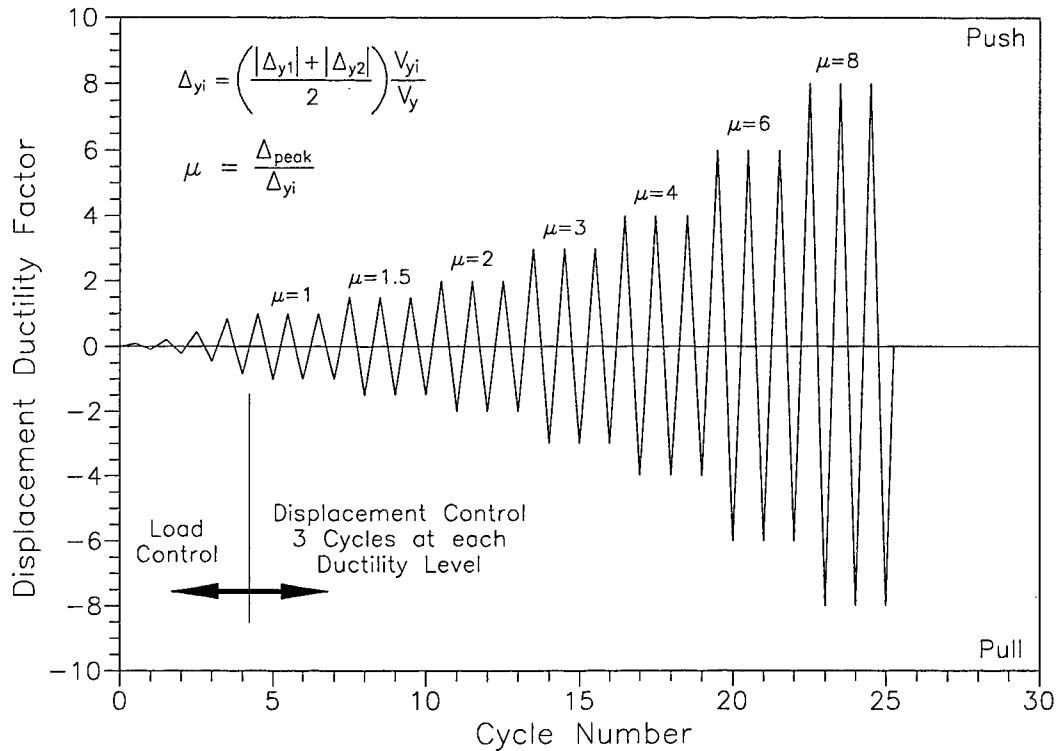


Figure 6.11: Recommended Loading History

In the force control test phase, load levels are required to be increased stepwise to the theoretical yield force level in 25% increments with one complete fully reversed cycle each. From the measured displacements  $\Delta_1$  and  $\Delta_2$ , a theoretical first yield, the effective yield displacement can be extrapolated as

$$\Delta_{yi} = \left( \frac{|\Delta_{y1}| + |\Delta_{y2}|}{2} \right) \frac{V_{yi}}{V_y}$$

and subsequent testing is specified to proceed in displacement control with three complete cycles to ductility levels  $\mu_\Delta = 1, 1.5, 2, 3, 4, 6, 8$ , etc. While this or similar

procedures may be used at testing facilities, the inherent danger is that a lot of energy in repetitive large displacement cycles is introduced into the test specimen which can result in premature low cycle fatigue of the column reinforcement itself. On the other hand, three full cycles are necessary at each level to establish stability of the hysteretic response. To be considered structurally sound, the retrofitted systems are required to meet the following criteria:

1. Displacement ductility, as defined in Figure 6.10, should be at least twice the displacement ductility of a comparable unretrofitted column specimen.
2. Displacement ductility of the retrofitted test specimen should be at a minimum 6, which represents 1.5 times the typical design ductility level of  $\mu_{\Delta} = 4$ .
3. Test specimens should fail in the pretest predicted failure mode and at displacement levels exceeding the design displacement. Failure is defined as a capacity reduction below 85% of the maximum test capacity.

#### **6.4 Overview of Tests Conducted Following the HITEC Protocol<sup>1</sup>**

Tables 6.2 – 6.7 compare parameters as set by the HITEC evaluation panel with those used in tests by the four systems evaluated (Xxsys, Fyfe, Hexcel, and CMI). The lack of an entry for a participant under a specific class of test signifies that no data was admitted under that classification. It is noted that in some cases, the parameters used for the individual tests do not meet the exact requirements of the specified test protocol, but are close enough to be admissible. The data was derived from reports submitted by each of the participants and are listed in the bibliography at the end of the chapter.

---

<sup>1</sup> Under the specifications set by CERF, the participants were required to submit data pertaining to tests completed that each felt met the requirements listed in the previous section. This data was assessed for compliance and was admitted if it met the overall criteria for testing. No new tests were conducted as part of this evaluation.

Table 6.2: Test Parameters for Circular Shear Columns

Parameter	Range	Fyfe	Hexcel	CMI	XXsys
Test Column Scale	1/3 to Full	40%	40%		40%
Column Diameter	1 ft to 6 ft	2 ft	2 ft		2 ft
Shear Span	H/D < 3	2	2		2
Longitudinal Reinforcement Ratio	1 to 5%	2.53%	2.53%		2.53%
Transverse Reinforcement Ratio	< 1%	0.17%	0.17%		0.17%
Axial Load Ratio $P / (f'_c \cdot A_g)$	5 to 30%	5.88%	5.88%		5.88%

Table 6.3: Test Parameters for Rectangular Shear Columns

Parameter	Range	Fyfe	Hexcel	CMI	XXsys
Test Column Scale	1/3 to Full	40%	40%		40%
Column Depth	1 ft to 6 ft	2'-0" x 1'-4"	2'-0" x 1'-4"		2'-0" x 1'-4"
Shear Span	H/D < 3	2	2		2
Side Aspect Ratio	1:1 to 1:2	1:1½	1:1½		1:1½
Longitudinal Reinforcement Ratio	1 to 5%	2.52%	2.52%		2.52%
Transverse Reinforcement Ratio	< 1%	0.22%	0.22%		0.22%
Axial Load Ratio $P / (f'_c \cdot A_g)$	5 to 30%	5.94%	5.94%		5.94%

Table 6.4: Test Parameters for Circular Flexure (Continuous) Columns

Parameter	Range	Fyfe	Hexcel	CMI	XXsys
Test Column Scale	1/3 to Full				40%
Column Depth	1 ft to 6 ft				2 ft
Shear Span	H/D > 4				6
Longitudinal Reinforcement Ratio	1 to 5%				5.09%
Transverse Reinforcement Ratio	< 1%				0.17%
Axial Load Ratio $P / (f'_c \cdot A_g)$	5 to 30%				17.68%

Table 6.5: Test Parameters for Rectangular Flexure (Continuous) Columns

Parameter	Range	Fyfe	Hexcel	CMI	XXsys
Test Column Scale	1/3 to Full	40%	40%		40%
Column Depth	1 ft to 6 ft	28 <sup>3</sup> / <sub>4</sub> " x 19 <sup>1</sup> / <sub>4</sub> "	28 <sup>3</sup> / <sub>4</sub> " x 19 <sup>1</sup> / <sub>4</sub> "		28 <sup>3</sup> / <sub>4</sub> " x 19 <sup>1</sup> / <sub>4</sub> "
Shear Span	H/D > 4	5	5		5
Side Aspect Ratio	1:1 to 1:2	1:1½	1:1½		1:1½
Longitudinal Reinforcement Ratio	1 to 5%	5.03%	5.03%		5.03%
Transverse Reinforcement Ratio	< 1%	0.18%	0.18%		0.18%
Axial Load Ratio $P / (f'_c \cdot A_g)$	5 to 30%	14.46%	14.46%		14.46%

Table 6.6: Test Parameters for Circular Flexure (Lap Splice) Columns

Parameter	Range	Fyfe	Hexcel	CMI	XXsys
Test Column Scale	1/3 to Full			50%	40%
Column Diameter	1 ft to 6 ft			2 ft	2 ft
Shear Span	H/D > 4			4	6
Longitudinal Reinforcement Ratio	1 to 5%			1.95%	2.53%
Transverse Reinforcement Ratio	< 1%			0.18%	0.17%
Axial Load Ratio $P / (f'_c \cdot A_g)$	5 to 30%			7.29%	17.68%
Lap Splice Length	20d <sub>b</sub> to 40d <sub>b</sub>			20d <sub>b</sub> = 15 in.	20d <sub>b</sub> = 15 in.

Table 6.7: Test Parameter for Rectangular Flexure (Lap Splice) Columns

Parameter	Range	Fyfe	Hexcel	CMI	XXsys
Test Column Scale	1/3 to Full	40%	40%		40%
Column Depth	1 ft to 6 ft	28 <sup>3</sup> / <sub>4</sub> " x 19 <sup>1</sup> / <sub>4</sub> " 19 <sup>1</sup> / <sub>4</sub> " x 28 <sup>3</sup> / <sub>4</sub> "	28 <sup>3</sup> / <sub>4</sub> " x 19 <sup>1</sup> / <sub>4</sub> " 19 <sup>1</sup> / <sub>4</sub> " x 28 <sup>3</sup> / <sub>4</sub> "		28 <sup>3</sup> / <sub>4</sub> " x 19 <sup>1</sup> / <sub>4</sub> "
Shear Span	H/D > 4	5 7 <sup>1</sup> / <sub>2</sub>	5 7 <sup>1</sup> / <sub>2</sub>		5
Side Aspect Ratio	1:1 to 1:2	1:1 <sup>1</sup> / <sub>2</sub> 1:0.67	1:1 <sup>1</sup> / <sub>2</sub> 1:0.67		1:1 <sup>1</sup> / <sub>2</sub>
Longitudinal Reinforcement Ratio	1 to 5%	5.03%	5.03%		5.03%
Transverse Reinforcement Ratio	< 1%	0.18%	0.18%		0.18%
Axial Load Ratio $P / (f'_c \cdot A_g)$	5 to 30%	14.46%	14.46%		14.46%
Lap Splice Length	20d <sub>b</sub> to 40d <sub>b</sub>	20d <sub>b</sub> = 15 in.	20d <sub>b</sub> = 15 in.		20d <sub>b</sub> = 15 in.

## 6.5 Assessment of Performance

An overall assessment of performance, as measured by comparison with three specific criteria required, is provided for the systems tested in Tables 6.8 – 6.14. Comparisons with un-retrofitted (i.e. as-built) column specimens are provided in each case. It should be noted that  $\Delta_{yi}$  values vary between sets of these tests thus influencing the ultimate values of ductility,  $\mu_{\Delta}$ .

Table 6.8: Overall Performance Evaluation of Circular Shear Test Columns

System	Theoretical Ideal Yield Displacement (in.) 2	Unretrofitted "As-Built" Column				Retrofitted Column			Performance Criteria		
		Ideal Yield Displacement (in.) 3	Ultimate Ductility Capacity ( $\mu_{\Delta}$ ) 4	Ultimate Displacement (in.) 5	Ideal Yield Displacement (in.) 6	Ultimate Ductility Capacity ( $\mu_{\Delta}$ ) 7	Ultimate Displacement (in.) 8		① $\frac{\text{Column 8}}{\text{Column 5}} \geq 2$	② $\frac{\text{Column 8}}{4 \times \text{Col 2}} \geq 1.5$	③ Column 8
Fyfe <sup>a</sup> Column 1 Column 2	0.341	0.727	1	0.727	0.876	6	5.256		7.2	3.9	6.0
	0.341	0.727	1	0.727	0.703	8	5.624		7.7	4.1	8.0
Hexcel <sup>a</sup> Column 1 Column 2	0.341	0.727	1	0.727	0.876	6	5.256		7.2	3.9	6.0
	0.341	0.727	1	0.727	0.703	8	5.624		7.7	4.1	8.0
CMI											
XXsys <sup>b</sup>	0.233	0.414	2	0.828	0.399	10.5	4.190		5.1	4.5	10.5

Notes:

a: Grade 60 longitudinal reinforcement

b: Grade 40 longitudinal reinforcement

Column 2 jacket thickness slightly less than that of column 1



Table 6.9: Overall Performance Evaluation of Rectangular Shear Test Columns

System	Theoretical Ideal Yield Displacement (in.) 2	Unretrofitted "As-Built" Column				Retrofitted Column			Performance Criteria		
		Ideal Yield Displacement (in.) 3	Ultimate Ductility Capacity ( $\mu_d$ ) 4	Ultimate Displacement (in.) 5	Ideal Yield Displacement (in.) 6	Ultimate Ductility Capacity ( $\mu_d$ ) 7	Ultimate Displacement (in.) 8	Column 8 Column 5 $\geq 2$	Column 8 Column 8 $\geq 1.5$	Column 8	Column 8
1											
Fyfe <sup>a</sup>	0.317	0.69	1.5	1.035	0.563	8	4.504	4.4	3.6	8.0	
Hexcel <sup>a</sup>	0.317	0.69	1.5	1.035	0.563	8	4.504	4.4	3.6	8.0	
CMI											
XXsys <sup>b</sup>	0.208	0.44	3	1.320	0.36	12	4.320	3.3	5.2	12.0	

Notes:

a: Grade 60 longitudinal reinforcement

b: Grade 40 longitudinal reinforcement

Table 6.10: Overall Performance Evaluation of Circular Flexure (Continuous Reinforcement) Test Columns

System	Theoretical Ideal Yield Displacement (in.) 2	Unretrofitted "As-Built" Column			Retrofitted Column			Performance Criteria	
		Ideal Yield Displacement (in.) 3	Ultimate Ductility Capacity ( $\mu_{\Delta}$ ) 4	Ultimate Displacement (in.) 5	Ideal Yield Displacement (in.) 6	Ultimate Ductility Capacity ( $\mu_{\Delta}$ ) 7	Ultimate Displacement (in.) 8	$\frac{\text{Column 8}}{\text{Column 5}}$ $\geq 2$	$\frac{\text{Column 8}}{4 \times \text{Col 2}}$ $\geq 1.5$
1									
Fyfe									
Hexcel									
CMI									
XXsys <sup>1</sup>	1.633	2.24	1.5	3.360	2.24	6.86	15.366	4.6	2.4
								6.9	

Notes:

1: Repaired Column

Table 6.11: Overall Performance Evaluation of Rectangular Flexure (Continuous Reinforcement)

System	Theoretical Ideal Yield Displacement (in.) 2	Unretrofitted "As-Built" Column			Retrofitted Column			Performance Criteria		
		Ideal Yield Displacement (in.) 3	Ultimate Ductility Capacity ( $\mu_{\Delta}$ ) 4	Ultimate Displacement (in.) 5	Ideal Yield Displacement (in.) 6	Ultimate Ductility Capacity ( $\mu_{\Delta}$ ) 7	Ultimate Displacement (in.) 8	① $\frac{\text{Column 8}}{\text{Column 5}}$ $\geq 2$	② $\frac{\text{Column 8}}{4 \times \text{Col 2}}$ $\geq 1.5$	③ Column 8
Fyfe	0.841	1.22	3	3.660	1.1	6	6.600	1.8	2.0	6.0
Hexcel	0.841	1.22	3	3.660	1.1	6	6.600	1.8	2.0	6.0
CMI										
XXsys	0.841	1.22	3	3.660	1.2	7	8.400	2.3	2.5	7.0

Table 6.12: Overall Performance Evaluation of Circular Flexure (Lap Spliced Reinforcement) Test Columns

System	Theoretical Ideal Yield Displacement (in.) 2	Unretrofitted "As-Built" Column			Retrofitted Column			Performance Criteria		
		Ideal Yield Displacement (in.) 3	Ultimate Ductility Capacity ( $\mu_{\Delta}$ ) 4	Ultimate Displacement (in.) 5	Ideal Yield Displacement (in.) 6	Ultimate Ductility Capacity ( $\mu_{\Delta}$ ) 7	Ultimate Displacement (in.) 8	① $\frac{\text{Column 8}}{\text{Column 5}} \geq 2$	② $\frac{\text{Column 8}}{4 \times \text{Col 2}} \geq 1.5$	③ Column 8
1										
Fyfe										
Hexcel										
CMI Column 1 Column 2 <sup>a</sup>	0.667 0.667	0.625 0.625	1 1	0.625 0.625	0.63 0.63	5.7 6	3.563 3.750	5.7 6.0	1.3 <sup>b</sup> 1.4 <sup>b</sup>	5.7 6.0
XXsys Column 1 Column 2 <sup>a</sup>	1.127 1.127	1.3 1.3	1.5 1.5	1.950 1.950	1.30 1.00	7.5 10	9.750 10.000	5.0 5.1	2.2 2.2	7.5 10.0

Notes:

a: Column 2 jacket thickness slightly greater than that of Column 1

b: Does not meet criterion 2 completely

Table 6.13: Overall Performance Evaluation of Rectangular Flexure (Lap Spliced Reinforcement) Test Columns

System	Theoretical Ideal Yield Displacement (in.) 2	Unretrofitted "As-Built" Column			Retrofitted Column			Performance Criteria		
		Ideal Yield Displacement (in.) 3	Ultimate Capacity ( $\mu\Delta$ ) 4	Ultimate Displacement (in.) 5	Ideal Yield Displacement (in.) 6	Ultimate Capacity ( $\mu\Delta$ ) 7	Ultimate Displacement (in.) 8	Column 8 Column 5 $\geq 2$	Column 8 4xCol 2 $\geq 1.5$	Column 8
Fyfe Column 1 <sup>a</sup> Column 2 <sup>b</sup>	0.821	0.892	1	0.892	0.773	10	5.256	8.7	2.4	10.0
	1.179	1.103	2	2.206	0.93	8	5.624	3.4	1.6	8.0
Hexcel <sup>a</sup> Column 1 <sup>a</sup> Column 2 <sup>b</sup>	0.821	0.892	1	0.892	0.773	10	5.256	8.7	2.4	10.0
	1.179	1.103	2	2.206	0.93	8	5.624	3.4	1.6	8.0
CMI										
XXsys	0.821	0.892	1	0.892	0.76	8	6.080	6.8	1.9	8.0

Notes:

a: Loading in the strong direction

b: Loading in the weak direction

## References

- [1] AC125 (2001), Acceptance Criteria for Concrete and Reinforced and Unreinforced Masonry Strengthening Using Fiber-Reinforced Polymer (FRP) Composite Systems, ICBO Evaluation Service.
- [2] HITEC Evaluation Plan for Composite Column Wrap Systems, CERF, 1997

## Bibliography

- [1] Shkurti, F. P., Lin, Y., Gamble, W. L. and Hawkins, N.M. (1995), "Testing of Bridge Piers Poplar Street Bridge Approach East St. Louis, IL", A Report to The Illinois Department of Transportation on Project IHR 330, University of Illinois of Urbana-Champaign.
- [2] Xiao, Y. and Martin, G. C. (1994), "Compression Test Results of Concrete Stub Columns Confined In Snap-Tite Composite Jackets", Final Testing Report to NCF Industries, Inc., University of Southern California.
- [3] Xiao, Y., Martin, G.R., Yin, Z. and Ma, R. (1995), "Bridge Column Retrofit Using Snap-Tite Composite Jacketing for Improved Seismic Performance", Report No. USC-SERR95/02, University of Southern California.
- [4] Priestley, M.J., and Seible, F. (1993), "High Strength Fiber", Final Report for Contract Number 59P841, Seqad Engineering Inc. for Fyfe Associates, Inc.
- [5] Priestley, M.J.N. and Seible, F. (undated) "Column Retrofit Using Prestressed Fiberglass/Epoxy Jackets", Fyfe Associates, Inc., University of California, San Diego.
- [6] Priestley, M.J.N. and Seible, F. (1991), "High Strength Fiber Repair of Circular Shear Tests", Research Report to Caltrans Under Contract Number 59P841, Fyfe Associates, Inc.
- [7] Priestley, M.J.N. and Seible, F. (1993), "Review of Reports on "High Strength Fiber Wrap System", Seqad Consulting Engineers, Inc. Report
- [8] Priestley, M.J.N. and Seible, F. (1993), "Design Aids for Retrofit of Columns Using Hexcel/Fyfe Fiber/ Epoxy Jackets", Report No. #93/12, Seqad Consulting Engineers.
- [9] Priestley, M.J.N. and Seible, F. (1993), "Repair of Shear Column Using Fiberglass/Epoxy Jacket and Epoxy Injection", Report No. #93/04, Seqad Consulting Engineers.
- [10] Priestley, M.J.N. and Seible, F. (1990), "Flexural Test of a High Strength Fiber Retrofitted Column", Report No. #90/06, Seqad Consulting Engineers.
- [11] Seible, F. (1992), "Rectangular Shear Column Test Report and (2) Square or Octagonal Columns", Seqad Consulting Engineers Report.
- [12] Priestley, M.J.N. and Seible, F. (1996), "Axial Load Characteristics of Rectangular Columns Wrapped With Tyfo-S Jackets", Report No. 96/04, Seqad Consulting Engineers.
- [13] Priestley, M.J.N. and Seible, F. (1993), "Seismic Retrofit of Bridge Columns Using High Strength Fiberglass/Epoxy Jackets", Report No. #93/07, Seqad Consulting Engineers.

- [14] Priestley, M.J.N. and Seible, F. (1991), "Shear Column Test No. 2", Report No. #91/07, Seqad Consulting Engineers.
- [15] Priestley, M.J.N. and Seible, F. (undated) "Column Seismic Retrofit Using Fiberglass/Epoxy Jackets, University of California, San Diego, Report to Fyfe Co.
- [16] Priestley, M.J.N. and Seible, F. (1992), "High Strength Fiber Rectangular Column Shear and No-Lap Splice Flexural Tests", Report to Caltrans Under Contract Number 59P841, Fyfe Associates, Inc.
- [17] Seible, F., Hegemier, G., Priestley, M.J.N. and Innamorato, D. (1994), "Seismic Retrofitting of Squat Circular Bridge Piers With Carbon Fiber Jackets", Report No. ACCT-94/04, University of California, San Diego.
- [18] Seible, F., Hegemier, G., Priestley, M.J.N., Innamorato, D., Weeks, J. and Policelli, F. (1994), "Carbon Fiber Jacket Retrofit Test of Circular Shear Bridge Column, CRC-2", Report No. ACTT-94/02, University of California, San Diego.
- [19] Seible, F., Hegemier, G., Priestley, M.J.N. and Innamorato, D. (1995), "Rectangular Carbon Fiber Jacket Retrofit Test of a Shear Column With 2.5% Reinforcement", Report No. ACTT-95/05, University of California, San Diego.
- [20] Seible, F., Hegemier, G., Priestley, M.J.N., Innamorato, D. and Ho, F. (1995), "Carbon Fiber Jacket Retrofit Test of Circular Flexural Columns With Lap Spliced Reinforcement", Report No. ACTT-95/04, University of California, San Diego.
- [21] Seible, F., Hegemier, G., Karbhari, V., Policelli, F., Randolph, R., Belknap, F. and Innamorato, D. (1995), "Earthquake Retrofit of Bridge Columns With Continuous Carbon Fiber Jackets- Volume I, Executive Summary", Report No. ACTT-95/07, University of California, San Diego.
- [22] Seible, F. and Innamorato, D. (1995), "Earthquake Retrofit of Bridge Columns With Continuous Carbon Fiber Jackets- Volume II, Design Guidelines", Report No. ACTT-95/08, University of California, San Diego.
- [23] Karbhari, V., Hegemier, G., Belknap, F., Policelli, F. and Randolph, R. (1995), "Earthquake Retrofit of Bridge Columns With Continuous Carbon Fiber Jackets- Volume III, Materials", Report No. ACTT-95/09, University of California, San Diego.
- [24] Seible, F., Hegemier, G., Priestley, M.J.N., Innamorato, D. and Ho, F. (1995), "Advanced Composites Technology Transfer Consortium", Report No. ACTT-95/02, University of California, San Diego.
- [25] Seible, F., Hegemier, G., Priestley, M.J.N., Ho, F. and Innamorato, D. (1995), "Rectangular Carbon Jacket Retrofit of Flexural Column With 5% Continuous Reinforcement", Report No. ACTT-95/03, University of California, San Diego.

## CHAPTER 7: DURABILITY TEST PROTOCOLS

### 7.1 Introduction

Although FRP composites have been successfully used in markets such as corrosion equipment, the automotive, marine and aerospace sectors, there are critical differences in loading, environment and even the types of materials and processes used in these applications as compared to the materials-process-load combinations that are likely to be used in civil infrastructure applications. FRP composites have also been successfully applied in pipelines, underground storage tanks, building facades, and architectural components, and anecdotal evidence provides substantial reason to believe that if appropriately designed and fabricated, these systems can provide longer lifetimes and lower maintenance than equivalent structures fabricated from conventional materials. However, actual data on durability is sparse, not well documented, and in cases where available – not easily accessible to the civil engineer. In addition, there is a wealth of contradictory data published in a variety of venues that tends to confuse the practicing engineer. The reasons for the apparent contradictions on durability are related to reporting of data without sufficient detail of the actual materials used, use of different forms of materials and processing techniques, and even changes in the materials systems with time (especially as related to resin formulations which are specified only by generic names). There is also some evidence of rapid degradation of specific types of FRP composites when exposed to certain environments found in the civil engineering environment. Given that composites used in civil infrastructure applications, including for purposes of seismic retrofit, are likely to be fabricated and/or installed in the field, under ambient conditions without significant control of the environment during processing and cure, and that the structures are likely to face varied environmental conditions with almost no routine inspection, and very little maintenance, it is critical that the durability of these materials and the resulting systems is both characterized and



understood in terms of probable service life and deterioration of pertinent properties over time.

It should be noted that although the term durability is widely used, its meaning and implications are often ambiguous. Often it is erroneously taken to refer only to the effect of natural or solution based weathering/degradation of a composite, whereas in reality this is only a small aspect of the overall phenomenon. FRP composites (and their constituents) can be affected by a variety of factors (including those related to the natural and surrounding environment), and the actual effect of each of these factors, or combinations thereof, can be substantially effected by the presence or absence of defects or other damage to the composite (or constituents thereof). A variety of different constituent materials are commercially available and the appropriate combination of these constituents allows for the development of a FRP composite system that provides the performance attributes for its intended use. Thus, the durability of a material or structure is defined as its ability to resist cracking, oxidation, chemical degradation, delamination, wear, and/or the effects of foreign object damage for a specified period of time, under the appropriate load conditions, under specified environmental conditions. This concept is realized in design through the application of sound design principles and the principles of damage tolerance whereby levels of performance are guaranteed through relationships between performance levels and damage/degradation accrued over specified periods of time. In this sense, damage tolerance is defined as the ability of a material or structure to resist failure and continue performing at prescribed levels of performance in the presence of flaws, cracks or other forms of damage/degradation for a specified period of time under specified environmental conditions. The overall concept is shown schematically in Figure 7.1. The use of this concept allows for the design of a structure using performance values that change with time based on external influences as long as the values do not fall below prescribed minimum levels, thereby accommodating limited degradation that is likely to take place with any material system due to mechanical, physical, or chemical factors.

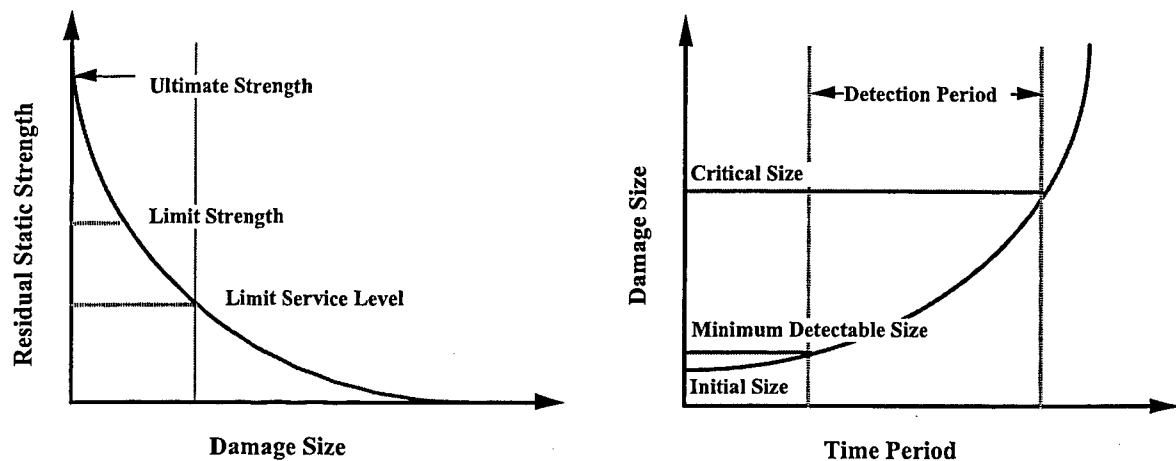


Figure 7.1: Schematic Showing Application of Concepts of Durability and Damage Tolerance to Design

Intrinsic to the determination of durability of a material, and the resulting system, are the definition of test methods and protocols for the characterization of pertinent properties and the assessment of deterioration under specific environmental conditions. Since the environmental conditions are likely to change with geographical location and time, and are difficult to reproduce reliably in a laboratory, simulated test conditions such as immersion in solution, exposure to dry heat etc. are often used for purposes of durability assessment. Three specific protocols for the determination of durability of composites used for the seismic retrofit of concrete columns are described in this chapter. Of the three the HITEC protocol is considered as the most comprehensive and extensively deliberated due to its being developed through participation of representatives from AASHTO member states.

## 7.2 Caltrans Test Matrix

The California Department of Transportation initiated a program for the evaluation of composite materials for seismic retrofit in 1995 [1-3] and later developed in collaboration with the Aerospace Corporation a set of durability tests and criteria [4]. The test matrix for environmental durability assessment required under this program is given in Table 7.1. Exposures are conducted on individual test panels of materials with edges sealed.

The effect of each exposure condition and period is evaluated through measurement of tensile properties (strength, modulus and ultimate strain), short-beam-shear strength, Shore D hardness, and glass transition temperature.

*Table 7.1: Durability Test Matrix*

<b>Environment</b>	<b>Test Condition</b>	<b>Duration of Exposure</b>
Water resistance	100% humidity at 38 C	1000, 3000 and 10000 hours
Salt water resistance	Immersion at 23 C	1000, 3000 and 10000 hours
Alkali resistance	Immersion in CaCO <sub>3</sub> at pH 9.5 and 23 C	1000, 3000 and 10000 hours
Dry heat resistance	Furnace at 60 C	1000, and 3000 hours
Fuel resistance	Immersion at 23 C	4 hours
Ultraviolet light resistance	Cycle between UV at 60 C and condensate at 40 C	4 hours per condition with 100 cycles
Freeze/Thaw resistance	Cycle between 100% humidity at 38 C and Freezer at -18 C	24 hour cycle for 20 cycles

The conditions for water resistance were chosen to represent an accelerated test. The salt water immersion was used to simulate effects of prolonged marine exposure with substitute ocean water prepared following ASTM D1141. CaCO<sub>3</sub> was used to create a pH of 9.5 for assessment of alkali resistance. The dry heat resistance conditions were selected to represent the maximum exposure temperature anticipated in service. Since degradation at this temperature was expected to be rapid a shorter period of total exposure (3000 hours rather than 10000 hours was chosen). UV exposure conditions were selected in accordance with ASTM G53 with exposure being one-sided. The freeze-thaw exposure conditions were developed to simulate effects of freezing following significant water absorption (attained by preconditioning of specimens at 100% humidity at 38 C for two weeks prior to the initiation of the exposure conditions [4]). The change from freeze to thaw conditions was achieved through placing the panels in a freezer at the beginning of a work day followed by its return to the humidity chamber at the end of the day, resulting in a cycle consisting approximately of 9 hours in the freezer and 15 hours in the humidity chamber [4] with very little control of intermediate ramps. It is noted that tests were not conducted immediately after removal from the exposure, but rather within 7 days of removal [4].

### 7.3 ICBO Test Matrix

AC125 [5] requires the determination of physical and mechanical properties of the composites for purposes of consideration in design criteria and limitations as listed in Table 7.2.

*Table 7.2: Test Details for Determination of "Physical Properties"*

Properties	Test Method	Number of Specimens
Tensile strength	ASTM D3039-95a	20
Tensile elongation	ASTM D3039-95a	20
Tensile modulus	ASTM D3039-95a	20
Coefficient of Thermal Expansion	ASTM D696-91 or E1142-97	5
Creep (3000 hours minimum)	ASTM D2900-95	5
Void content	ASTM D2584-94 or D3171-95	5
Glass Transition Temperature (T <sub>g</sub> )	ASTM D4065-95	20
Impact	ASTM D3029-94, Method I	5
Interlaminar Shear Strength	ASTM D2344-84	20

Specimen sets are restricted to those that exhibit a coefficient of variation (COV) of 6% or less with outliers to be treated per ASTM E178. In cases of material systems having a COV of greater than 6% AC 125 [5] requires that the listed number of specimens in Table 7.2 be doubled so as to consider the larger scatter bounds. Properties are required in each case to be determined both in the primary and the "cross" transverse direction. Since AC 125 [5] is not restricted just to seismic retrofit a criterion for impact is also added with the impact head being defined as being of 15.9 mm diameter. Impact coupons are to be of 102 mm x 152 mm size placed on supports of 76 mm x 127 mm. The minimum requirement for acceptance is a force of 250 lb-in at 0.1" thickness. Void content is restricted to a maximum of 6% and glass transition temperature is required to be a minimum of 140 F for both the control and exposed specimens.

The assessment of durability follows details listed in Table 7.3 with a minimum of 5 specimens being used for each condition and time period. Material properties are assessed through determination of tensile properties (ultimate strength, modulus, and

strain), short-beam-shear strength, and glass transition temperature. AC 125 [5] requires that as a criterion of acceptance all specimens show not less than 90% retention of properties after 1000 hours of exposure and not less than 85% retention after 3000 hours of exposure.

*Table 7.3: Details of Environmental Durability Tests*

<b>Exposure Condition</b>	<b>Relevant ASTM Specification</b>	<b>Test Conditions</b>	<b>Periods of Exposure</b>
Water resistance	D2247-97, E104-85	100% relative humidity, $100 \pm 2$ F	1000, 3000 hours
Saltwater resistance	D 1141-91, C581-94	Immersion at $73 \pm 2$ F	1000, 3000 hours
Alkali resistance	C581-94	Immersion in $\text{CaCO}_3$ at pH = 9.5 and $73 \pm 3$ F	1000, 3000 hours
<i>Dry heat resistance</i>	<i>D3045-92</i>	<i><math>140 \pm 5</math> F</i>	<i>1000, 3000 hours</i>

In addition to the conditions listed in Table 7.3 specimens are also to be tested after a minimum of 2000 hours weatherometer exposure with a minimum retention of 90% of the unexposed material properties. The weatherometer exposure follows ASTM G23-96 and uses a cycle of 102 minutes of light followed by 18 minutes of light and water spray at a black body temperature of 145 F. For purposes of freeze-thaw testing specimens are preconditioned at 100% relative humidity at 100 F for 3 weeks after which they are subject to 20 cycles at 0 F for a minimum of 4 hours and in a humidity chamber for a minimum of 12 hours at 100% relative humidity and 100 F. As before specimens are required to retain a minimum of 90% of their unexposed tensile properties (ultimate strength, modulus, and strain), short-beam-shear strength and glass transition temperature.

In cases where exposure to soil is possible in the actual application, a further test for alkaline soil following ASTM D3083-89, section 9.5 is required for 1000 hours with the 90% retention requirement for tensile properties (ultimate strength, modulus, and strain), short-beam-shear strength and glass transition temperature.

Fire-resistance, where applicable, is to be assessed according to Section 703 of the Uniform Building Code (UBC) or the International Building Code (IBC).

Fuel resistance, where applicable, is to be assessed according to ASTM C581-94 with immersion in a diesel reagent for a minimum of 4 hours.

In the case of prefabricated specimens adhesive lap strength is required to be assessed following ASTM D3165-95 using conditions and retention requirements of Table 7.2 and freeze-thaw and fuel resistance. This requirement would only apply to seismic retrofit in the case of adhesive bonding of prefabricated shells. Although AC125 [5] presents requirements of a bond test to the concrete substrate following ASTM C297-94 after exposures following Table 7.3, this is generally not applied to systems for seismic retrofit by ICBO.

#### **7.4 HITEC Test Matrix**

The HITEC evaluation protocol [6] is based on the assumption that composites used for the seismic retrofit of concrete columns are designed predominantly with fiber orientation in the hoop direction. Further, it considers that since the use of composites for the seismic retrofit of columns requires placement of the jackets around the column for purposes of confinement, processing details are likely to significantly affect material and system properties. In this case testing of flat coupons is unlikely to provide a clear indication of combined materials-systems effects and hence a NOL- (Naval Ordnance Laboratory) burst test is conducted on a 510 mm (20" nominal) internal diameter ring with internal pressurization which would result in the stressing of the material in a fashion closely simulating the system during concrete dilation. The details of the test specimen specifications are provided in Figure 7.1. It is emphasized that this configuration not only provides an assessment of materials performance in the actual structural configuration of use in the field, but also enables a direct characterization of process related defects and final failure mechanisms. Details on the test and its

applicability in this application are given by Policelli [7] and Karbhari [8]. It should be noted that the tensile strength,  $\sigma_{ult}$ , and hoop modulus,  $E_{hoop}$ , as characterized by the NOL-ring burst test can be determined as

$$\sigma_{ult} = \frac{P_{ult} (ID + t)}{2t} \quad \dots \quad (7.1)$$

$$E_{hoop} = s \left( \frac{ID + t}{2t} \right) \quad \dots \quad (7.2)$$

where  $P_{ult}$  is the ultimate burst pressure recorded, ID is the inner diameter of a NOL ring of thickness,  $t$ , and  $s$  is the slope of the pressure versus strain curve between levels of 1,000 and 6,000 microstrain.

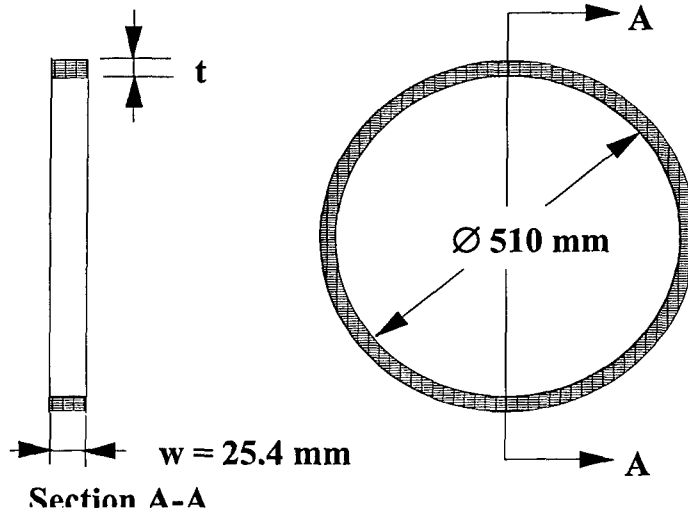


Figure 7.1: Schematic of the Burst Test Ring

In order to simulate conditions of actual jacket fabrication as much as possible specimens are required to be fabricated using procedures similar to those practiced by the manufacturer in the field, such that blanks of 178 mm height (7") and 510 mm (20") internal diameter are fabricated to enable the systems to be exposed to environmental conditions in the jacket, rather than ring, configuration. Once exposures are completed, 4 NOL-rings each of 25 mm (1") height are cut from the central portion of each blank with a fifth ring being also cut from the same section for specimens to be tested in short-beam-shear and for assessment of glass transition temperature ( $T_g$ ). In order to provide ease of

comparison and to reduce uncertainty due to operator judgement the glass transition temperature is to be determined from the peak of the  $\tan \delta$  curve resulting from Dynamic Mechanical Thermal Analysis conducted on specimens.

The use of test specimens from the central region of each test blank, rejecting edge areas, enables almost complete elimination of edge effects during environmental exposure which could, otherwise, result in nonuniformity and testing of specimens with moisture contents and attendant damage not likely to be encountered by the overall jacket in the field. In order to provide a standard baseline for design of test specimens for purposes of durability assessment, manufacturers are required to fabricate blanks to meet a predetermined internal pressure rating of 17.2 MPa (2,500 psi) for E-glass fiber based systems and 34.5 MPa (5,000 psi) for carbon fiber based systems with a maximum thickness constraint of 11.5 mm (0.45"). These specifications were selected to match existing Caltrans requirements [9] at the flat coupon level.

*Table 7.4: Details of Environmental Conditions*

<b>Exposure Condition</b>	<b>Test Details</b>	<b>Periods of Exposure</b>
Ambient Ageing	Conditioning in an environmental chamber at 23° C and 55% RH	6, 12 and 18 months
Water exposure	Immersion in water at 23° C	6, 12 and 18 months
Accelerated water exposure	Immersion in water at 60° C	6, 12 and 18 months
Concrete based alkaline exposure	Immersion in a concrete leachate at pH 10.5-11 at 23° C	6, 12 and 18 months
Simulated alkaline exposure	Immersion in a $\text{CaCO}_3 + \text{Ca(OH)}_2$ based alkaline solution at pH 9-9.5 at 23° C	6, 12 and 18 months
Freeze	Exposure at -26° C	6 and 12 months
Freeze-Thaw	Exposure between -26° C and +60° C after salt soak in a 5% NaCl solution for 5 weeks.	6 and 12 months

Environmental exposure conditions required under the HITEC protocol are listed in Table 7.4. All specimens are required to be tested using the burst tests (tensile strength strain and modulus), short-beam-shear tests, gravimetric moisture uptake, and DMTA for assessment of glass transition temperature. It is noted that the initial draft of the HITEC



procedure required a minimum retention of 85% but the requirement was modified in the final draft to being listed as a recommendation, leaving the final decision to the engineer.

Ambient ageing is assessed in the HITEC procedure since most composite systems used in seismic retrofit use an ambient cure in the field which will intrinsically result in changes in properties with time as cure progresses. It is noted that although this is not the case with the prefabricated shells, ambient cure is still used for the adhesive and therefore the system itself is still subject to these changes. The use of two alkaline solutions is based on the lack of clear definition as to the constituents of pore water and its actual effects. Whereas the first solution provides a pH that is also specified in the Caltrans and ICBO test protocols the HITEC panel was unconvinced about the realism of this simulation and desired a test using actual leachate from cured concrete as defined by the second alkaline solution. Similarly, the requirements for freeze-thaw were based on the number of cycles likely to be attained in the field rather than just the shorter requirement of 20 as given in the ICBO specifications.

## References

- [1] Sultan, M. (1997), "Evaluating Advanced Composites for Applications in Transportation Structures," SAMPE Journal, 33[3].
- [2] Sultan, M., Hawking, G., and Sheng, L. (1995), "Caltrans Program for the Evaluation of Fiber Reinforced Plastics for Seismic Retrofit and Rehabilitation of Structures," in the Proceedings of the FHWA National Conference.
- [3] Sultan, M., Sheng, L. and Steckel, G.L. (1997), "Evaluating Advanced Composites for Applications in Transportation Structures," in the Proceedings of the FHWA National Conference.
- [4] Steckel, G.L., Hawkins, G.F. and Bauer, J.L., Jr. ((1999), "Environmental Durability of Composites for Seismic Retrofit of Bridge Columns," Proceedings of the NIST Workshop on Standards Developments for the Use of Fiber

Reinforced Polymers for the Rehabilitation of Concrete and Masonry Structures, pp. 3/83-3-96.

- [5] AC125 (2001), Acceptance Criteria for Concrete and Reinforced and Unreinforced Masonry Strengthening Using Fiber Reinforced Polymer (FRP) Composite Systems, ICBO Evaluation Service.
- [6] Evaluation Plan for Composite Column Wrap Systems, Civil Engineering Research Foundation, Highway Innovative Technology Evaluation Center (1997).
- [7] Policelli, F. (1995), "Checkout of 20-Inch NOL Ring Equipment," Structural Systems Research Project, University of California, San Diego, Report ACTT/BIR-95/19.
- [8] Karbhari, V.M. (2000), "Composites in the Renewal of Civil Infrastructure – Materials, Manufacturing, Design and Durability," Proceedings of the 9<sup>th</sup> US-Japan Conference on Composite Materials, Mishima, Japan, pp. 41-48.
- [9] Caltrans Memorandum to Designers, 20-4 (1996), Attachment B: Composite Column Casing, and Standard Specification. I.48\_AENC.DOC

## CHAPTER 8: REVIEW OF HITEC DURABILITY RESULTS

### 8.1 Introduction

This chapter presents the results of the evaluation conducted to assess materials and durability characteristics of four specific systems through an assessment of system response after a variety of laboratory based exposures defined in the HITEC protocol presented in Chapter 7.

Four different systems encompassing a range of materials, forms, and processing techniques were investigated, as listed in Table 8.1.

*Table 8.1: Details of Column Wrap Systems*

Set	Process	Materials	Cure Conditions
A	Adhesive bonding of prefabricated sections	Unidirectional E-glass impregnated with polyester. Polyurethane adhesive with glass scrim	Ambient for adhesive
B	Wet layup of fabric	Woven fabric with reinforcement (E-glass) primarily in the warp direction and aramid tracers in weft direction	Elevated for prefabricated sections Ambient
C	Wet layup of fabric	E-glass woven fabric with reinforcement primarily in the warp direction	Ambient
D	Automated winding	12k Carbon/epoxy prepreg tow	Elevated temperature

All four systems represent commercially available sets, which have already been demonstrated in the field. System A is representative of the prefabricated class wherein a hollow circular cross-sectional shell is first fabricated under carefully controlled factory conditions, including elevated temperature cure over an extended period of time. This cylinder is then slit down the length to create an opening and after the addition of

adhesive to the inner surface is pulled over a column. Subsequent layers are added with the position of the slit being staggered to enable good overlap with the overall configuration being akin to that of an onionskin. Bonding is achieved under ambient conditions with external pressure applied by separate circumferential straps tightened manually and removed after a period of time. The primary difference in systems B and C is that in B an Aramid tracer tow is used whereas system C incorporates E-glass strands. The original purpose of the tracer was for the facilitation of manual assessment of fiber orientation. System D is the only system using carbon fibers, which are wound using an automated winder and then cured at elevated temperature, through the enclosure of the jacketed column in a shell with heating elements thereby enabling cure following a pre-specified temperature cycle consisting of ramps and dwells culminating in the achievement of a 121°C (250°F) temperature level.

Following procedures detailed in Chapter 7 and further elucidated in [1] specimens were fabricated using procedures similar to those practiced by the manufacturer in the field, such that blanks of 178 mm height (7") were fabricated to enable the systems to be exposed to environmental conditions in the jacket, rather than ring, configuration. The specimens were exposed to the following controlled laboratory conditions for a period of 18 months:

1. Storage at 23° C and 55% RH
2. Immersion in water at 23° C
3. Immersion in water at 60° C (to serve as an accelerated ageing environment)
4. Immersion in a  $\text{CaCO}_3 + \text{Ca}(\text{OH})_2$  based alkaline solution at pH 9-9.5 at 23° C
5. Immersion in concrete based alkaline solution (pH 10.5-11) at 23° C
6. Exposure to -26° C
7. Freeze-thaw exposure between -26° C and +60° C after salt soak in a 5% NaCl solution

In addition to tests conducted prior to the initiation of environmental exposure, tests were also conducted on blanks removed after each period of 6 months. Once exposures were completed, 4 NOL-rings each of 25 mm (1") height were cut from the central portion of each blank with a fifth ring being also cut from the same section for specimens to be

tested in short-beam-shear (sbs) using specimens of nominal span-to-depth ratio of 5:1, assessment of glass transition temperature ( $T_g$ ), moisture content, and microscopic investigations. A set of 5 samples was tested in each of these cases. In order to provide ease of comparison and to reduce uncertainty due to operator judgment the glass transition temperature was determined from the peak of the  $\tan \delta$  curve resulting from Dynamic Mechanical Thermal Analysis conducted on specimens. The use of test specimens from the central region of each test blank, rejecting edge areas (Figure 8.1), enabled almost complete elimination of edge effects during environmental exposure which could, otherwise, have resulted in non-uniformity and testing of specimens with moisture contents and attendant damage not likely to be encountered by the overall jacket in the field.

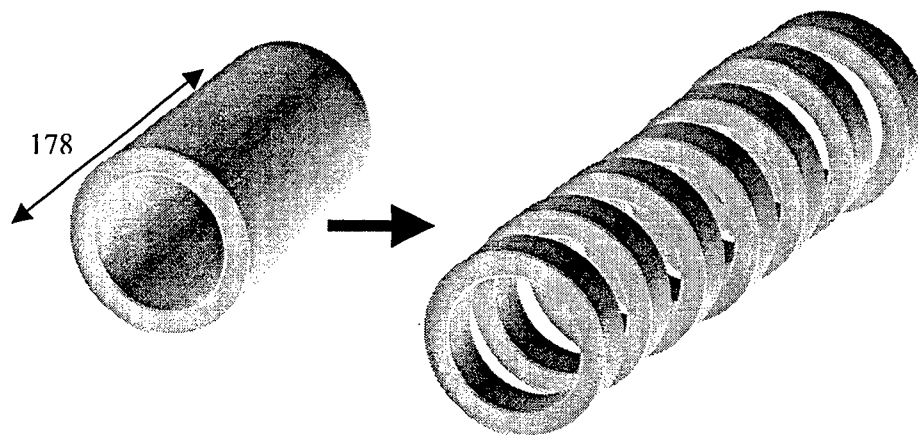


*Figure 8.1: Schematic of Test Blank and Ring Specimens*

In order to provide a standard baseline for design of test specimens for purposes of durability assessment, manufacturers were asked to fabricate blanks to meet a predetermined internal pressure rating of 17.2 MPa (2500 psi) for E-glass fiber based systems and 34.5 MPa (5000 psi) for carbon fiber based systems with a maximum thickness constraint of 11.5 mm (0.45"). These specifications were selected to match existing requirements specified by the California Department of Transportation at the flat coupon level [2].

## 8.2 Characterization of Unexposed Specimens:

Since the systems are cured on a concrete plug prior to removal (to simulate actual processing conditions used in the field), and with the exception of system D, under ambient conditions, it is of interest to compare results of critical material characteristics based on tests conducted both prior to the beginning of the period of exposure and at the end of the 18 month period to assess effects over that period of time. Results are given for the four systems in Table 8.2. As can be seen the only property that essentially changed over the period of time was the modulus which can be traced to the effect of residual cure over the 18 month period of time. It is noted, however, that the prepreg based system showed a substantially lower glass transition temperature than would be expected. Further analysis showed that this was due to a combination of moisture entrapment and resin instability.

*Table 8.2: Performance Characteristics of Ambient Exposed Specimens (Standard Deviations are in [ ])*

Properties	System A		System B		System C		System D	
	0 months	18 months	0 months	18 months	0 months	18 months	0 months	18 months
Strength (MPa)	365.4 [13.79]	386.1 [13.79]	468.9 [34.48]	468.9 [27.58]	606.8 [6.89]	613.7 [6.90]	1372.1 [75.85]	1441.1 [48.27]
Hoop modulus (GPa)	34.3 [2.62]	40.7 [1.03]	25.3 [2.14]	28.8 [0.97]	26.3 [0.48]	29.2 [0.69]	108.7 [3.52]	117.9 [4.69]
SBS Strength (MPa)	22.5 [0.76]	23.4 [2.41]	26.3 [1.10]	26.3 [1.10]	31.0 [1.31]	31.0 [0.48]	36.3 [2.95]	41.7 [1.97]
Tg (°C)	164 <sup>1</sup>	158 <sup>1</sup>	68	72	73	75	86	83

<sup>1</sup> Measured on composite alone

## 8.3 Results After Solution Based Environmental Exposure

Tables 8.3-8.6 list the residual performance values for the four different systems as a result of the different solution based laboratory exposure conditions.

*Table 8.3: Effect of Laboratory Exposure on Percentage Retention of Properties for System A*

Time (Months)	Strength			Modulus			SBS Strength			Tg		
	6	12	18	6	12	18	6	12	18	6	12	18
Water at 23°C	89	89	89	96	91	93	93	90	89	101	101	98
Water at 60°C	73	30	-	90	-	-	55	35	-	101	98	-
Alkaline Solution	102	98	84	104	91	98	86	84	81	108	106	96
Concrete Based Alkali	95	79	73	98	88	88	85	88	93	110	108	93

*Table 8.4: Effect of Laboratory Exposure on Percentage Retention of Properties for System B*

Time (Months)	Strength			Modulus			SBS Strength			Tg		
	6	12	18	6	12	18	6	12	18	6	12	18
Water at 23°C	99	76	65	104	94	89	61	65	54	94	108	100
Water at 60°C	50	50	46	104	104	94	67	68	77	119	128	128
Alkaline Solution	76	79	74	96	90	92	68	77	73	97	107	99
Concrete Based Alkali	103	100	97	103	103	103	106	101	89	111	104	93

*Table 8.5: Effect of Laboratory Exposure on Percentage Retention of Properties for System C*

Time (Months)	Strength			Modulus			SBS Strength			Tg		
	6	12	18	6	12	18	6	12	18	6	12	18
Water at 23°C	85	83	81	92	92	93	93	90	92	96	105	92
Water at 60°C	38	37	37	92	94	98	60	60	62	112	128	111
Alkaline Solution	88	88	83	96	93	97	90	88	88	95	107	95
Concrete Based Alkali	90	85	78	97	98	96	90	89	89	99	101	96

*Table 8.6: Effect of Laboratory Exposure on Percentage Retention of Properties for System D*

Time (Months)	Strength			Modulus			SBS Strength			Tg		
	6	12	18	6	12	18	6	12	18	6	12	18
Water at 23°C	73	76	76	99	99	97	81	88	87	86	99	89
Water at 60°C	54	55	-	95	96	-	39	35	22	77	89	72
Alkaline Solution	90	85	85	98	100	99	94	86	84	110	84	73
Concrete Based Alkali	84	85	85	95	96	91	92	88	87	120	94	80

As can be seen from Table 8.2 the maximum degradation in System A is due to immersion in water at 60°C. Although this can be considered to be a very aggressive environment it is noted that the failure is completely within the adhesive layer with complete unraveling of the sections. It is seen that this mechanism of failure is common also to the specimens immersed to water at 23° C and to the concrete based alkaline solution (having a pH between 11 and 11.5), (Figure 8.2). In each case the loss of adhesive integrity was noticed at the 6-month level of exposure and increased with time of exposure.

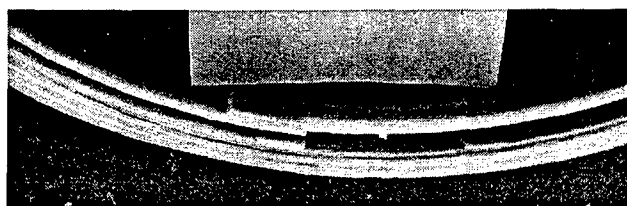


*Figure 8.2: System A Failure Through Separation of Prefabricated Layers*

System B specimens show a level of delamination with significant hoop splitting and tearing of fabric with pull-out of the aramid fibers (Figure 8.3) in all cases except the exposure to water at 60° C wherein failure was through fiber fracture (Figure 8.4). Microscopic examination of the specimens showed a level of fiber degradation after exposure to water at 60° C for 18 months.



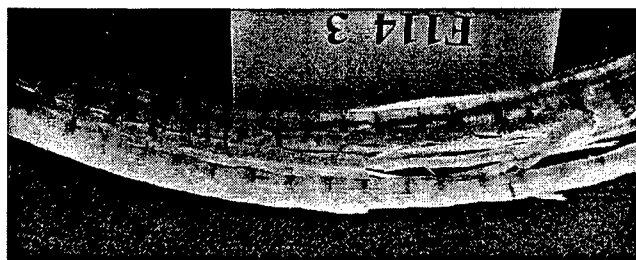


*Figure 8.3: System B Failure Through Hoop Splitting and Tearing*



*Figure 8.4: System B Failure After Exposure to Water at 60° C*

It is noted, however that immersion in water at the higher temperature results in an increase in glass transition temperature. Although one may be tempted to relate the increase in  $T_g$  to residual curing it is noted that such increases in  $T_g$  could also be due to the leaching of low molecular weight flexibilizing segments leading to the embrittlement of the network, which corresponds to the change in failure modes, and the sbs response.

Although system D consists of carbon fibers in an epoxy matrix cured at elevated temperature it is seen that failure is primarily through unraveling and inter-tow debonding suggesting instability, or moisture sensitivity, of the resin system (Figure 8.5). This is further emphasized through the dramatic decrease in sbs strength after immersion in water at 60° C. It is noted that although cure was conducted at elevated temperature there is a consistent drop in  $T_g$  after all exposure conditions with the reduction being the highest of all four systems under consideration.



*Figure 8.5: System D Failure Through Unraveling and Inter-Tow Debonding*

#### 8.4: Results After Freeze and Freeze-Thaw Exposure

Freeze and freeze-thaw cycling was conducted for a period of 12 months. Overall results in terms of percentage retention of properties are reported in Tables 8.7 and 8.8. There is very little change in the strength of systems A and B due to the  $-26^{\circ}\text{C}$  exposure, whereas system C shows a 6.8% decrease in strength and system D shows as much as a 13.1% decrease after 12 months of exposure.

*Table 8.7: Effect of Laboratory Exposure on NOL-Ring Based Strength and Hoop Modulus (Expressed as Residual Percentage)*

	System A		System B		System C		System D	
	$\sigma$	E	$\sigma$	$\sigma$	$\sigma$	E	$\sigma$	E
Freeze	116	113	100	112	93	105	87	104
Freeze-Thaw	84	94	88	100	88	92	90	99

*Table 8.8: Effect of Laboratory Exposure on Short Beam Shear strength and Tg (Expressed as Residual Percentage)*

	System A		System B		System C		System D	
	SBS	Tg	SBS	Tg	SBS	Tg	SBS	Tg
Freeze	95	104	93	104	99	99	103	118
Freeze-Thaw	79	95	75	96	92	92	102	87

This decrease after exposure to sub-zero temperatures can be traced to matrix hardening and increase in density of microcracks. The greater drop in the carbon/epoxy system, system D, in comparison to the glass/epoxy system, system C, is probably due to a combination of two factors, namely the higher cure temperature and anisotropy of carbon

fibers on one hand, and secondly due to the fact that the carbon/epoxy specimens were fabricated from tow rather than fabric providing greater potential for waviness. Further, as elucidated in [3] lower temperatures cause failure surfaces of carbon/epoxy to become smoother as a result of interfacial debonding dominated failure in an increasingly brittle matrix. This effect was also noted in a comparison of failure surfaces and is in fact discernable on comparison of failed ring specimens as in Figure 8.6, wherein it can be seen that the specimen after exposure to  $-26^{\circ}\text{C}$  shows more pronounced unraveling of tow and matrix dominated interlayer fracture and debonding with significantly reduced tensile fiber fracture as compared to the unexposed specimen.

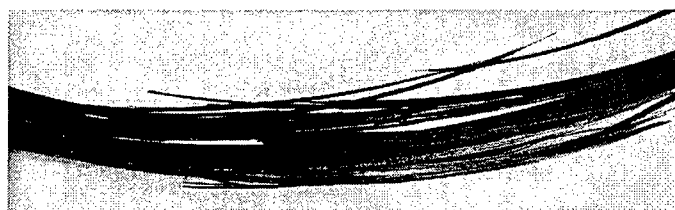


*Figure 8.6: Pronounced Unraveling of Tow and Matrix Dominated Interlayer Failure due to "Freeze" Exposure*

Specimens from system C appear to show a change in failure mode from one representative of tensile fracture to one showing a combination of hoop splitting and interlayer separation as a result of the  $-26^{\circ}\text{C}$  exposure after 6 months of exposure (Figure 8.7).



*Figure 8.7: Interlayer Separation (Delamination) in System C*

It is important to point out that polymeric resins tend to increase stiffness on cooling and this effect can clearly be seen in the increase in modulus of system A of 12.7% after 6 months of exposure to the freeze environment which also results in a transition to a more

brittle and catastrophic mode of failure (Figure 8.8). As can be seen from Figure 8.8(a) the specimens tested without low temperature exposure shows failure in the adhesive bond interphase resulting in separation of layers, whereas exposure to freeze conditions results in a combination of brittle interface failure and fracture of the composite locally in brittle tensile fashion (Figure 8.8(b)). It should be noted that at the six month level failure is still through an unraveling mode but with initiation of some tensile pullout and fracture, emphasizing the effect of time period of exposure on the transition in failure modes from adhesive to composite based.

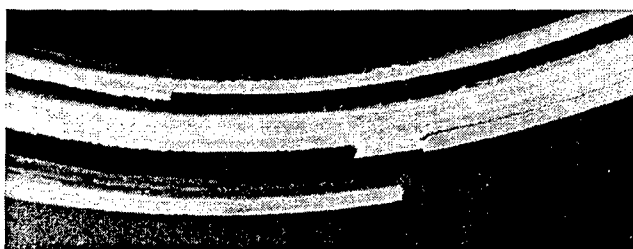


*Figure 8.8(a): System A Failure After Ambient Exposure Conditions.*

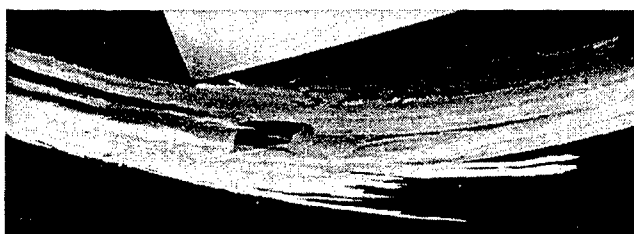


*Figure 8.8(b): System A Failure After "Freeze" Exposure Conditions.*

The absorption of moisture into a composite is known to cause swelling and a combination of reversible and irreversible changes in the polymer and at the interphase between the fiber and the matrix. In addition freeze-thaw cycling can cause growth of microcracks and initiation of cracks from existing voids and defects in the composite leading to increased levels of performance degradation. All four systems show a general decrease in tensile strength levels with the maximum being shown by system A, of -16%, wherein failure is clearly at the adhesive-composite interphase with some tensile microcracking and failure within the adhesive itself. Unlike the unexposed specimens

where there is partial unraveling of the separate shell segments, after freeze-thaw exposure the separation is complete with all layers debonding from each other. The visible degradation of the adhesive and the adhesive-composite interphase is also evident from the decrease in hoop modulus of 6% as well as the decrease in short-beam-shear strength. In fact, interlaminar cracks formed fairly early during short-beam-shear testing of these specimens. Both the glass/epoxy systems show roughly equivalent levels of tensile strength degradation, although system B has a significantly higher level of degradation in short-beam-shear strength (25.3% as compared to 7.8% for system C). This can be traced both to local degradation around the aramid tows, as well as to a more pronounced level of separation between layers in system B. System B NOL-ring specimens fail through a combination of local fabric tearing, fracture and interlayer separation, whereas system C NOL-ring specimens show failure through localized splitting, tearing and fracture. After 12 months of freeze-thaw exposure the dominance of areas with excessive voids is clearly seen with failure being shear dominated between layers. In comparison, the elevated cure carbon/epoxy system, D, shows only degradation in strength with very little change in hoop modulus or short-beam-shear strength that is in line with the higher durability of such systems to moisture and cycling related degradation. Failure of NOL-rings is through a combination of hoop splitting and tow level debonding. A reduction in splitting and an increase in the debonding mode are seen after 12 months of exposure with some evidence of moisture and cycling related degradation. It is noted that due to freeze-thaw cycling all the systems showed a decrease in NOL-ring based burst strength with the reductions being at the levels of 16.06%, 11.77%, 12.38% and 10.05%, for systems A, B, C and D, respectively. This corresponds to a total of 180 cycles over a period of 12 months with initial moisture contents of 0.24%, 0.66%, 0.67% and 1.41% for systems A, B, C and D, respectively. However, in reality it is likely that over an extended period of time in the field, at least the outer layers would reach higher levels of moisture absorption (weight gain). Following the procedure for prediction of effects due to freeze and freeze-thaw presented in [4] and assuming that void/defect/crack volume grows only by 5% over the time period it can be predicted that reductions of strength for systems A, B, C and D, of 25%, 18%, 23% and 30%, respectively, will be realized. This emphasizes the deleterious effect of moisture-coupled

freeze-thaw. However, it should be noted that since some of the systems already show transition in materials behavior due to increased defect sensitivity due to low temperature induced matrix hardening, these values should not be considered as conservative.

## **8.5 Summary**

Results show a range of effects, which are dominated by aspects related to fabrication, such as the bond-line within the adhesively bonded specimens, and moisture uptake. System A failures are adhesive dominated with degradation being as early as the 6 month level. Systems B and C fail primarily through delaminations and separation of layers, and splitting between bundles, suggesting moisture induced resin and interface degradation. Fiber fracture was only seen to be the dominant mode after the severe elevated temperature exposures. System D failures were primarily through unraveling and intertow debonding and it is seen that process conditions, especially as related to voids and cure related residual stresses, can have a significant effect on failure modes. It is necessary to note that while the laboratory exposures considered in this investigation could be considered as not simulating field conditions to the full extent and in some cases being more severe, due to the extended continuous periods of constant exposure regime, the results do provide the basis for rational selection of materials systems and for the future development of materials design allowables and durability evaluation, in addition to the identification and characterization of failure modes.

Of the three test protocols described in Chapter 7 it is noted that AC 125 [5] requires that as a criterion of acceptance all specimens show not less than 90% retention of properties after 1000 hours of exposure and not less than 85% retention after 3000 hours of exposure. The 1000 hour period relates to about 42 days whereas the 3000 hour level relates to about 125 days. The latter time frame is lower than the first period of exposure of 6 months under the HITEC protocol and further the environmental conditions are themselves different. However, a comparative assessment can be made using the two closest conditions – immersion in water at 23 °C and immersion in alkaline solution. It is

seen that System B specimens fall below the 85% level for strength after immersion in alkaline solution (76% retention) and for short beam shear strength after immersion in both solutions (61% and 68% retention in water and alkaline solution, respectively). System D specimens also fall below this level insofar as tensile strength and short-beam-shear strength after immersion in water (73% and 81% retention, respectively). The reader is, however, cautioned that the tests are themselves different and that further reductions are seen in these and other systems over longer time periods of exposure and hence this assessment cannot be considered in absolute terms.

## References

- [1] Reynaud, D., Karbhari, V. M. and Seible, F., "The HITEC Evaluation Program for Composite Column Wrap Systems for Seismic Retrofit," *Proceedings of International Composites Exposition, Cincinnati, OH*, 1999, pp. 4A/1-6.
- [2] Caltrans Memorandum to Designers, 20-4,1996, Attachment B: Composite Column Casing, and Standard Specification. I.48\_AENC.DOC, 1996.
- [3] Dutta, P. K. and Taylor, S., "A Fractographic Analysis of Graphite/Epoxy Composites Subjected to Low Temperature Thermal Cycling," *Proceedings of the International Symposium for Testing and Failure Analysis*, Los Angeles, CA, 1989, pp. 429-435.
- [4] Karbhari, V.M., "Response of Fiber Reinforced Polymer Confined Concrete Exposed to Freeze and Freeze-Thaw Regimes," *American Society of Civil Engineers Journal of Composites for Construction*, Vol. 6 (1), 2002, pp. 35-40.
- [5] AC125 (2001), Acceptance Criteria for Concrete and Reinforced and Unreinforced Masonry Strengthening Using Fiber Reinforced Polymer (FRP) Composite Systems, ICBO Evaluation Service.

## **CHAPTER 9: FIELD EXPOSURE BASED DURABILITY ASSESSMENT OF FRP COLUMN WRAP SYSTEMS**

### **9.1 Introduction**

To date, a number of FRP column wrap systems have been extensively evaluated through large- and full-scale testing in laboratories, and there is an increasing use of these systems in the field, with perhaps the largest number of columns being on the Yolo causeway in Sacramento, California [1]. Although substantial sets of durability data can be collected on the basis of tests conducted after carefully controlled exposure experiments in a laboratory setting, for the most part these experiments only provide data bases for materials de-selection and provide approximate and short-term trends of potential materials response. Due to the effect of combined environmental conditions and factors, and time varying conditions, field exposures, in general, can result in different rates and even mechanisms of degradation than those determined on the basis of controlled laboratory exposures. In addition, in a large number of cases, design allowables, generated through the use of laboratory simulations only, can result in grossly over-conservative designs that ultimately result in negatively impacting the cost-efficiency of a system.

In order to provide a validated basis for the characterization and comparison of representative FRP composite systems used for the seismic retrofit of columns a detailed evaluation program was initiated by the Civil Engineering Research Foundation (CERF) in conjunction with the Federal Highway Administration (FHWA) and the State Departments of Transportation under the auspices of the Highway Innovative Technology Evaluation Center (HITEC) program. The primary objectives of the program were the assessment of structural tests completed on representative systems, evaluation of durability through controlled laboratory exposures, and field evaluation of durability [2]. This chapter describes results of an investigation into the field applicability and durability of two specific FRP composite systems evaluated at multiple bridge sites in Tacoma, Washington.



## 9.2 Bridge Site Details

In order to ensure that field tests duplicated conditions at actual bridge locations, specimens for the durability evaluation were fabricated at the same time, and following the same process details, as the actual retrofit of columns on bridges at the selected field locations. Washington State Department of Transportation (WSDOT) has 188 bridges with single column supports, which fall within the WSDOT Priority Group 3 as related to seismic retrofit in that they are considered to be of high seismic risk [3]. A set of these bridges in the Tacoma area (as shown in Figure 9.1) were chosen for retrofit using both steel and FRP composite jackets. Column diameters ranged from 1220 mm (4') to 2134 mm (7'). In all cases excavation below existing ground level was required prior to placement of the steel casing or FRP composite jacket. However, none of the columns were located in areas having water.

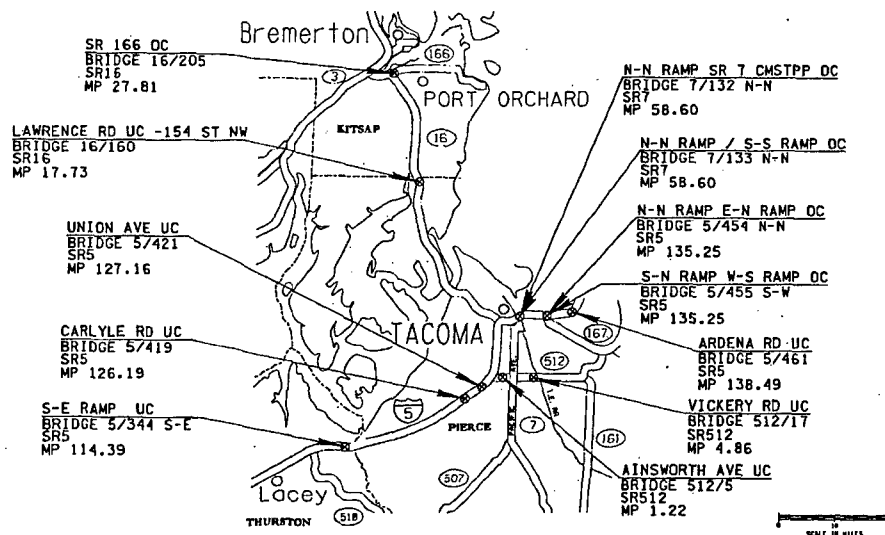
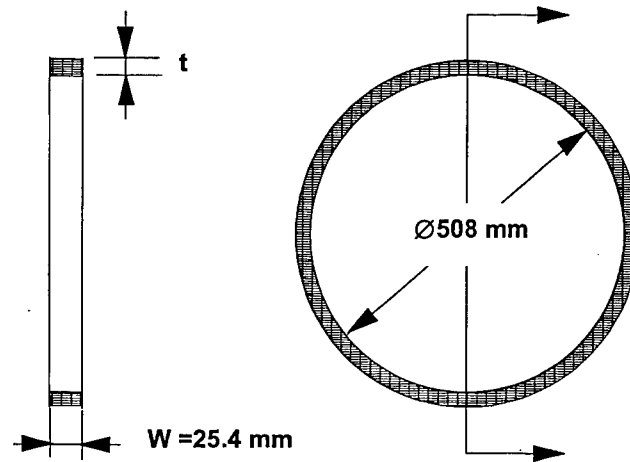


Figure 9.1: Map Showing Vicinity of Demonstration Columns and Field Exposure Sites

## 9.2 Methodology for Durability Assessment

Following the HITEC test protocol described in Chapter 7 durability is assessed through the use of a ring burst test which not enables assessment of parameters that not only characterize materials response but also characterize combined materials-structural systems effects which can

directly be used by structural engineers and designers. The details of the test specimen specifications are provided in Figure 9.2.



*Figure 9.2: Dimension of Ring Test Unit*

The use of actual bridge sites enables the assessment of environmental exposure at two levels. The first is related to condition assessment of the actual jackets placed around bridge columns. Since these jackets serve a structural purpose and are bonded to the concrete column substrate it is not possible to remove these, in the short term, without decreasing seismic retrofit integrity or otherwise damaging the system. Thus, the assessment at this level, for the purposes of this investigation would be through visual and rudimentary non-destructive inspection (tap test to pinpoint areas of gross delamination, materials degradation and/or separation), although more invasive tests are planned for the longer time period. The second level of assessment, which is the topic of the current investigation, relates to the fabrication of blanks, or exposure specimens, using the same process and materials as used in the actual retrofit of the columns, and fabricated at the same time as the jackets themselves. These blanks are of 178 mm (7") height and 59 mm (20") internal diameter, fabricated to enable the systems to be placed adjacent to the actual retrofitted columns, thus subjected to the same exposure conditions as the columns, and be exposed in the actual structural configuration, rather than merely as a materials sample. After exposure, individual ring specimens are cut from each blank with edge elements being discarded to ensure that results are not obscured by edge effects from exposure. In order to assess the effect of the encapsulated concrete, if any, on the results, samples were to be placed both using a

solid concrete core and as hollow blanks. These test specimens could then be retrieved from the field after appropriate periods of exposure and tested in the laboratory.

### 9.3 Materials and Fabrication Details

The two FRP composite systems, designated as A and B, consist of a prefabricated shell system which is adhesively bonded layer by layer in the field, and a fabric based system which is fabricated in the field using the wet lay-up process (Table 9.1).

*Table 9.1: Description of Systems Evaluated*

System	Constituent Materials	Process and Form	Conditions of Cure
A	Unidirectional E-glass fabric with aerial weight of 1668 g/m <sup>2</sup> (49.21 oz/sq yd) and polyester mat stitched as backing Isophthalic polyester resin with cumene hydroperoxide catalyst  Two-part Polyurethane adhesive with 148% elongation at 23 °F	Cylindrical shells with fiber weight fraction of 71% ± 3% fabricated by wrapping/winding on a mandrel. Tensile strength and modulus of each layer is 620 MPa and 34.5 GPa, respectively. T <sub>g</sub> = 94 °C Shells are split longitudinally and then adhesively bonded in the field with staggered joints	Elevated temperatures under controlled factory conditions     Ambient cure in the field under strap-based pressure
B	E-glass woven fabric with fibers primarily in the warp direction with aramid tracers in the weft direction. Nominal thickness of layer in composite form: 2.6 mm  Two-part epoxy resin with 5% elongation	Wet Lay-up using an impregnator Minimum tensile strength, modulus and ultimate strain per layer = 552 MPa, 28 GPa and 2%, respectively	Ambient cure in the field

Since the jacket thickness varies based on the column being retrofit, a standard baseline aimed at meeting an internal pressure rating of 17.2 MPa (2,500 psi) was required for the design of the test blanks for purposes of durability assessment. This specification was selected to match existing Caltrans requirements [4] at the flat coupon level.

## 9.4 Periods of Exposure and Test Procedures

One blank from each system was tested after attainment of cure in the field to serve as a baseline, whereas subsequent sets were removed from the field site after nominal intervals of 6 months each for a total nominal period of exposure of 18 months. The exact periods of exposure for each system are listed in Table 9.2.

*Table 9.2: Periods of Field Exposure*

Exposure Period	System A	System B
Baseline	-	-
1	38 weeks	31 weeks
2	59 weeks	52 weeks
3	82 weeks	89 weeks

Once exposures were completed, 4 NOL-rings, each of 24 mm (1") height, were cut from the central portion of each blank for burst testing with a fifth ring being also cut from the same section for specimens to be tested in short-beam-shear and for assessment of glass transition temperature ( $T_g$ ). In order to provide ease of comparison and to reduce uncertainty due to operator judgment the glass transition temperature was determined from the peak of the  $\tan \delta$  curve resulting from Dynamic Mechanical Thermal Analysis conducted on specimens. The use of these specimens from the central region of each test blank, rejecting edge areas, enabled almost complete elimination of edge effects related to environmental exposure. It should be noted that these anomalous effects could, otherwise, have resulted in non-uniformity in specimens with moisture contents and attendant damage not likely to be encountered by the overall jacket in the field.

## 9.5 Test Results

Specimens received from the field were carefully examined for defects and measured for dimensions. Both systems appeared to have a thicker level of protective coating on the test blanks than on the actual columns. Whereas this could be due to difficulties related to the application of the coating on smaller surface areas it should be noted that while the presence of

this additional thickness would not be expected to substantially alter the unexposed (i.e. baseline) performance values, it could reasonably be expected to enhance the durability of the systems to conditions of field exposure.

An overall record of temperature variation, precipitation, and dew point measured in the general vicinity of the bridges over the time period of field exposure is plotted in Figures 9.3 and 9.4. As can be seen the maximum temperature, minimum temperature, and maximum variation in temperature recorded during this time period were 35.6 °C, -2 °C, and 22.3 °C, respectively.

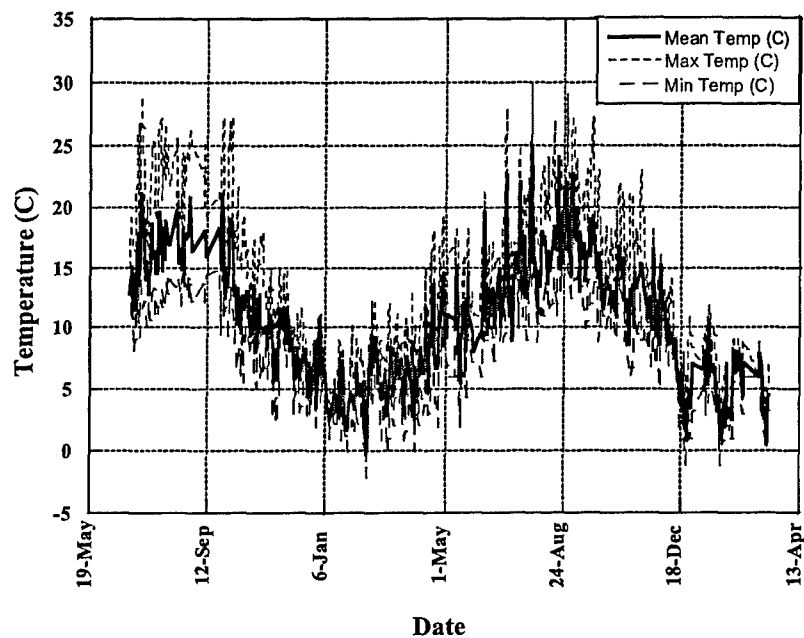


*Figure 9.3: Temperature Records in the Vicinity of the Test Area*

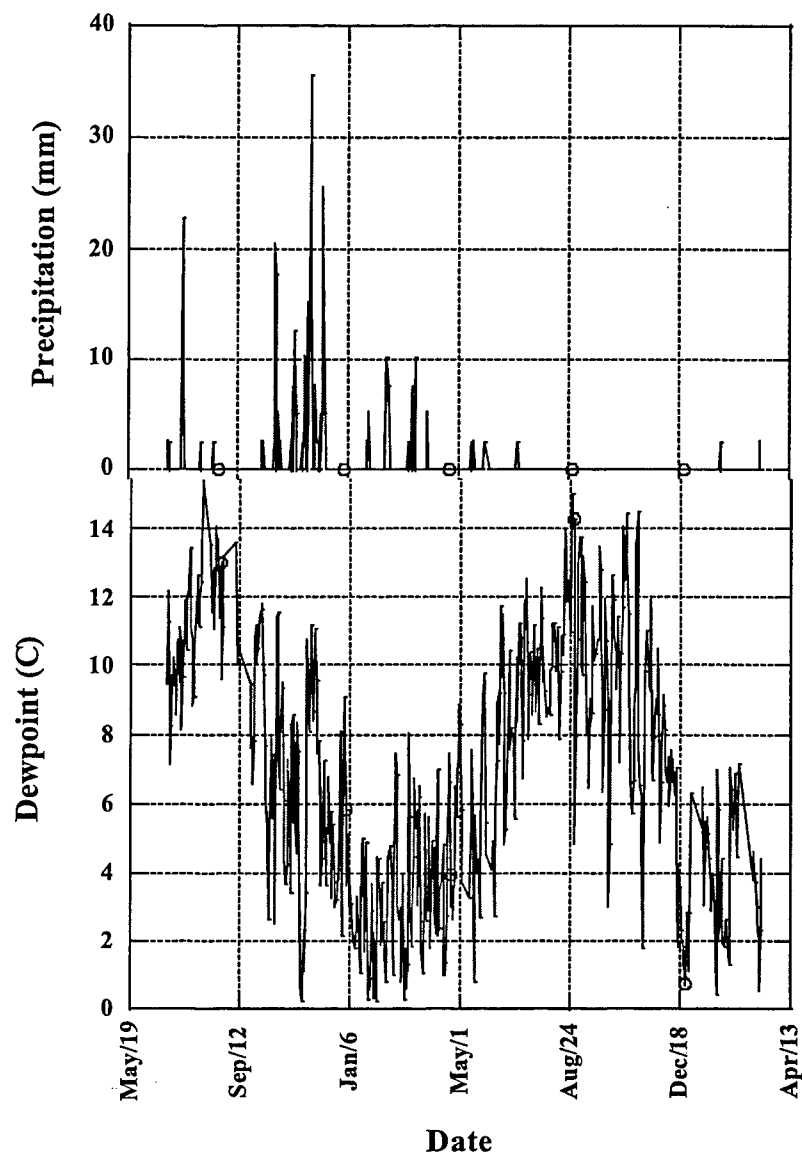


*Figure 9.4: Precipitation and Dew Point Records for the Local Geographical Region*

The base-line (unexposed) performance values, as measured through NOL-burst, short-beam-shear, and DMTA testing, for the two specimens, are listed in Table 9.3. Burst pressures for the specimens were 14.4 MPa and 17.9 MPa on average, for specimens from systems A and B, respectively. The two systems had differing thicknesses of 12.2 mm and 8.6 mm, respectively. It is noted that the larger thickness and lower recorded burst pressure of system A was due to the

presence of the adhesive between layers of the FRP composite shell and the resulting shear-lag effect due to the large bond-line thickness and gap between individual shell ends.

*Table 9.3: Base-line Performance Values*

Performance Metrics	System A	System B
NOL-ring based tensile strength (MPa)	386.1 [13.79]	530.9 [20.69]
NOL-ring based hoop modulus (GPa)	40.7 [1.03]	28.9 [1.12]
Short-beam-shear strength (MPa)	23.4 [2.41]	32.1 [2.9]
Glass transition temperature (°C)	158	87

The change in levels of performance metrics is shown as a function of exposure period in Figures 9.4 and 9.5, respectively. A comparison of Figures 9.5 and 9.6 shows that system B undergoes a higher drop in tensile strength at each of the exposure periods, although the final change in glass transition temperature is about the same. It should be noted that moisture absorption causes both a depression in glass transition temperature and changes in mechanical properties. In both systems standard deviation of results is seen to substantially increase over the second period of exposure, which can be correlated to non-uniform through-thickness moisture absorption levels and gradients. The prolonged exposure through the third period results in the attainment of a more uniform level of moisture through the thickness resulting in a decrease in scatter bounds.

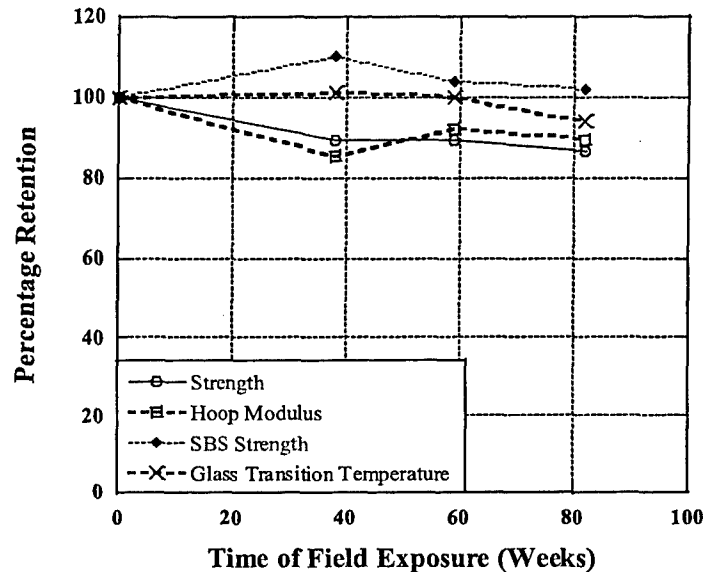


*Figure 9.5: Percentage Retention of System A Properties as a Function of Exposure Time*

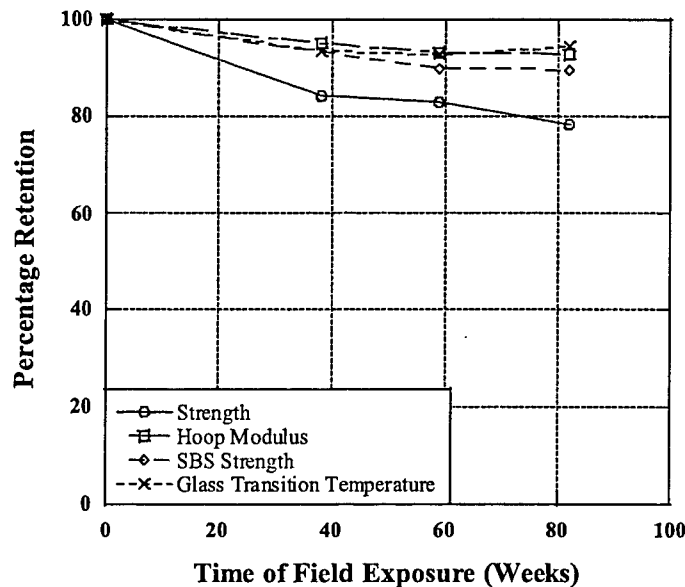


*Figure 9.6: Percentage Retention of System B Properties as a Function of Exposure Time*

Although strength depends largely on the intrinsic properties of the composite itself, in the configuration tested, the hoop modulus is largely affected by inter-layer effects. Since system A depends on the adhesive for stress transfer between layers of the factory-fabricated shell segments the change in adhesive properties as a result of exposure causes greater flexibility and inter-layer slip resulting in a greater drop in hoop modulus over the period of exposure. This flexibilization also results in a higher apparent toughness resulting in an almost negligible change in inter-laminar shear strength as measured through short-beam-shear testing. It is noted, however, that this is an indication of adhesive deterioration, and a higher level of overall performance degradation, including disbond initiation could reasonably be expected with a high probability after further exposure, especially if a higher degree of moisture were absorbed by the adhesive.

It is of interest to note that the failure mechanisms for system A closely mimic those seen in the laboratory after prolonged immersion in water [5] and a freeze-thaw environment [6] in that the primary mode of failure was through separation/de-bonding along the adhesive interfaces as shown in Figures 9.7(a) – 9.7(c).



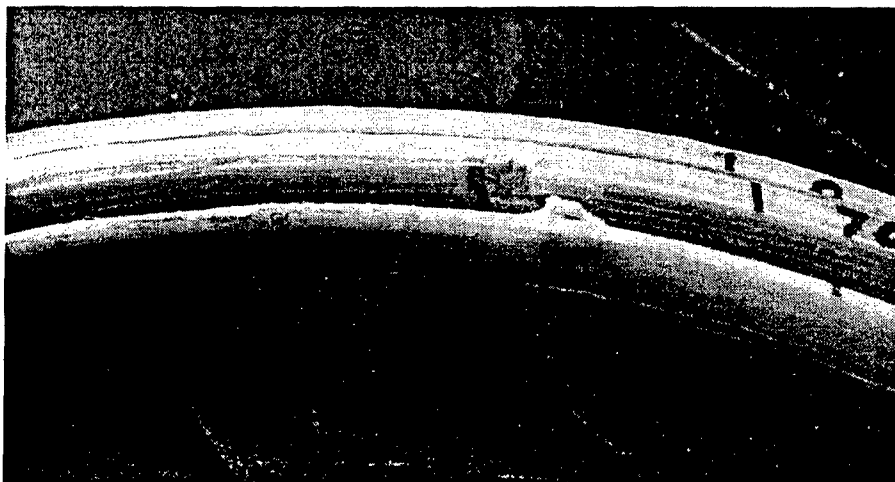


*Figure 9.7(a): Close-Up of Failure Mode for System A Showing Layer Separation With Failure at Adhesive Plug Between Layer Ends, and Pull-out From Scrim*

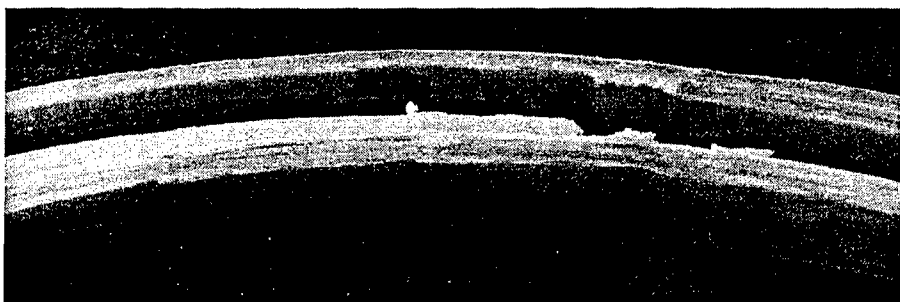


*Figure 9.7(b): Close-up Showing Brittle Failure of Adhesive Between Layers*

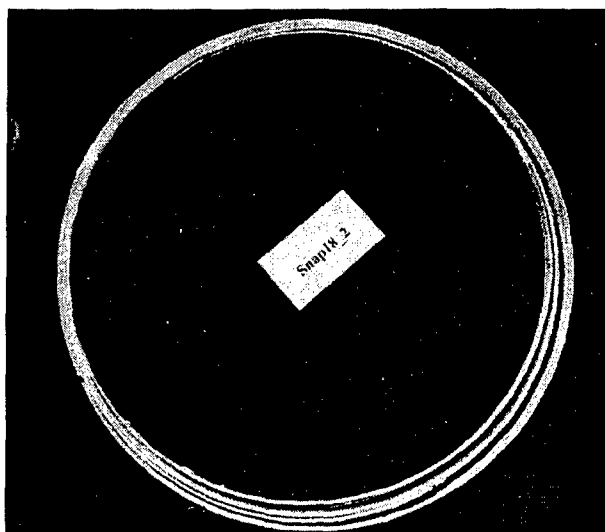


*Figure 9.7(c): Overall View of Representative Failure at the End of the Field Exposure Period*

After the first period of field exposure (38 weeks) the adhesive within the gaps between the ends of prefabricated shell sections was seen to fracture in brittle fashion and can be seen to cause the initiation of debonds along the adjoining surfaces. Samples examined at the end of the full period of exposure show significant degradation and cracking in the adhesive rather than the composite which showed very little change in characteristics when analyzed through Differential Scanning Calorimetry (DSC) and DMTA techniques. Specimens tested in the NOL-burst fixture show clear separation and debonding along the adhesive bond lines, as seen in Figure 9.7(c), with some pullout and tearing of the scrim placed between layers.

The rings from system B tested after the first period of field exposure (30 weeks) failed primarily through separation of the outer ply and local tearing/splitting through the thickness as shown in Figure 9.8(a). The separation of the outermost ply was without fiber pullout and indicated local moisture induced degradation of the interface causing a drop in inter-laminar properties. A significant (15.6%) drop in NOL-strength was also recorded for specimens at this stage of exposure. Rings tested after the second period of field exposure (52 weeks) failed through a combination of inter-layer splitting, Figure 9.8(b) and fracture of bundles akin to a "brooming" type failure de-bonding. Transverse aramid tows in general were not fractured although some local tearing and movement was seen along areas of hoop splitting in the bulk jacket material, Figure 9.8(c) along with significant pull-out and tearing of the E-glass fibers in the hoop direction. The rings showed significant disbonds and cracks in areas next to the aramid tows, Figure 9.8(d) and these potentially could have been areas of stress concentration leading to inter-layer separation and failure. Rings examined prior to testing after the full period of field exposure showed discoloration of the outer coating with some local indications of fiber exposure. Failure through burst testing was again characterized by local splitting/tearing in the hoop direction with bundle fracture being accomplished by pullout of the aramid tows. It is also significant that there was an increase in level of moisture absorption during the third period of field exposure resulting in a consequent drop in burst strength. The increase in absorbed moisture during this period is hypothesized to occur due to enhanced wicking along tows and into local areas of disbond and cracks.

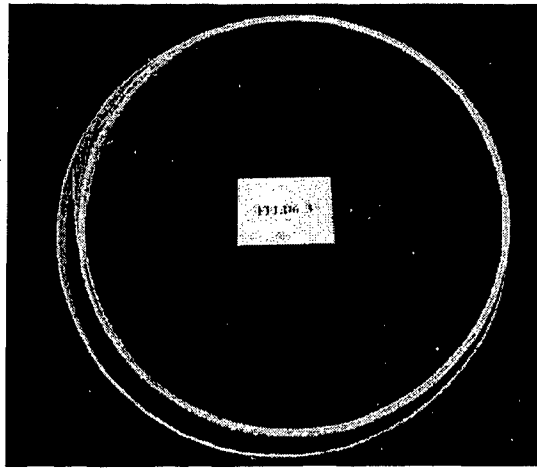


*Figure 9.8(a): Overall View of System B Showing Representative Failure After the First Period of Field Exposure Showing Ply Separation and Local Tearing/Splitting*

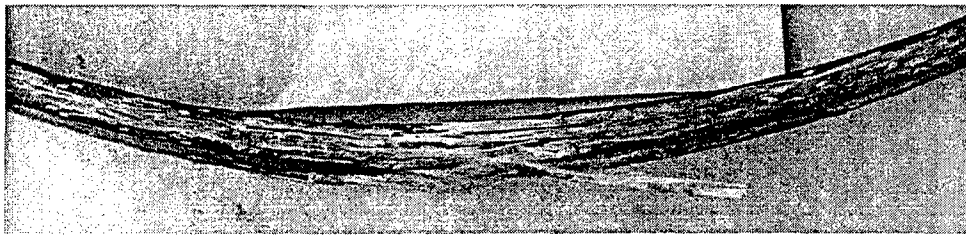


*Figure 9.8(b): Close-up Showing Interlayer Splitting*

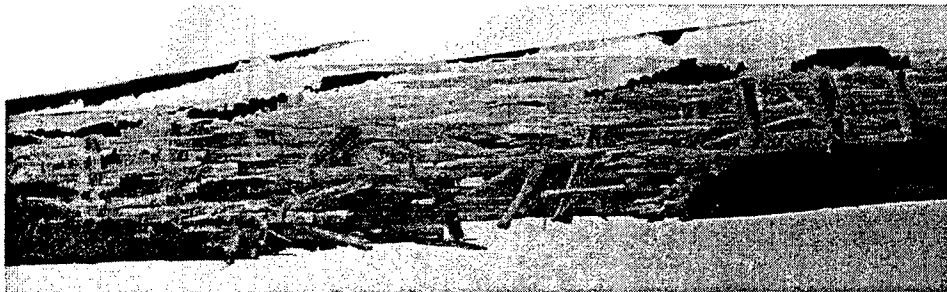


*Figure 9.8(c): Close-up of Fracture Area Showing Intact Aramid Tows*



*Figure 9.8(d): Close-up Showing Areas of Local Disbond/Voids Adjacent to Aramid Tows*

## 9.6 Summary and Conclusions

Tests conducted after periods of field exposure show that the degradation mechanisms and failure modes of the two systems under consideration are very different. System A is dominated by degradation of the adhesive and bond-line with very little change in mechanical performance of the prefabricated composite sections. These sections, cured at elevated temperature show moisture absorption levels of over 1%, but with the exception of fiber exposure in local areas, do not show signs of degradation beyond minor debonding at the fiber-matrix interfacial level. The ambient cured system, B, in contrast, depicts moisture-induced degradation at the level of the resin and fiber-matrix bond, and in cracking adjacent to the aramid tows which appear to have a substantially higher moisture uptake than the bulk. Thus, mechanisms are substantially different and hence generic design rules cannot be used without context over these systems. Rather each system (wet layup, adhesively bonded etc.) needs to be considered separately. Changes in NOL-ring based properties for both systems show similarities with results obtained from laboratory-based exposure to water and free-thaw conditions. Tests are seen to correlate well with the jackets on actual columns in the field as related to moisture absorption and surface conditions.

Preliminary comparisons of the methods of field installation show that both methods are very attractive for rapid retrofit and are faster than the installation of steel jackets. Space requirements are also lower which is advantageous in terms of less traffic disruption in areas where the placement process of jackets could result in local blockage of traffic lanes. However, a comparison of costs based on the average over all bridges shows that on the whole, the FRP

composite systems, at least on acquisition cost, are two to three times higher than steel jacketing [3]. Some of these additional costs are attributable to the use of over-conservative design equations, and a lower level of familiarity with these materials as compared to steel. It is noted that cost reductions accruing from speed of completion were not factored into the determination of these costs. No actual factors for life-cycle durability were explicitly considered in design, except as part of the overall high factor of safety, and further work needs to be conducted in this area.

### References

- [1] Karbhari, V.M. and Seible, F. (1999), "Fibre-Reinforced Polymer composites for Civil Infrastructure in the USA," *Structural Engineering International*, Vol. 9 [4], pp. 274-277.
- [2] Reynaud, D., Karbhari, V.M. and Seible, F. (1999), "The HITEC Evaluation Program for Composite Column Wrap Systems for Seismic Retrofit," Proceedings of the International Composites Exposition, Cincinnati, OH, pp. 4A/1-6.
- [3] Roper, T.H. (2000), "Post-Construction Report – Experimental Feature Project Bridge Column Seismic Retrofit Using Fiber Reinforced Polymer Wrap Systems," Report to Washington State Department of Transportation.
- [4] Caltrans Memorandum to Designers 20-4 (1996), Attachment B: Composite Column Casing and Standard Specification, I.48-AENC.DOC, California Department of Transportation.
- [5] Karbhari, V.M. and Zhang, J.S. (2001), "Correlation of Laboratory and Field Studies of Aging and Degradation of Composite systems in Civil Infrastructure," Proceedings of DURACOSYS, Tokyo, Japan 8 pp.
- [6] Zhang, S., Karbhari, V.M. and Reynaud, D. (2001), "NOL-Ring Based Evaluation of Freeze and Freeze-Thaw Exposure Effects on FRP Composite Column Wrap Systems," *Composites, Part-B: Engineering*, Vol. 32 [7], pp. 589-598.

## CHAPTER 10: REVIEW OF DURABILITY RESULTS FROM THE CALTRANS QUALIFICATION PROGRAM

### 10.1 Introduction

This chapter presents a summary of the results of a qualification program initiated by the California Department of Transportation focused on composite materials for seismic retrofit. Details related to the test protocol and exposure conditions are reported in Chapter 7. The testing was conducted by the Aerospace Corporation and results are summarized, with permission from [1].

*Table 10.1: Details of Composite Systems*

Supplier	Fiber/Resin	Description
Fyfe Co. & Hexcel	E-Glass/Epoxy	2 systems using SEH51 and SEH51S E-glass fabric impregnated using the wet layup technique
	Carbon/ Epoxy	1 system using SCH41 carbon fabric impregnated using the wet layup technique
Xxsys Technologies Inc.	Carbon/Epoxy	3 Tow based systems cured at elevated temperature using AS4D/MIOE, Akzo (48k)/UF 3325-90 and Zoltek (48k)/UF 3325-90.
	Carbon Epoxy	1 system using Akzo 48k tow based fabric impregnated with Shell Epon 828 Epoxy Resin under ambient temperature conditions
Hardcore Composites	E-glass/Vinylester	2 Prefabricated systems using different adhesives – epoxy and vinylester
Myers Technologies, Inc.	E-glass/Vinylester	1 prefabricated system with a polyurethane adhesive
Tonen Corporation	Carbon/Epoxy	2 wetlayup systems using the CF-130 fabric with one resin system from Japan and another from Master Builders, Inc.
Mitsubishi Chemical Corp.	Carbon/Epoxy	1 Wet-layup systems using L700S-LS using Replark 30 fabric
Mitsubishi/Obayashi	Carbon/Epoxy	1 wet winding based system
Mitsubishi/Toray	Carbon/Epoxy	1 wet layup system using Toray's UT70-30 fabric with Mitsubishi's L700S-LS resin system

14 different systems as listed in Table 10.1 were evaluated under the aegis of this program, of which evaluations were completed for 11 systems, with the other 3 being in various stages of testing. Complete data sets were not available for all systems due to the

proprietary nature of the test contract and as a result the data presented in this chapter is also not directly identified by supplier.

## **10.2 Overall Results**

Overall reduction in tensile modulus for all systems was seen to be less than 5%. Stress-strain curves, even after exposure, were nearly linear to fracture. Exposure to the elevated temperature (60°C) aqueous conditions was reported to have no degrading effect on the mechanical and physical properties, although a 0.1-1% decrease in mass was noted after dry-out. Glass transition temperatures were seen to increase after exposure for the ambient temperature cure systems. In addition short-beam-shear strengths were also noted as having increased by 5-10%. With the exception of one E-glass/polymer and 1 Carbon/epoxy system, which showed 10% reduction in tensile strength and failure strain after immersion in diesel fuel, the systems were not affected by the 4 hour immersion.

A number of polymer matrices were reported to soften as a result of plasticization due to moisture absorption with attendant reductions in glass transition temperatures and short-beam-shear strengths. Hardness, as measured at the surface, was however, reported to remain unchanged.

## **10.3 Environmental Durability of E-Glass/Polymer Systems**

The three E-glass systems are denoted as G1 (polyester matrix and an essentially unidirectional fabric), G2 (epoxy matrix and a woven fabric) and G3 (vinylester matrix and an essentially unidirectional fabric). The E-glass fibers for G1 and G3 came from the same supplier, but no check was made on type of fiber sizing which could have been different in all cases. Overall moisture uptake traces exposure to 100% humidity at 100°F are shown in Figure 10.1.

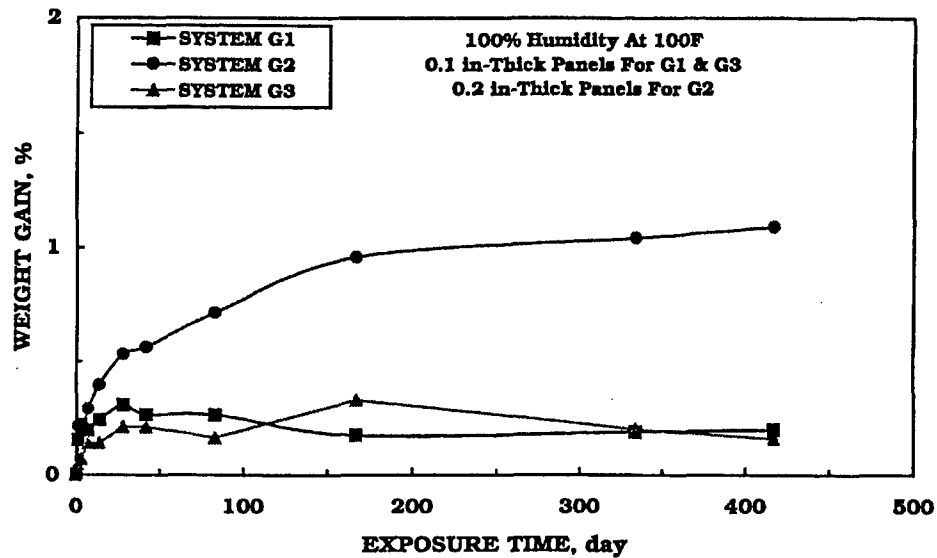


Figure 10.1: Moisture Uptake as a Function of Time Due to Exposure at 100% Humidity and 100°F (G1 and G3 samples are 0.1" thick, G2 samples are 0.2" thick).

It is noted that G2 samples show the highest uptake and also that they have not reached saturation. However, the data in Figure 10.1 needs to be considered carefully since equilibrium uptake levels of the 3 resins, even if processed under optimal conditions, will intrinsically be different. Further, it is difficult to directly compare effects based on different thicknesses and without consideration of fiber volume fractions (which are not reported). Also since G2 is a woven fabric it is likely to have substantially more paths for wicking along fiber interfaces than the other two essentially unidirectional composites. A determination of diffusion coefficients would have made a comparison more viable. It can also be seen that G3 appears to show less of weight after a period of 160 days. This phenomena is not commented on in [1] but may be an important clue of irreversible damage due to leaching. Although no data is provided for other environments it is reported that similar trends in uptake as in Figure 10.1 were seen due to immersion in salt water and pH 9.5 alkali solutions.

Degradation in tensile strength is shown in Figures 10.2 and 10.3 for sets G2 , and G1 and G3, respectively. System G2 showed the highest level of degradation when exposed



to 100% humidity at 100°F reaching about 35% at 417 days. Although this can be considered as an accelerated environment the rate of degradation and its irreversibility on redrying are of concern. In salt water and alkali the degradation was approximately 20% but again there was no regain on drying. Although no microscopic investigations were reported, degradation was hypothesized to be due to degradation at the level of the fibers or the fiber-resin interface. Similar results were seen in G1 and G3 but with regain on drying out. The moist environments, however, resulted in a change in failure mode indicating changes at the level of the fiber-matrix bond or matrix itself.

No reduction in strength was noted after freeze-thaw exposure and UV exposure, although the report [1] notes that the test duration was too short and recommends use of a longer duration. System G2 was noted to show degradation in short-beam-shear strength as well.

Tensile strength was noted to be unaffected at the 125 day level after exposure of specimens to humidity, salt water and alkaline solutions, but that significant degradation was noted beyond 417 days making it "impossible to predict the effects of exposure times longer than 417 days."

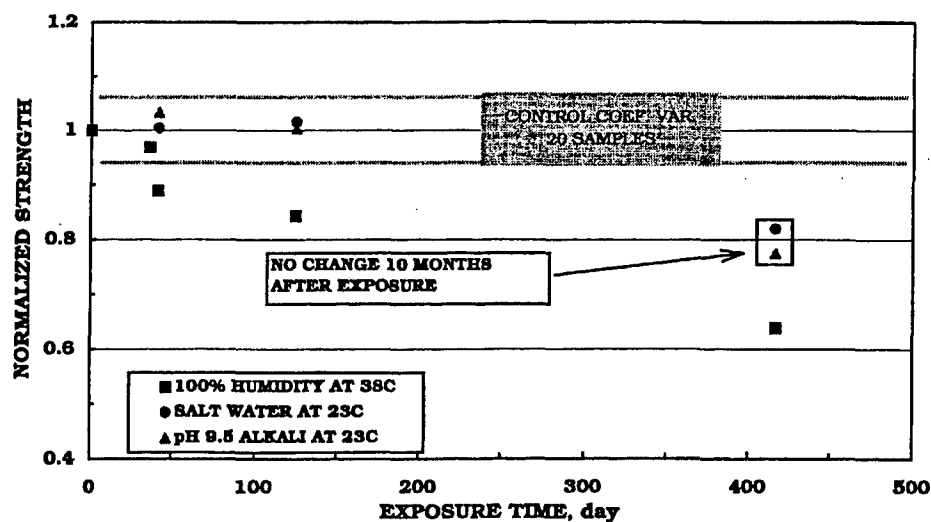


Figure 10.2: Normalized Tensile Strength for System G2

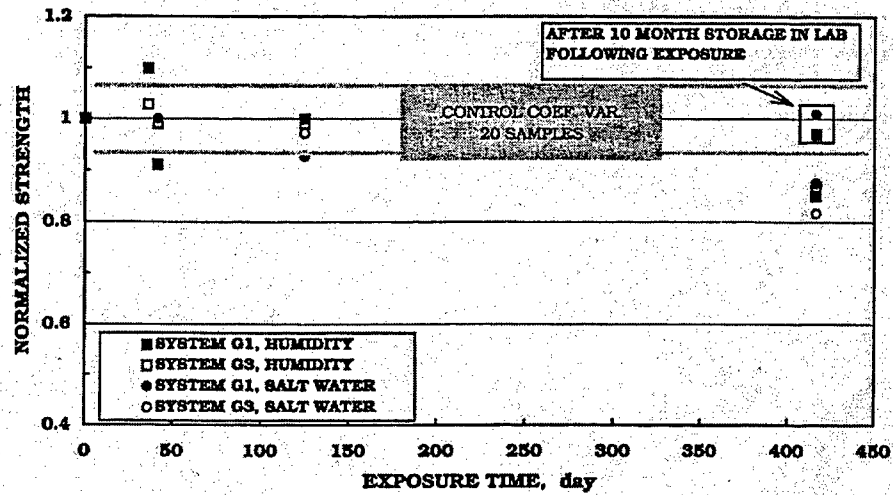


Figure 10.3: Normalized Tensile Strength for Systems G1 and G3

#### 10.4 Environmental Durability of Carbon/Polymer Systems

Moisture uptake curves for a few of the systems tested are shown in Figure 10.4.

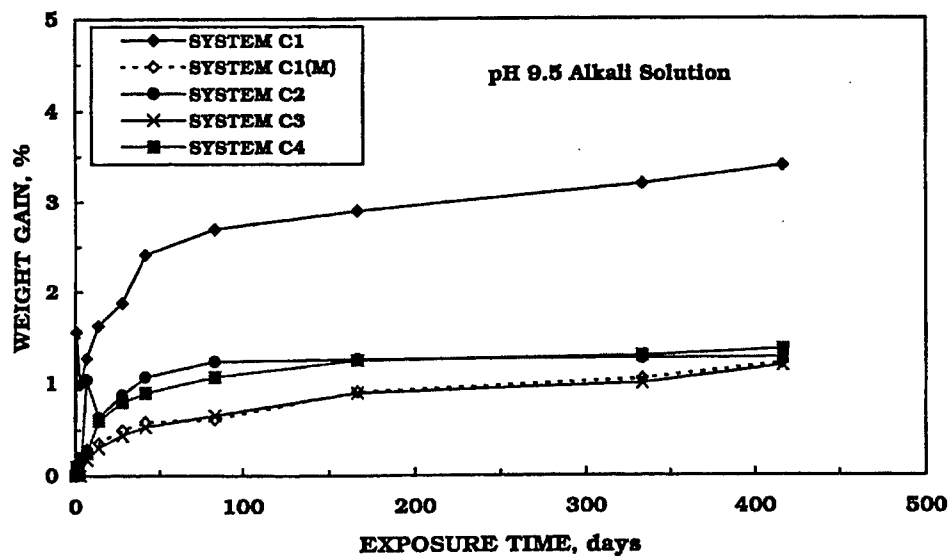


Figure 10.4: Moisture Uptake as a Function of Time for Systems C1, C1(M), C2, C3 and C4

It is noted that the curves are representative of specimens exposed to humidity and salt water as well.

Changes in glass transition temperature as a function of the same exposure is shown in Figure 10.5 and it can be seen that the largest reductions are seen in systems C3, C7 and C8, which were all cured at elevated temperature. System C1, which showed the maximum uptake also shows the lowest  $T_g$  of about 50°C.

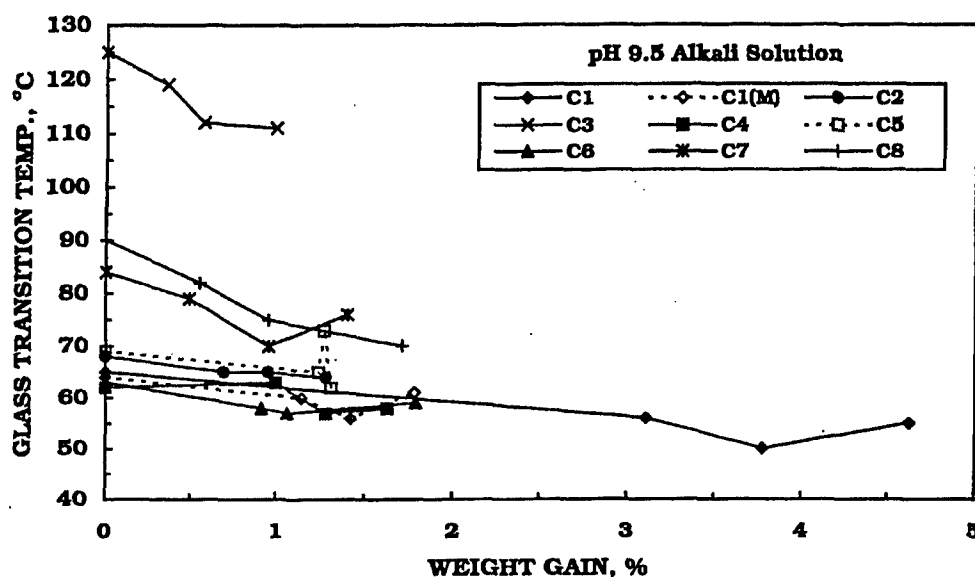


Figure 10.5: Change in  $T_g$  as a Function of Moisture Uptake

Changes in short-beam-shear strength in an alkaline solution are depicted in Figure 10.6 with the base-line varying between 5.5-8.5 ksi. System C2 which had a woven fabric architecture showed significant scatter in results, reportedly as a result of porosity at cross-over points. Maximum reductions at the 417 day level were about 20% except for system C1 which showed a loss of up to 50%.

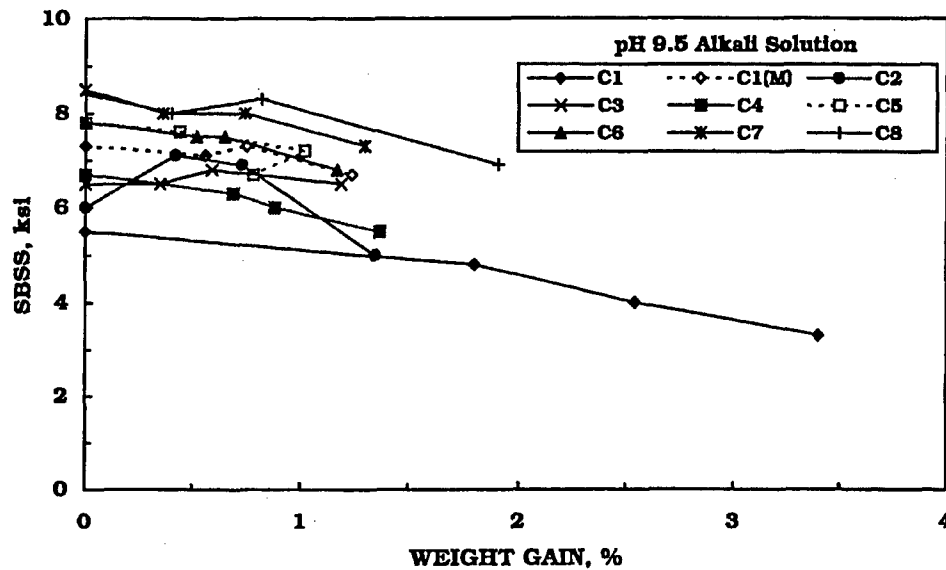


Figure 10.6: Change in Short-Beam-Shear Strength as a Function of Moisture Uptake

Although no data was reported for tensile strength after exposures it was noted that some systems had not cured completely and these were more susceptible to moisture degradation.

### 10.5 Environmental Durability of Adhesives

The coefficients of variation for the lap shear tests were reported to be between 15-20% for the control specimens while result due to exposure showed changes within this very band. Due to this no conclusions were drawn on environmental exposure effects.

### 10.6 Summary

The carbon/epoxy systems were noted to show excellent durability. However, it was noted that moisture uptake could cause significant reduction in  $T_g$  in the ambient

temperature cure systems bringing  $T_g$  level to within or near the service temperature range. This was noted to cause unacceptable reductions in tensile properties.

E-glass/polymer systems showed reduction in strength after exposure with one system showing an irreversible reduction of 35% in tensile strength and 20% in sbs strength even after redrying. Further investigations were recommended to clarify the differences in response and reasons for them [1].

The UV radiation/condensate exposure was seen to result in no degradation to all systems but the time period was noted to be too short and a recommendation was made that it be increased from 100 cycles to 1250 cycles in the future [1].

#### REFERENCES

- [1] Steckel, G.L., Hawkins, G.F. and Bauer, J.L., Jr. (1999), "Qualifications for Seismic Retrofitting of Bridge Columns Using Composites. Volume 1: Composite Properties Characterization," Aerospace Report No. ATR-99(7524)-2, Volume 1.

## CHAPTER 11: EXAMPLES OF COMMERCIALY AVAILABLE SYSTEMS

### 12.1 Introduction

Although wraps/jackets for the seismic retrofit of concrete columns can be fabricated using a number of methods (as described in Chapter 4) only a limited number of systems are commercially available. Further, a number of companies that pioneered the use of some of these systems, such as Xxsys Technologies Inc. (automated prepreg tow winding) and CMI, Inc (adhesive bonding of prefabricated shells having a single slit) are no longer active. The system related to wet winding of tow is also rarely used today, although it could easily be implemented since the tow and resin can be purchased directly from the manufacturers of the raw materials themselves. However, there are numerous suppliers and applicators of fabrics and impregnating resin systems for wet layup, and of prefabricated strips and adhesive for adhesively bonded systems. A partial list of manufacturers/suppliers in each of these categories is given in Table 12.1.

*Table 12.1: Examples of Retrofit Systems*

<b>Fabric Based</b>	<b>Prefabricated Component Based</b>
Hexcel Mitsubishi Sika Edge Structural Composites Fyfe Co. Watson Bowman Acme Corp. SCCI Freyssinet	Hardcore Composites Sika Fyfe Co. Watson Bowman Acme Corp.

Table 12.1 and the sections in this chapter provide examples of such systems. The list and descriptions are provided only as a reference for the assessment of system availability rather than as a comprehensive collection of all available systems. It is essential to note, however, that in general the system constituents (fabric and impregnating resin, prefabricated component and adhesive) are not interchangeable between suppliers.

## 12.2 Hexcel Civil Engineering and Construction Systems [1]

Hexcel has a number of fabric based systems for the wet layup process using both E-glass and carbon fibers. The properties of the fibers derived from Hexcel data sheets and brochures are listed in Tables 12.2 and 12.3 for glass and carbon fiber, respectively, and those for fabrics are listed in Table 12.4.

*Table 12.2: Properties of Glass Fibers*

Fabric Type	100,101, 106, 107, 116, 430
Tensile Strength (GPa)	2.3
Tensile Modulus (GPa)	76
% Elongation	2.8
Density (glcc).	2.56

*Table 12.3: Properties of Carbon Fibers*

Fabric Type	103	103HS	113,230	117
Tensile Strength (GPa)	3.8	4.8	3.4	4.2
Tensile Modulus (GPa)	234	234	234	230
% Elongation	1.5	1.5	1.5	1.8
Density (glcc)	1.8	1.8	1.76	1.78
Tow Size	24k	24k	12k	12k

*Table 12.4: Details for Fabrics*

Fabric Type	Style (Warp/Weft)	Aerial Weight (g/m <sup>2</sup> )	Weight %	Heat Set	Theoretical Thickness (mm)
Glass Fabric					
100	Weave(E- Glass/Polymide)	920	98% / 2%	Yes	0.36
101	±45	600			
106	0/90	325			
107	Weave (E-Glass/Aramid)	920	98% / 2%	Yes	0.36
116	±45 with 17 glm <sup>2</sup> mat	610			
430	Unidirectional	440			
Carbon Fabric					
103	Weave (24k carbon/polyamide)	610	99% / 1%	Heat Set	0.34
103HS	Weave (24k carbon/polyamide)	610			
113	0/90	195			
117	Weave (12k carbon/polyamide)	300	99% / 1%	Heat Set	0.17
230	Weave (12k carbon/polyamide)	230	99% / 1%	Heat Set	0.12

Two primary resin systems, both epoxies, denoted as Hex-3R Epoxy 300 and Hex-3R Epoxy 306, are used in conjunction with the fabrics. Properties for these resin systems are listed in Table 12.5.

*Table 12.5: Characteristics and Properties of Neat Resins*

Characteristic/Property	HEX-3R Epoxy 300	HEX-3R Epoxy 306
Service Temperature Range (°C)	-40°C to +60°	-40°C to +60°
Application Temperature Range (°C)	10°C to 40°	10°C to 40°
Shelf Life (years)	2 years (unopened)	2 years (unopened)
Pot Life (hours)	4 hours at 21°C	3 hours at 21°C
Cure Time (days)	5 days at 21°C	5 days at 21°C
Gel Time (hours)	14 hours at 21°C	5 hours at 21°C
Tack Free Time (hours)	20 hours at 21°C	16 hours at 21°C
Viscosity (cps)	Part A: 13000cps at 25°C	Part A: 44000 cps at 25°C
	Part B: 17 cps at 25°C	Part B: 18 cps at 25°C
Glass Transition Temperature (°C)	51 °C after 7 days at 23°C	48 °C after 7 days at 25°C
	79°C after 5 days at 23°C and 48 hours at 60°C	80°C after 5 days at 25°C and 48 hours at 60°C
Tensile Strength (MPa)	68	65
Tensile Modulus (GPa)	3.4	3.56
Elongation at Failure (%)	3.1	3.5
Flexural Strength (MPa)	116	103
Flexural Modulus (GPa)	3.19	2.92
Cured Specific Gravity (glcc)	1.16	1.14

Nominal properties for impregnated and cured systems are given in Table 12.6 – Table 12.17. The reader is cautioned that these properties are for purposes of reference only.



*Table 12.6: Laminate Properties for Hex-3R Wrap 100 Material  
(after 70-75°F for 5 days and 48 hours at 140°F)*

Property	Hex 3R Epoxy 300		Hex-3R Epoxy 306XR	
	Average	Design <sup>1</sup>	Average	Design <sup>1</sup>
Tensile Strength (MPa)*	612	558	575	514
Tensile Modulus (GPa)*	26.12	24.44	25.30	21.80
% Elongation*	2.45	2.23	2.31	2.03
Tensile Strength @ 140°F (MPa)	551	531	477	446
Tensile Modulus @ 140°F (GPa)	25.69	23.36	22.78	21.24
% Elongation @ 140°F	2.28	2.14	2.19	2.01
Compressive Strength (MPa)	597	542	517	470
Compressive Modulus (GPa)	29.72	25.49	29.27	24.47
90° Tensile Strength (MPa)	30	30	34	26
90° Tensile Modulus (GPa)	6.65	6.32	5.65	5.15
90° % Elongation	0.46	0.34	0.66	0.52
±45° In-Plane Shear Strength (MPa)	40	34	42	39
±45° In-Plane Shear Modulus (GPa)	2.31	2.11	2.32	2.14
Ply thickness (mm)	1.016		1.016	

\* 24 coupons per test series; all other values based on 6 coupon test series

<sup>1</sup> Design Value = Average Value – 2(Standard Deviation)

*Table 12.7: Laminate Properties for Hex-3R Wrap 101 Material  
(after 70-75°F for 5 days and 48 hours at 140°F)*

Property	Hex 3R Epoxy 300		Hex-3R Epoxy 306XR	
	Average	Design <sup>1</sup>	Average	Design <sup>1</sup>
Tensile Strength (MPa)*	284	234	274	234
Tensile Modulus (GPa)*	16.54	15.77	16.39	15
% Elongation*	2.17	1.81	2.06	1.50
Tensile Strength @ 140°F (MPa)	262	238	239	210
Tensile Modulus @ 140°F (GPa)	14.80	13.59	14.74	13.69
% Elongation @ 140°F	2.34	1.98	2.10	1.92
Compressive Strength (MPa)	643	385	**	**
Compressive Modulus (GPa)	**	**	**	**
90° Tensile Strength (MPa)	**	**	**	**
90° Tensile Modulus (GPa)	**	**	**	**
90° % Elongation	**	**	**	**
±45° In-Plane Shear Strength (MPa)	**	**	**	**
±45° In-Plane Shear Modulus (GPa)	**	**	**	**
Ply thickness (mm)	0.686	**	0.686	**

\* 24 coupons per test series; all other values based on 6 coupon test series

<sup>1</sup> Design Value = Average Value – 2(Standard Deviation)

\*\* Not Available

*Table 12.8: Laminate Properties for Hex-3R Wrap 106G Material  
(after 70-75° for 5 days and 48 hours at 140°F)*

Property	Hex 3R Epoxy 300		Hex-3R Epoxy 306XR	
	Average Value	Design Value <sup>1</sup>	Average Value	Design Value
Tensile Strength (MPa)*	280	243	274	196
Tensile Modulus (GPa)*	18.70	16.26	17.98	16.06
% Elongation*	1.79	1.43	1.78	1.42
Tensile Strength @ 140°F (MPa)	242	231	192	178
Tensile Modulus @ 140°F (GPa)	16.88	16.45	12.97	12.12
% Elongation @ 140°F	1.59	1.43	1.69	1.47
Compressive Strength (MPa)	314	289	252	216
Compressive Modulus (GPa)	23.33	21.13	20.34	20.30
90° Tensile Strength (MPa)	280	243	274	196
90° Tensile Modulus (GPa)	18.70	16.26	18.24	16.32
90° % Elongation	1.79	1.43	1.78	1.40
±45° In-Plane Shear Strength (MPa)	66	63	64	59
±45° In-Plane Shear Modulus (GPa)	2.60	2.45	2.30	2.18
Ply thickness (mm)	0.356		0.356	

*Table 12.9: Laminate Properties for Hex-3R Wrap 107 Material  
(after 70-75° for 5 days and 48 hours at 140°F)*

Property	Hex 3R Epoxy 300		Hex-3R Epoxy 306XR	
	Average Value	Design Value <sup>1</sup>	Average Value	Design Value
Tensile Strength (MPa)*	648	597	604	544
Tensile Modulus (GPa)*	26.14	24.58	25.54	23.96
% Elongation*	2.57	2.33	2.43	2.18
Tensile Strength @ 140°F (MPa)	603	574	501	462
Tensile Modulus @ 140°F (GPa)	25.23	24.09	22.93	21.59
% Elongation @ 140°F	2.55	2.43	2.34	2.12
Compressive Strength (MPa)	572	495	496	409
Compressive Modulus (GPa)	29.50	22.22	28.08	24.64
90° Tensile Strength (MPa)	50	32	47	23
90° Tensile Modulus (GPa)	8.58	6.73	7.20	6.79
90° % Elongation	1.20	1.08	0.78	0.60
±45° In-Plane Shear Strength (MPa)	45	43	64	59
±45° In-Plane Shear Modulus (GPa)	2.38	1.11	2.30	2.18
Ply thickness (mm)	1.02		1.02	

\* 24 coupons per test series; all other values based on 6 coupon test series

\* Design Value = Average Value – 2(Standard Deviation)

*Table 12.10: Laminate Properties for Hex-3R Wrap 116 Material  
(70-75° for 5 days and 48 hours at 140°F)*

Property	Hex 3R Epoxy 300		Hex-3R Epoxy 306XR	
	Average Value	Design Value <sup>1</sup>	Average Value	Design Value
Tensile Strength (MPa)*	256	219	245	207
Tensile Modulus (GPa)*	15.88	15	14.51	13.04
% Elongation*	1.97	1.67	1.99	1.73
Tensile Strength @ 140°F (MPa)	175	150	203	179
Tensile Modulus @ 140°F (GPa)	10.88	9.56	12.43	11.17
% Elongation @ 140°F	1.84	1.72	1.91	1.59
Compressive Strength (MPa)	269	222	223	200
Compressive Modulus (GPa)	21.21	19.33	19.23	17.35
90° Tensile Strength (MPa)	**	**	**	**
90° Tensile Modulus (GPa)	**	**	**	**
90° % Elongation	**	**	**	**
±45° In-Plane Shear Strength (MPa)	164	130	167	134
±45° In-Plane Shear Modulus (GPa)	8.29	8.20	8.04	7.39
Ply thickness (mm)	0.94		0.94	

\* 24 coupons per test series; all other values based on 6 coupon test series

<sup>1</sup> Design Value = Average Value -2(Standard Deviation)

\*\* Not Available

*Table 12.11: Laminate Properties for Hex-3R Wrap 430 Material (70-75° for 5 days and 48 hours at 140°F)*

Property	Hex 3R Epoxy 300		Hex-3R Epoxy 306XR	
	Average Value	Design Value <sup>1</sup>	Average Value	Design Value
Tensile Strength (MPa)*	537	504		
Tensile Modulus (GPa)*	26.49	15		
% Elongation*	2.21	1.93		
Tensile Strength @ 140°F (MPa)	477	449		
Tensile Modulus @ 140°F (GPa)	24.83	23.69		
% Elongation @ 140°F	2.01	1.87		
Compressive Strength (MPa)	**	**		
Compressive Modulus (GPa)	**	**		
90° Tensile Strength (MPa)	23	15		
90° Tensile Modulus (GPa)	7.07	5.98		
90° % Elongation	0.32	0.24		
±45° In-Plane Shear Strength (MPa)	**	**		
±45° In-Plane Shear Modulus (GPa)	**	**		
Ply thickness (mm)	0.508			

\* 24 coupons per test series; all other values based on 6 coupon test series

<sup>1</sup> Design Value = Average Value -2(Standard Deviation)

\*\* Not available

*Table 12.12: Laminate Properties for Hex-3R Wrap 430 Material  
(70-75° for 5 days and 48 hours at 140°F)*

Properties	Hex-3R Epoxy 300	Hex-3R Epoxy 306
Tensile Strength (MPa)	450	360
Tensile Modulus (GPa)	21.5	20.5
% Elongation	1.9	1.6
Ply thickness (mm)	0.5	0.65

\* Listed at 95% confidence level, i.e. Average – 1.96 (Standard Deviation)

*Table 12.13: Laminate Properties for Hex-3R Wrap 103 Material  
(after 5 days at 70-75° and 48 hour post-cure at 140°F)*

Property	Hex 3R Epoxy 300		Hex-3R Epoxy 306XR	
	Average Value	Design Value	Average Value	Design Value <sup>1</sup>
Tensile Strength (MPa)*	849	717	801	668
Tensile Modulus (GPa)*	70.55	65.09	67.21	58.02
% Elongation*	1.12	0.98	1.13	0.99
Tensile Strength @ 140°F (MPa)	847	699	811	708
Tensile Modulus @ 140°F (GPa)	69.84	63.09	69.64	65.31
% Elongation @ 140°F	1.13	0.97	1.10	0.94
Compressive Strength (MPa)	779	715	643	385
Compressive Modulus (GPa)	67.01	61.53	67.21	59.80
90° Tensile Strength (MPa)	24	16	28	23
90° Tensile Modulus (GPa)	4.86	3.97	4.49	4.04
90° % Elongation	0.45	0.33	0.64	0.52
±45° In-Plane Shear Strength (MPa)	52	46	49	42
±45° In-Plane Shear Modulus (GPa)	2.50	2.39	2.37	2.25
Ply thickness (mm)	1.016		1.016	

\* 24 coupons per test series; all other values based on 6 coupon test series

<sup>1</sup> Design Value = Average Value – 2(Standard Deviation)

*Table 12.14: Laminate Properties for Hex-3R Wrap 103 HS Material  
(after 70-75°F for 5 days and 48 hours at 140°F)*

Property	Hex 3R Epoxy 300		Hex-3R Epoxy 306XR	
	Average Value	Design Value	Average Value	Design Value <sup>1</sup>
Tensile Strength (MPa)*	1022	918		
Tensile Modulus (GPa)*	71.72	56.15		
% Elongation*	1.31	1.15		
Tensile Strength @ 140°F (MPa)	**	**		
Tensile Modulus @ 140°F (GPa)	**	**		
% Elongation @ 140°F	**	**		
Compressive Strength (MPa)	**	**		
Compressive Modulus (GPa)	**	**		
90° Tensile Strength (MPa)	**	**		
90° Tensile Modulus (GPa)	**	**		
90° % Elongation	**	**		
±45° In-Plane Shear Strength (MPa)	**	**		
±45° In-Plane Shear Modulus (GPa)	**	**		
Ply thickness (mm)	1.016			

\* 24 coupons per test series; all other values based on 6 coupon test series

<sup>1</sup> Design Value = Average Value -2(Standard Deviation)

\*\* Not available

*Table 12.15: Laminate Properties for Hex-3R Wrap 113C Material  
(70-75°F for 5 days and 48 hours at 140°F)*

Property	Hex 3R Epoxy 300		Hex-3R Epoxy 306XR	
	Average Value	Design Value	Average Value	Design Value <sup>1</sup>
Tensile Strength (MPa)*	609	546	595	536
Tensile Modulus (GPa)*	50.89	15	45.84	40.42
% Elongation*	1.20	1.08	1.25	1.07
Tensile Strength @ 140°F (MPa)	538	493	395	351
Tensile Modulus @ 140°F (GPa)	45.99	45.32	34.12	29.65
% Elongation @ 140°F	1.18	1.06	1.19	0.93
Compressive Strength (MPa)	393	318	340	287
Compressive Modulus (GPa)	48.65	47.63	39.93	36.00
90° Tensile Strength (MPa)	609	546	595	502
90° Tensile Modulus (GPa)	50.89	50.48	45.84	40.42
90° % Elongation	1.20	1.08	1.25	1.07
±45° In-Plane Shear Strength (MPa)	106	98	88	83
±45° In-Plane Shear Modulus (GPa)	**	**	3.02	2.85
Ply thickness (mm)	0.254		0.254	

\* 24 coupons per test series; all other values based on 6 coupon test series

<sup>1</sup> Design Value = Average Value -2(Standard Deviation)

\*\* Not available

*Table 12.16: Laminate Properties for Hex-3R Wrap 117 Material  
(70-75°F for 5 days and 48 hours at 140°F)*

Properties	Hex-3R Epoxy 300	Hex-3R Epoxy 306
Tensile Strength (MPa)	740	600
Tensile Modulus (GPa)	65	59
% Elongation	1	0.9
Ply thickness (mm)	0.52	0.58

\* Listed at 95% confidence level, i.e. Average – 1.96 (Standard Deviation)

*Table 12.17: Laminate Properties for Hex-3R Wrap 230 Material  
(after 5 days at 70-75°F)*

Property	HEX-3R Epoxy 300		HEX-3R Epoxy 306XR		Sikadur 330	
	Avg. Value	Design Value <sup>1</sup>	Avg. Value	Design Value <sup>1</sup>	Avg Value	Design Value <sup>1</sup>
Tensile Strength (MPa)*	954	820	903	776	894	715
Tensile Modulus (GPa)*	66.33	61.24	67.71	63.11	65.40	61.01
% Elongation*	1.33	1.19	1.23	1.07	1.33	1.09
Tensile Strength @ 140°F (MPa)	948	890	664	606	814	703
Tensile Modulus @ 140°F (GPa)	70.35	66.32	54.99	51.92	66.70	59.70
% Elongation @ 140°F	1.25	1.15	1.17	0.87	1.16	1.00
Compressive Strength (MPa)	696	651	619	542	779	668
Compressive Modulus (GPa)	65.09	59.46	55.11	53.33	67.00	63.60
90° Tensile Strength (MPa)	24	17	41	37	27	23
90° Tensile Modulus (GPa)	5.16	4.84	5.10	4.77	5.88	5.50
90° % Elongation	0.48	0.38	0.85	0.71	0.46	0.40
±45° In-Plane Shear Strength (MPa)	67	67	74	64	63	56
±45° In-Plane Shear Modulus (GPa)	2.34	2.26	2.78	2.56	2.90	2.80
Ply thickness (mm)	0.381		0.381		0.381	

\* 24 coupons per test series; all other values based on 6 coupon test series

<sup>1</sup> Design Value = Average Value – 2(Standard Deviation)

### 12.3 Mitsubishi Chemical Corporation [2-4]

Mitsubishi Chemical Corporation (often in conjunction with the Sumitomo Corporation in the US) provides systems of stabilized unidirectional carbon fabric under the trade-name Replark™.

The Replark systems consist of carbon fibers stabilized through use of a glass mesh attached using binder and then placed on removable paper backing for stability. Due to this structure the system cannot be impregnated using an impregnator and wet layup has to be done on the structure itself using rollers and squeegees. The fabrics are available in 4 varieties as listed in Table 12.18, with the first 3 being used commonly.

*Table 12.18: Replark™ Sheet Characteristics*

Characteristics	Grade 20	Grade 30	Grade HM	Grade MM
Fiber Density (glcc)	1.80	1.80	2.10	1.80
Fabric Areal Weight (glm <sup>2</sup> )	200	300	300	300
Nominal Thickness (mm)	0.111	0.167	0.143	0.167
Nominal Tensile Strength (MPa)	3820	3820	2330	3820
Design Tensile Strength (MPa)	2940	2940	1960	2940
Tensile Modulus (GPa)	230	230	640	390
Elongation (%)	1.2	1.2	0.3	0.7
Color of Glass Mesh	White	Black	Green	Variable

An epoxy resin system is used in two varieties based on the surrounding temperature and these are generally referred to as the “Spring” or “Cool Season” system and the “Summer” or “Warm Season” system. Overall characteristics for the primer, and resin are listed in Table 12.19.

*Table 12.19: Characteristic of Polymeric Systems*

Characteristic	Primer		Resin	
	PS 301	PS 401	L 700W	L 700-LS
Season	Cool	Warm	Cool	Warm
Temperature Range (°C)	5-25	20-35	5-15	15-35
Mix Proportion (Main-Hardener)	2:1	2:1	2:1	2:1
Specific Gravity at 25°C – Main	1.11	1.11	1.13	1.13
Hardener	1.02	0.97	1.05	0.99
Tensile Strength at 23°C (MPa)	-	-	29.4	29.4
Flexural Strength at 23°C (MPa)	-	-	39.2	39.2
Shear Strength at 23°C (MPa)	-	-	9.8	9.8
Adhesive Strength at 23°C to Steel (MPa)	4.9	4.9	4.9	4.9
Adhesive Strength at 23°C to Concrete (MPa)	1.5	1.5	1.5	1.5
Viscosity at 23°C (mPa.s)	500	500	3500	2700
Pot Life at 23°C (minutes)	40	240	20	120
Tack Free Time at 23°C (hours)	3.5	7.0	3.5	7.0
Curing Time at 23°C (Days)	-	-	7	7

Typical composite properties for purposes of reference are given in Table 12.20. It is noted that the composite is taken to consist of a layer of resin undercoat, one layer of reinforcing fabric, and a layer of resin overcoat. The reader is directed to the footnotes for details on calculation of tensile strength and modulus as presented by Mitsubishi.

*Table 12.20: Typical Constituent and Composite Properties*

Property	Carbon Fabric			Resin	Composite		
	20	30	HM		20	30	HM
Thickness (mm)	0.111	0.167	0.143	0.636	0.474	0.803	0.779
Tensile Strength (MPa) <sup>1</sup>	3820	3820	2330	5	567	794	427
Tensile Modulus (GPa) <sup>1</sup>	230	230	640	1.5	34	48	117
Minimum Breaking Load (kgf/cm)	-	-	-	-	441.7	664.5	363.2
Guaranteed Breaking Load (kgf/cm)	-	-	-	-	436	656	341

<sup>1</sup> Since tensile strength of the resin is very low when compared to the fiber it is neglected.

$$\text{Tensile strength} = \text{Tensile modulus of fabric} \times \frac{\text{fabric thickness}}{\text{composite thickness}}$$

<sup>2</sup> Since tensile modulus of the resin is very low when compared to the fiber it is neglected.

$$\text{Tensile modulus} = \text{Tensile modulus of fabric} \times (\text{fabric thickness/composite thickness})$$

In addition to the Replark™ systems Mitsubishi has on occasion also used a lightly stitch carbon fabric designated as UT70-30. No specifications for this are available from Mitsubishi but the system was evaluated under the Caltrans Durability program in conjunction with the L700S-LS resin system and results from that study\* are reported herein. The areal weight of the fabric is reported as 300 glm<sup>2</sup> with a nominal thickness of 0.167 mm. In composite form the properties were reported as in Table 12.21.

*Table 12.21: Properties for UT70-30/L700-LS Composite[3]*

Characteristic	Value
Tensile Modulus (GPa)	220.6 ± 11.03
Tensile Strength (GPa)	4.54 ± 0.26
Failure Strain (%)	1.86 ± 0.10
Short Beam Shear Strength (MPa)	53.78 ± 2.07
Glass Transition Temperature (C°)	63.25 (Average of 4 measurements)
Shore D Hardness	91 ± 3



## 12.4 Hardcore, LLC [5]

Hardcore Composites provide the Hardshell Composite Strengthening System which consists of E-glass/Vinylester prefabricated sections which can be used to form a jacket around a column by adhesive bonding. The sections are either slightly less than half the column circumference, or the entire circumference with a vertical slit to enable stretching open and positioning. In both cases, the jacket is formed by using several layers ensuring that joints are staggered. 4 different systems, each comprising of a different reinforcing architecture for the fabric, are available as listed in Table 12.22, of which the first, WM-4505, is used primarily for seismic retrofit.

Table 12.22: Characteristics of the Hardshell System

Property <sup>1</sup>	WM4505	QM6408	QE9100	WR2400
Description	Unidirectional	0/±45/90 (balanced 0,90)	0/±45/90 (0° enhanced)	Bidirectional
Primary direction <sup>2</sup> Tensile strength (MPa)	620	435	510	400
Secondary direction <sup>3</sup> Tensile strength (MPa)	70	325	240	415
Primary direction <sup>2</sup> Tensile modulus (GPa)	35	25	30	21
Secondary direction <sup>3</sup> Tensile modulus (GPa)	3	16	13	23
Primary direction Ultimate Strain (%)	2	1.8	1.8	1.8
Fiber volume fraction (%)	50	50	50	50

<sup>1</sup> Minimum properties

<sup>2</sup> Primary direction is the hoop direction for seismic retrofit

<sup>3</sup> Secondary direction is the axial direction for seismic retrofit

## 12.5 Freyssinet, LLC [6]

Freyssinet markets a single fabric based system under the trade name of TFC. The fabric is a 4-harness satin (a bi-directional weave) of carbon fibers woven by Porcher with an areal weight of 500 g/m<sup>2</sup> and 70% of the fibers in the warp direction. The carbon fibers are PAN based from Soficar and are used in 12k and 24k tow sizes with properties as in Table 12.23.

*Table 12.23: Properties of T700SC Fibers (12/24k at 50°)*

Property	Maximum	Nominal	Minimum
Tensile Strength (MPa)	-	4900	4510
Tensile Modulus (GPa)	240	230	221
Ultimate Strain (%)	-	2.1	1.8
Mass of 12k tow (g/1000m)	824	800	776
Mass of 24k tow (g/1000m)	1700	1650	1600
Density (g/cc)	1.84	1.8	1.76

The impregnating resin system is a two component epoxy manufactured by Atofindley and denoted as XEP 3935A/2919B, representing the resin and hardener. The resin has a density of 1.32-1.36 g/cc whereas the hardener has a density of 1.00-1.04 g/cc. The ratio of resin to hardener is 100:40 by weight and 2:1 by volume. Neat resin properties are given in Table 12.24.

*Table 12.24: Properties of XEP 3935A/2919B Resin System (after 7 days at 23°)*

Characteristic	Value
Tensile Strength (MPa)	29.3 ± 1.2
Tensile Modulus (MPa)	2300 ± 120
Ultimate Strain (%)	2.4 ± 0.3
Compressive Strength (MPa)	56.3 ± 0.7
Compressive Modulus (MPa)	2000 ± 100
Ultimate Strain in Compression (%)	4.7 ± 0.1
Bond Strength on dry concrete (MPa)	2.5 <sup>1</sup>
Bond Strength on moist concrete (MPa)	2.0 <sup>1</sup>

<sup>1</sup>Failure in concrete

Composite properties determined at a sample thickness of 0.86mm and normalized to a fiber volume fraction of 65% are given in Table 12.25.

*Table 12.25: Composite Properties*

Characteristic	Wrap Direction	Weft Direction
Tensile Strength (MPa)	1649	692
Tensile Modulus (GPa)	104	40.8
Ultimate Strain (%)	1.63	1.73

For purposes of design a breaking stress of 1400MPa, a modulus of 105 GPa and an ultimate strain of 1.3% are recommended.

## 12.6 Edge Structural Composites

Edge Structural Composites markets two fabric based systems for wetlayup, one consisting of standard modulus carbon fibers and the other of E-glass fibers. Both are primarily unidirectional fabrics with transverse threads, and characteristics as listed in Table 12.26. The resin system is a 2-phase 100% solids epoxy with resin and hardener mixed in a ratio of 100:62 by weight and 100:70 by volume. The components are listed as having a shelf life of 12 months. The mixed viscosity at 25°C is 2,200 cps with a pot life of 45 minutes 25°C. Characteristics of the neat resin are given in Table 12.27 with characteristics of cured composite being listed in Table 12.28.

*Table 12.26: Fabric Characteristics*

Characteristic	Carbon Fiber	E-Glass Fiber
Areal Weight (g/m <sup>2</sup> )	335	875
Thickness <sup>1</sup> (cm <sup>2</sup> /m)	1.75	3.45
Tensile Strength (MPa)	4480	2275
Tensile Modulus (GPa)	234.4	72.39
Ultimate Strain (%)	1.9	4

<sup>1</sup> Based on the theoretical fiber area

*Table 12.27: Resin System Characteristics*

Characteristic	Value
Tensile Strength (MPa)	44.8
Tensile Modulus (GPa)	2.07
Ultimate Strain (%)	5.5
Hardness (Shore D)	77
Compressive Strength (MPa)	71
Compressive Modulus (GPa)	2
Shear Bond Strength (MPa)	15
Glass Transition Temperature (C°)	63

*Table 12.28: Design Values for Composite Material*

Characteristic	Carbon Fiber Composite	E-Glass Fiber Composite
Ply thickness (mm)	0.584	1.1
Tensile Strength (MPa)	1035	552
Tensile Modulus (GPa)	70	27.6
Ultimate Strain (%)	1.5	2.2
Bond Strength to Concrete (N/mm <sup>2</sup> )	4.68	4.68

## 12.7 Watson Bowman Acme [8]

Systems for both wet-layup of fabric and for adhesive bonding of precured laminates are available. 5 different reinforcing fabrics are available based on type of fiber with all being unidirectional fabrics. The impregnating resin systems are available in two primary types – the conventional resins that are 100% solids amine cured epoxied and a specially formulated set of systems which are moisture permeable. Characteristics of these systems are provided in Tables 12.29 and 12.30, respectively.

*Table 12.29: Characteristics of Encapsulating Resin Systems*

Characteristic	Wabo Mbrace Primer	Wabo Mbrace Saturant LTC	Wabo Mbrace Saturant
Mix Ratio (A:B)	3 to 1 by volume	3 to 1 by volume	3 to 1 by volume
	100 to 30 by weight	100 to 34 by weight	100 to 34 by weight
Working Time at 25°C (minutes)	20	10	45
Viscosity at 25°C (cps)	400	1150	1350
Shelf life at 21°C	18	18	18
Density (kg/m <sup>3</sup> )	1102	983	983
Tensile Yield Strength (MPa)	14.5	14	54
Tensile Strain at Yield (%)	2	1.3	2.5
Tensile Modulus (MPa)	717	1138	3034
Tensile Strength (MPa)	17.2	14	55.2
Ultimate Strain (%)	40	5.3	3.5
Poisson's Ratio	0.48	0.4	0.4
Compressive Yield Strength (MPa)	26.2	36	86.2
Compressive Strain at Yield (%)	4	2.3	5
Compressive Modulus (MPa)	670	1585	2620
Compressive Strength (MPa)	28.3	36	86.2
Ultimate Strain (%)	10	5	5
Flexural Yield Strength (MPa)	24.1	225	138
Flexural Strain at Yield (%)	4	4.5	3.8
Flexural Modulus (MPa)	595	552	3724
Flexural Strength (MPa)	24.1	25	138
Ultimate Strain (%)	No rupture	5	5
Coefficient of Thermal Expansion (/°C)	$35 \times 10^{-6}$	$35 \times 10^{-6}$	$35 \times 10^{-6}$
Thermal Conductivity (W/m <sup>2</sup> °k)	0.2	0.21	0.21
Glass Transition Temperature (°C)	77	71	71

Table 12.30: Characteristics of Moisture Permeable Systems

Characteristic	MBrace Resicem Saturant LTC	MBrace Resicem Saturant
Mix Ratio (A to B)	3 to 1 by volume	3 to 1 by volume
	100 to 34 by weight	100 to 34 by weight
Working Time at 25°C (minutes)	10	45
Sag resistance (mm)	0.5	0.625
Use Temperature Range (°C)	4-21	10-50
Shelf Life at 21°C	18	18

Properties of resulting composites using the 5 different types of fibers in a unidirectional fabric form using the wet layup process are listed in Table 12.31.

Table 12.31: Characteristics of Composite<sup>1</sup>

Characteristics	CF130	CF160	CF530	AK60	EG900
Fiber Type	HS Carbon	HS Carbon	HM Carbon	Kevlar	E- Glass
Areal Weight (g/m <sup>2</sup> )	300	600	300	600	900
Nominal Thickness <sup>2</sup> (mm)	0.165	0.33	0.165	0.28	0.353
Coefficient of Thermal Expansion (x10 <sup>-6</sup> /°C)	0.38	0.38	0.83		3.27
Conductivity (W/m°K)	9.38		68.7		1.29
Resistivity (Ω-cm)	1.6x10 <sup>-3</sup>		1x10 <sup>-3</sup>		
Tensile Strength (MPa)	3800	3800	3500	2000	1517
Tensile Modulus (GPa)	227	227	373	120	72.4
Tensile Strength/Unit Width <sup>3</sup> (kN/mm/ply)	0.625	1.25	0.577	0.559	0.536
Tensile Modulus/Unit Width <sup>3</sup> (kN/mm/ply)	38	76	62	33.5	25.6
Ultimate Strain (%)	1.67	1.67	0.94	1.55	2.1

<sup>1</sup> Properties in the fiber direction (0°)

<sup>2</sup> Based on total area of fibers only in a unit width. Actual cured thickness of a single ply is 0.6-1.0 mm.

<sup>3</sup> Tensile properties for design obtained by dividing strength and modulus per unit width from D3039 by nominal fabric thickness.

The Wabo MBrace system also makes available prefabricated carbon/epoxy laminates that can be adhesively bonded onto the concrete substrate. Characteristics of these laminates (designated as Wabo MBrace S&P laminates) are given in Table 12.32.

*Table 12.32: Characteristics of Prefabricated S&P Laminates*

Characteristic	10/1.4	501.4	100/1.4
Fiber Volume Fraction (%)	70	70	70
Nominal Width (mm)	10	50	100
Nominal Thickness (mm)	1.4	1.4	1.4
Design Area (sq mm)			
Tensile Modulus (GPa)			
Tensile Strength (MPa)			

## 12.8 Sika [9]

Sika has both prefabricated (pultruded) strips systems used by adhesive bonding, and fabric based systems which are used through the wet layup process. The company has an agreement with Hexcel enabling it to market a number of the same systems as marketed by the Hexcel Civil Engineering and Construction Systems division (see section 12.2 of this chapter) but under the Sika name.

The prefabricated systems are available under the CarboDur® trade name and consist of carbon fibers pultruded with an epoxy resin into strips. The strips have a fiber volume fraction of over 68% and a temperature resistance of about 150°C. Overall characteristics of the three primary types of systems (differentiated on the basis of mechanical properties, primarily modulus) are given in Table 12.33.

*Table 12.33: Mechanical Characteristics of the CarboDur Systems (at 23°C and 50% RH)*

Characteristic	Type S	Type M	Type H
Description	Standard Modulus	Intermediate Modulus	High Modulus
Longitudinal Tensile Modulus (GPa)	165	210	300
Longitudinal Tensile Strength (GPa)	2.8	2.4	1.3
Ultimate Strain (%)	>1.7%	>1.2%	>0.45%
Density (g/cm <sup>3</sup> )	1.5	1.6	1.6

The strips are available in a number of widths and thicknesses as listed in Table 12.34.



*Table 12.36: Impregnating Resin Characteristics*

Characteristic	Sikadur 300	Sikadur 306	Sikadur Hex 300/306	Sikadur 330
Storage Conditions (°C)	4-35	4-35	4-35	4-35
Minimum Use Temperature (°F)	65-75	65-75	65-75	65-75
Viscosity (cps)	300-500	306-2500	300-550,306-7000	Paste
Service Temperature Range (°F)	-40 to 140	-40 to 140	-40 to 140	
Tensile Strength <sup>1</sup> (MPa)	64.8	52.4	72.4	30.0
Tensile Modulus <sup>1</sup> (GPa)	2.1	2.2	3.2	-
Ultimate Strain <sup>1</sup> (MPa)	3.9	3.1	4.8	1.5
Flexural Strength <sup>1</sup> (MPa)	86.2	64.1	123.4	-
Flexural Modulus <sup>1</sup> (GPa)	3.9	3.4	3.1	3.8

<sup>1</sup>After 14 day cure at 23°C and 50% RH.

The fabrics used in wet layup are just renamed versions of fabrics from Hexcel already described in detail in section 12.2 of this chapter and are hence not reported herein. However, a correspondence between the fabrics is listed in Table 12.37.

*Table 12.37: Correspondence Between Sika and Hexcel Fabrics (Properties are given in Section 12.2)*

Fiber Type	Sika Designation	Hexcel Designation
Glass	Sika Wrap Hex 100G	Hex-3R Wrap 100
Carbon	Sika Wrap Hex 103C	Hex-3R Wrap 103
Glass	Sika Wrap Hex 106G	Hex-3R Wrap 106
Glass	Sika Wrap Hex 107G	Hex-3R Wrap 107
Carbon	Sika Wrap Hex 113C	Hex-3R Wrap 113
Carbon	Sika Wrap Hex 117C	Hex-3R Wrap 117
Carbon	Sika Wrap Hex 230C	Hex-3R Wrap 230

## 12.9 Structural Composite Construction, Inc. (SCCI) [10]

SCCI uses the wet layup process with fabrics consisting of both E-glass and carbon fiber reinforcements. Two impregnating epoxies are used, the primary properties of which are given in Table 12.38. Both are two part epoxies with 2:1 mix ratios by volume.



*Table 12.38: Characteristics of SCCI Expoxies*

Characteristic	Fiber Matrix I	Fiber Matrix II
Gel Time at 23°C (minutes)	60	36-42
Tack Free Time at 24°C (hours)	4.5	2-4
Tensile Strength at 14 days (MPa)	41	48
Ultimate Strain (%)	2-4	1.6
Flexural Strength at 14 days (MPa)	52	52
Compressive Yield Strength at 24 hours (MPa)	22	22
Compressive Yield Strength at 7 days (MPa)	72	72
Bond Strength (2 days) (MPa)	8.2	8.3
Water Absorption in 24 hours (%)	0.08	0.5

Characteristics of the composites formed using the 3 primarily unidirectional fabric systems are given in Table 12.39.

*Table 12.39: Characteristics of Fabric Systems*

Characteristic	SCCI-C1	SCCI-C2	SCCI-C3
Fiber Type	T-700 Carbon	T-700 Carbon	E-Glass
Fiber Tow Size	12k	24k	
Fabric Basis Weight (g/cc)	305	610	610
Nominal Thickness (mm)	0.508	1.016	1.041
Tensile Strength (MPa)	888.8	861.9	542.6
Tensile Modulus (GPa)	78.6	79.3	30.3
Ultimate Strain (%)	1.1	1.2	4.5

A prefabricated strip which is adhesively bonded to the concrete substrate using a two part high solids content epoxy is also available. However, no properties or specifications were available from the company at the time of writing.

#### **12.10 Fyfe Co. LLC [11]**

Both fabric based and prefabricated, pull formed, strip systems are available. The fabric based systems are either impregnated using rollers or directly in an impregnating machine. Characteristics of 3 commonly used resins, all of which are 2 part epoxies, are given in Table 12.40.

*Table 12.40: Characteristics of Impregnating Epoxies*

Characteristic	Tyfo TC	Tyfo T	Tyfo S
Description	Primarily tack coat or between layers	High Temperature Use ( $\approx 121^{\circ}\text{C}$ )	Standard
Mix Ratio, A:B, by volume	100:30	100:30	100:42
Mix Ratio, A:B, by weight	100:25	100:30	100:35.4
Minimum Application Temperature ( $^{\circ}\text{C}$ )	4	4	4
Pot Life (hours)	1-2 between $21-32^{\circ}\text{C}$	$\approx 2$ hours between $16-27^{\circ}\text{C}$	3-6 hours at $20^{\circ}\text{C}$
Viscosity (cps)	-	-	600-700

Properties of the standard, high elongation system, Tyfo S after 72 hours post cure at  $60^{\circ}\text{C}$  are listed in Table 12.41.

*Table 12.41: Properties of Neat Cured Tyfo S*

Property	ASTM Method	Typical Value
Glass Transition Temperature ( $^{\circ}\text{C}$ )		82
Tensile Strength (MPa)	D-638 (1)	72.4
Tensile Modulus (GPa)		3.18
Ultimate Strain (%)	D-638 (1)	5
Flexural Strength (MPa)	D-790	123.4
Flexural Modulus (GPa)	D-790	3.12

The fabrics for wet layup are available using E-glass, carbon and aramid fibers. Often a second fiber is used in the transverse direction as a tracer in an otherwise essentially unidirectional fabric.

Typical dry fiber and fabric characteristics are given in Tables 12.42-12.44 for the E-glass, Carbon, and Aramid fiber based fabrics, respectively.

*Table 12.42: Dry Fiber and Fabric Properties – Glass Fabric*

Characteristic	BC	SEH-51	SEH-51A
Fabric Description	Bidirectional with $\pm 45^\circ$ orientation	Unidirectional glass with aramid at $90^\circ$	Unidirectional glass, Yellow colored glass at $90^\circ$
Tensile Strength (GPa)	3.24	3.24	3.24
Tensile Modulus (GPa)	72.4	72.4	72.4
Ultimate Strain (%)	4.5	4.5	4.5
Density (g/cc)	2.55	2.55	2.55
Basis Weight (g/m <sup>2</sup> )	813	915	915
Fabric Thickness (mm)	-	0.36	0.36

*Table 12.43: Dry Fiber and Fabric Properties – Carbon Fabric*

Characteristic	SCH-11UP	SCH-35	SCH-41	SCH-415
Fabric Description	Unidirectional	Unidirectional stitched	Unidirectional with glass veil	Unidirectional with aramid cross fibers
Tensile Strength (GPa)	3.79		3.79	3.79
Tensile Modulus (GPa)	230		230	230
Ultimate Strain (%)	1.7		1.7	1.7
Density (g/cc)	1.74		1.74	1.74
Basis Weight (g/m <sup>2</sup> )	298		644	644
Fabric Thickness (mm)	0.127		0.28	0.28

*Table 12.44: Dry Fiber and Fabric Properties – Aramid Fabric*

Characteristic	SAH-41	BA
Fabric Description	Unidirectional weave	Unidirectional weave
Tensile Strength (GPa)	3.1	3.1
Tensile Modulus (GPa)	114	114
Ultimate Strain (%)	2.8	2.8
Density (g/cc)	1.4	1.4
Basis Weight (g/m <sup>2</sup> )	650	650

Typical gross laminate properties using the fabrics listed in Tables 12.42-12.44 with the Tyfo-S Epoxy are listed in Tables 12.45-12.47, respectively.

*Table 12.45: Typical Gross Glass Fabric Laminate Properties  
[Primary Fiber Direction (0°) Unless Specified]*

Characteristic	BC		SEH-51		SEH-51A	
	Typical	Design	Typical	Design	Typical	Design
Tensile Strength (MPa)	279	223	575	460	575	460
Tensile Modulus (GPa)	18.6	14.9	26.1	20.9	26.1	20.9
Ultimate Strain (%)	1.5	1.5	2.2	2.2	2.2	2.2
Laminate Thickness	0.864	0.864	1.3	1.3	1.3	1.3
90° Tensile Strength (MPa)	279	223	43	34.4	25.8	20.7

*Table 12.46: Typical Gross Carbon Fabric Laminate Properties  
[Primary Fiber Direction (0°) Unless Specified]*

Characteristics	SCH-11UP		SCH-35	SCH-41		SCH-41S	
	Typical	Design	Typical	Typical	Design	Typical	Design
Tensile Strength (MPa)	1062	903	991	876	745	876	745
Tensile Modulus (GPa)	102	86.9	78.6	72.4	61.5	72.4	61.5
Ultimate Strain (%)	1.05	1.05	1.26	1.2	1.2	1.2	1.2
Laminate Thickness	0.25	0.25	0.89	1.0	1.0	1.0	1.0
90° Tensile Strength (MPa)	-	-	-	-	-	40.6	34.5

*Table 12.47: Typical Gross Aramid Fabric Laminate Properties  
[Primary Fiber Direction (0°) Unless Specified]*

Characteristics	SAH-41		BA	
	Typical	Design	Typical	Design
Tensile Strength (MPa)	696.4	557.1	696.4	557.1
Tensile Modulus (GPa)	40	32	40	32
Ultimate Strain (%)	1.7	1.7	1.7	1.7
Laminate Thickness	1.3	1.3	1.3	1.3

The prefabricated strip system uses a two component adhesive, Tyfo TC, as the Tyfo S epoxy system. Properties of the laminates available as strips are listed in Table 12.48.

*Table 12.48: Characteristics of Laminate Strip Systems*

Characteristic	UG	UC	
	Typical	Typical	Design
Fiber	E-Glass	Carbon	Carbon
Tensile Strength (GPa)	0.89	2.79	2.51
Tensile Modulus (GPa)	41.4	155	139
Ultimate Strain (%)	2.2	1.8	1.8

A variety of strip widths and thicknesses are available with the standard thicknesses being 1.4 and 1.9mm, at widths of 50.8 and 101.6mm.

## 12.10 Summary

It should be noted that the preceding sections provide summaries of only the most common systems. A number of other systems may be available, as well as variations of these supplied through secondary contractors. The reader is cautioned in the use of performance values for design since the values were taken directly from manufacturer supplied brochures in most cases, and a number of different systems are used by each to determine properties (gross area, fiber area only, normalized fabric area, etc.) and hence direct comparisons between systems need to be made cautiously.

## REFERENCES

- [1] Hexcel Civil Engineering and Construction Systems Data Sheets.
- [2] Technical Manual, Replark™ System, Revision 2.0 ( January 2000)
- [3] Steckel, G.L. (199), "Environmental Durability of Replark 30/L700-LS and UT70-30/L700S Carbon/Epoxy Composites," Aerospace Corporation Report ATR-99 (7455)-1.
- [4] Karbhari, V.M. (1998), Use of Composite Materials in Civil Infrastructure in Japan, WTEC Monograph, WTEC, National Science Foundation, ISBN-1-883712-50-5
- [5] Hardcore Composites, Hardshell Composite Strengthening Jackets Brochure (2003).
- [6] Doghri, K. (2001), "Testing Documentation of the TFC™"
- [7] Edge Structural Composites (20001), Technical Data Sheets
- [8] Watson Bowman Acme (2002), Wabo Data Sheets
- [9] Sika (2002), Construction Products Catalog
- [10] SCCI (2003), Data Sheets from L. McCauley
- [11] Fyfe Co. LLC (2003), Data Sheets from E. Fyfe